

**MITIGATION OF NITROUS OXIDE EMISSIONS
FROM ARABLE SOILS**

PÕLLUMULLAST ERALDUVA DILÄMMASTIKOKSIIDI
VÄHENDAMINE

JORDI ESCUER GATIUS

A Thesis for applying for the degree of
Doctor of Philosophy in Agriculture

Väitekirj
filosoofiadoktori kraadi taotlemiseks
põllumajanduse erialal

Eesti Maaülikooli doktoritööd
Doctoral Theses of the
Estonian University of Life Sciences

**MITIGATION OF NITROUS OXIDE EMISSIONS
FROM ARABLE SOILS**

PÕLLUMULLAST ERALDUVA DILÄMMASTIKOKSIIDI
VÄHENDAMINE

JORDI ESCUER GATIUS

A Thesis for applying for the degree of
Doctor of Philosophy in Agriculture

Väitekirj
filosoofiadoktori kraadi taotlemiseks
põllumajanduse erialal

Institute of Agricultural and Environmental Sciences
Estonian University of Life Sciences

According to verdict No 6-14/14-2 of May 23, 2022, the Doctoral Committee of the Agricultural and Natural Sciences of the Estonian University of Life Sciences has accepted the thesis for the defence for the degree of Doctor of Philosophy in Agriculture.

Opponent: **Prof. Dr. Klaus Butterbach-Bahl**
Institute of Meteorology and Climate Research,
Atmospheric Environmental Research (IMK-IFU)
Karlsruhe Institute of Technology (KIT)

Supervisors: **Assoc. Prof. Merrit Shanskiy**
Institute of Agricultural and Environmental Sciences
Estonian University of Life Sciences

Assoc. Prof. Kaido Soosaar
Institute of Ecology and Earth Sciences
University of Tartu

Prof. Alar Astover
Institute of Agricultural and Environmental Sciences
Estonian University of Life Sciences

Defence of the thesis: Estonian University of Life Sciences, room 2A1,
Fr. Kreutzwaldi 5, Tartu on June 30, 2022, at 10.00

The English in the current thesis was revised by
Dr. Alex Boon and the Estonian by the Language
Centre of the Estonian University of Life Sciences.

© Jordi Escuer Gatius, 2022

ISSN 2382-7076

ISBN 978-9916-669-52-5 (trükis)

ISBN 978-9916-669-53-2 (pdf)

CONTENTS

LIST OF ORIGINAL PUBLICATIONS	7
ABBREVIATIONS	8
1. INTRODUCTION	9
2. LITERATURE REVIEW	12
2.1. Fertilisation and N losses	12
2.3. Soil N ₂ O emissions mitigation strategies in agriculture	16
2.3.1. Nitrification inhibitors	17
2.3.2. Biochar	18
2.3.3. Crop residue management.....	19
3. HYPOTHESES AND AIMS OF THE STUDY	21
4. MATERIAL AND METHODS	22
4.1. Experimental sites and set-up	22
4.1.1. Organic fertilisers (I, III, IV)	23
4.1.2. Biochar experiment (I)	24
4.1.3. Crop residue experiment (II)	25
4.1.4. Nitrification inhibitor (III, IV).....	25
4.2. Nitrous oxide flux measurements and analyses (I, II, III, IV)	26
4.3. Environmental parameter measurements (II, III, IV)	27
4.4. Statistical analyses	28
5. RESULTS	29
5.1. Nitrous oxide fluxes	29
5.2. Biochar and organic fertiliser experiment (I)	29
5.3. Crop residue experiment (II)	31
5.4. Field experiment with cattle slurry and nitrification inhibitor application (III, IV)	31
6. DISCUSSION	33
6.1. N ₂ O emissions mitigation by biochar	34
6.2. N ₂ O emissions mitigation by nitrification inhibitors	36
6.3. N ₂ O emissions after plant residue incorporation	37
6.4. N ₂ O emissions during a full growing season of winter rapeseed (IV)	39
6.5. Limitations and future research	41
7. CONCLUSIONS	43
REFERENCES	45

SUMMARY IN ESTONIAN	69
ORIGINAL PUBLICATIONS	77
CURRICULUM VITAE	162
ELULOOKIRJELDUS	164
LIST OF PUBLICATIONS	166

LIST OF ORIGINAL PUBLICATIONS

The present thesis is based on the following research papers, referred to by their Roman numerals (I–IV in the text). Papers are reproduced by kind permission of the journals concerned.

- I Escuer-Gatius, J.**, Shanskiy, M., Soosaar, K., Astover, A., Raave, H. 2020. High-Temperature Hay Biochar Application into Soil Increases N₂O Fluxes. *Agronomy* 10(1), 109. doi: 10.3390/agrono-my10010109
- II Stegarescu, G., Escuer-Gatius, J.**, Soosaar, K., Kauer, K., Tõnutare, T., Astover, A., Reintam, E. 2020. Effect of Crop Residue Decomposition on Soil Aggregate Stability. *Agriculture* 10(11), 527. doi: 10.3390/agriculture10110527
- III Escuer-Gatius, J.**, Shanskiy, M., Mander, Ü., Kauer, K., Astover, A., Vahter, H., Soosaar, K. 2020. Intensive rain hampers the effectiveness of nitrification inhibition in controlling N₂O emissions from dairy slurry fertilised soils. *Agriculture* 10(11), 497. doi: 10.3390/agriculture10110497
- IV Escuer-Gatius, J.**, Lõhmus, K., Shanskiy, M., Kauer, K., Vahter, H., Mander, Ü., Astover, A., Soosaar, K. 2022. Critical points for closing the carbon and nitrogen budgets in a winter rapeseed field. *Nutrient Cycling in Agroecosystems*. doi: 10.1007/s10705-022-10202-8

The contributions of the authors to the papers:

Paper	Idea and study design	Data collection/ analyses	Data analysis	Manuscript preparation
I	HR AA JEG	JEG MS HR	JEG KS	JEG HR KS
II	GS, ER, TT	GS KK TT	GS JEG ER	GS ER AA KK TT JEG KS
III	KS, KK JEG	JEG KK MS HV	JEG KS	JEG KS ÜM MS AA HV
IV	KS, KK, KL JEG	JEG KK HV	JEG KL KS	JEG KL KS ÜM MS AA HV

JEG – Jordi Escuer Gatius; **MS** – Merrit Shanskiy; **KS** – Kaido Soosaar; **AA** – Alar Astover; **GS** – Gheorghe Stegarescu; **HR** – Henn Raave; **KK** – Karin Kauer; **KL** – Krista Lõhmus; **ÜM** – Ülo Mander; **TT** – Tõnu Tõnutare; **ER** – Endla Reintam; **HV** – Hanna Vahter.

ABBREVIATIONS

AOB	Ammonia oxidizing bacteria
ASN	Ammonium sulphate nitrate
BC	Biochar
BNF	Biological nitrogen fixation
CAN	Calcium ammonium nitrate
DCD	Dicyandiamide
DMPP	3,4-dimethylpyrazole phosphate
EEF	Enhanced efficiency fertiliser
EF	Emission Factor
GHG	Greenhouse gasses
GWP	Global warming potential
NET	Negative emissions technology
NI	Nitrification inhibitor
NUE	Nitrogen Use Efficiency
SOC	Soil organic carbon
WFPS	Water-filled pore space

1. INTRODUCTION

The increase of atmospheric concentrations of greenhouse gases (GHGs), which are responsible for global warming (Mosier, 1998), is one of the greatest environmental concerns of our time, as concentrations of the three main GHGs, carbon dioxide (CO₂), nitrous oxide (N₂O), and methane (CH₄), have been increasing since the beginning of the industrial revolution (NOAA, 2021).

Agriculture is facing the challenge of meeting food demands from a growing human population while maintaining environmental and economic sustainability (Zhang et al., 2015; OECD, 2021), all in the context of the shifting environmental and socio-economic conditions resulting from climate change (Wheeler and von Braun, 2013; Challinor et al., 2014). The growing world population, combined with a higher per capita food demand in developing countries (Baldos and Hertel, 2014), is projected to increase agricultural produce demand by around 50% between 2013 and 2050 (FAO, 2017). The intensification of agricultural production may cause higher GHG emissions, and increased use of nitrogen (N) fertilisers to improve soil fertility and crop productivity can enhance soil N₂O emissions (Davidson, 2009). Nutrient losses also have a negative economic effect on agriculture, as they increase the need for inputs (e.g., fertilisation), eventually making agriculture unsustainable (Oenema and Velthof, 2002). Nutrient losses in agro-ecosystems are related to leaching, gaseous emissions, and surface runoff (FAO/IFA, 2001). The intensification of agriculture can also lead to soil erosion and degradation; loss of wildlife habitats; depletion of soil carbon (C), further enhancing GHG emissions; eutrophication of freshwater and ecosystems; ozone formation, resulting in high tropospheric ozone concentrations; and soil acidification (EEA, 2000; Ammann et al., 2009; Bosch-Serra et al., 2020).

Goals to reduce GHG emissions are included in several worldwide international agreements and reports such as the Kyoto Protocol (UNFCCC, 1997), the Paris Agreement (UNFCCC, 2015), and the “Global Warming of 1.5°C” report (IPCC, 2018), as well as regional and national legislation, such as “The European Green Deal” (European commission, 2019). To achieve these GHG reduction goals, it is necessary to implement effective emissions mitigation strategies.

Although industry and transportation usually receive the most attention, as they represent the largest sources of total anthropogenic GHG emissions, agriculture is responsible for approximately 10%–12% of total global GHG emissions (IPCC, 2007). Moreover, agriculture is the main anthropogenic source of non-CO₂ emissions, which include N₂O and CH₄. Anthropogenic emissions represent approximately 50% of the total global N₂O emissions (Ciais et al., 2013), and agriculture is responsible for around two-thirds of those emissions (Davidson and Kanter, 2014). This is especially important because N₂O has a global warming potential 273 times that of CO₂ (IPCC, 2021) and is currently the main stratospheric ozone-depleting substance (Revell et al., 2015). The European Green Deal, which aims to achieve zero net emissions of greenhouse gases by 2050, places a particular focus on agriculture with the “Farm to Fork Strategy” (European commission, 2020), with the aim of developing a food system that helps to mitigate climate change.

The use of N fertilisers is a key factor in the high N₂O emissions from agriculture (Dobbie and Smith, 2003; Davidson, 2009; Ussiri and Lal, 2013). Davidson (2009) estimated that 2% and 2.5% of the N applied with manure and inorganic fertiliser, respectively, had been emitted as N₂O between 1860 and 2005, explaining the increase of N₂O concentrations in the atmosphere during this period. Many studies have shown that organic fertilisers, including animal slurries, are linked to higher N₂O emissions than synthetic fertilisers (Pelster et al., 2012; Zhou et al., 2013) because of their C content. However, the question of whether N₂O emissions are larger from organic or inorganic fertilisation remains a matter for debate (Chen et al., 2014). The incorporation of plant residues can also result in high N₂O emissions (Zhou et al., 2013). In fact, in organic farming, the highest fluxes are often measured after the incorporation of plant residues (Hansen et al., 2019), and the effect of crop residue incorporation into the soil on N₂O emissions can be similar to that of mineral fertilisation (Chen et al., 2013).

Several strategies have been proposed to mitigate N₂O emissions from the soil, but the variety and complexity of the influencing factors (soil properties, agro-ecosystem management, climatology, and plant cover, among others) as well as the interaction between them (Machefert et al., 2002; Venterea et al., 2012; Butterbach-Bahl et al., 2013), makes it difficult to estimate their effectiveness.

Biochar and nitrification inhibitors are two of the tools that have been proposed as N₂O emissions mitigation tools (Zaman et al., 2021). Besides the potential positive environmental effects in reducing soil N₂O emissions and nitrate (NO₃⁻) leaching, their application can also increase yields (PASDA et al., 2001) or produce the same yield with a smaller amount of fertiliser application (Wang et al., 2016). However, their use has resulted in mixed or contradictory results (Sánchez-García et al., 2014; Shi et al., 2016; Thers et al., 2019), especially for biochar, because its properties vary considerably according to the feedstock and production process (Joseph et al., 2021).

Most importantly, there is a lack of experimental data of N₂O emissions from arable soils for the hemiboreal zone and specifically for Estonia. Moreover, this is the first study to examine the use of the nitrification inhibitor DMPP (3,4-dimethylpyrazole phosphate) in Estonia and one of the first in the Baltic countries. Finally, this work quantifies for the first time all the relevant N fluxes in an agro-ecosystem with intensively managed rapeseed field in Estonia.

2. LITERATURE REVIEW

Soil health, the ability of soil to function as a living ecosystem that can sustain animal and plant life, is threatened by several agents, such as organic matter losses, pollution, salinisation, erosion, compaction, and decreased biodiversity (European Commission, 2006).

2.1. Fertilisation and N losses

Fertilisation influences soil health by affecting factors such as organic matter content, microbial communities and soil acidity (Singh, 2018). Excessive or unbalanced fertilisation and the inappropriate use of pesticides are two major factors threatening soil health in agro-ecosystems. Inadequate fertilisation practices can cause high nutrient losses, with detrimental economic and environmental consequences, especially NO_3^- leaching and gaseous N emissions (FAO/IFA, 2001; Ma et al., 2022) including N_2O , dinitrogen gas (N_2), nitrogen oxides (NO_x), and ammonia (NH_3). Other threats to soil health include drainage of wetlands or mechanical disturbance, which can result in increased C mineralisation (Lohila et al., 2004).

Organic fertilisers are those derived from organic animal or plant matter and include manure and slurry, crop residues, and compost (Kiiski et al., 2000; Wei et al., 2020), as well as sewage sludge and industrial wastes (Thomas et al., 2019). Manure slurry and digestate are often used as fertilisers (Bosch-Serra et al., 2020). The recycling of organic waste and the use of by-products as fertiliser serves a double purpose as it also removes the requirement for disposal in landfills or similar sites (Thomas et al., 2019), which is in accordance with the directives of the Circular Economy Package from the European Union (European Commission, 2016). The main drawbacks of the use of organic fertilisers are the great variability in nutrient content depending on the source materials (Davis, 2015; KeChrist et al., 2017) and the reported higher N_2O emissions than those of synthetic fertiliser for the same amount of applied N (van Groenigen et al., 2004; Jones et al., 2007). However, the use of manure instead of synthetic fertilisers can increase the soil organic carbon (SOC) pool (Lal, 2007). Smith et al. (1997) estimated that SOC in the European croplands could be increased by 5.5% following the application of 10t ha^{-1} of manure over 100 years. Cattle slurry, the semi-liquid mixture of animal excreta from cattle, rich in ammonium (NH_4^+), is a common organic fertiliser (van der Molen et al., 1990; Thompson and Meisinger, 2002). Slurry digestate is

the by-product of the anaerobic digestion of slurry, which is also used for fertilisation (Marchaim, 1992), and can have a higher NH_4^+ content than the undigested slurry (Ciborowski, 2001), but a lower C content (Amon et al., 2006), which can result in lower N_2O emissions (Petersen, 1999; Chantigny et al., 2007). Both cattle slurry and slurry digestate can produce high gaseous N-related emissions when applied to the soil because of their high NH_4^+ content. Vinasse is an industrial organic residue, a by-product of sugar and ethanol production, and its application in the soil as fertiliser has also been shown to increase N_2O emissions relative to inorganic fertilisers (Carmo et al., 2013; Lourenço et al., 2019).

Nitrogen is an essential element for plants, being a component of chlorophyll, plant proteins, and DNA (FAO, 2006). Nitrogen constitutes the most determinant mineral element of crop yield obtained from the soil by plants (Allison, 1957; Wang and Li, 2019). Low fertiliser efficiency is one of the main problems associated with fertilisation, and especially N fertilisation. For example, while using N-fertilisers, losses from croplands can reach 37% in maize, 46% in wheat, and 56% in rice (Prasad and Hobbs, 2018). Globally, only 47% of the reactive N added into croplands with fertilisation is converted into harvest (Lassaletta et al., 2014). Liu et al. (2016) estimated that only 38% of total N applied was harvested (Figure 1), with over 30% of applied N lost with leaching and gaseous emissions, while other studies have proposed even lower values of harvested

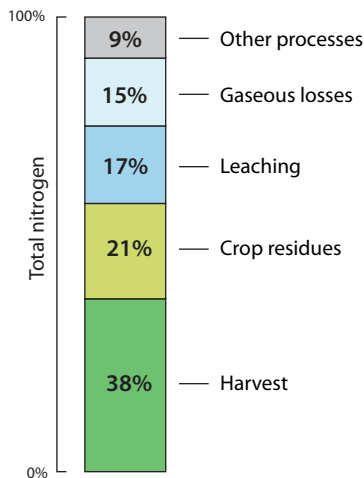


Figure 1. The fate of total nitrogen input applied with fertilisation (data from Liu et al., 2016).

N, such as only 33% (Raun and Johnson, 1999; Galloway and Cowling, 2002) and 50% when considering harvest and crop residue together (Galloway and Cowling, 2002). Similar values of apparent N recovery have been estimated by Lal and Stewart (2018) for cereals, with 63% for maize, 54% for wheat, and 44% for rice.

Nitrogen losses are often related to over-fertilisation (Weinbaum et al., 1992; Vilas et al., 2019), sometimes because of an overestimation of the potential crop yield (Thorburn and Wilkinson, 2013), but most commonly as a consequence of the lack of synchrony between N fertilisation and crop uptake (Crews and Peoples, 2005; Dahlin et al., 2005; Hansen et al., 2019; Vilas et al., 2019). Fertilisation can also result in possible nutrient imbalances as a consequence of excessive N addition (Bosch-Serra et al., 2020).

Fertilisation increases the soil NO_3^- concentration (Quan et al., 2016). This may occur directly from the NO_3^- added with the fertiliser, and indirectly through nitrification, the oxidation of NH_4^+ to NO_3^- . As NO_3^- is soluble, it may be easily lost from the soil through leaching (Cameron et al., 2013; Norton and Ouyang, 2019). The NO_3^- lost by leaching contaminates drinking water and leads to eutrophication of freshwater and marine ecosystems (Hansen et al., 2017). It has thus become one of the main threats to the Baltic Sea (HELCOM, 2009). Plants can absorb N in both NO_3^- and NH_4^+ forms (FAO, 1984); however, the low soil retention of NO_3^- (Bouchet et al., 2016) increases the chances of losses through leaching. Subsequently, reducing nitrification, decreases N losses due to leaching of NO_3^- beyond the reach of roots (Yu et al., 2017). In addition, NO_3^- can be transformed into N_2 through denitrification, or into N_2O if denitrification is incomplete, and lost to the atmosphere (Cameron et al., 2013; Vilas et al., 2019). Reducing nitrification will also indirectly reduce the denitrification rate as there is no additional source of NO_3^- , the main substrate for denitrification. However, NH_4^+ can be transformed into ammonia (NH_3) and also lost through gaseous emissions (Velthof et al., 2012). Deposition of NH_3 can cause soil acidification and eutrophication of rivers and lakes, and it is also a source of indirect N_2O emissions (Lam et al., 2017). The volatilisation of NH_3 also negatively affects human health, acting as a precursor for the formation of secondary aerosols (Sanz-Cobena et al., 2014; Herr et al., 2020).

2.2. Soil N₂O emissions

Nitrous oxide is a powerful GHG, with a global warming potential of 273 (IPCC, 2021), and a major ozone-depleting substance (Ravishankara et al., 2009). Agriculture is the main anthropogenic source of N₂O (Reay et al., 2012) and the two main processes involved in N₂O emissions from the soil are nitrification and denitrification (Firestone and Davidson, 1989; Parton et al., 1996; Bremner, 1997; Braker, 2011), although considerable emissions have also been attributed to nitrifier denitrification under certain conditions, such as low O₂ content (Wrage et al., 2001; Zhu et al., 2013; Wrage-Mönnig et al., 2018). Nitrification is the aerobic oxidation of NH₃ or NH₄⁺ into NO₃⁻, a process that can be divided into two steps: the oxidation of NH₄⁺ into NO₂⁻, with hydroxylamine as an intermediate product; and the oxidation of NO₂⁻ to NO₃⁻ (Figure 2). Denitrification is the anaerobic reduction of NO₃⁻ to N₂, with NO₂⁻, NO, and N₂O as intermediate products (Figure 2). In nitrifier denitrification, NO₂⁻ is reduced to NO without intermediate oxidation to NO₃⁻.

The key factors regulating nitrification and denitrification in soils are soil water content, temperature and pH, soil NH₄⁺ and NO₃⁻ contents, and C availability (Parton et al., 1996; Bremner, 1997; Mosier et al., 1998;

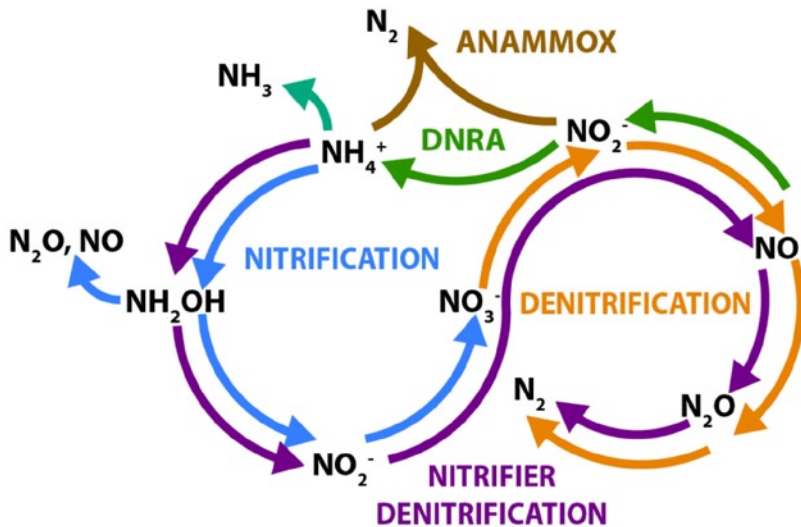


Figure 2. The main processes involved in the production of N₂O and other relevant N-gases in soil (Giles et al., 2012; Levy-Booth et al., 2014).

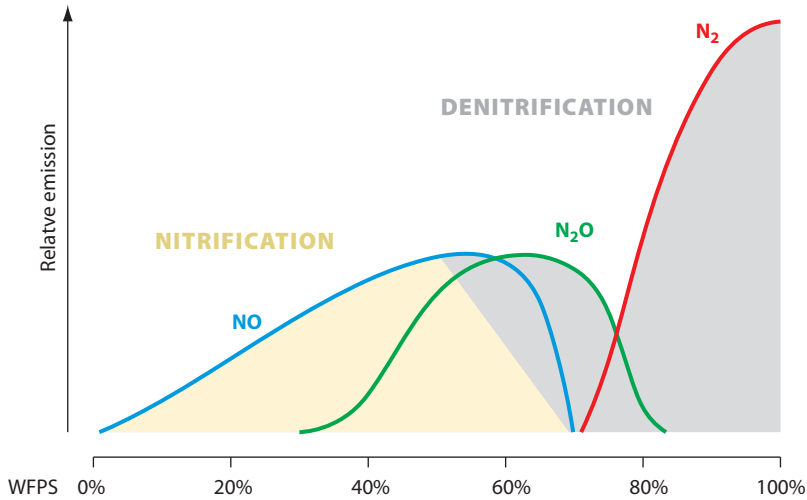


Figure 3. Water-filled pore space (WFPS) and the role of nitrification and denitrification in NO, N₂O, and N₂ production (adapted from Davidson, 1991; Davidson et al., 2000).

Dobbie and Smith, 2003). Soil moisture, presented as water-filled pore space (WFPS), which also considers soil porosity, is a useful indirect measure of oxygen (O₂) availability. As nitrification is an aerobic process and denitrification is anaerobic, the importance of each of these processes is directly controlled by O₂ availability in the soil. Consequently, WFPS is usually used to estimate the prevalence of nitrification or denitrification (Bouwman, 1996; Ruser et al., 2006) Figure 3). Nitrification is thought to be predominant at WFPS below 50% and denitrification at WFPS values above 70%, with both processes coexisting between 50% and 70% WFPS (Figure 3). The optimum WFPS for N₂O generation lies between 30% and 90% because nitric oxide (NO) is generated at WFPS below 30%, whereas N₂ gas is produced at WFPS above 90% (Focht, 1978; Ussiri and Lal, 2013).

2.3. Soil N₂O emissions mitigation strategies in agriculture

Emissions of GHG can be directly reduced through the use of agrotechnologies that increase the efficiency in the management of C and N inputs in agricultural ecosystems. Strategies to improve N fertilisation efficiency and reduce N losses while maintaining the yield include:

plant improvement, soil analyses to characterise field needs, precision application, use of slow-release fertilisers, use of urease inhibitors or nitrification inhibitors, improved synchronisation between application and plant demand, reduced or no-tillage, implementation of crop rotation, use of cover crops, precise irrigation, use of deep-root crops, crop residue incorporation, improved organic amendment application, extensification, change of land use (e.g., arable land to grassland or woodland), and switching from annual to perennial crops (Mosier et al., 1998; Smith, 2004; Smith et al., 2008; Horowitz and Gottlieb, 2010; Byrne et al., 2020).

2.3.1. Nitrification inhibitors

Enhanced efficiency fertilisers (EEFs) are fertilisers developed to achieve a better synchronisation between supply of N and crop demand, reducing the risk of N losses, and thereby improving N use efficiency (NUE) in crop production systems (Li et al., 2018; Vilas et al., 2019). EEFs can act through two different mechanisms: slowing down the release of N into soils, and stabilising N in the soil in a form that is less susceptible to losses (Vilas et al., 2019). Nitrification inhibitors (NIs) are an example of the second strategy.

Nitrification inhibitors have been proposed as a tool to reduce N losses from agriculture after fertilisation (Alexander, 1965; Ruser and Schulz, 2015) and after crop residues incorporation (Chaves et al., 2005; Duan et al., 2017), by inhibiting the first step of the nitrification process. By slowing down nitrification, NIs stabilise N in the soil in the form of NH_4^+ , which can be then gradually absorbed by plants (Di and Cameron, 2016). By reducing the production of NO_3^- , which is much more soluble and prone to leaching than NH_4^+ , NIs can also reduce N losses through leaching (Abalos et al., 2022a).

Of all commercially available NIs, 3,4-dimethylpyrazole phosphate (DMPP) has received increasing attention in recent years. This is because it has been reported to be very effective in inhibiting the activity of ammonia-oxidising bacteria (AOB), and increasing NUE and crop yield, whilst showing lower toxicity than other NIs and no negative effects on non-target soil microorganisms (Yang et al., 2016; Kong et al., 2018). DMPP slows down the activity of AOB (Corrochano-Monsalve et al., 2021a) and specifically of the genus *Nitrosomonas* spp. (Zerulla et al., 2001; Guillaumes and Villar, 2004; Trenkel, 2010; Corrochano-Monsalve et al.,

2021b). The mechanism is assumed to be chelation of the copper involved in NH_4 oxidation (Corrochano-Monsalve et al., 2021a). The effectiveness of NIs, and specifically of DMPP, has been widely reported in the literature (Di and Cameron, 2011; Menéndez et al., 2012; Di and Cameron, 2016; Gilsanz et al., 2016; Barrena et al., 2017; Duan et al., 2017; Yin et al., 2017). A meta-analysis by Yang et al. (2016) established an average reduction of N_2O emissions of 47.6% for DMPP, compared with 44.7% for dicyandiamide (DCD), another popular NI.

2.3.2. Biochar

Biochar is a C-rich material produced from organic matter by heating under low O_2 conditions (pyrolysis) (Lehmann and Joseph, 2009; Sohi, 2012). It has been proposed as an amendment that can improve soil conditions and increase crop yield, but also reduce N losses through N_2O emissions into the atmosphere and NO_3^- leaching (Borchard et al., 2019). Biochar is a specific type of organic amendment, as the main purpose of its application is to improve soil physical properties and modify the pH, and the addition of nutrients is only a secondary objective.

Biochar has been proposed as a possible negative emissions technology (NET; Smith et al. (2015); Smith (2016); Frank et al. (2017)), an anthropogenic activity that deliberately extracts CO_2 from the atmosphere (Fuss et al., 2016). Biochar has also been proposed as a tool for the mitigation of N_2O emissions. Several meta-analyses have shown average reductions of N_2O emissions after biochar application, compared with a non-amended control, of between 12% and 54% (Cayuela et al., 2014; Verhoeven et al., 2017; Liu et al., 2018; Borchard et al., 2019), but some studies have found no effect (Scheer et al., 2011; Suddick and Six, 2013; Rittl et al., 2018; Buchkina et al., 2019), or even an increase in emissions after biochar application (Zwieten et al., 2009; Clough et al., 2010; Verhoeven and Six, 2014).

The mechanisms by which biochar amendment reduces N_2O emissions are not completely clear (Verhoeven and Six, 2014; Wang et al., 2015), and several different hypotheses have been proposed:

- NO_3^- immobilisation (Borchard et al., 2019);
- reduction of organic matter degradation and soil C mineralisation, which increases with higher biochar production temperatures (Christel et al., 2016). The availability of biochar to sequester C, reducing available labile C, also affects the denitrification rate;

- alteration of the microbial denitrifying communities (Wang et al., 2013; Krause et al., 2018), including the increase in abundance of N_2O reductase bacteria, resulting in a reduced $N_2O:N_2$ ratio (Harter et al., 2014). This has been attributed to the increase of soil pH after biochar application (Hüppi et al., 2015; Obia et al., 2015). Cayuela et al. (2013) proposed that biochar also facilitated the transfer of electrons to soil denitrifying microorganisms.

Increased N_2O emissions, after biochar addition, have generally been attributed to increased nitrification, as biochar addition generally increases populations of soil ammonia-oxidising microbes, increasing the nitrification rate (Nelissen et al., 2012; Prommer et al., 2014; Sánchez-García et al., 2014), although the opposite effect has also been reported (Wang et al., 2015).

2.3.3. Crop residue management

Most of the plant biomass produced annually by agriculture is found in crop residues (Smil, 1999). Of their total mass, straw and other residues generally contain around 40% C, but also 0.7% N, 0.1% P, and 1.3% K (Lal, 2009b). Crop residue management allows the modification of soil properties, both physical and chemical, and biological functions (Blanco-Canqui and Lal, 2009; Sarkar et al., 2020). Incorporation of the plant residues improves several soil characteristics such as soil organic matter, cation exchange capacity, water-holding capacity, and fertility; reduces soil erosion (Mosier et al., 1998; Lal, 2009a; Jordán et al., 2010); and also improves soil conditions for earthworms (Bhattacharya et al., 2017). Conversely, removal of crop residue, such as for biofuel production, can have a negative effect on the soil and environment quality (Blanco-Canqui and Lal, 2009). Furthermore, the burning of crop-residues remains common in many agroecosystems (Smil, 1999; Mathur and Srivastava, 2018), as it constitutes a simple and cheap alternative to residue removal. Nevertheless, burning of crop-residues results in a loss of nutrients since they are no longer incorporated into the soil. Burning of crop residue also produces emissions of GHG and other air pollutants (e.g., particulate matter, NO_x , and NH_3), with negative environmental, health, and economic consequences (Smil, 1999; Mathur and Srivastava, 2018; Chen et al., 2019).

Crop residue incorporation can also promote GHG emissions, as it constitutes an addition of C and N into the soil, which in turn stimulates microbial activity and even promotes oxidation and denitrification,

alongside the decomposition of SOC (Badagliacca et al., 2017). Soil N₂O emissions after incorporation of plant residues depend on the N mineralisation rate (Duan et al., 2018). The crop residue mineralisation rate is conditioned by different environmental factors, such as soil temperature and moisture, soil properties, and the crop residue characteristics (Abalos et al., 2022b), but also agronomic practices (Smil, 1999; Badagliacca et al., 2017). The most commonly reported property of crop residue, predicting the mineralisation rate and N₂O emissions, is the C/N ratio (Baggs et al., 2000; Duan et al., 2018; Abalos et al., 2022a). The C/N ratio shapes the balance between net N mineralisation and immobilisation (Abalos et al., 2022a). Thus, the C/N ratio determines N₂O emissions, with higher emissions being measured after the incorporation of low-C/N-ratio residues and lower N₂O emissions being measured after the incorporation of high-C/N-ratio residues (Baggs et al., 2000; Badagliacca et al., 2017).

3. HYPOTHESES AND AIMS OF THE STUDY

The main aim of this PhD thesis is to contribute to the understanding of the mechanisms behind N₂O emissions, and to provide the first data of N₂O emissions from arable soils in Estonia, focusing especially on novel potential mitigation strategies in agriculture, and specifically after organic matter incorporation.

The specific aims of the thesis are as follows:

1. to study the mitigation potential of N₂O emissions of two proposed tools: biochar (**I**) and nitrification inhibitor (**III**);
2. to quantify potential N₂O emissions from the incorporation of different crop residues into the soil (**II**);
3. to analyse soil N₂O emissions during an entire growing season in a winter rapeseed field (**IV**).

To achieve the aims mentioned above, the following hypotheses were assessed:

1. soil amendment with biochar reduces N₂O emissions from soil and the mitigation effect varies with the biochar production temperature (**I**);
2. fresh rapeseed and rye residues, and wheat straw incorporation in the soil results in different N₂O emissions, depending on their C/N ratio (**II**);
3. the addition of DMPP to slurry prior to application reduces N₂O emissions from soil (**III**);
4. fertiliser (both organic and inorganic) application during a full winter rapeseed growing season will result in peaks of N₂O emissions (**IV**).

4. MATERIAL AND METHODS

4.1. Experimental sites and set-up

Three experiments were conducted from 2016 to 2020 under lab and field conditions (Table 1) to study the soil N₂O emissions after the application of different amendments:

- Experiment 1 (**I**), hereafter ‘biochar experiment’.
A pot experiment involving the application of three different organic fertilisers and three biochars produced at different production temperatures under controlled conditions.
- Experiment 2 (**II**), hereafter ‘crop residue experiment’.
A pot experiment involving the incorporation of three different types of crop residues under controlled conditions.
- Experiment 3 (**III, IV**), hereafter ‘nitrification inhibitor experiment’.
A field experiment involving the application of slurry and a nitrification inhibitor in a winter rapeseed field in Central Estonia.

Table 1. Overview of the conducted experiments

Paper	Experi- ment	Year	Type	Location	Amendment*	Crop
I	1	2017	Pot experi- ment	Estonian University of Life Sciences, Tartu, Estonia	Organic ferti- lisers (3), biochars (3)	Ryegrass (<i>Lolium perenne</i> L.)
II	2	2019	Pot experi- ment	Estonian University of Life Sciences, Tartu, Estonia	Crop residues (3)	–
III	3	2016	Field experi- ment	Kehtna Parish, Rapla County, Estonia (58°55′21″N, 24°50′52″E)	Organic ferti- liser (1), nitrifi- cation inhibitor (1)	Winter rapeseed (<i>Brassica napus</i>)
IV	3	2016– 2017	Field experi- ment	Kehtna Parish, Rapla County, Estonia (58°55′21″N, 24°50′52″E)	Organic ferti- liser (1), nitrifi- cation inhibitor (1)	Winter rapeseed (<i>Brassica napus</i>)

* In parenthesis, the number of different treatments

Table 2. Characteristics of the soils used in the different experiments

Experiment	Soil classification*	Soil type	pH _{KCl}	C N		P	K	Ca	Mg
				g kg ⁻¹					
1 (I)	Dystric Endostagnic Glossic Retisol	Sandy loam	4.46	12.4	0.7	210	710	530	1480
2 (II)	Albic Stagnic Luvisol	Sandy loam	5.70	14.8	1.2	300	270	1910	430
3 (III, IV)	Gleysol	Sandy loam	4.75	64.5	6.3	50	120	2320	330

* WRB, 2015

Characteristics of the soils used in these three experiments are presented in Table 2. In the lab experiments (I, II), three random samples of soil were used for analysis. In the field experiment (III, IV), three separate soil samples were collected for both plots next to the chambers, with the aid of a soil probe, initially every two days, with decreasing frequency thereafter, to monitor the evolution of the soil C and N content. Soil sampling in the field experiment was limited by soil freezing and waterlogging of the study sites. The corresponding manuscripts (I, II, III, and IV) include a detailed description of the soil, leachate, and slurry analysis methodologies.

4.1.1. Organic fertilisers (I, III, IV)

Three different organic fertilisers were applied to the soil in the biochar and nitrification inhibitor experiments: cattle slurry, slurry digestate, and vinasse. Cattle slurry was applied in the biochar and the nitrification inhibitor experiment, whereas slurry digestate and vinasse were applied only in the biochar experiment. In both experiments, fertiliser was applied before sowing. The cattle slurries and the slurry digestate had very similar application rates (27.4–30 t ha⁻¹), whereas vinasse was applied at a much lower rate (1.8 t ha⁻¹) as it had higher dry matter and NH₄⁺ contents (Table 3). Vinasse was also characterised by lower pH than the other organic fertilisers and a higher K content. The cattle slurry used in the nitrification inhibitor experiment (III, IV) had a much higher N content in NH₄⁺ content (0.613%) than the organic fertilisers used in the nitrification inhibitor experiment (0.214%–0.270%).

Table 3. Chemical properties of the organic fertilisers applied in the experiments

	Cattle Slurry 1 (I)	Cattle Slurry 2 (III, IV)	Slurry Digestate (I)	Vinasse (I)
Application rate (t ha ⁻¹)	27.4	30	27.4	1.8
Dry Matter (%)	10.7	7.9	7.1	67.0
pH _{KCl}	7.5	8.02	7.9	4.5
NH ₄ ⁺ -N (%) ¹	0.214	0.613	0.257	0.27
NO ₃ ⁻ -N (%) ¹	<md	<md	<md	<md
P (%) ²	0.112	0.96	0.102	0.101
K (%) ²	0.362	2.37	0.302	13.25
Ca (%) ²	0.182	1.42	0.162	2.061
Mg (%) ²	0.066	0.59	0.041	0.161

¹: content in fresh matter

²: content in dry matter

md: minimum detectable concentration

4.1.2. Biochar experiment (I)

A lab experiment was carried out to test the effectiveness of biochar produced under various different temperatures in reducing soil N₂O emissions in unamended soil and after the application of three different organic fertilisers (cattle slurry, slurry digestate, and vinasse). The rate of application of the organic fertilisers was 27.4 t ha⁻¹ for cattle slurry and slurry digestate, and 1.8 t ha⁻¹ for vinasse (I, Table 1). The difference in application rate was a consequence of the higher dry matter and NH₄⁺ content in vinasse. The chemical properties of the organic fertilisers applied in the experiment are presented in Table 3.

Biochar was produced via different procedures and at various temperatures as follows: torrefaction at 300°C (BC300), torrefaction at 300°C followed by pyrolysis at 550°C (BC550), and torrefaction at 300°C followed by pyrolysis at 850°C (BC850). In all treatments, biochar was mixed into the soil at a common rate of 915.8 g m⁻². The pH of the different biochars was 6.8, 10.8, and 11.8 for BC300, BC550, and BC850, respectively, while the C/N ratio was 19.0, 22.6, and 26.6 for BC300, BC550, and BC850, respectively (I, Table 2).

The treatments included the three organic fertilisers and the three different biochars mixed into the soil alone or in combination. A list of detailed treatments can be found in manuscript I (Table 1). Four rep-

lications were used for all treatments. The pots used in the experiment, made from PVC and with a volume of 2.4 L, were filled in two different layers: a lower layer (depth between 10 and 27 cm) of 2000 g of air-dry soil, and an upper layer (depth between 0 and 10 cm) where 1200 g of soil was mixed with biochar and/or the organic fertiliser depending on the treatment (I, Table 1).

4.1.3. Crop residue experiment (II)

Three different plant residues were used to assess the effect on soil N₂O emissions arising from the incorporation of different crop residues into the soil: oilseed rape stems and leaves, wheat straw, and rye stems and leaves. The experiment consisted of soil without any amendment and soil incorporating each of the different crop residues separately. Three replications were used for each treatment. The dry matter and total C and N contents of the collected plant materials were measured to characterise the different crop residues (II, Table 2). The different plant residues were incorporated into the soil at a common rate of 6 g C kg⁻¹ of soil (equivalent to 10.6 t C ha⁻¹) after chopping the crop residue into 4-cm-long fragments.

The pots used in this experiment had a volume of 4 L, and 3000 g of soil was incorporated into each pot in total. The pots were incubated for 105 days at 23°C and were watered on Days 1, 11, 26, 46, and 75 (taking Day 0 as the day of residue incorporation).

4.1.4. Nitrification inhibitor (III, IV)

The effectiveness of the DMPP in reducing N₂O emissions after the addition of dairy slurry (Cattle Slurry 2) was tested in a field experiment in Central Estonia (Kehtna, Raplamaa, 58°55′21″N, 24°50′52″E). The 18.13 ha study field was divided into two plots (control and treatment) depending on the local drainage system. This division allowed the collection of representative leaching samples from both plots separately. Winter rapeseed (*Brassica napus* ‘DK Sequoia’) was sown in both plots on August 10, 2016 and harvested on August 26, 2017. On August 6, 2016, a dairy slurry was applied to the field at a rate of 30 t ha⁻¹ via injection, followed by a rotary harrow. On the control plot, the slurry was applied alone, whereas on the treatment plot, the slurry was mixed with DMPP, at a rate of 3 L ha⁻¹. During the growing season, mineral fertilisation was applied

on three occasions in 2017: April 4, 250 kg ha⁻¹ of calcium ammonium nitrate (CAN) 27; May 1, 160 kg ha⁻¹ of ammonium sulphate nitrate (ASN) 26N+13S; and May 8, 160 kg ha⁻¹ of ASN 26N+13S.

Manuscript **III** describes the N₂O emissions during the initial 50 days; this period was chosen to cover both the higher emissions resulting from slurry application and also the expected effect of DMPP. Manuscript **IV** presents the soil N₂O fluxes during from the whole growing season of winter rapeseed.

4.2. Nitrous oxide flux measurements and analyses (I, II, III, IV)

Trace gas flux measurements were carried out in the lab and field experiments with the closed chamber method (Hutchinson and Livingston, 1993; Mander et al., 2015). Opaque PVC chambers, but with different chamber designs and dimensions, were used for the gas measurement in the three experiments. The volumes of the chambers used in the lab were 2.85 L (**I**) and 2.4 L (**II**), and the volume of the chamber used in the field (**II**, **III**) was 65.5 L. In all cases, gas samples for trace gas measurement were collected during an hour at 20-min intervals (0, 20, 40, and 60 min) into 20-ml pre-evacuated (0.04 mbar) bottles.

Three chambers were used as replications in the lab experiments for each treatment (**I**, **II**). Five chambers were used in the field experiment as replications for each plot (**III**, **IV**). Collars were installed in the soil at the field experiment 24 hours before the first measurement, to avoid soil disruption influencing the measurements. Trace gas fluxes were measured from August 5, 2016 until August 22, 2017, and were carried out at a 2–3 day interval during the first two weeks after the application of the slurry, and then with decreasing frequency until reaching a weekly frequency, which was maintained for the rest of the period.

In all cases, the soil N₂O flux was calculated from the slope of the least-squares linear regression of the N₂O concentrations versus time (dC/dt), using the following equation (Livingston and Hutchinson, 1995):

$$f = \frac{dC}{dt} \cdot \frac{V}{A} \quad (\text{Eq. 1})$$

where f is the N₂O flux (ppm[v] s⁻¹); dC/dt is the change of concentration (slope) in a period of time t ; C is the concentration in the chamber head-space (ppm[v]); t is time (s); V is the volume (m³); and A is the surface (m²) covered by the chamber.

The resulting measurements were filtered according to the adjusted R^2 values of the linear regression, as described in the manuscripts. Cumulative fluxes were calculated by integration of total daily fluxes (time-integration) over the whole period, after linear interpolation between sampling points (Vinzent et al., 2018).

The emission factors (EF) were calculated as the unit of N emitted in N_2O emissions per unit of applied N (Smith et al., 1999) with the organic fertilisers (**I**, **III**, **IV**) or crop residue (**II**).

A common period of six weeks (42 days) was chosen to compare N_2O fluxes between experiments, being the duration of the shortest experiment (**I**). This period is considered to include the effect of slurry application (Lessard et al., 1996; Mosier, 1998; Dobbie and Smith, 2003) and also the DMPP mitigation effect (Villar and Guillaumes, 2010).

4.3. Environmental parameter measurements (**II**, **III**, **IV**)

Climatic and field data were used to characterise the state of the field during the emissions. Hourly climatic data (air pressure, precipitation, relative humidity, sunshine duration, air temperature at different heights, ground temperature, visibility before observation, and wind speed and direction) for the field experiment (**III**, **IV**) were obtained from the Kuusiku weather station (Estonian Weather Service, WMO code 26134, 58°58'23.3"N 24°44'02.4"E), located approximately 11 km from the experimental field.

In the field experiment (**III**, **IV**), soil temperature was measured at four different depths (5, 10, 20, and 30 cm) with a four-channel temperature data logger S0141 together with four PT1000 sensors (COMET SYSTEM, Rožnov pod Radhoštěm, Czech Republic). For the crop residue and the field experiments (**II**, **III**, **IV**), soil moisture and electrical conductivity were measured with a GS3 sensor connected to a ProCheck handheld reader (Decagon Devices, Pullman, WA, USA), for each plot. Field parameters were measured on each GHG flux measurement day in both experiments.

The WFPS was calculated using the following equation (Linn and Doran, 1984; Oo et al., 2018):

$$WFPS (\%) = 100 \cdot \frac{VWC}{TP} \quad (\text{Eq. 2})$$

where *VWC* is the volumetric water content ($\text{m}^3 \text{m}^{-3}$) and *TP* is total porosity (%). Linear interpolation was used to estimate missing data for field parameters and the soil and leachate data (Øygarden and Botterweg, 1998; Kersebaum et al., 2004) used for the correlation analysis.

4.4. Statistical analyses

All statistical analyses were carried out using the R programming language (R Core Team, 2016). The normality of the data was tested using the Shapiro–Wilk test. When transformation of non-normally distributed data was not sufficient, non-parametric tests were used. Analysis of variance (ANOVA), followed by a post-hoc Tukey HSD was used for pairwise comparisons (**I**, **II**) when there were more than two treatments, and the Mann–Whitney U test (Wilcoxon–Mann–Whitney test) was used when there were only two treatments (**III**, **IV**). The Spearman’s rank correlation coefficient (ρ) was used to analyse correlations between GHG fluxes and other parameters (soil and leachate chemical parameters and environmental data). Statistical differences were considered significant at a level of $p < 0.05$. All results are presented as mean and standard error.

5. RESULTS

5.1. Nitrous oxide fluxes

The highest mean soil N₂O fluxes among the three experiments for the initial 42-day period were measured after incorporation of rye and rape-seed plant residues (2580 ± 148 and 1956 ± 82 $\mu\text{g N m}^{-2} \text{h}^{-1}$, respectively; Table 4), followed by cattle slurry application in the field experiment (1180 ± 75 and 1701 ± 93 $\mu\text{g N m}^{-2} \text{h}^{-1}$, for control and treatment plots). Similar maximum values were reached for both the plant residues and field experiments (6514 $\mu\text{g N m}^{-2} \text{h}^{-1}$ for the treatment plot in the field experiment and 6039 $\mu\text{g N m}^{-2} \text{h}^{-1}$ for incorporation of rye residues). The maximum values were reached for all experiments during the first 42 days.

The highest mean and maximum soil N₂O flux values in the biochar experiment, after addition of the three organic fertilisers and/or biochar, were much lower than those measured in the two other experiments (26 ± 3.8 and 173 $\mu\text{g N m}^{-2} \text{h}^{-1}$).

5.2. Biochar and organic fertiliser experiment (I)

Organic fertiliser addition to soil increased N₂O emissions (I, Figure 2), an increase measured almost exclusively during the first two weeks after slurry application (I, Figure 4), but no significant differences were found among the different organic fertilisers. The average N₂O flux from the soil mixed with organic fertilisers ranged between 4.33 ± 1.11 and 7.52 ± 1.32 $\mu\text{g N m}^{-2} \text{h}^{-1}$, whereas the flux from the soil without amendment (control) was slightly negative (-1.27 ± 0.62 $\mu\text{g N m}^{-2} \text{h}^{-1}$).

The addition of biochar into the soil increased soil N₂O flux values, although only the highest production temperature (BC850) showed fluxes that were significantly higher than control (I, Figure 3). Among all treatments, the highest soil N₂O flux peak was observed in the BC850+SD treatment (173.35 $\mu\text{g N m}^{-2} \text{h}^{-1}$), followed by BC550+SD (93.03 $\mu\text{g N m}^{-2} \text{h}^{-1}$) and BC850+VN (79.99 $\mu\text{g N m}^{-2} \text{h}^{-1}$).

The highest cumulative fluxes were measured in the three treatments in which BC850 was applied in combination with organic fertilisation (16.12 ± 2.93 to 24.89 ± 3.56 mg N m^{-2}). Cumulative N₂O emissions during the experiment were related to the release of both C and N from the biochar during the observation period (I, Figure 5).

Table 4. Soil N₂O fluxes ($\mu\text{g N m}^{-2} \text{h}^{-1}$) for all the treatments in the three experiments. S: Soil. BC300: biochar produced by torrefaction at 300°C; BC550: biochar produced by torrefaction at 300°C, followed by pyrolysis at 550°C; and BC850: biochar produced by torrefaction at 300°C, followed by pyrolysis at 850°C. Slurry: cattle slurry; and Digestate: slurry digestate.

Experiment	Treatment	Mean \pm SE soil	Maximum N ₂ O
		N ₂ O flux for the initial 42 days	flux during the experiment
		$\mu\text{g N m}^{-2} \text{h}^{-1}$	
1 (I)	S	-1.3 \pm 0.6	10
	S+BC300	1.1 \pm 0.6	14
	S+BC300+Slurry	7.2 \pm 1.3	42
	S+BC300+Digestate	15 \pm 1.7	57
	S+BC300+Vinasse	10 \pm 1.1	39
	S+BC550	1.9 \pm 1.0	36
	S+BC550+Slurry	9.1 \pm 1.8	65
	S+BC550+Digestate	14 \pm 2.3	93
	S+BC550+Vinasse	7.7 \pm 1.0	36
	S+BC850	8.0 \pm 1.3	56
	S+BC850+Slurry	17 \pm 2.6	78
	S+BC850+Digestate	26 \pm 3.8	173
	S+BC850+Vinasse	17 \pm 2.3	80
	S+CS	4.3 \pm 1.1	34
	S+SD	7.5 \pm 1.3	40
S+VN	5.5 \pm 1.4	48	
2 (II)	Control	26 \pm 1.8	105
	Rapeseed	1956 \pm 82	3346
	Rye	2580 \pm 148	6039
	Wheat	269 \pm 3.1	185
3 (III, IV)	Control	1180 \pm 75	6433
	DMPP	1701 \pm 93	6514

In several treatments, soil N₂O fluxes became negative after the initial peak of emissions following slurry and/or biochar application (I, Figure 4). This resulted in lower mean and cumulative fluxes over 42 days (results presented here) compared with the initial 20 days (I, Figure 1). This is especially important for the soil-only treatment, as it resulted in negative cumulative emissions.

5.3. Crop residue experiment (II)

Soil N₂O fluxes were significantly higher following rapeseed and rye plant residue incorporation compared with that of control and wheat straw, but there was no significant difference between them (911.70 ± 59.97 and $1087.95 \pm 91,83 \mu\text{g N m}^{-2} \text{ h}^{-1}$, respectively; **II**, Figure 3). The highest flux was measured for rye ($6039 \mu\text{g N m}^{-2} \text{ h}^{-1}$), followed by rapeseed ($3346 \mu\text{g N m}^{-2} \text{ h}^{-1}$). The N₂O fluxes were not significantly different between the control and the wheat straw treatment (14.02 ± 0.94 and $11.80 \pm 1.42 \mu\text{g N m}^{-2} \text{ h}^{-1}$, respectively). Cumulative emissions followed the same pattern.

Soil N₂O emissions were positively correlated with soil moisture ($\rho = 0.30$, $p < 0.001$), while no significant correlation was observed between soil temperature and N₂O ($p > 0.05$). The N₂O fluxes were also positively correlated with both soil total C and total N ($\rho = 0.43$, $p < 0.001$; $\rho = 0.44$, $p < 0.001$). Soil N₂O fluxes were positively correlated with plant total N content ($\rho = 0.95$, $p < 0.001$) and negatively correlated with plant residues total C content ($\rho = -0.94$, $p < 0.001$).

The N₂O emission factors (EF) for the crop residue application during the 42 days of duration of the experiment were 0.11 for rapeseed, 0.01 for wheat, and 0.15 kg N₂O-N per kg N applied for rye.

5.4. Field experiment with cattle slurry and nitrification inhibitor application (III, IV)

The N₂O emissions were negligible through the full period, except during the initial high peaks of emissions, immediately after the application of the slurry, with more than half of the N₂O fluxes being recorded in the first 50 days after slurry application (**III**, Figure 2), and during two smaller peaks in December 2016 and March-April 2017 (**IV**, Figure 1). The average N₂O fluxes for the first 42 days were 1180.11 ± 75.44 and $1700.75 \pm 93.03 \mu\text{g N m}^{-2} \text{ h}^{-1}$ for the control and treatment plots, respectively, while the average N₂O fluxes for the duration of the whole experiment were 244.49 ± 12.36 and $335.59 \pm 16.50 \mu\text{g N m}^{-2} \text{ h}^{-1}$. The maximum peaks of measured fluxes were 6433 for the control and 6514 $\mu\text{g N m}^{-2} \text{ h}^{-1}$ for the treatment plots.

The final cumulative flux for the whole period was 2200 ± 244 and 3029 ± 298 mg N m⁻² for control and treatment plots, respectively, with 53.64% and 56.12% of N₂O emissions occurring during the first 42 days.

The EF for the slurry application after 50 days considered in manuscript **III** were 0.19 and 0.27 kg N₂O-N per kg N applied for the control and treatment plots, and 0.10 and 0.14 kg N₂O-N per kg N applied at the end of the growing season (one year).

6. DISCUSSION

According to the previous studies summarised in the literature review, NIs and biochar are effective tools for reducing soil N₂O emissions from agriculture, but our results show that this mitigation effect is not universal. The environmental conditions during the application of the amendments (in the case of the NI) or the characteristics of the amendments (in the case of biochar) can hamper their mitigation potential and even result in enhanced emissions.

The results from the field and lab experiments confirmed that peaks of soil N₂O emissions follow slurry application (**I**, **III**, **IV**). In the field experiment, approximately 55% of the total N₂O emissions during the full growing season occurred in the first 42 days after slurry application (**III**, **IV**). No significant differences were observed among the different organic fertilisers used in the biochar experiment (**I**, Figure 2); however, anaerobic digestion of slurry resulted in slightly, but not significantly, higher values of soil N₂O emissions after application. The high soil N₂O emissions that followed slurry application, reaching almost 6 mg m⁻² h⁻¹ in the NI experiment both highlight the need for mitigation measures and suggest strong possibilities for mitigation during or after organic fertiliser application (Myrgiotis et al., 2019). This underlines the need for the mitigation options discussed in the literature review section, and specifically biochar and nitrification inhibitors. However, neither the application of biochar (**I**) nor that of the nitrification inhibitor (**II**) reduced N₂O emissions in our experiments, in fact, higher emissions than in the unamended control were recorded.

After slurry application, the average N₂O fluxes for the NI experiment (**III**) in the first 42 days after slurry application were more than 100-times higher than those in the biochar experiment (**I**) in the same period. Several factors can explain this difference. First, and probably the most important, is a difference in NH₄⁺ content in the applied slurry in the biochar and NI experiments (0.214% and 0.613%, respectively). This is especially relevant considering that the response of N₂O emissions to N input with fertilisation is exponential rather than linear (Shcherbak et al., 2014; Walter et al., 2014; Scheer et al., 2016; Ni et al., 2021). The lower slurry application rate in the biochar experiment than in the NI experiment (27.4 and 30 t ha⁻¹), could have been partially compensated by the slightly higher DM content of the slurry used in the biochars experiment.

The differences in C and N contents in the soils of the biochars and the NI experiments also contributed to these differences. Soil C content was 12.4 g kg^{-1} for the biochar experiment and 64.5 g kg^{-1} for the NI experiment, while soil N content was 0.7 g kg^{-1} for the biochar experiment and 6.3 g kg^{-1} for the field experiment. The C/N ratio was also higher in the soil of the biochar experiment (17.7 and 10.2 for the pot and NI experiment, respectively), resulting in lower mineralisation and higher N immobilisation rates (Flavel and Murphy, 2006; Quan et al., 2016). Lower soil C/N ratio, means that N can be more easily utilised by nitrifiers and denitrifiers, resulting in higher N_2O emissions (Feng and Zhu, 2017). In fact, the C/N ratio can be used as a scalar parameter to predict N_2O emissions (Klemmedtsson et al., 2005). In the nitrification inhibitor experiment, decomposition of the crop residues from the previous season provided an additional source of labile C (Saggar et al., 2013). Finally, in the field experiment, re-wetting of the soil by precipitation after a dry period occurred simultaneously with the manure application (III, Figure 2). It is known that rewetting after drought boosts mineralisation and denitrification (Guo et al., 2014), and that rainfall events usually produce immediate peaks in N_2O emissions (Flessa et al., 1995; Dobbie and Smith, 2003). These factors and their interaction could explain the difference in the measured values of N_2O flux after slurry application in the biochar and NI experiments.

Increased soil N_2O emissions after crop residue incorporation are common, especially for crop residue with a low C/N ratio (Chen et al., 2013; Li et al., 2021). However, the huge emissions measured after the incorporation of rapeseed and rye residues can only be attributed to a combination of factors, such as the effect of re-wetting of the soil, as in the case of the field nitrification inhibitor. Furthermore, the higher pH and the lower C/N ratio in the soil of the crop residues experiment compared with the soil used in the biochar experiment could partially explain the difference in the magnitude of the emissions.

6.1. N_2O emissions mitigation by biochar

Soil amendment with biochar did not reduce N_2O emissions but in fact resulted in higher emissions. Reduction of soil N_2O emissions after biochar application is generally attributed to a reduction in the denitrification rate (Cayuela et al., 2013), which has been explained by different mechanisms, most commonly by adsorption of NO_3^- and reduction

of available C. Conversely, increases in emissions of N_2O after biochar application are generally attributed to an increase in nitrification activity (Sánchez-García et al., 2014), due to the increase of pH after biochar application, and related to the above-mentioned sensitivity of nitrifier bacteria to low pH. This is likely to be most relevant in acid soils such as the one used in this experiment (Borchard et al., 2019).

The high N content and low C/N values (I, Table 2) of the three different production temperature biochars could explain the absence of mitigating effect on N_2O emissions, with the C/N values located in the lower range of those reported in the literature (Borchard et al., 2019), even when considering exclusively biochar produced from herbaceous residues (Cayuela et al., 2014). Previous research has documented that N-rich biochars with low C/N ratios had no mitigation effect on N_2O emissions (Borchard et al., 2019), and a meta-analysis by Cayuela et al. (2014) found that biochars with a low C/N ratio (<30) did not reduce N_2O emissions. In contrast, those biochars characterised by low N content and higher C/N effectively reduce N_2O emissions (Liu et al., 2018; Borchard et al., 2019). Spokas and Reicosky (2009) found that biochars with high N content, high labile organic matter, and a low C/N ratio increased N_2O emissions. Clough et al. (2013) showed that biochar could increase N_2O emissions if several conditions are met: adequate soil moisture for denitrification, and large release of C and N from biochar. In our studied biochars, the significant relationship between released C and N and total N_2O emissions (I, Figure 5) supports the idea that the enhancing effect of biochar on N_2O emissions arises from the nutrient release, with the biggest release of C and N measured for BC850, which had the highest N_2O emissions (I, Figure 5). The higher release of nutrients measured for biochar with higher production temperature could be caused by the pH of the soil–biochar interface being closer to the optimal pH value for ammonification, thus increasing the mineralisation rate of biochar.

The increase of substrate and labile C availability from enhanced mineralisation would have promoted denitrification. However, emissions of N_2O from denitrification would be partly mitigated as the increase of pH should also favour the last step of denitrification (Cayuela et al., 2013; Borchard et al., 2019).

Soil N_2O fluxes became negative after an initial period of variable duration (between 16 and 30 days) of positive fluxes (emissions) following

the slurry and/or biochar application for several of the treatments (**I**, Figure 4). This resulted in lower values of cumulative fluxes for the period of 42 days than those that had been reported for the initial 20 days and were presented in manuscript **I** (Figure 1). These negative fluxes are most likely the result of the soil becoming a net sink of N_2O . Chapuis-Lardy et al. (2007) discussed the mechanisms that result in the soil acting as a sink: reduction of N_2O to N_2 , with absorption of N_2O in soil water, and subsequent reduction of N_2O . Many studies have linked low availability of soil mineral N with N_2O capture from the atmosphere (Chapuis-Lardy et al., 2007), which is in accordance with the low N content of the soil used in the biochar experiment.

6.2. N_2O emissions mitigation by nitrification inhibitors

The effectiveness of the studied nitrification inhibitor was undermined by the predominance of denitrification-originated N_2O emissions after slurry application (**II**), as a result of the high soil moisture content.

The WFPS is commonly used as a proxy of water content that determines the predominance of nitrification or denitrification. The WFPS values measured during the nitrification inhibitor experiment were between 50% and 90%. In this range of WFPS values, both nitrification and denitrification (50%–70%), or only denitrification (70%–90%) occurred, indicating that denitrification was the dominant process (**III**, Figure 3). Higher emissions were also correlated to higher WFPS values (**III**, Table S2).

Precipitation was a key factor controlling the N_2O flux during the experiment: an intense precipitation period, especially when compared with pre-experiment conditions, started on the same day as the application of the slurry and DMPP, and altered soil moisture conditions. The effectiveness of NIs is known to be conditioned by soil moisture, rainfall, soil pH, and soil temperature (Di et al., 2014; Barrera et al., 2017). Soil moisture determines the availability of O_2 , which is one of the key factors regulating nitrification and denitrification activity (Firestone and Davidson, 1989). Denitrification, which is enabled by anaerobic conditions, is not affected by the inhibitory effect of DMPP (Müller et al., 2002; Duan et al., 2017). Rainfall and soil water content are the main factors controlling N_2O emissions from denitrification (Ryden, 1983; Mori et al., 2010; Keil et al., 2015), and several studies have reported that denitrification is the main process responsible for N_2O emissions following rainfall events (Thorn-

ton et al., 1998; Cantarel et al., 2010; Herr et al., 2020). WFPS has been found to be the principal factor controlling denitrification when other factors, such as soil NO_3^- content and temperature, are not limiting (Loro et al., 1997; Dobbie and Smith, 2003). Other factors, such as the addition of labile C with the slurry (Lazcano et al., 2021), together with labile C from mineralisation of the crop residue of the previous year, would have enhanced denitrification activity (Beck and Christensen, 1987; Saggarr et al., 2013; Herr et al., 2020). Moreover, the low values of soil pH can also result in a decrease of the $\text{N}_2/\text{N}_2\text{O}$ ratio, because of the high sensitivity of nitrous oxide reductase to low pH (Simek and Cooper, 2002; McMillan et al., 2016; Hénault et al., 2019), promoting N_2O production.

To guarantee the effectiveness of NI in mitigating soil N_2O emissions after slurry application, it would be advisable to apply the NI at a moment in which the soil moisture is appropriate for nitrification, and to avoid a period when precipitation is forecasted. However, it is important to consider that the absence of precipitation, though positive for enabling the action of the nitrification inhibitor through shifting the source of N_2O emissions from denitrification to nitrification, can result in higher NH_3 emissions, as precipitation during or after slurry application reduces NH_3 emissions (Thompson and Meisinger, 2002).

6.3. N_2O emissions after plant residue incorporation

The incorporation of plant residues significantly increased N_2O emissions for rapeseed and rye plant residues but not for wheat straw (II, Figure 3). The N_2O emission peaks that followed the application of rapeseed and rye plant residue (II, Figure 3) were less immediate than those identified after slurry application, but reached maximum values even higher than those measured after slurry application (Table 4). Soil N_2O emissions after crop residue incorporation were the result of mineralisation of the residues, but also of the appearance of denitrification hotspots due to the reduction of O_2 as a result of degradation of organic matter in the areas surrounding the incorporated residues (Duan et al., 2018).

The C and N contents of the plant residues, and therefore the C/N ratio, were the main factors determining differences in N_2O fluxes. Lower C/N ratio resulted in higher emissions, indicating that it was not the total C nor the total N content but the recalcitrancy of the residues in the plant residues that was the determining factor. It is well-known that the C/N

ratio is one of the key factors affecting mineralisation speed (Villar et al., 2019), and therefore the availability of substrates for nitrification and denitrification and thus the N₂O emissions (Chen et al., 2013; Hansen et al., 2019). Moreover, microbial respiration, after crop residue incorporation, increases O₂ consumption, generating anaerobic conditions and promoting denitrification (Pfab et al., 2010). Baggs et al. (2000) found that N₂O emissions increased with decreasing C/N ratio of the incorporated plant residues in different soil types. In the current study, brassica and rye residues were characterised by a low C/N ratio (**II**, Table 2), which facilitates their decomposition and the subsequent release both of C and N (Akkal-Corfini et al., 2009). In a meta-analysis, Chen et al. (2013) found that crop residue with a C/N ratio below 45 significantly increased soil N₂O emissions after incorporation. In contrast, C/N ratio values above 100 had a limited mitigation effect on N₂O emissions. The wheat straw residues used in our experiment had a C/N ratio of 98, thus some mitigation could result from the addition of these residues, but this effect was not observed as no N₂O emissions were recorded from the control treatment (**II**, Figure 3). Li et al. (2013), however, found that under aerobic conditions, incorporation of nine different plant residues with C/N ratios ranging from 14 to 297 always resulted in increased soil N₂O emissions.

The plant residues applied in the current study can be divided into two groups based on their dry matter content, with rye and rapeseed residues having dry matter contents of 194 and 153 g kg⁻¹, respectively, and wheat straw having a dry matter content of 796 g kg⁻¹ (**II**, Table 2). The water content is relevant because a lower N mineralisation rate has been reported in dry residues compared with fresh residues (Moore et al., 1988; Breland, 1994). In our study, N₂O emissions were correlated to both water content in the plant residues and soil moisture (**II**, Table 6). Moreover, more advanced decomposition, with lower dry matter content, but also with lower C/N ratio, produces organic matter that is more porous and retains more water (Iqbal et al., 2012). The significant positive correlation between N₂O emissions and soil moisture may also indicate that denitrification was the dominant source of soil N₂O emissions. In contrast, no significant correlation was observed between soil temperature and N₂O fluxes.

The EF resulting from the measured emissions for wheat straw was 0.01 kg N₂O-N per kg N applied, which is in the range proposed in the 2019 Refinement to the 2006 IPCC Guidelines for National Greenhouse

Gas Inventories (IPCC, 2019) of 0.001–0.011. However, the EFs for the rye and rapeseed residues (0.15 and 0.11 kg N₂O-N per kg N applied, respectively) were approximately ten times higher than the upper limit of this range. This is probably due to its much lower C/N ratio and higher water content.

A possible approach to reduce N₂O emissions from fresh residues incorporation would be drying the residues before incorporation. This would reduce the immobilisation rate of the residues once incorporated, and subsequently, reduce losses through soil N₂O emissions and NO₃⁻ leaching. Reduction of NO₃⁻ leaching from crop residues with reduced and delayed tillage has been shown in similar climatological conditions in several studies in southern Scandinavia and Finland (Aronsson et al., 2016).

Another potential approach to N₂O mitigation after crop residue incorporation is the application of an NI in the moment of incorporation (Abalos et al., 2022a). The NI should reduce oxidation of the mineralised NH₄⁺ by nitrification (Chaves et al., 2005) reducing soil N₂O emissions from nitrification directly, and indirectly, from the lower NO₃⁻ availability, from denitrification.

The high N₂O emissions recorded after incorporation of some of the plant residues are especially relevant considering that the use of cover crops and green manures (cover crops that are incorporated into the soil) is promoted as a measure to increase SOC or reduce leaching (European Council, 1991; Directorate-General for Climate Action - European Commission, 2014; Berge et al., 2017), but this could result in nutrient losses through GHG emissions that surpass the reduction of losses through leaching. The use of such techniques could be suitable for areas with low SOC and/or erosion risk, such as the Mediterranean region (EIP-AGRI, 2015). However, under northern conditions, N mineralisation, after tillage in the end of summer and early fall, combined with precipitation can result in high N losses (Aronsson et al., 2016).

6.4. N₂O emissions during a full growing season of winter rapeseed (IV)

In the field experiment, outside the peak that followed organic fertilisation (August 2016; discussed in manuscript **III**), only two peaks of soil N₂O emissions could be identified (December 2016 and March–April

2017). These higher emissions were observed when the temperatures fluctuated around 0°C and were attributed to freeze-thaw events (IV, Figure 2).

High emissions from freeze-thaw can be explained by two different mechanisms: the first being the release of N₂O physically trapped under and/or inside ice (Tietema et al., 1991; Burton and Beauchamp, 1994); and the second relating to the increase of biological activity after the physical and chemical changes triggered by thawing, especially mass microbial death and the destruction of soil aggregates (Risk et al., 2013). Freeze-thaw N₂O fluxes are usually associated with denitrification resulting from the increased soil moisture and the availability of C and N substrates due to the combination of microbial mass death and the ease of release following soil aggregate destruction (Flessa et al., 1995; Risk et al., 2013). For instance, Ludwig et al. (2004) found that denitrification contributed 83% of the total N₂O emissions in a Luvisol soil during a freeze-thaw event; and Mørkved et al. (2006) found that nitrification contributed less than 5% to N₂O production during freeze-thaw in a Mollic Gleysol.

No noticeable peaks were detected after mineral fertilisation (IV, Figure 1). The higher fluxes measured at the end of March and beginning of April cannot be attributed to mineral fertilisation as the peak of emissions for this period was measured on 31 March, before the first mineral fertilisation took place (4 April). These fluxes are therefore more likely to be related to freeze-thaw. Nonetheless, mineral fertilisation could have partially contributed to the emissions measured between 4 and 28 April. The combination of the following mechanisms could explain the absence of emission peaks after mineral fertilisation:

- The lack of soil disturbance from tillage during synthetic fertiliser application.
- The lack of soil moisture increase associated with the mineral fertilisation.
- The lack of additional C addition, which can be used as energy source by denitrifiers.
- The weather conditions during and after mineral fertilisation, with no re-wetting effect from precipitation at the moment of mineral fertilisation (Duan et al., 2018).
- Uptake by plants, which although still small, were already present when mineral fertiliser was applied and could thus take up part of the N input from mineral fertilisation.

6.5. Limitations and future research

The large number of factors influencing soil N₂O fluxes, especially soil properties, landscape characteristics, and environmental factors, makes it difficult to predict the magnitude of N₂O fluxes or even whether the flux will be positive or negative. In the case of application of amendments, this is often aggravated by the diverse nature of these amendments, hence the importance of standardisation, especially in the case of biochar (Meyer et al., 2017). Nevertheless, the main factors controlling soil N₂O fluxes are well known (soil moisture and temperature and availability of necessary substrates). Future studies should consider how the applied amendments interact or modify these parameters in a specific soil, because more knowledge is needed before these amendments can be effectively used by farmers. This is particularly important to avoid undesired environmental or economic trade-offs.

The type of experiment is also a major factor when analysing and comparing the results of different studies as differences in the results of lab and field experiments are common (Xu et al., 2019), and high variations can even occur in the same experiment and with the same biochar (Felber et al., 2014). Therefore, it is necessary to be cautious when interpreting and extrapolating the results of either type of experiment. Field experiments are limited by the uncontrollable nature of environmental factors, such as the levels of temperature, precipitation, and sunshine. Precipitation is the key factor controlling soil N₂O emissions, as it controls the soil water content, and subsequently nitrification and denitrification, thus it can significantly alter N₂O fluxes in field experiments. Conversely, lab experiments cannot include all the factors at play in the natural environment. Even the factors that are considered in the lab experimental design are subject to some level of regularity that rarely mimics the variability and unpredictability present in nature.

Measurement frequency is a key factor affecting the representativeness of the measurements. A low frequency can hamper the temporal representativeness, but a high frequency is often economically and/or logistically non-viable. Weekly measurements are common practice but can miss the variability in soil N₂O fluxes, especially in field experiments, when disruptive weather events are common. High-frequency measurements, such as those provided by automated chamber systems, can solve this limitation. More data, considering more measured parameters and

a higher frequency for the parameters that have been already measured, can help to model the processes involved in soil N₂O fluxes. This will, in turn, clarify how the studied amendments interact with the soil physical and chemical properties, and how this affects N₂O emissions.

The quantification of nitrification and denitrification and the disentanglement of the source of soil N₂O emissions can also shed light on the mechanisms behind the success or failure of the mitigation tool used. This can be highly useful for mitigation strategies, such as biochar, where opposite results have been reported for both nitrification and denitrification.

The potential of the soil to act as an N₂O sink also deserves further research. Negative fluxes could significantly affect annual N₂O budgets, as it could be a significant source of error when measurements focus only in the period following fertilisation.

Finally, the study of techniques for the mitigation of N₂O emissions should not ignore possible trade-offs (e.g., increased NH₃ emissions after NI application), which are often neglected (Wu et al., 2021), as these strategies can result in higher emissions of other GHGs, especially CO₂ (Zhang et al., 2020). Non-GHG but also prejudicial gases, such as NH₃ emissions (Wu et al., 2021) could also be considered as they can have negative environmental effects and even result in indirect GHG emissions (Denmead et al., 2008).

7. CONCLUSIONS

Two lab experiments and a full growing season field experiment were conducted to study the effect of organic amendment application and crop residues incorporation on soil N₂O emissions and to evaluate the mitigation potential of biochar and the nitrification inhibitor DMPP.

Previous research has shown that, in general, NIs and biochar effectively reduce soil N₂O emissions from agriculture. However, our results show that this mitigation is not universal. The environmental conditions in the moment of application of the NI hampered its effectiveness, and the properties of the studied biochars could explain the enhanced emissions after biochar application.

In all cases, fertilisation with organic amendments (cattle slurry, slurry digestate, and vinasse) resulted in higher soil N₂O emissions than the untreated control. Although this increase in emissions was observed for all treatments with organic fertilisation, no significant differences were found among the different organic amendments when used in the same soil and under the same experimental conditions. The measured emissions after application of different cattle slurries were much higher in the field experiment than in the lab biochar experiment.

In contrast to organic fertilisation, the use of the two different mineral fertilisers (calcium ammonium nitrate and ammonium sulphate nitrate) applied in the field experiment did not result in significantly higher soil N₂O fluxes. This lack of a measurable effect was attributed to the lack of soil tillage, the lack of additional C provided by the mineral fertilisation, the weather conditions at the moment of application, and the effect of plant uptake.

The incorporation of plant residues in the pot experiment resulted in significantly higher emissions for fresh rapeseed and rye biomass but not for wheat straw. The C/N ratio of the residues was a major factor explaining the differences in N₂O fluxes. A higher decomposition rate of the organic matter, linked to a lower C/N ratio, resulted in a higher substrate availability for nitrification and denitrification. This indicates that, under specific conditions, high soil N₂O emissions from crop residue incorporation might counterbalance the potential benefits of leaching reduction and soil carbon sequestration associated with the use of cover crops and green manures.

Biochar application did not reduce soil N₂O emissions and addition of the high-temperature (850°C) biochar significantly increased emissions. This was related to the high N content and low C/N ratio of the studied biochars, resulting in a release of nutrients instead of the desired nutrient adsorption. This was supported by the linear relationship between C and N released from the biochars and the measured soil N₂O emissions. These results show that biochar application is not a universal tool for reducing GHG emissions and certain biochars can even induce higher soil N₂O emissions. The mechanisms behind these increased emissions are not fully understood, highlighting the need for further research on the topic.

Contrary to our hypothesis, NI application did not reduce emissions. The effectiveness of the studied nitrification inhibitor (DMPP) was hampered by the intensive rain during the period following slurry application. Soil N₂O emissions from denitrification after the soil water increase, and not nitrification, explain the lack of observed effect in the treatment with the NI. It is known that soil moisture at the moment of application of NI is a key factor in its effectiveness, but our results show that NI action on soil N₂O emissions can be completely hampered by temporary field conditions. This highlights the importance of the timing of the treatment to avoid unsuitable weather conditions.

The results of this work constitute the first direct quantification of N₂O emissions from arable soils in Estonia, and one of the first to study the mitigation potential of the nitrification inhibitor DMPP and biochar on N₂O emissions in the region.

Future research should focus on filling the gaps in the knowledge of the relationships between soil amendment properties and soil N₂O emissions, especially when amending with diverse materials such as biochar. However, characterisation of the amendment to be applied to the soil is insufficient: the timing of the application is also critical, as shown in the NI experiment. Correspondingly, tools should be developed to assist farmers in identifying the optimum moment of application, considering soil properties, field conditions, present weather conditions, and weather forecasting.

REFERENCES

- Abalos D., Recous S., Butterbach-Bahl K., De Notaris C., Rittl T.F., Topp C.F.E., Petersen S.O., Hansen S., Bleken M.A., Rees R.M., Olesen J.E. 2022a. A review and meta-analysis of mitigation measures for nitrous oxide emissions from crop residues. *Sci Total Environ*; 828: 154388. doi:10.1016/j.scitotenv.2022.154388
- Abalos D., Rittl T.F., Recous S., Thiebeau P., Topp C.F.E., van Groenigen K.J., Butterbach-Bahl K., Thorman R.E., Smith K.E., Ahuja I., Olesen J.E., Bleken M.A., Rees R.M., Hansen S. 2022b. Predicting field N₂O emissions from crop residues based on their biochemical composition: A meta-analytical approach. *Sci Total Environ*; 812: 152532. doi:10.1016/j.scitotenv.2021.152532
- Akkal-Corfini N., Morvan T., Menasseri-Aubry S., Bissuel-Bélaygue C., Poulain D., Orsini F., Leterme P. 2009. Nitrogen mineralization, plant uptake and nitrate leaching following the incorporation of (15N)-labeled cauliflower crop residues (*Brassica oleracea*) into the soil: a 3-year lysimeter study. *Plant and Soil*; 328: 17-26. doi:10.1007/s11104-009-0104-0
- Alexander M. 1965. Nitrification. In: Bartholomew WV, Clark FE, editors. *Soil Nitrogen*. 10. American Society of Agronomy, Madison, WI, USA, pp. 307-343.
- Allison F.E. 1957. Nitrogen and Soil Fertility. *Yearbook of Agriculture 1957*. United States Department of Agriculture, Washington, WA, United States, pp. 784.
- Ammann C., Spirig C., Leifeld J., Neftel A. 2009. Assessment of the nitrogen and carbon budget of two managed temperate grassland fields. *Agriculture, Ecosystems & Environment*; 133: 150-162. doi:10.1016/j.agee.2009.05.006
- Amon B., Kryvoruchko V., Amon T., Zechmeister-Boltenstern S. 2006. Methane, nitrous oxide and ammonia emissions during storage and after application of dairy cattle slurry and influence of slurry treatment. *Agriculture, Ecosystems & Environment*; 112: 153-162. doi:10.1016/j.agee.2005.08.030
- Aronsson H., Hansen E.M., Thomsen I.K., Liu J., Ogaard A.F., Kankanen H., Ulen B. 2016. The ability of cover crops to reduce nitrogen and phosphorus losses from arable land in southern Scandinavia and Finland. *Journal of Soil and Water Conservation*; 71: 41-55. doi:10.2489/jswc.71.1.41

- Badagliacca G., Ruisi P., Rees R.M., Saia S. 2017. An assessment of factors controlling N₂O and CO₂ emissions from crop residues using different measurement approaches. *Biol Fertil Soils*; 53: 547-561. doi:10.1007/s00374-017-1195-z
- Baggs E.M., Rees R.M., Smith K.A., Vinten A.J.A. 2000. Nitrous oxide emission from soils after incorporating crop residues. *Soil Use and Management*; 16: 82-87. doi:10.1111/j.1475-2743.2000.tb00179.x
- Baldos U.L.C., Hertel T.W. 2014. Global food security in 2050: the role of agricultural productivity and climate change. *Australian Journal of Agricultural and Resource Economics*; 58: 554-570. doi:10.1111/1467-8489.12048
- Barrena I., Menéndez S., Correa-Galeote D., Vega-Mas I., Bedmar E.J., González-Murua C., Estavillo J.M. 2017. Soil water content modulates the effect of the nitrification inhibitor 3,4-dimethylpyrazole phosphate (DMPP) on nitrifying and denitrifying bacteria. *Geoderma*; 303: 1-8. doi:10.1016/j.geoderma.2017.04.022
- Beck H., Christensen S. 1987. The effect of grass maturing and root decay on N₂O production in soil. *Plant and Soil*; 103: 269-273. doi:10.1007/bf02370399
- Berge H.F.M.t., Schroder J.J., Olesen J.E., Giraldez Cervera J.V. 2017. Research for AGRI Committee - Preserving agricultural soils in the EU. Directorate-General for Internal Policies - European Parliament, Brussels, Belgium.
- Bhattacharya S., Adhya T.K., Pathak H., Raghuram N., Sharma C. 2017. Issues and Policies for Reactive Nitrogen Management in the Indian Region. *The Indian Nitrogen Assessment*, pp. 491-513.
- Blanco-Canqui H., Lal R. 2009. Crop Residue Removal Impacts on Soil Productivity and Environmental Quality. *Critical Reviews in Plant Sciences*; 28: 139-163. doi:10.1080/07352680902776507
- Borchard N., Schirrmann M., Cayuela M.L., Kammann C., Wrage-Monnig N., Estavillo J.M., Fuertes-Mendizabal T., Sigua G., Spokas K., Ippolito J.A., Novak J. 2019. Biochar, soil and land-use interactions that reduce nitrate leaching and N₂O emissions: A meta-analysis. *Sci Total Environ*; 651: 2354-2364. doi:10.1016/j.scitotenv.2018.10.060
- Bosch-Serra A.D., Yague M.R., Valdez A.S., Domingo-Olive F. 2020. Dairy cattle slurry fertilization management in an intensive Mediterranean agricultural system to sustain soil quality while enhanc-

- ing rapeseed nutritional value. *J Environ Manage*; 273: 111092. doi:10.1016/j.jenvman.2020.111092
- Bouchet A.-S., Laperche A., Bissuel-Belaygue C., Snowdon R., Nesi N., Stahl A. 2016. Nitrogen use efficiency in rapeseed. A review. *Agronomy for Sustainable Development*; 36. doi:10.1007/s13593-016-0371-0
- Bouwman A.F. 1996. Direct emission of nitrous oxide from agricultural soils. *Nutrient Cycling in Agroecosystems*; 46: 53-70. doi:10.1007/bf00210224
- Braker G.C., Ralf. 2011. Diversity, Structure, and Size of N₂O-Producing Microbial Communities in Soils—What Matters for Their Functioning? *Advances in Applied Microbiology*. 75. Academic Press, Cambridge, MA, pp. 33-70.
- Breland T.A. 1994. Enhanced mineralization and denitrification as a result of heterogeneous distribution of clover residues in soil. *Plant and Soil*; 166: 1-12. doi:10.1007/bf02185475
- Bremner J.M. 1997. Sources of nitrous oxide in soils. *Nutrient Cycling in Agroecosystems*; 49: 7-16. doi:10.1023/a:1009798022569
- Buchkina N.P., Hüppi R., Leifeld J. 2019. Biochar and short-term N₂O and CO₂ emission from plant residue-amended soil with different fertilisation history. *Zemdirbyste-Agriculture*; 106: 99-106. doi:10.13080/z-a.2019.106.013
- Burton D.L., Beauchamp E.G. 1994. Profile Nitrous Oxide and Carbon Dioxide Concentrations in a Soil Subject to Freezing. *Soil Science Society of America Journal*; 58: 115-122. doi:10.2136/sssaj1994.03615995005800010016x
- Butterbach-Bahl K., Baggs E.M., Dannenmann M., Kiese R., Zechmeister-Boltenstern S. 2013. Nitrous oxide emissions from soils: how well do we understand the processes and their controls? *Philos Trans R Soc Lond B Biol Sci*; 368: 20130122. doi:10.1098/rstb.2013.0122
- Byrne M.P., Tobin J.T., Forrester P.J., Danaher M., Nkwonta C.G., Richards K., Cummins E., Hogan S.A., O'Callaghan T.F. 2020. Urease and Nitrification Inhibitors—As Mitigation Tools for Greenhouse Gas Emissions in Sustainable Dairy Systems: A Review. *Sustainability*; 12. doi:10.3390/su12156018
- Cameron K.C., Di H.J., Moir J.L. 2013. Nitrogen losses from the soil/plant system: a review. *Annals of Applied Biology*; 162: 145-173. doi:10.1111/aab.12014

- Cantarel A.A.M., Bloor J.M.G., Deltroy N., Soussana J.-F. 2010. Effects of Climate Change Drivers on Nitrous Oxide Fluxes in an Upland Temperate Grassland. *Ecosystems*; 14: 223-233. doi:10.1007/s10021-010-9405-7
- Carmo J.B.d., Filoso S., Zotelli L.C., de Sousa Neto E.R., Pitombo L.M., Duarte-Neto P.J., Vargas V.P., Andrade C.A., Gava G.J.C., Rossetto R., Cantarella H., Neto A.E., Martinelli L.A. 2013. Infield greenhouse gas emissions from sugarcane soils in Brazil: effects from synthetic and organic fertilizer application and crop trash accumulation. *GCB Bioenergy*; 5: 267-280. doi:10.1111/j.1757-1707.2012.01199.x
- Cayuela M.L., Sanchez-Monedero M.A., Roig A., Hanley K., Enders A., Lehmann J. 2013. Biochar and denitrification in soils: when, how much and why does biochar reduce N₂O emissions? *Sci Rep*; 3: 1732. doi:10.1038/srep01732
- Cayuela M.L., van Zwieten L., Singh B.P., Jeffery S., Roig A., Sánchez-Monedero M.A. 2014. Biochar's role in mitigating soil nitrous oxide emissions: A review and meta-analysis. *Agriculture, Ecosystems & Environment*; 191: 5-16. doi:10.1016/j.agee.2013.10.009
- Challinor A.J., Watson J., Lobell D.B., Howden S.M., Smith D.R., Chhetri N. 2014. A meta-analysis of crop yield under climate change and adaptation. *Nature Climate Change*; 4: 287-291. doi:10.1038/nclimate2153
- Chantigny M.H., Angers D.A., Rochette P., Belanger G., Masse D., Cote D. 2007. Gaseous nitrogen emissions and forage nitrogen uptake on soils fertilized with raw and treated swine manure. *J Environ Qual*; 36: 1864-72. doi:10.2134/jeq2007.0083
- Chapuis-Lardy L., Wrage N., Metay A., Chotte J.-L., Bernoux M. 2007. Soils, a sink for N₂O? A review. *Global Change Biology*; 13: 1-17. doi:10.1111/j.1365-2486.2006.01280.x
- Chaves B., Opoku A., De Neve S., Boeckx P., Van Cleemput O., Hofman G. 2005. Influence of DCD and DMPP on soil N dynamics after incorporation of vegetable crop residues. *Biology and Fertility of Soils*; 43: 62-68. doi:10.1007/s00374-005-0061-6
- Chen H., Li X., Hu F., Shi W. 2013. Soil nitrous oxide emissions following crop residue addition: a meta-analysis. *Glob Chang Biol*; 19: 2956-64. doi:10.1111/gcb.12274
- Chen J., Gong Y., Wang S., Guan B., Balkovic J., Kraxner F. 2019. To burn or retain crop residues on croplands? An integrated analysis of

- crop residue management in China. *Sci Total Environ*; 662: 141-150. doi:10.1016/j.scitotenv.2019.01.150
- Chen Z., Ding W., Luo Y., Yu H., Xu Y., Müller C., Xu X., Zhu T. 2014. Nitrous oxide emissions from cultivated black soil: A case study in Northeast China and global estimates using empirical model. *Global Biogeochemical Cycles*; 28: 1311-1326. doi:10.1002/2014gb004871
- Christel W., Zhu K., Hoefler C., Kreuzeder A., Santner J., Bruun S., Magid J., Jensen L.S. 2016. Spatiotemporal dynamics of phosphorus release, oxygen consumption and greenhouse gas emissions after localised soil amendment with organic fertilisers. *Sci Total Environ*; 554-555: 119-29. doi:10.1016/j.scitotenv.2016.02.152
- Ciais P., Sabine C., Bala G., Bopp L., Brovkin V., Canadell J., Chhabra A., DeFries R., Galloway J., Heimann M., Jones C., Quéré C.L., Myneni R.B., Piao S., Thornton P. 2013. Carbon and Other Biogeochemical Cycles. In: Stocker TF, Qin D, Plattner G-K, Tignor M, Allen SK, Boschung J, et al., editors. *Climate Change 2013: The Physical Science Basis. Contribution of Working Group I to the Fifth Assessment Report of the Intergovernmental Panel on Climate Change*. Cambridge University Press, Cambridge, United Kingdom.
- Ciborowski P. 2001. *Anaerobic Digestion of Livestock Manure for Pollution Control and Energy Production: A Feasibility Assessment*, Minnesota, U.S.A., pp. 233.
- Clough T., Condon L., Kammann C., Müller C. 2013. A Review of Biochar and Soil Nitrogen Dynamics. *Agronomy*; 3: 275-293. doi:10.3390/agronomy3020275
- Clough T.J., Bertram J.E., Ray J.L., Condon L.M., O'Callaghan M., Sherlock R.R., Wells N.S. 2010. Unweathered Wood Biochar Impact on Nitrous Oxide Emissions from a Bovine-Urine-Amended Pasture Soil. *Soil Science Society of America Journal*; 74. doi:10.2136/sssaj2009.0185
- Corrochano-Monsalve M., Gonzalez-Murua C., Bozal-Leorri A., Lezama L., Artetxe B. 2021a. Mechanism of action of nitrification inhibitors based on dimethylpyrazole: A matter of chelation. *Sci Total Environ*; 752: 141885. doi:10.1016/j.scitotenv.2020.141885
- Corrochano-Monsalve M., Gonzalez-Murua C., Estavillo J.M., Estonba A., Zarraonaindia I. 2021b. Impact of dimethylpyrazole-based nitrification inhibitors on soil-borne bacteria. *Sci Total Environ*; 792: 148374. doi:10.1016/j.scitotenv.2021.148374

- Crews T.E., Peoples M.B. 2005. Can the Synchrony of Nitrogen Supply and Crop Demand be Improved in Legume and Fertilizer-based Agroecosystems? A Review. *Nutrient Cycling in Agroecosystems*; 72: 101-120. doi:10.1007/s10705-004-6480-1
- Dahlin S., Kirchmann H., Kätterer T., Gunnarsson S., Bergström L. 2005. Possibilities for Improving Nitrogen Use From Organic Materials in Agricultural Cropping Systems. *AMBIO: A Journal of the Human Environment*; 34: 288-295. doi:10.1579/0044-7447-34.4.288
- Davidson E.A. 1991. Fluxes of nitrous oxide and nitric oxide from terrestrial ecosystems. In: Rogers JE, Whitman WB, editors. *Microbial production and consumption of greenhouse gases: Methane, nitrogen oxides, and halomethanes*. American Society for Microbiology, Washington, WA, United States, pp. 219–235.
- Davidson E.A. 2009. The contribution of manure and fertilizer nitrogen to atmospheric nitrous oxide since 1860. *Nature Geoscience*; 2: 659-662. doi:10.1038/ngeo608
- Davidson E.A., Kanter D. 2014. Inventories and scenarios of nitrous oxide emissions. *Environmental Research Letters*; 9. doi:10.1088/1748-9326/9/10/105012
- Davidson E.A., Keller M., Erickson H.E., Verchot L.V., Veldkamp E. 2000. Testing a Conceptual Model of Soil Emissions of Nitrous and Nitric Oxides. *BioScience*; 50. doi:10.1641/0006-3568(2000)050[0667:tacmos]2.0.co;2
- Davis A. 2015. *Feed and Feeding Practices in Aquaculture*.
- Denmead O.T., Chen D., Griffith D.W.T., Loh Z.M., Bai M., Naylor T. 2008. Emissions of the indirect greenhouse gases NH₃ and NO_x from Australian beef cattle feedlots. *Australian Journal of Experimental Agriculture*; 48. doi:10.1071/ea07276
- Di H.J., Cameron K.C. 2011. Inhibition of ammonium oxidation by a liquid formulation of 3,4-Dimethylpyrazole phosphate (DMPP) compared with a dicyandiamide (DCD) solution in six new Zealand grazed grassland soils. *Journal of Soils and Sediments*; 11: 1032-1039. doi:10.1007/s11368-011-0372-1
- Di H.J., Cameron K.C. 2016. Inhibition of nitrification to mitigate nitrate leaching and nitrous oxide emissions in grazed grassland: a review. *Journal of Soils and Sediments*; 16: 1401-1420. doi:10.1007/s11368-016-1403-8
- Di H.J., Cameron K.C., Podolyan A., Robinson A. 2014. Effect of soil moisture status and a nitrification inhibitor, dicyandiamide, on

- ammonia oxidizer and denitrifier growth and nitrous oxide emissions in a grassland soil. *Soil Biology and Biochemistry*; 73: 59-68. doi:10.1016/j.soilbio.2014.02.011
- Directorate-General for Climate Action - European Commission. 2014. Mainstreaming climate change into rural development policy post 2013 : final report. European Union, Luxembourg.
- Dobbie K.E., Smith K.A. 2003. Nitrous oxide emission factors for agricultural soils in Great Britain: the impact of soil water-filled pore space and other controlling variables. *Global Change Biology*; 9: 204-218. doi:10.1046/j.1365-2486.2003.00563.x
- Duan Y.F., Hallin S., Jones C.M., Prieme A., Labouriau R., Petersen S.O. 2018. Catch Crop Residues Stimulate N₂O Emissions During Spring, Without Affecting the Genetic Potential for Nitrite and N₂O Reduction. *Front Microbiol*; 9: 2629. doi:10.3389/fmicb.2018.02629
- Duan Y.F., Kong X.W., Schramm A., Labouriau R., Eriksen J., Petersen S.O. 2017. Microbial N Transformations and N₂O Emission after Simulated Grassland Cultivation: Effects of the Nitrification Inhibitor 3,4-Dimethylpyrazole Phosphate (DMPP). *Appl Environ Microbiol*; 83. doi:10.1128/AEM.02019-16
- EEA. 2000. Down to earth: soil degradation and sustainable development in Europe. Copenhagen, Denmark: European Environment Agency.
- EIP-AGRI. 2015. Focus Group on Soil Organic Matter content in Mediterranean regions: Final Report. EIP-AGRI, Brussels, Belgium.
- European Commission. 2006. Thematic Strategy for Soil Protection In: European Commission, editor. COM(2006)231 final, Belgium, Brussels.
- European Commission. 2016. Circular economy: New Regulation to boost the use of organic and waste-based fertilisers. The Commission presents first deliverable of Circular Economy Package with new rules on organic and waste-based fertilisers in the EU, Brussels, Belgium.
- European Commission. 2019. Communication From The Commission: The European Green Deal. In: Commission E, editor, Brussels, Belgium.
- European Commission. 2020. Farm to Fork strategy - For a fair, healthy and environmentally-friendly food system. European Commission, Brussels, Belgium.
- European Council. 1991. Council Directive of 12 December 1991 concerning the protection of waters against pollution caused by nitrates

- from agricultural sources (91/676/EEC). In: European Council, editor, Brussels, Belgium.
- FAO. 1984. Fertilizer and plant nutrition guide. Vol 9. Rome, Italy: FAO.
- FAO. 2006. Plant nutrition for food security - A guide for integrated nutrient management. Vol 16. Rome, Italy: FAO.
- FAO. 2017. The Future of Food and Agriculture: Trends and Challenges. Rome, Italy: FAO.
- FAO/IFA. 2001. Global estimates of gaseous emissions of NH₃, NO and N₂O from agricultural land. Rome, Italy: Food and Agriculture Organization of the United Nations / International Fertilizer Association.
- Felber R., Leifeld J., Horák J., Neftel A. 2014. Nitrous oxide emission reduction with greenwaste biochar: comparison of laboratory and field experiments. *European Journal of Soil Science*; 65: 128-138. doi:10.1111/ejss.12093
- Feng Z., Zhu L. 2017. Impact of biochar on soil N₂O emissions under different biochar-carbon/fertilizer-nitrogen ratios at a constant moisture condition on a silt loam soil. *Sci Total Environ*; 584-585: 776-782. doi:10.1016/j.scitotenv.2017.01.115
- Firestone M.K., Davidson E.A. 1989. Microbiological Basis of NO and N₂O Production and Consumption in Soils. In: Andreae MO, Schimel, D.S., editor. *Exchange of Trace Gases between Terrestrial Ecosystems and the Atmosphere*. John Willey and Sons, New York, United States, pp. 7-21.
- Flavel T.C., Murphy D.V. 2006. Carbon and nitrogen mineralization rates after application of organic amendments to soil. *J Environ Qual*; 35: 183-93. doi:10.2134/jeq2005.0022
- Flessa H., Dörsch P., Beese F. 1995. Seasonal variation of N₂O and CH₄ fluxes in differently managed arable soils in southern Germany. *Journal of Geophysical Research*; 100. doi:10.1029/95jd02270
- Focht D.D. 1978. Methods for Analysis of Denitrification in Soils. In: Nielsen DR, MacDonald JG, editors. *Soil-Plant-Nitrogen Relationships*, pp. 433-490.
- Frank S., Havlík P., Soussana J.-F., Levesque A., Valin H., Wollenberg E., Kleinwechter U., Fricko O., Gusti M., Herrero M., Smith P., Hasegawa T., Kraxner F., Obersteiner M. 2017. Reducing greenhouse gas emissions in agriculture without compromising food security? *Environmental Research Letters*; 12. doi:10.1088/1748-9326/aa8c83

- Fuss S., Jones C.D., Kraxner F., Peters G.P., Smith P., Tavoni M., van Vuuren D.P., Canadell J.G., Jackson R.B., Milne J., Moreira J.R., Nakicenovic N., Sharifi A., Yamagata Y. 2016. Research priorities for negative emissions. *Environmental Research Letters*; 11. doi:10.1088/1748-9326/11/11/115007
- Galloway J.N., Cowling E.B. 2002. Reactive nitrogen and the world: 200 years of change. *Ambio*; 31: 64-71. doi:10.1579/0044-7447-31.2.64
- Giles M., Morley N., Baggs E.M., Daniell T.J. 2012. Soil nitrate reducing processes - drivers, mechanisms for spatial variation, and significance for nitrous oxide production. *Front Microbiol*; 3: 407. doi:10.3389/fmicb.2012.00407
- Gilsanz C., Báez D., Misselbrook T.H., Dhanoa M.S., Cárdenas L.M. 2016. Development of emission factors and efficiency of two nitrification inhibitors, DCD and DMPP. *Agriculture, Ecosystems & Environment*; 216: 1-8. doi:10.1016/j.agee.2015.09.030
- Guillaumes E., Villar J.M. 2004. Effects of DMPP [3,4-dimethylpyroazole phosphate] on the growth and chemical composition of ryegrass (*Lolium perenne* L.) raised on calcareous soil. *Spanish Journal of Agricultural Research*; 2. doi:10.5424/sjar/2004024-115
- Guo X., Drury C.F., Yang X., Daniel Reynolds W., Fan R. 2014. The Extent of Soil Drying and Rewetting Affects Nitrous Oxide Emissions, Denitrification, and Nitrogen Mineralization. *Soil Science Society of America Journal*; 78: 194-204. doi:10.2136/sssaj2013.06.0219
- Hansen S., Berland Frøseth R., Stenberg M., Stalenga J., Olesen J.E., Krauss M., Radzikowski P., Doltra J., Nadeem S., Torp T., Pappa V., Watson C.A. 2019. Reviews and syntheses: Review of causes and sources of N₂O emissions and NO₃ leaching from organic arable crop rotations. *Biogeosciences*; 16: 2795-2819. doi:10.5194/bg-16-2795-2019
- Harter J., Krause H.M., Schuettler S., Ruser R., Fromme M., Scholten T., Kappler A., Behrens S. 2014. Linking N₂O emissions from biochar-amended soil to the structure and function of the N-cycling microbial community. *ISME J*; 8: 660-74. doi:10.1038/ismej.2013.160
- HELCOM. 2009. Eutrophication in the Baltic Sea. An integrated thematic assessment of the effects of nutrient enrichment in the Baltic Sea region. 115. Helsinki Commission, pp. 148.
- Hénault C., Bourennane H., Ayzac A., Ratié C., Saby N.P.A., Cohan J.P., Eglin T., Gall C.L. 2019. Management of soil pH promotes nitrous

- oxide reduction and thus mitigates soil emissions of this greenhouse gas. *Sci Rep*; 9: 20182. doi:10.1038/s41598-019-56694-3
- Herr C., Mannheim T., Müller T., Ruser R. 2020. Effect of Nitrification Inhibitors on N₂O Emissions after Cattle Slurry Application. *Agronomy*; 10. doi:10.3390/agronomy10081174
- Horowitz J.K., Gottlieb J. 2010. The Role of Agriculture in Reducing Greenhouse Gas Emissions. *Economic Brief*. 15. United States Department of Agriculture (USDA). Economic Research Service, Washington, DC, United States, pp. 8.
- Hüppi R., Felber R., Neftel A., Six J., Leifeld J. 2015. Effect of biochar and liming on soil nitrous oxide emissions from a temperate maize cropping system. *Soil*; 1: 707-717. doi:10.5194/soil-1-707-2015
- IPCC. 2007. *Climate Change 2007: Mitigation. Contribution of Working Group III to the Fourth Assessment Report of the Intergovernmental Panel on Climate Change* Cambridge, United Kingdom: Cambridge University Press.
- IPCC. 2018. *Global warming of 1.5°C. An IPCC Special Report on the impacts of global warming of 1.5°C above pre-industrial levels and related global greenhouse gas emission pathways, in the context of strengthening the global response to the threat of climate change, sustainable development, and efforts to eradicate poverty.* In: Masson-Delmotte V, P. Zhai, H.-O. Pörtner, D. Roberts, J. Skea, P.R. Shukla, A. Pirani, W. Moufouma-Okia, C. Péan, R. Pidcock, S. Connors, J.B.R. Matthews, Y. Chen, X. Zhou, M.I. Gomis, E. Lonnoy, T. Maycock, M. Tignor, and T. Waterfield, editor, Geneva, Switzerland, pp. 630.
- IPCC. 2019. Chapter 11: N₂O Emissions from Managed Soils, and CO₂ Emissions from Lime and Urea Application. In: Calvo Buendia E, Tanabe K, Kranjc A, Baasansuren J, Fukuda M, Ngarize S, et al., editors. *2019 Refinement to the 2006 IPCC Guidelines for National Greenhouse Gas Inventories. Volume 4: Agriculture, Forestry and Other Land Use.* IPCC, Geneva, Switzerland.
- IPCC. 2021. *Climate Change 2021: The Physical Science Basis. Contribution of Working Group I to the Sixth Assessment Report of the Intergovernmental Panel on Climate Change.* IPCC, Geneva, Switzerland.
- Iqbal A., Beaugrand J., Garnier P., Recous S. 2012. Tissue density determines the water storage characteristics of crop residues. *Plant and Soil*; 367: 285-299. doi:10.1007/s11104-012-1460-8

- Jones S.K., Rees R.M., Skiba U.M., Ball B.C. 2007. Influence of organic and mineral N fertiliser on N₂O fluxes from a temperate grassland. *Agriculture, Ecosystems & Environment*; 121: 74-83. doi:10.1016/j.agee.2006.12.006
- Jordán A., Zavala L.M., Gil J. 2010. Effects of mulching on soil physical properties and runoff under semi-arid conditions in southern Spain. *Catena*; 81: 77-85. doi:10.1016/j.catena.2010.01.007
- Joseph S., Cowie A.L., Van Zwieten L., Bolan N., Budai A., Buss W., Cayuela M.L., Graber E.R., Ippolito J.A., Kuzyakov Y., Luo Y., Ok Y.S., Palansooriya K.N., Shepherd J., Stephens S., Weng Z., Lehmann J. 2021. How biochar works, and when it doesn't: A review of mechanisms controlling soil and plant responses to biochar. *GCB Bioenergy*; 13: 1731-1764. doi:10.1111/gcbb.12885
- KeChrist O., Sampson M., Golden M., Nwabunwanne N. 2017. Slurry Utilization and Impact of Mixing Ratio in Biogas Production. *Chemical Engineering & Technology*; 40: 1742-1749. doi:10.1002/ceat.201600619
- Keil D., Niklaus P.A., von Riedmatten L.R., Boeddinghaus R.S., Dormann C.F., Scherer-Lorenzen M., Kandeler E., Marhan S. 2015. Effects of warming and drought on potential N₂O emissions and denitrifying bacteria abundance in grasslands with different land-use. *FEMS Microbiol Ecol*; 91. doi:10.1093/femsec/fiv066
- Kersebaum K.C., Hecker J.-M., Mirschel W., Wegehenkel M. 2004. Modelling water and nutrient dynamics in soil-crop systems. Springer Netherlands, Müncheberg, Germany, pp. VIII, 272.
- Kiiski H., Dittmar H., Drach M., Vosskamp R., Trenkel M.E., Gutser R., Steffens G. 2000. Fertilizers, 2. Types. Ullmann's Encyclopedia of Industrial Chemistry. Wiley-VCH Verlag GmbH & Co. KGaA, Weinheim, Germany.
- Klemetsson L., Von Arnold K., Weslien P., Gundersen P. 2005. Soil CN ratio as a scalar parameter to predict nitrous oxide emissions. *Global Change Biology*; 11: 1142-1147. doi:10.1111/j.1365-2486.2005.00973.x
- Kong X., Eriksen J., Petersen S.O. 2018. Evaluation of the nitrification inhibitor 3,4-dimethylpyrazole phosphate (DMPP) for mitigating soil N₂O emissions after grassland cultivation. *Agriculture, Ecosystems & Environment*; 259: 174-183. doi:10.1016/j.agee.2018.02.029
- Krause H.-M., Hüppi R., Leifeld J., El-Hadidi M., Harter J., Kappler A., Hartmann M., Behrens S., Mäder P., Gattinger A. 2018.

- Biochar affects community composition of nitrous oxide reducers in a field experiment. *Soil Biology and Biochemistry*; 119: 143-151. doi:10.1016/j.soilbio.2018.01.018
- Lal R. 2007. Carbon sequestration. *Philos Trans R Soc Lond B Biol Sci*; 363: 815-30. doi:10.1098/rstb.2007.2185
- Lal R. 2009a. Soil quality impacts of residue removal for bioethanol production. *Soil and Tillage Research*; 102: 233-241. doi:10.1016/j.still.2008.07.003
- Lal R. 2009b. Use of crop residues in the production of biofuel. *Handbook of Waste Management and Co-Product Recovery in Food Processing*, pp. 455-478.
- Lal R., Stewart B.A. 2018. *Soil Nitrogen Uses and Environmental Impacts*.
- Lam S.K., Suter H., Mosier A.R., Chen D. 2017. Using nitrification inhibitors to mitigate agricultural N₂O emission: a double-edged sword? *Glob Chang Biol*; 23: 485-489. doi:10.1111/gcb.13338
- Lassaletta L., Billen G., Grizzetti B., Anglade J., Garnier J. 2014. 50 year trends in nitrogen use efficiency of world cropping systems: the relationship between yield and nitrogen input to cropland. *Environmental Research Letters*; 9. doi:10.1088/1748-9326/9/10/105011
- Lazcano C., Zhu-Barker X., Decock C. 2021. Effects of Organic Fertilizers on the Soil Microorganisms Responsible for N₂O Emissions: A Review. *Microorganisms*; 9. doi:10.3390/microorganisms9050983
- Lehmann J., Joseph S. 2009. *Biochar for Environmental Management: Science and Technology*. London, United Kingdom: Earthscan.
- Lessard R., Rochette P., Gregorich E.G., Pattey E., Desjardins R.L. 1996. Nitrous Oxide Fluxes from Manure-Amended Soil under Maize. *Journal of Environment Quality*; 25. doi:10.2134/jeq1996.00472425002500060029x
- Levy-Booth D.J., Prescott C.E., Grayston S.J. 2014. Microbial functional genes involved in nitrogen fixation, nitrification and denitrification in forest ecosystems. *Soil Biology and Biochemistry*; 75: 11-25. doi:10.1016/j.soilbio.2014.03.021
- Li T., Zhang W., Yin J., Chadwick D., Norse D., Lu Y., Liu X., Chen X., Zhang F., Powlson D., Dou Z. 2018. Enhanced-efficiency fertilizers are not a panacea for resolving the nitrogen problem. *Glob Chang Biol*; 24: e511-e521. doi:10.1111/gcb.13918

- Li X., Hu F., Shi W. 2013. Plant material addition affects soil nitrous oxide production differently between aerobic and oxygen-limited conditions. *Applied Soil Ecology*; 64: 91-98. doi:10.1016/j.apsoil.2012.10.003
- Li Z., Reichel R., Xu Z., Vereecken H., Brüggemann N. 2021. Return of crop residues to arable land stimulates N₂O emission but mitigates NO₃⁻ leaching: a meta-analysis. *Agronomy for Sustainable Development*; 41. doi:10.1007/s13593-021-00715-x
- Linn D.M., Doran J.W. 1984. Effect of Water-Filled Pore Space on Carbon Dioxide and Nitrous Oxide Production in Tilled and Nontilled Soils. *Soil Science Society of America Journal*; 48: 1267-1272. doi:10.2136/sssaj1984.03615995004800060013x
- Liu J., Ma K., Ciais P., Polasky S. 2016. Reducing human nitrogen use for food production. *Sci Rep*; 6: 30104. doi:10.1038/srep30104
- Liu Q., Zhang Y., Liu B., Amonette J.E., Lin Z., Liu G., Ambus P., Xie Z. 2018. How does biochar influence soil N cycle? A meta-analysis. *Plant and Soil*; 426: 211-225. doi:10.1007/s11104-018-3619-4
- Lohila A., Aurela M., Tuovinen J.-P., Laurila T. 2004. Annual CO₂ exchange of a peat field growing spring barley or perennial forage grass. *Journal of Geophysical Research*; 109. doi:10.1029/2004jd004715
- Loro P.J., Bergstrom D.W., Beauchamp E.G. 1997. Intensity and Duration of Denitrification following Application of Manure and Fertilizer to Soil. *Journal of Environmental Quality*; 26: 706-713. doi:10.2134/jeq1997.00472425002600030016x
- Lourenço K.S., Rossetto R., Vitti A.C., Montezano Z.F., Soares J.R., Sousa R.M., do Carmo J.B., Kuramae E.E., Cantarella H. 2019. Strategies to mitigate the nitrous oxide emissions from nitrogen fertilizer applied with organic fertilizers in sugarcane. *Sci Total Environ*; 650: 1476-1486. doi:10.1016/j.scitotenv.2018.09.037
- Ludwig B., Wolf I., Teepe R. 2004. Contribution of nitrification and denitrification to the emission of N₂O in a freeze-thaw event in an agricultural soil. *Journal of Plant Nutrition and Soil Science*; 167: 678-684. doi:10.1002/jpln.200421462
- Ma R., Yu K., Xiao S., Liu S., Ciais P., Zou J. 2022. Data-driven estimates of fertilizer-induced soil NH₃, NO and N₂O emissions from croplands in China and their climate change impacts. *Glob Chang Biol*; 28: 1008-1022. doi:10.1111/gcb.15975

- Machefert S.E., Dise N.B., Goulding K.W.T., Whitehead P.G. 2002. Nitrous oxide emission from a range of land uses across Europe. *Hydrology and Earth System Sciences*; 6: 325-338. doi:10.5194/hess-6-325-2002
- Marchaim U. 1992. *Biogas processes for sustainable development* Rome, Italy: FAO.
- Mathur R., Srivastava V.K. 2018. *Crop Residue Burning: Effects on Environment. Greenhouse Gas Emissions*. Springer Nature Singapore Private Limited, Singapore, pp. 127-140.
- McMillan A.M.S., Pal P., Phillips R.L., Palmada T., Berben P.H., Jha N., Saggar S., Luo J. 2016. Can pH amendments in grazed pastures help reduce N₂O emissions from denitrification? – The effects of liming and urine addition on the completion of denitrification in fluvial and volcanic soils. *Soil Biology and Biochemistry*; 93: 90-104. doi:10.1016/j.soilbio.2015.10.013
- Menéndez S., Barrena I., Setien I., González-Murua C., Estavillo J.M. 2012. Efficiency of nitrification inhibitor DMPP to reduce nitrous oxide emissions under different temperature and moisture conditions. *Soil Biology and Biochemistry*; 53: 82-89. doi:10.1016/j.soilbio.2012.04.026
- Meyer S., Genesio L., Vogel I., Schmidt H.-P., Soja G., Someus E., Shackley S., Verheijen F.G.A., Glaser B. 2017. Biochar Standardization and Legislation Harmonization. *Journal of Environmental Engineering and Landscape Management*; 25: 175-191. doi:10.3846/16486897.2016.1254640
- Moore J.C., Walter D.E., Hunt H.W. 1988. Arthropod Regulation of Micro- and Mesobiota in Below-Ground Detrital Food Webs. *Annual Review of Entomology*; 33: 419-435. doi:10.1146/annurev.en.33.010188.002223
- Mori T., Ohta S., Ishizuka S., Konda R., Wicaksono A., Heriyanto J., Hardjono A. 2010. Effects of phosphorus addition on N₂O and NO emissions from soils of an *Acacia mangium* plantation. *Soil Science and Plant Nutrition*; 56: 782-788. doi:10.1111/j.1747-0765.2010.00501.x
- Mørkved P.T., Dörsch P., Henriksen T.M., Bakken L.R. 2006. N₂O emissions and product ratios of nitrification and denitrification as affected by freezing and thawing. *Soil Biology and Biochemistry*; 38: 3411-3420. doi:10.1016/j.soilbio.2006.05.015

- Mosier A.R. 1998. Soil processes and global change. *Biology and Fertility of Soils*; 27: 221-229. doi:10.1007/s003740050424
- Mosier A.R., Duxbury J.M., Freney J.R., Heinemeyer O., Minami K. 1998. Assessing and Mitigating N₂O Emissions from Agricultural Soils. *Climatic Change*; 40: 7-38. doi:10.1023/a:1005386614431
- Müller C., Stevens R.J., Laughlin R.J., Azam F., Ottow J.C.G. 2002. The nitrification inhibitor DMPP had no effect on denitrifying enzyme activity. *Soil Biology and Biochemistry*; 34: 1825-1827. doi:10.1016/s0038-0717(02)00165-7
- Myrgiotis V., Williams M., Rees R.M., Topp C.F.E. 2019. Estimating the soil N₂O emission intensity of croplands in northwest Europe. *Biogeosciences*; 16: 1641-1655. doi:10.5194/bg-16-1641-2019
- Nelissen V., Rütting T., Huygens D., Staelens J., Ruyschaert G., Boeckx P. 2012. Maize biochars accelerate short-term soil nitrogen dynamics in a loamy sand soil. *Soil Biology and Biochemistry*; 55: 20-27. doi:10.1016/j.soilbio.2012.05.019
- Ni B., Zhang W., Xu X., Wang L., Bol R., Wang K., Hu Z., Zhang H., Meng F. 2021. Exponential relationship between N₂O emission and fertilizer nitrogen input and mechanisms for improving fertilizer nitrogen efficiency under intensive plastic-shed vegetable production in China: A systematic analysis. *Agriculture, Ecosystems & Environment*; 312. doi:10.1016/j.agee.2021.107353
- NOAA. 2021. Trends in Atmospheric Carbon Dioxide.
- Norton J., Ouyang Y. 2019. Controls and Adaptive Management of Nitrification in Agricultural Soils. *Front Microbiol*; 10: 1931. doi:10.3389/fmicb.2019.01931
- Obia A., Cornelissen G., Mulder J., Dorsch P. 2015. Effect of Soil pH Increase by Biochar on NO, N₂O and N₂ Production during Denitrification in Acid Soils. *PLoS One*; 10: e0138781. doi:10.1371/journal.pone.0138781
- OECD. 2021. OECD Global Forum on Agriculture 2021: Policies for a more resilient agro-food sector. OECD, Paris, France.
- Oenema O., Velthof G.L. 2002. Balanced fertilization and regulating nutrient losses from agriculture. In: Steenvorden J, Claessen F, Willems J, Steenvoorden J, editors. *Agricultural effects on ground and surface waters: research at the edge of science and society*. 273. IAHS, Wageningen, The Netherlands.

- Oo A.Z., Gonai T., Sudo S., Thuzar Win K., Shibata A. 2018. Surface application of fertilizers and residue biochar on N₂O emission from Japanese pear orchard soil. *Plant, Soil and Environment*; 64: 597-604. doi:10.17221/114/2018-pse
- Øygarden L., Botterweg P. 1998. *Measuring Runoff and Nutrient Losses from Agricultural Land in Nordic Countries: A Guideline for Good Measurement Practices*. Copenhagen, Denmark: Nordic Council of Ministers.
- Parton W.J., Mosier A.R., Ojima D.S., Valentine D.W., Schimel D.S., Weier K., Kulmala A.E. 1996. Generalized model for N₂ and N₂O production from nitrification and denitrification. *Global Biogeochemical Cycles*; 10: 401-412. doi:10.1029/96gb01455
- Pasda G., Hähndel R., Zerulla W. 2001. Effect of fertilizers with the new nitrification inhibitor DMPP (3,4-dimethylpyrazole phosphate) on yield and quality of agricultural and horticultural crops. *Biology and Fertility of Soils*; 34: 85-97. doi:10.1007/s003740100381
- Pelster D.E., Chantigny M.H., Rochette P., Angers D.A., Rieux C., Vanasse A. 2012. Nitrous oxide emissions respond differently to mineral and organic nitrogen sources in contrasting soil types. *J Environ Qual*; 41: 427-35. doi:10.2134/jeq2011.0261
- Petersen S.O. 1999. Nitrous Oxide Emissions from Manure and Inorganic Fertilizers Applied to Spring Barley. *Journal of Environment Quality*; 28. doi:10.2134/jeq1999.00472425002800050027x
- Pfab H., Palmer I., Buegger F., Fiedler S., Müller T., Ruser R. 2010. N₂O fluxes from a Haplic Luvisol under intensive production of lettuce and cauliflower as affected by different N-fertilization strategies. *Journal of Plant Nutrition and Soil Science*; 174: 545-553. doi:10.1002/jpln.201000123
- Prasad R., Hobbs P.R. 2018. Efficient Nitrogen Management in the Tropics and Subtropics. In: Lal R, Stewart BA, editors. *Soil Nitrogen Uses and Environmental Impacts*, New York, NY, United States, pp. 392.
- Prommer J., Wanek W., Hofhansl F., Trojan D., Offre P., Urich T., Schleper C., Sassmann S., Kitzler B., Soja G., Hood-Nowotny R.C. 2014. Biochar decelerates soil organic nitrogen cycling but stimulates soil nitrification in a temperate arable field trial. *PLoS One*; 9: e86388. doi:10.1371/journal.pone.0086388

- Quan Z., Huang B., Lu C., Shi Y., Chen X., Zhang H., Fang Y. 2016. The fate of fertilizer nitrogen in a high nitrate accumulated agricultural soil. *Sci Rep*; 5: 21539. doi:10.1038/srep21539
- R Core Team. 2016. R: A language and environment for statistical computing. R Foundation for Statistical Computing.
- Raun W.R., Johnson G.V. 1999. Improving Nitrogen Use Efficiency for Cereal Production. *Agronomy Journal*; 91: 357-363. doi:10.2134/agronj1999.00021962009100030001x
- Ravishankara A.R., Daniel J.S., Portmann R.W. 2009. Nitrous oxide (N₂O): the dominant ozone-depleting substance emitted in the 21st century. *Science*; 326: 123-5. doi:10.1126/science.1176985
- Reay D.S., Davidson E.A., Smith K.A., Smith P., Melillo J.M., Dentener F., Crutzen P.J. 2012. Global agriculture and nitrous oxide emissions. *Nature Climate Change*; 2: 410-416. doi:10.1038/nclimate1458
- Revell L.E., Tummon F., Salawitch R.J., Stenke A., Peter T. 2015. The changing ozone depletion potential of N₂O in a future climate. *Geophysical Research Letters*; 42: 10,047-10,055. doi:10.1002/2015gl065702
- Risk N., Snider D., Wagner-Riddle C. 2013. Mechanisms leading to enhanced soil nitrous oxide fluxes induced by freeze-thaw cycles. *Canadian Journal of Soil Science*; 93: 401-414. doi:10.4141/cjss2012-071
- Rittl T.F., Butterbach-Bahl K., Basile C.M., Pereira L.A., Alms V., Dannenmann M., Couto E.G., Cerri C.E.P. 2018. Greenhouse gas emissions from soil amended with agricultural residue biochars: Effects of feedstock type, production temperature and soil moisture. *Biomass and Bioenergy*; 117: 1-9. doi:10.1016/j.biombioe.2018.07.004
- Ruser R., Flessa H., Russow R., Schmidt G., Buegger F., Munch J.C. 2006. Emission of N₂O, N₂ and CO₂ from soil fertilized with nitrate: effect of compaction, soil moisture and rewetting. *Soil Biology and Biochemistry*; 38: 263-274. doi:10.1016/j.soilbio.2005.05.005
- Ruser R., Schulz R. 2015. The effect of nitrification inhibitors on the nitrous oxide (N₂O) release from agricultural soils-a review. *Journal of Plant Nutrition and Soil Science*; 178: 171-188. doi:10.1002/jpln.201400251
- Ryden J.C. 1983. Denitrification loss from a grassland soil in the field receiving different rates of nitrogen as ammonium nitrate. *Journal of Soil Science*; 34: 355-365. doi:10.1111/j.1365-2389.1983.tb01041.x

- Saggar S., Jha N., Deslippe J., Bolan N.S., Luo J., Giltrap D.L., Kim D.G., Zaman M., Tillman R.W. 2013. Denitrification and N₂O: N₂ production in temperate grasslands: processes, measurements, modelling and mitigating negative impacts. *Sci Total Environ*; 465: 173-95. doi:10.1016/j.scitotenv.2012.11.050
- Sánchez-García M., Roig A., Sánchez-Monedero M.A., Cayuela M.L. 2014. Biochar increases soil N₂O emissions produced by nitrification-mediated pathways. *Frontiers in Environmental Science*; 2. doi:10.3389/fenvs.2014.00025
- Sanz-Cobena A., Lassaletta L., Estellés F., Del Prado A., Guardia G., Abalos D., Aguilera E., Pardo G., Vallejo A., Sutton M.A., Garnier J., Billen G. 2014. Yield-scaled mitigation of ammonia emission from N fertilization: the Spanish case. *Environmental Research Letters*; 9. doi:10.1088/1748-9326/9/12/125005
- Sarkar S., Skalicky M., Hossain A., Brestic M., Saha S., Garai S., Ray K., Brahmachari K. 2020. Management of Crop Residues for Improving Input Use Efficiency and Agricultural Sustainability. *Sustainability*; 12. doi:10.3390/su12239808
- Scheer C., Grace P.R., Rowlings D.W., Kimber S., Van Zwieten L. 2011. Effect of biochar amendment on the soil-atmosphere exchange of greenhouse gases from an intensive subtropical pasture in northern New South Wales, Australia. *Plant and Soil*; 345: 47-58. doi:10.1007/s11104-011-0759-1
- Scheer C., Rowlings D.W., Grace P.R. 2016. Non-linear response of soil N₂O emissions to nitrogen fertiliser in a cotton-fallow rotation in sub-tropical Australia. *Soil Research*; 54. doi:10.1071/sr14328
- Shcherbak I., Millar N., Robertson G.P. 2014. Global metaanalysis of the nonlinear response of soil nitrous oxide (N₂O) emissions to fertilizer nitrogen. *Proc Natl Acad Sci U S A*; 111: 9199-204. doi:10.1073/pnas.1322434111
- Shi X., Hu H., He J., Chen D., Suter H.C. 2016. Effects of 3,4-dimethylpyrazole phosphate (DMPP) on nitrification and the abundance and community composition of soil ammonia oxidizers in three land uses. *Biology and Fertility of Soils*; 52: 927-939. doi:10.1007/s00374-016-1131-7
- Simek M., Cooper J.E. 2002. The influence of soil pH on denitrification: progress towards the understanding of this interaction over the last 50 years. *European Journal of Soil Science*; 53: 345-354. doi:10.1046/j.1365-2389.2002.00461.x

- Singh B. 2018. Are Nitrogen Fertilizers Deleterious to Soil Health? *Agronomy*; 8. doi:10.3390/agronomy8040048
- Smil V. 1999. Crop Residues: Agriculture's Largest Harvest. *BioScience*; 49: 299-308. doi:10.2307/1313613
- Smith K., Bouwman L., Braatz B. 1999. N₂O: Direct Emissions from Agricultural Soils. In: IPCC, editor. Background Paper to IPCC Good Practice Guidance and Uncertainty Management in National Greenhouse Gas Inventories, pp. 361-380.
- Smith P. 2004. Carbon sequestration in croplands: the potential in Europe and the global context. *European Journal of Agronomy*; 20: 229-236. doi:10.1016/j.eja.2003.08.002
- Smith P. 2016. Soil carbon sequestration and biochar as negative emission technologies. *Glob Chang Biol*; 22: 1315-24. doi:10.1111/gcb.13178
- Smith P., Davis S.J., Creutzig F., Fuss S., Minx J., Gabrielle B., Kato E., Jackson R.B., Cowie A., Kriegler E., van Vuuren D.P., Rogelj J., Ciais P., Milne J., Canadell J.G., McCollum D., Peters G., Andrew R., Krey V., Shrestha G., Friedlingstein P., Gasser T., Grübler A., Heidug W.K., Jonas M., Jones C.D., Kraxner F., Littleton E., Lowe J., Moreira J.R., Nakicenovic N., Obersteiner M., Patwardhan A., Rogner M., Rubin E., Sharifi A., Torvanger A., Yamagata Y., Edmonds J., Yongsung C. 2015. Biophysical and economic limits to negative CO₂ emissions. *Nature Climate Change*; 6: 42-50. doi:10.1038/nclimate2870
- Smith P., Martino D., Cai Z., Gwary D., Janzen H., Kumar P., McCarl B., Ogle S., O'Mara F., Rice C., Scholes B., Sirotenko O., Howden M., McAllister T., Pan G., Romanenkov V., Schneider U., Towprayoon S., Wattenbach M., Smith J. 2008. Greenhouse gas mitigation in agriculture. *Philos Trans R Soc Lond B Biol Sci*; 363: 789-813. doi:10.1098/rstb.2007.2184
- Smith P., Powlson D., Glendining M., Smith J.O. 1997. Potential for carbon sequestration in European soils: preliminary estimates for five scenarios using results from long-term experiments. *Global Change Biology*; 3: 67-79. doi:10.1046/j.1365-2486.1997.00055.x
- Sohi S.P. 2012. Carbon storage with benefits. *Science*; 338: 1034-5. doi:10.1126/science.1225987
- Spokas K.A., Reicosky D.C. 2009. Impacts of Sixteen Different Biochars on Soil Greenhouse Gas Production. *Annals of Environmental Science*; 3: 179-193.

- Suddick E.C., Six J. 2013. An estimation of annual nitrous oxide emissions and soil quality following the amendment of high temperature walnut shell biochar and compost to a small scale vegetable crop rotation. *Sci Total Environ*; 465: 298-307. doi:10.1016/j.scitotenv.2013.01.094
- Thers H., Petersen S.O., Elsgaard L. 2019. DMPP reduced nitrification, but not annual N₂O emissions from mineral fertilizer applied to oilseed rape on a sandy loam soil. *GCB Bioenergy*; 11: 1396-1407. doi:10.1111/gcbb.12642
- Thomas C.L., Acquah G.E., Whitmore A.P., McGrath S.P., Haeefe S.M. 2019. The Effect of Different Organic Fertilizers on Yield and Soil and Crop Nutrient Concentrations. *Agronomy*; 9. doi:10.3390/agronomy9120776
- Thompson R.B., Meisinger J.J. 2002. Management factors affecting ammonia volatilization from land-applied cattle slurry in the Mid-Atlantic USA. *J Environ Qual*; 31: 1329-38. doi:10.2134/jeq2002.1329
- Thorburn P.J., Wilkinson S.N. 2013. Conceptual frameworks for estimating the water quality benefits of improved agricultural management practices in large catchments. *Agriculture, Ecosystems & Environment*; 180: 192-209. doi:10.1016/j.agee.2011.12.021
- Thornton F.C., Shurpali N.J., Bock B.R., Reddy K.C. 1998. N₂O and no emissions from poultry litter and urea applications to Bermuda grass. *Atmospheric Environment*; 32: 1623-1630. doi:10.1016/s1352-2310(97)00390-7
- Tietema A., Bouten W., Wartenbergh P.E. 1991. Nitrous oxide dynamics in an oak-beech forest ecosystem in the Netherlands. *Forest Ecology and Management*; 44: 53-61. doi:10.1016/0378-1127(91)90197-4
- Trenkel M.E. 2010. Slow- and Controlled-Release and Stabilized Fertilizers: An Option for Enhancing Nutrient Use Efficiency in Agriculture. International Fertilizer Industry Association (IFA), Paris, France.
- UNFCCC. 1997. Kyoto Protocol to the United Nations Framework Convention on Climate Change. In: (UNFCCC) UNFCCC, editor, Kyoto, Japan.
- UNFCCC. 2015. Adoption of the Paris Agreement FCCC/CP/2015/L.9/Rev.1 United Nations Framework Convention on Climate Change. In: (UNFCCC) UNFCCC, editor, 21st Conference of the Parties, Paris, France.

- Ussiri D., Lal R. 2013. Soil Emission of Nitrous Oxide and its Mitigation. Vol XVIII: Springer Netherlands.
- van der Molen J., van Faassen H.G., Leclerc M.Y., Vriesema R., Chardon W.J. 1990. Ammonia volatilization from arable land after application of cattle slurry. 1. Field estimates. Netherlands Journal of Agricultural Science; 38: 145-158. doi:10.18174/njas.v38i2.16601
- van Groenigen J.W., Kasper G.J., Velthof G.L., van den Pol-van Dasselaar A., Kuikman P.J. 2004. Nitrous oxide emissions from silage maize fields under different mineral nitrogen fertilizer and slurry applications. Plant and Soil; 263: 101-111. doi:10.1023/b:plso.0000047729.43185.46
- Velthof G.L., van Bruggen C., Groenestein C.M., de Haan B.J., Hoo-geveen M.W., Huijsmans J.F.M. 2012. A model for inventory of ammonia emissions from agriculture in the Netherlands. Atmospheric Environment; 46: 248-255. doi:10.1016/j.atmosenv.2011.09.075
- Venterea R.T., Halvorson A.D., Kitchen N., Liebig M.A., Cavigelli M.A., Grosso S.J.D., Motavalli P.P., Nelson K.A., Spokas K.A., Singh B.P., Stewart C.E., Ranaivoson A., Strock J., Collins H. 2012. Challenges and opportunities for mitigating nitrous oxide emissions from fertilized cropping systems. Frontiers in Ecology and the Environment; 10: 562-570. doi:10.1890/120062
- Verhoeven E., Pereira E., Decock C., Suddick E., Angst T., Six J. 2017. Toward a Better Assessment of Biochar-Nitrous Oxide Mitigation Potential at the Field Scale. J Environ Qual; 46: 237-246. doi:10.2134/jeq2016.10.0396
- Verhoeven E., Six J. 2014. Biochar does not mitigate field-scale N₂O emissions in a Northern California vineyard: An assessment across two years. Agriculture, Ecosystems & Environment; 191: 27-38. doi:10.1016/j.agee.2014.03.008
- Vilas M.P., Verburg K., Thorburn P.J., Probert M.E., Bonnett G.D. 2019. A framework for analysing nitrification inhibition: A case study on 3,4-dimethylpyrazole phosphate (DMPP). Sci Total Environ; 672: 846-854. doi:10.1016/j.scitotenv.2019.03.462
- Villar J.M., Guillaumes E. 2010. Use of nitrification inhibitor DMPP to improve nitrogen recovery in irrigated wheat on a calcareous soil. Spanish Journal of Agricultural Research; 8. doi:10.5424/sjar/2010084-1241
- Villar N., Aranguren M., Castellon A., Besga G., Aizpurua A. 2019. Soil nitrogen dynamics during an oilseed rape (*Brassica napus* L.)

- growing cycle in a humid Mediterranean climate. *Sci Rep*; 9: 13864. doi:10.1038/s41598-019-50347-1
- Vinzent B., Fuß R., Maidl F.-X., Hülsbergen K.-J. 2018. N₂O emissions and nitrogen dynamics of winter rapeseed fertilized with different N forms and a nitrification inhibitor. *Agriculture, Ecosystems & Environment*; 259: 86-97. doi:10.1016/j.agee.2018.02.028
- Walter K., Don A., Fuß R., Kern J., Drewer J., Flessa H. 2014. Direct nitrous oxide emissions from oilseed rape cropping – a meta-analysis. *GCB Bioenergy*; 7: 1260-1271. doi:10.1111/gcbb.12223
- Wang C., Lu H., Dong D., Deng H., Strong P.J., Wang H., Wu W. 2013. Insight into the effects of biochar on manure composting: evidence supporting the relationship between N₂O emission and denitrifying community. *Environ Sci Technol*; 47: 7341-9. doi:10.1021/es305293h
- Wang W., Park G., Reeves S., Zahmel M., Heenan M., Salter B. 2016. Nitrous oxide emission and fertiliser nitrogen efficiency in a tropical sugarcane cropping system applied with different formulations of urea. *Soil Research*; 54. doi:10.1071/sr15314
- Wang Z.-H., Li S.-X. 2019. Nitrate N loss by leaching and surface runoff in agricultural land: A global issue (a review), pp. 159-217.
- Wang Z., Zong H., Zheng H., Liu G., Chen L., Xing B. 2015. Reduced nitrification and abundance of ammonia-oxidizing bacteria in acidic soil amended with biochar. *Chemosphere*; 138: 576-83. doi:10.1016/j.chemosphere.2015.06.084
- Wei X., Chen J., Gao B., Wang Z. 2020. Chapter 39 - Role of controlled and slow release fertilizers in fruit crop nutrition. *Fruit Crops. Diagnosis and Management of Nutrient Constraints*. Elsevier Inc., Amsterdam, The Netherlands, pp. 555-566.
- Weinbaum S.A., Johnson R.S., DeJong T.M. 1992. Causes and Consequences of Overfertilization in Orchards. *HortTechnology*; 2: 112b-121. doi:10.21273/HORTTECH.2.1.112b
- Wheeler T., von Braun J. 2013. Climate change impacts on global food security. *Science*; 341: 508-13. doi:10.1126/science.1239402
- Wrage-Mönnig N., Horn M.A., Well R., Müller C., Velthof G., Oenema O. 2018. The role of nitrifier denitrification in the production of nitrous oxide revisited. *Soil Biology and Biochemistry*; 123: A3-A16. doi:10.1016/j.soilbio.2018.03.020

- Wrage N., Velthof G.L., van Beusichem M.L., Oenema O. 2001. Role of nitrifier denitrification in the production of nitrous oxide. *Soil Biology and Biochemistry*; 33: 1723-1732. doi:10.1016/s0038-0717(01)00096-7
- Wu D., Zhang Y., Dong G., Du Z., Wu W., Chadwick D., Bol R. 2021. The importance of ammonia volatilization in estimating the efficacy of nitrification inhibitors to reduce N₂O emissions: A global meta-analysis. *Environ Pollut*; 271: 116365. doi:10.1016/j.envpol.2020.116365
- Xu X., Yan L., Xia J. 2019. A threefold difference in plant growth response to nitrogen addition between the laboratory and field experiments. *Ecosphere*; 10. doi:10.1002/ecs2.2572
- Yang M., Fang Y., Sun D., Shi Y. 2016. Efficiency of two nitrification inhibitors (dicyandiamide and 3, 4-dimethylpyrazole phosphate) on soil nitrogen transformations and plant productivity: a meta-analysis. *Sci Rep*; 6: 22075. doi:10.1038/srep22075
- Yin S., Zhang X., Jiang Z., Zhu P., Li C., Liu C. 2017. Inhibitory Effects of 3,4-Dimethylpyrazole Phosphate on CH₄ and N₂O Emissions in Paddy Fields of Subtropical China. *Int J Environ Res Public Health*; 14. doi:10.3390/ijerph14101177
- Yu L., Kang R., Mulder J., Zhu J., Dörsch P. 2017. Distinct fates of atmgogenic NH₄⁺ and NO₃⁻ in subtropical, N-saturated forest soils. *Biogeochemistry*; 133: 279-294. doi:10.1007/s10533-017-0332-y
- Zaman M., Kleineidam K., Bakken L., Berendt J., Bracken C., Butterbach-Bahl K., Cai Z., Chang S.X., Clough T., Dawar K., Ding W.X., Dörsch P., dos Reis Martins M., Eckhardt C., Fiedler S., Frosch T., Goopy J., Görres C.M., Gupta A., Henjes S., Hofmann M.E.G., Horn M.A., Jahangir M.M.R., Jansen-Willems A., Lenhart K., Heng L., Lewicka-Szczebak D., Lucic G., Merbold L., Mohn J., Molstad L., Moser G., Murphy P., Sanz-Cobena A., Šimek M., Urquiaga S., Well R., Wrage-Mönnig N., Zaman S., Zhang J., Müller C. 2021. Climate-Smart Agriculture Practices for Mitigating Greenhouse Gas Emissions. *Measuring Emission of Agricultural Greenhouse Gases and Developing Mitigation Options using Nuclear and Related Techniques*, pp. 303-328.
- Zerulla W., Barth T., Dressel J., Erhardt K., Horchler von Locquenghien K., Pasda G., Rädle M., Wissemeyer A. 2001. 3,4-Dimethylpyrazole phosphate (DMPP) - a new nitrification inhibitor for agriculture and

- horticulture. *Biology and Fertility of Soils*; 34: 79-84. doi:10.1007/s003740100380
- Zhang Q., Xiao J., Xue J., Zhang L. 2020. Quantifying the Effects of Biochar Application on Greenhouse Gas Emissions from Agricultural Soils: A Global Meta-Analysis. *Sustainability*; 12. doi:10.3390/su12083436
- Zhang X., Davidson E.A., Mauzerall D.L., Searchinger T.D., Dumas P., Shen Y. 2015. Managing nitrogen for sustainable development. *Nature*; 528: 51-9. doi:10.1038/nature15743
- Zhou M., Zhu B., Brüggemann N., Bergmann J., Wang Y., Butterbach-Bahl K. 2013. N₂O and CH₄ Emissions, and NO₃⁻ Leaching on a Crop-Yield Basis from a Subtropical Rain-fed Wheat–Maize Rotation in Response to Different Types of Nitrogen Fertilizer. *Ecosystems*; 17: 286-301. doi:10.1007/s10021-013-9723-7
- Zhu X., Burger M., Doane T.A., Horwath W.R. 2013. Ammonia oxidation pathways and nitrifier denitrification are significant sources of N₂O and NO under low oxygen availability. *Proc Natl Acad Sci U S A*; 110: 6328-33. doi:10.1073/pnas.1219993110
- Zwieten L.V., Singh B., Joseph S., Kimber S., Cowie A., Chan K.Y. 2009. Biochar and Emissions of Non-CO₂ Greenhouse Gases from Soil. In: Johannes Lehmann SJ, editor. *Biochar for Environmental Management. Science and Technology*. Routledge, London.

SUMMARY IN ESTONIAN

PÕLLUMULLAST ERALDUVA DILÄMMASTIKOKSIIDI VÄHENDAMINE

Sissejuhatus

Kasvuhoonegaaside kontsentratsiooni suurenemine atmosfääris, mis on tinginud Maa globaalse soojenemisest (vt nt Mosier, 1998), on meie aja üks suurimaid keskkonnaprobleeme. Kolme peamise kasvuhoonegaasi (süsihappegaasi CO₂, dilämmastikoksiidi e naerugaasi N₂O, ja metaani CH₄) kontsentratsioon on suurenenud alates tööstusrevolutsiooni algusest (NOAA, 2021). Maalt atmosfääri lenduvast N₂O kogusest on ligikaudu 50% inimtekkeline (Ciais *et al.*, 2013), sellest omakorda umbes kaks kolmandikku on pärit põllumajandusest (Davidson ja Kanter, 2014).

Lämmastikukadu põllumajanduses, näiteks liigne N₂O lendumine ja NO₃ leostumine on suur oht keskkonnale ja põllumajanduse jätkusuutlikkusele. Globaalselt suudavad taimed omastada väetistega põllumaale viidud lämmastikust 47%, ning see suurusjärk on viimase 50 aasta jooksul vähenenud (Lassaletta *et al.*, 2014). Liu *et al.* (2016) andmetel väärindatakse lämmastikväetisest põllul saagina ainult 38% ning üle 30% läheb leostumise ja emissiooni teel mullast kaduma. Sellest tulenevalt otsitakse üha enam lahendusi, kuidas saagikust säilitades vähendada väetiste kasutamisega kaasnevat N₂O lendumist.

Nitrifikatsiooni inhibiitorid on ühendid, mis aeglustavad ammooniumi oksüdeerumist nitrititeks (Kong *et al.*, 2016). Nitrifikatsiooni aeglustamine säilitab lämmastikku NH₄⁺ kujul, mis on vähem tundlik leostumisele, ning vähendab ka lämmastiku lendumist NO, N₂O ja N₂ kujul, kuigi võib suurendada NH₃ lendumist. Varasemad uuringud on näidanud, et nitrifikatsiooni inhibiitor 3,4-dimetüülpüraasoolfosfaat (DMPP) vähendab tõhusalt N₂O lendumist (Barrena *et al.*, 2017; Di ja Cameron, 2011; Di ja Cameron, 2016; Duan *et al.*, 2017; Gilsanz *et al.*, 2016; Menéndez *et al.*, 2012; Yin *et al.*, 2017). Metaanalüüs (Yang *et al.*, 2016) näitas, et DMPP-d kasutades vähenes N₂O lendumine keskmiselt 47,6%. Teine populaarne nitrifikatsiooni inhibiitor ditsüaandiamiid (DCD) vähendas lendumist 44,7%. Nitrifikatsiooni inhibiitorite toime kohta Eesti kliimatilistes ja mullastikutingimustes tingimustes on teadmisi praegu vähe.

Biosüsi on suure süsinikusaldusega materjal, mida toodetakse orgaanilisest ainest seda hapnikuvaeses keskkonnas kuumutades (Lehmann ja Joseph, 2009; Sohi, 2012). Biosütti soovitatakse mullaparandajana, et suurendada saagikust ja vähendada lämmastikukadu N_2O lendumise ja NO_3 leostumise kaudu (Borchard *et al.*, 2019). Metaanalüüsid sedastavad biosöe kasutamise korral N_2O eraldumise keskmist vähenemist 12,4% kuni 54% (Borchard *et al.*, 2019; Cayuela *et al.*, 2014; Liu *et al.*, 2018; Verhoeven *et al.*, 2017). Kõik uurimused ei ole sellist mõju siiski täheldanud (Buchkina *et al.*, 2019; Rittl *et al.*, 2018; Scheer *et al.*, 2011; Suddick ja Six, 2013) või on tuvastatud isegi N_2O lendumise suurenemist biosöe kasutamise tagajärjel (Clough *et al.*, 2010; Verhoeven ja Six, 2014; Zwieten *et al.*, 2009). Suuremat N_2O lendumist pärast biosöe lisamist mulda seostatakse peamiselt nitrifikatsiooni suurenemisega (Sánchez-García *et al.* 2014).

Taimse biomassi muldaviimine võib soodustada kasvuhoonegaaside heidet, sest sellega lisandub mulda süsinikku ja toiteelemente, mis soodustavad mikroorganismide aktiivsust ja mulla orgaanilise süsiniku lagunemist, oksüdatsiooni ja denitrifikatsiooni (Badagliacca *et al.*, 2017). Mullast N_2O eraldumine sõltub orgaanilise aine mineraliseerumise määra. Taimejääkide lagunemismäära ja kasvuhoonegaaside heitkoguse kõige olulisem näitaja on süsiniku ja lämmastiku (C/N) suhe (Baggs *et al.*, 2000; Duan *et al.*, 2018). Madala C/N suhtega taimemassi muldaviimise korral tuvastatakse suuremaid heitkoguseid (Badagliacca *et al.*, 2017; Baggs *et al.*, 2000).

Eesmärgid ja hüpoteesid

Doktoritöö eesmärk on avardada põllumajanduses teadmisi N_2O lendumise mehhanismide ja eraldumise vähendamise strateegiate kohta, eriti orgaaniliste väetiste ja lisandite kasutamise korral. Uurimistöö annab uudset teadmist biosöe, taimejäänuste ja nitrifikatsiooni inhibiitori mõjust N_2O lendumisele ning käsitleb Eestis esmakordselt empiirilist tõendust agroökosüsteemi olulisematest lämmastikuvoogusid intensiivselt majandatud rapsipõllu näitel. Töö eesmärgid on:

1. uurida biosöe (I) ja nitrifikatsiooni inhibiitori (III) mõju N_2O eraldumise vähendamisel;
2. määrata erinevate taimejäänuste muldaviimise mõju N_2O lendumisele (II);
3. analüüsida N_2O mullast eraldumist talirapsipõllul kogu kasvuperioodi vältel (IV).

Eesmärkide saavutamiseks püstitati järgmised hüpoteesid.

1. Mullaomaduste parandamine biosöe abil vähendab N_2O eraldumist mullast; eraldumise vähendamise mõju on erinev ja sõltub biosöe tootmise temperatuurist (**I**).
2. Rapsi, rukki ja nisu biomassi muldaviimisega kaasnevad erinevad N_2O heitkogused olenevalt C/N suhtest (**II**).
3. Nitrifikatsiooni inhibiitori DMPP lisamine lägale vähendab N_2O eraldumist mullast (**III**).
4. Orgaaniliste ja mineraalväetiste kasutamine on N_2O eraldumise peamine põhjus talirapsi kasvatamisel (**IV**).

Materjal ja meetodika

Katsed viidi läbi aastatel 2016–2020 labori- ja välitingimustes eesmärgiga selgitada välja N_2O lendumist mullast pärast erinevate väetis- ja lisainete muldaviimist.

Laborkatses (**I**) testiti erineva tootmistemperatuuriga biosöe tõhusust N_2O mullast lendumise vähendamiseks väetamata mullas, ning kombinatsioonis kolme orgaanilise väetisega (veiseläga, läga kääritusjääk ja vinass). Orgaaniliste väetiste kasutusnorm oli $27,4 \text{ t ha}^{-1}$ veiseläga ja läga kääritusjäägi korral, ning $1,8 \text{ t ha}^{-1}$ vinassi kasutamisel.

Mulda segati kolme erinevat luhahaina biomassist toodetud biosütt ($915,8 \text{ g m}^{-2}$): (i) $300 \text{ }^\circ\text{C}$ (BC300) temperatuuril torrefikatsioonil, (ii) $550 \text{ }^\circ\text{C}$ (BC550) temperatuuril pürolüüsil, (iii) $850 \text{ }^\circ\text{C}$ (BC850) temperatuuril pürolüüsil. Kahe viimase biosöe lähtematerjaliks oli eelnevalt $300 \text{ }^\circ\text{C}$ juures torrefitseeritud süsi. Biosöe pH oli BC300, BC550 ja BC850 puhul vastavalt 6,8; 10,8 ja 11,8, ning C/N suhe oli 19,0; 22,6 ja 26,6 (**I**, tabel 2).

Teises laborkatses (**II**) kasutati kolme sorti taimemassi: rapsi ja rukki maa-pealset haljasmassi ning nisupõhku. Taimejäänused hakiti 4 cm pikkus-teks tükkideks ja viidi mulda keskmise normiga 6 g C kg^{-1} . Rapsi, rukki ja nisu biomassi C/N suhe oli vastavalt 10, 12 ja 98.

Nitrifikatsiooni inhibiitori DMPP tõhusust N_2O eraldumise vähendamiseks pärast piimalehmade läga muldaviimist katsetati Kesk-Eestis (**III**, Kehtna, Raplamaa, $58^\circ55'21''\text{N}$, $24^\circ50'52''\text{E}$) talirapsipõllul (*Brassica napus* 'DK Sequoia'). Kontrollalal viidi mulda ainult läga koguses 30 t ha^{-1} ; katselapil segati läga nitrifikatsiooni inhibiitoriga DMPP koguses 3 l ha^{-1} .

Kasvuperioodil 2017. a lisati kolmel korral ka mineraalväetist: 4. aprillil 250 kg ha⁻¹ kaltsiumammooniumnitraati (CAN) 27; 1. mail 160 kg ha⁻¹ ammooniumsulfaatnitraati (ASN) 26N+13S, ja 8. mail 160 kg ha⁻¹ ASN 26N+13S. Samal katses hinnati ka kogu talirapsi kasvuperioodi N bilanssi (IV).

Tulemused ja arutelu

Orgaanilise väetise lisamine mulda suurendas N₂O eraldumist (I, joonis 2 ja 4), kusjuures orgaaniliste väetiste vahel olulisi erinevusi ei täheldatud. N₂O keskmine voog orgaaniliste väetistega segatud mullast oli vahemikus 4,33 ± 1,11 ja 7,52 ± 1,32 µg N m⁻² h⁻¹, ning N₂O voog väetamata mullast oli nõrgalt negatiivne (-1,27 ± 0,62 µg N m⁻² h⁻¹).

Biosöe lisamine suurendas laboritingimustes nõukatses mulla N₂O voo näitajaid. Kuid tunduvalt suuremad olid vood võrreldes kontrolliga ainult kõige kõrgema tootmistemperatuuriga biosöe korral (BC850; I, joonis 3), ning keskmine voog oli 1,13 ± 0,63 BC300, 1,87 ± 1,05 BC550 ja 7,97 ± 1,35 µg N m⁻² h⁻¹ BC850.

Nõukatse kontrollvariandi ja nisupõhuga võrreldes olid rapsi ja rukki biomassi muldaviimisel N₂O vood mullast märgatavalt suuremad, kuid neil ei olnud omavahel märgatavat erinevust (vastavalt 911,70 ± 59,97 ja 1087,95 ± 91,83 µg N m⁻² h⁻¹; II, joonis 3). Kõige suurem voog mõõdeti rukki biomassi lisamisel (6039 µg N m⁻² h⁻¹), millele järgnes raps (3346 µg N m⁻² h⁻¹). Kontrolli ja nisupõhuga töödeldud mulla N₂O vood ei erinevad märgatavalt (vastavalt 14,02 ± 0,94 ja 11,80 ± 1,42 µg N m⁻² h⁻¹).

Talirapsi põldkatses mõõdeti katseaasta jooksul ainult kolmel korral märkimisväärset N₂O emissiooni mullast: esimesel korral vahetult pärast läga muldaviimist, seejärel registreeriti esimesel 50 päeval pärast läga muldaviimist üle poole N₂O voogudest (III, joonis 2), ning kaks väiksemat tippu 2016. a detsembris ja 2017. a märtsis–aprillis (IV, joonis 1 ja joonis 2).

Kontrollalal ja katselapil oli esimese 42 päeva keskmine N₂O voog vastavalt 1180,11 ± 75,44 ja 1700,75 ± 93,03 µg N m⁻² h⁻¹; keskmised vood kogu kasvuperioodil olid 24,49 ± 12,36 ja 335,59 ± 16,50 µg N m⁻² h⁻¹. Mõõdetud voogude maksimaalsed tipud olid kontrollalal 6433 ja katselapil 6514 µg N m⁻² h⁻¹.

Põld- ja laborkatsete tulemused kinnitasid, et mullast N₂O eraldumise tipp seostub läga muldaviimisega (I, III, IV). Põldkatsel toimus ligikaudu 55% N₂O kogueraldumisest 42 päeva jooksul pärast läga muldaviimist (III, IV). Samades tingimustes erinevate orgaaniliste väetiste muldaviimisel ei tuvastatud N₂O eraldumises olulisi erinevusi (I, joonis 2).

Biosöe kasutamine tekitab suuremat N₂O eraldumist. Kolme erineva tootmistemperatuuriga biosöe suur lämmastikusisaldus ja madalad C/N näitajad (I, tabel 2) võivad olla põhjuseks, miks N₂O eraldumine ei vähene. Spokas ja Reicosky (2009) andmetel suurendab suure lämmastikusisalduse, väga labiilse orgaanilise aine ja väikese C/N suhtega biosüsi N₂O eraldumist. Clough *et al.* (2013) näitasid, et biosüsi võib suurendada N₂O eraldumist, kui mullaniiskus on denitrifikatsiooniks piisav ning biosöest vabaneb rohkesti süsinikku ja lämmastikku.

Nitrifikatsiooni inhibiitori tõhusust põldkatses vähendas läga muldaviimise järgne denitrifikatsioonist tulenenud N₂O eraldumine, mis oli tingitud suurest mullaniiskusest. Tugevate vihmasadude periood, mis algas läga ja DMPP muldaviimise päeval, muutis mulla niiskustingimusi. Mitme uurimuse kinnitusele on N₂O vihmajärgse eraldumise peamine põhjus denitrifikatsioon (Cantarel *et al.*, 2010; Herr *et al.*, 2020; Thornton *et al.*, 1998). Teised tegurid, näiteks labiilse süsiniku lisamine lägale ning eelmise aasta taimejäänuste mineraliseerumine suurendavad denitrifikatsiooni (Beck ja Christensen, 1987; Herr *et al.*, 2020; Saggar *et al.*, 2013).

Rapsi ja rukki biomassi muldaviimine suurendas tunduvalt N₂O eraldumist, erinevalt nisupõhu muldaviimisest (II, joonis 3). Muldaviidud taimejäänuste mineraliseerumise tagajärjeks oli N₂O eraldumine (Duan *et al.*, 2018). C/N suhe mõjutab mineraliseerumise kiirust (Villar *et al.*, 2019), mis omakorda mõjutab substraatide kättesaadavust nitrifikatsiooniks ja denitrifikatsiooniks, mis viib N₂O eraldumiseni (Chen *et al.*, 2013; Hansen *et al.*, 2019). *Brassica* liikide ja rukki massi iseloomustab madal C/N suhe, eriti võrreldes nisupõhuga (II, tabel 2), soodustades lagunemist ning süsiniku ja lämmastiku vabanemist (Akkal-Corfini *et al.*, 2009). Chen *et al.* (2013) leidsid metaanalüüsis, et taimemass, mille C/N suhe on alla 45, suurendas pärast muldaviimist märgatavalt N₂O mullast eraldumist.

Põldkatses tuvastati lisaks orgaanilisele väetamisele järgnenud tipule (2016. a augustis) ainult kaks teist N₂O mullast eraldumise tippu (2016. a detsembris ja 2017. a märtsis–aprillis). Suuremaid emissioonikoguseid

mõõdeti ajal, kui temperatuur kõikus 0 °C juures (IV, joonis 3), seostudes jäätumis-sulamistsükliga. Mineraalväetiste kasutamise järel märgatavaid N₂O mullast eraldumise tippe ei täheldatud (IV, joonis 1).

Peamised järeldused

1. Orgaaniliste väetiste kasutamine (veiseläga, läga kääritusjääk, vinass) andis kõigil juhtudel suurema N₂O heite mullast kui töötlemata mullaga kontrollvariandis. Samades mullastiku- ja katsetingimustes ei leitud orgaaniliste väetiste vahel olulisi erinevusi.
2. Mineraalväetise (kaltsiumammooniumnitraadi ja ammooniumsulfaatnitraadi) muldaviimine ei põhjustanud suuremaid N₂O vooge mullast.
3. Rapsi ja rukki värske biomassi muldaviimine suurendas N₂O lendumist, ent nisupõhu mulda lisamine emissiooni ei suurendanud. Värske biomassi suurem lagunemismäär, mis seostus madalama C/N suhtega ja seetõttu suurema substraadihulgaga nitrifikatsiooni ja denitrifikatsiooni protsessiks, tekitas suuremad N₂O vood.
4. Vastupidiselt paljudele varasematele uuringutele põhjustas biosöe muldaviimine suuremaid N₂O vooge, kuigi suurenemine oli kõige märgatavam vaid kõrgeima tootmistemperatuuriga biosöe puhul (850 °C). See oli seotud uuritud biosöe suure lämmastikusisaldusega ja madala C/N suhtega, mis põhjustas toitainete adsorbeerimise asemel nende vabanemist.
5. Nitrifikatsiooni inhibiitori DMPP tõhusust vähendas läga muldaviimisele järgnenud intensiivne vihma periood, mida näitasid N₂O vood mullast.

Käesoleva uurimuse tulemused olid esimesed, mis otseselt kvantifitseerisid põllumulla N₂O heitkoguseid Eestis ning avardasid teadmisi nitrifikatsiooni inhibiitori DMPP ja biosöe potentsiaalset N₂O heitkoguste reguleerimisel. Kuigi DMPP ja biosöe kasutamist lämmastikukao vähendamiseks on varemgi uuritud, siis siinsed tulemused näitavad, et nende positiivne mõju ei pruugi kliimaatilistes ja mullastikutingimuste tõttu avalduda.

ACKNOWLEDGEMENTS

Aquesta tesi està dedicada als meus pares.

First of all, I would like to express my deepest gratitude to my supervisors for helping me and guiding me all the way until here. I would like to thank Ass. Prof. Merrit Shanskiy for giving me the opportunity to start this journey, Ass. Prof. Kaido Soosaar for making me a part of several exciting projects, and Prof. Alar Astover for making me a part of his team.

I want to thank everybody at the Chair of Soil Science, for their help and support, especially with the lab work.

I would like to thank all the co-authors in the papers where I was the lead author, without whose contribution the papers would not have been possible. A special thanks to Prof. Krista Lõhmus for sharing her knowledge. I would also like to thank everybody who allowed me to contribute to their work as a co-author.

I would also like to thank Prof. Ülo Mander, for the help in the manuscripts that are part of this thesis but also for allowing me to collaborate with his team, and everybody in the Chair of Physical Geography and Landscape Ecology of Tartu Ülikool.

I would like to thank my wife for her unconditional support, and my family both in Estonia and in Catalonia. Also, to my friends for their comprehension, and advise.

This research was funded by the Estonian Research Council and the EU through the European Regional Development Fund (Centre of Excellence EcolChange, Estonia).

This work was also supported by the Archimedes Foundation, through the Dora Plus programme, funding the participation in international conferences.

I would also like to thank Marko Satsi and Kehtna Mõisa OÜ for their help in the field experiment.

ORIGINAL PUBLICATIONS

I Escuer-Gatius, J., Shanskiy, M., Soosaar, K., Astover, A., Raave, H. 2020. High-Temperature Hay Biochar Application Into Soil Increases N₂O Fluxes. *Agronomy* 10(1), 109.

Article

High-Temperature Hay Biochar Application into Soil Increases N₂O Fluxes

Jordi Escuer-Gatius ^{1,*}, Merrit Shanskiy ¹, Kaido Soosaar ², Alar Astover ¹ and Henn Raave ¹

¹ Institute of Agricultural and Environmental Sciences, Estonian University of Life Sciences, 51006 Tartu, Estonia; merrit.shanskiy@emu.ee (M.S.); alar.astover@emu.ee (A.A.); henn.raave@emu.ee (H.R.)

² Department of Geography, Institute of Ecology and Earth Sciences, University of Tartu, 50090 Tartu, Estonia; kaido.soosaar@ut.ee

* Correspondence: Jordi.EscuerGatius@emu.ee

Received: 27 November 2019; Accepted: 8 January 2020; Published: 11 January 2020



Abstract: Biochar has been proposed as an amendment that can improve soil conditions, increase harvest yield, and reduce N losses through NO₃[−] leaching and N₂O emissions. We conducted an experiment to test the hay biochar mitigation effect on N₂O emissions depending on its production temperature. The pot experiment consisted of the soil amendment with three different production temperature biochars (300 °C, 550 °C, 850 °C) alone and in combination with three different organic fertilizers (cattle slurry, slurry digestate, vinasse), in growth chamber conditions. The effects of biochar and fertilizer were both significant, but the interaction biochar:fertilizer was not. The amendment with the three fertilizer types and with the highest production temperature biochar resulted in significantly higher cumulative N₂O fluxes. Biochar did not show a mitigation effect on N₂O emissions when applied with organic fertilizer. Cumulative emissions were higher with biochar addition, with increasing emissions for increasing biochar production temperature. Our results support the idea that biochar cannot be considered as a universal tool for the reduction of N₂O emissions.

Keywords: carbon; denitrification; nitrification; nitrous oxide; fertilization; pyrolysis

1. Introduction

The urge to reduce emissions of greenhouse trace gasses (GHG) is generally acknowledged [1], with special focus on nitrous oxide (N₂O) due to its high global warming potential [2], and for being the main ozone-depleting substance [3]. Anthropogenic sources of N₂O account for almost 40% of global emissions, of which, agriculture represents 67%–80% [4]. Nitrogen fertilization, both organic and inorganic, is the main factor explaining the contribution of agriculture to N₂O emissions [4,5].

N₂O emissions from the soil are the product of two main processes: nitrification and denitrification [6,7]. Soil water content, soil temperature, soil pH, soil ammonium and nitrate content and carbon (C) availability are some of the key factors that regulate the prevalence of one of these processes as well as its importance.

Organic fertilization is the main fate of manure slurry [8], a by-product of livestock farms rich in NH₄⁺, but it has been found to produce higher N₂O emissions than synthetic fertilizer for the same amount of applied nitrogen [9,10]. Slurry digestate is the by-product of anaerobic digestion of slurry, also used for fertilization [11], and can have a higher NH₄⁺ content than the original slurry [12]. Digestion of slurry reduces emissions of CH₄ [13] but does not significantly reduce N₂O emissions [14]. Vinasse is usually the by-product of sugar and ethanol production and it has also been reported to have higher N₂O emissions than inorganic fertilizers [15,16].

Biochar, a carbon-rich material produced from organic matter by heating under low oxygen conditions (pyrolysis) [17,18], has been proposed as an amendment that can improve soil conditions and increase crop yield, especially for soils with small cation exchange capacity and low organic carbon content and pH [19,20], but also reduce N losses through NO_3^- leaching and N_2O emissions into the atmosphere [21].

Recent meta-analyses have reported average reductions of N_2O emissions for lab and field experiments between 32% and 54% [21–23] after biochar application. However, there are also studies indicating no effect from biochar application on N_2O emissions [24–27] as well as increased emissions [28–30], and studies showing opposite outcomes by applying the same biochar to different soils [31–33].

The mechanisms by which biochar amendment reduces N_2O emissions are not completely understood [30], and different hypothesis have been proposed: NO_3^- immobilization by biochar [21], reduction of organic matter degradation and soil C mineralization, a reduction that increases as biochar production temperature increases [34], and alteration of the microbial denitrifying communities [35], including the increase in abundance of N_2O reductase bacteria, resulting in a reduced $\text{N}_2\text{O}:\text{N}_2$ ratio [36], likely due to the increase of soil pH after biochar application [37,38]. Biochar can also sequester C [21,39,40], reducing available labile C, which is one of the factors controlling denitrification. On the other hand, it has been reported that biochar amendment can increase N_2O emissions [33,41], what has been generally associated to an enhancement of nitrification [13,24]. Results of previous studies suggest that the effect of biochar on N_2O fluxes depends on its properties, which are influenced by feedstock material and pyrolysis temperature [42,43], with a key role of pyrolysis temperature as it influences biochar surface area and aromaticity [44], as well as pH [45], capacity to adsorb NO_3^- and NH_4^+ [23,46], and C sequestration [47]. The big variability in the effect on N_2O emissions reported for different types of biochar, depending of its feedstock, production temperature, and method, highlights the need for a comprehensive study of different types of biochar and its effect on N_2O emissions [48], especially in combination with other soil amendments commonly used in agriculture, like organic fertilizers.

We studied N_2O emissions from a soil amended with pelletized hay biochar produced at three different temperatures (300 °C, 550 °C, and 850 °C) and three organic fertilizers (cattle slurry, yeast industry residue vinasse, and slurry digestate) separately and in mixture.

We hypothesized that: (i) organic fertilizer would produce higher emissions, (ii) hay biochar application would result in reduced N_2O emissions both for fertilized and unfertilized soil, and (iii) the effect of biochar on N_2O emissions would depend on its production temperature.

2. Materials and Methods

2.1. Experimental Design

The experiment was conducted in a growing chamber in the Institute of Agricultural and Environmental Sciences of the Estonian University of Life Sciences, between June and August of 2017, under controlled conditions over 60 days. Two treatments were applied, biochar production temperature and type of organic fertilizer, each consisting in four different levels: control and biochar produced at 300 °C, 550 °C, and 850 °C (hereafter Control, BC300, BC550, and BC850, respectively) for biochar production temperature, control, cattle slurry, slurry digestate, and vinasse (hereafter Control, CS, SD, and VN, respectively), for the type of organic fertilizer, and pure soil.

Pots built from polyvinyl chloride (PVC) were used in the experiment. The dimensions of the pots were 110 mm diameter and 30 cm height, and the volume of soil in the pots was 2.4 L.

The substrate in the pots was divided in two layers: a lower layer (depth between 10 and 27 cm) of 2000 g of air-dry soil, and an upper layer (depth between 0 and 10 cm), where 1200 g of soil was mixed with biochar and/or organic fertilizer depending on the treatment. The characterization of this layer for the 16 combinations of the factor treatments can be found in Table 1. The amount of manure

applied was derived from common practices for croplands in the Baltic region [49]. The weight of fertilizer amendment was 0.053% for VN and 0.813% for CS and SD of the total weight of un-amended soil. The amount of biochar applied is the most common application rate [50]. The weight of biochar represented 0.272% of the total un-amended soil weight for all treatments.

Table 1. Mixture for the 0–10 cm depth layer for each of the treatments and amount of applied biochar and/or fertilizer (g m^{-2}). BC300: torrefied granules at 300 °C, BC550: BC300 pyrolyzed at 550 °C, BC850: BC300 pyrolyzed at 850 °C, CS: cattle slurry, SD: slurry digestate, VN: vinasse.

Treatment	0–10 cm Depth
Soil (S)	Soil without fertilizer or BC
S + CS	Soil + CS (2736 g m^{-2})
S + SD	Soil + SD (2736 g m^{-2})
S + VN	Soil + VN (178.9 g m^{-2})
S + BC ₃₀₀	Soil + BC ₃₀₀ (915.8 g m^{-2})
S + BC ₃₀₀ + CS	Soil + BC ₃₀₀ (915.8 g m^{-2}) + CS (2736 g m^{-2})
S + BC ₃₀₀ + SD	Soil + BC ₃₀₀ (915.8 g m^{-2}) + SD (2736 g m^{-2})
S + BC ₃₀₀ + VN	Soil + BC ₃₀₀ (915.8 g m^{-2}) + VN (178.9 g m^{-2})
S + BC ₅₅₀	Soil + BC ₅₅₀ (915.8 g m^{-2})
S + BC ₅₅₀ + CS	Soil + BC ₅₅₀ (915.8 g m^{-2}) + CS (2736 g m^{-2})
S + BC ₅₅₀ + SD	Soil + BC ₅₅₀ (915.8 g m^{-2}) + SD (2736 g m^{-2})
S + BC ₅₅₀ + VN	Soil + BC ₅₅₀ (915.8 g m^{-2}) + VN (178.9 g m^{-2})
S + BC ₈₅₀	Soil + BC ₈₅₀ (915.8 g m^{-2})
S + BC ₈₅₀ + CS	Soil + BC ₈₅₀ (915.8 g m^{-2}) + CS (2736 g m^{-2})
S + BC ₈₅₀ + SD	Soil + BC ₈₅₀ (915.8 g m^{-2}) + SD (2736 g m^{-2})
S + BC ₈₅₀ + VN	Soil + BC ₈₅₀ (915.8 g m^{-2}) + VN (178.9 g m^{-2})

The soil used in the experiment was a sandy loam (73% sand, 22% silt, 5% clay) excavated from the A horizon of a permanent grassland on Dystric Endostagnic Glossic Retisol (Colluvic) (FAO World Reference Base). Soil pH_{KCl} was 4.46, and N_{tot} , C_{tot} , P_{tot} , K_{tot} , Ca_{tot} , and Mg_{tot} concentrations were 0.7, 12.4, 0.214, 0.715, 0.538, and 1.48 g kg^{-1} , respectively.

2.2. Biochar

Hay from a permanent grassland dominated by reed canary grass (*Phalaris arundinacea* L.), cut at the seed ripening phase, was pressed into granules of 10–20 mm in length and 7 mm diameter. These granules were torrefied in the Fraunhofer Institute in Germany (Fraunhofer Institute for Environmental, Safety, and Energy Technology, Sulzbach-Rosenberg, Germany) at a temperature of 300 °C. Torrefaction is a mild pyrolysis, with lower temperatures, but also in the absence of oxygen [51,52]. These torrefied granules (hereafter BC300) were afterward pyrolyzed at 550 °C or 850 °C (hereafter BC550 and BC850, respectively) in the Lithuanian Energy Institute (Lietuvos Energetikos Institutas, Kaunas, Lithuania). The pyrolysis was performed with a slow pyrolysis reactor under laboratory conditions. A container filled with 22 L of the torrefied hay pellets was inserted into the furnace. Before heating, N_2 , at a rate of 15 L min^{-1} , was blown through the bottom of the furnace. The furnace was kept at the desired temperature (550 or 850 °C) for one hour. After the pyrolysis, the resulting biochar was left to cool in a closed device for 24 h. The pH for the different biochars ranged from 6.8 for BC300 to 11.8 for BC850 and the C/N ratio from 19.0 for BC300 to 26.6 for BC850 (Table 2). Further details of the different biochar properties can be found in Raave et al. [53].

Table 2. Biochar physical and chemical properties. BC300: torrefied granules at 300 °C, BC550: BC300 pyrolyzed at 550 °C, BC850: BC300 pyrolyzed at 850 °C.

Parameter	BC300	BC550	BC850
pH	6.8	10.1	11.8
Ash content (%)	10.4	20.3	23.0
Neutralization ability, CaCO ₃ (%)	4.35	8.15	8.11
Surface area (BET) ¹ (m ² g ⁻¹)	0.99	3.91	6.17
Cumulative pore volume (DFT) ² (cm ³ g ⁻¹)	0.002	0.018	0.008
N _{tot} (%)	2.82	2.92	2.56
C _{tot} (%)	53.5	65.9	68.1
C/N	19.0	22.6	26.6
P _{tot} (%)	0.24	0.54	0.60
K _{tot} (%)	2.28	4.62	5.10
Ca _{tot} (%)	0.93	2.11	2.44
Mg _{tot} (%)	0.47	0.93	1.03

¹ BET: Brunauer-Emmett-Teller method. ² DFT: density functional theory method.

2.3. Fertilizers

The fertilizers used in the experiment were cattle slurry (CS), yeast industry residue vinasse (VN), and cattle slurry digestate (SD). The pH of the three fertilizers was 4.5, 7.5, and 7.9 for vinasse, cattle slurry, and slurry digestate respectively (Table 3), and the NH₄⁺-N content ranged between 0.214 for cattle slurry and 0.27 (%) for vinasse, with no detectable presence of NO₃⁻-N.

Table 3. Dry Matter, pH_{KCl}, and nutrient content of the three fertilizers.

	Cattle Slurry	Slurry Digestate	Vinasse
Dry Matter (%)	10.7	7.1	67.0
pH	7.5	7.9	4.5
NH ₄ ⁺ -N (%) ¹	0.214	0.257	0.27
NO ₃ ⁻ -N (%) ¹	<md	<md	nd
P (%) ²	0.112	0.102	0.101
K (%) ²	0.362	0.302	13.25
Ca (%) ²	0.182	0.162	2.061
Mg (%) ²	0.066	0.041	0.161

¹ content in fresh material; ² content in dry matter. md: minimum detectable concentration, nd: not detected.

The combination of the amount of fertilizer applied (Table 1) and the dry matter content in each fertilizer results in the total amount of dry matter applied (cattle slurry: 29,275 kg/m²; slurry digestate: 19,425 kg/m²; vinasse: 11,986 kg/m²).

2.4. Cover Crop

The vegetation cover consisted of ryegrass (*Lolium perenne* L.). Into each pot, 100 ryegrass seeds were sown, after filling the pots with the substrate and watering to field capacity. During the experiment, the growth room air temperature was kept at 17 °C and air relative humidity at 60%, with a 13:11 h light:dark cycle. All pots were watered with the same amount of water three times a week, at a rate of 125 mL pot⁻¹ during the first growing period (0–30 days) and 150 mL pot⁻¹ during the second growing period (30–60 days). The water amount was calculated to avoid leaching and adjusted according to plant biomass size. Plants were harvested at the end of each growing period. The week before harvesting, watering was increased by 25 mL pot⁻¹.

2.5. Flux Measurements

Flux measurements were carried out by the static closed chamber method [54] between June and August of 2017. The PVC chambers had the same dimensions as the pots, with 110 mm diameter and 30 cm height, and a total volume of 2.4 L. They were designed to fit inside the neck of the pots, achieving a hermetic sealing. The chambers had two holes, one for the sample extraction pipe, and the second for the temperature sensor. Trace gas measurements were carried out weekly, always the next day after watering to assure that the pots had a similar moisture level during all measurement dates.

Gas samples were collected during one hour in 20 min intervals (0, 20, 40, 60 min) into 12 mL pre-evacuated (0.04 mbar) bottles [55].

The gas concentration in the collected air was determined using the Shimadzu GC-2014 gas chromatography system (Shimadzu Corporation, Kyoto, Japan) equipped with an electron capture detector (ECD) and a flame ionization detector (FID). The system is based on the automated gas chromatographic system described by Loftfield et al. [56] and is located in the Department of Geography of the Institute of Ecology and Earth Sciences at the University of Tartu (Estonia).

The N_2O flux was calculated from the slope of the least-squares linear regression of the N_2O concentrations versus time [57,58], using the equation:

$$f = \frac{dC}{dt} \cdot \frac{V}{A} \quad (1)$$

where f is the flux of N_2O ($\text{ppm}[\text{v}] \text{ s}^{-1} \text{ m}^{-2}$), C is the N_2O concentration in the chamber headspace ($\text{ppm}(\text{v})$), t is time (s), V is the volume of the chamber headspace (m^3), and A is the surface entailed by the chamber (m^2). Thus, dC/dt is the rate of change in concentration with time ($\text{ppm}(\text{v}) \text{ s}^{-1}$).

Three replicates for each of the treatments were sampled. The adjusted R^2 value of the linear regression is used to check the quality of the chamber measurement, and if necessary, one of the observations is discarded, using the remaining three for the linear fit [58].

The cumulative flux was calculated as the time-integration of the total daily fluxes, after gap-filling by linear interpolation between measurement points [59].

2.6. Fourier Transformed Infrared Spectrophotometer (FTIR) Analysis

Fourier transformed infrared spectrophotometer (FTIR) analyses of the different biochars was carried out using the Thermo-Nicolet iS10 Fourier transformed infrared spectrophotometer (FTIR, Thermo Fisher Scientific, Waltham, MA, USA), with a 4 cm^{-1} resolution over the range from 4000 to 400 cm^{-1} , and 32 scans per analysis. The resulting spectra were corrected against the ambient air spectrum as background, applying an automated baseline correction.

2.7. Statistical Analysis

Statistical analyses were carried out using R programming language [60]. The fulfillment of test assumptions was checked prior to analysis. A three-way analysis of variance (ANOVA) was performed to study the effect of biochar, fertilizer, and number of days and the interaction between them. A post-hoc Tukey's HSD (honest significant difference) analysis was performed after ANOVA to discriminate between groups for each treatment factor, with the package 'agricolae' in R [61]. The Pearson correlation coefficient was used for correlation analysis. Correlation analysis for fertilizer properties was performed after weighing, according to the application rate to compensate for the different amount of fertilizer applied, and for the differences in dry matter content. Cumulative fluxes are represented by box-and-whisker plots according to the conventions described by Tukey [62].

3. Results

The biochar and fertilizer amendment significantly increased N_2O emissions (Table 4, Figure 1). The effect of both factors ($\omega^2 = 0.039$ and $\omega^2 = 0.037$, for biochar and fertilizer) was similar. Among organic

fertilizers, the three studied fertilizers (CS, SD, and VN) had a significant impact on N₂O emissions (Figure 2). N₂O emissions between the three organic fertilizer treatments were not significantly different ($p > 0.05$) (Figure 1).

Table 4. Results of the three-way analysis of variance (ANOVA) and effect size (ω^2) testing the effects of biochar production temperature (BC), applied fertilizer type (FERT), days since beginning of the application of fertilizer (TIME), and the interactions between these factors on N₂O fluxes for the full duration of the experiment. † Stars indicate significance: ***: 0.001; **: 0.01; *: 0.05; ns: not significant.

	Df	Sum of Squares	Mean Square	F Value	Pr(>F)	Significance †	ω^2
BC	3	7057	2352	25.11	4.82×10^{-14}	***	0.039
FERT	3	6696	2232	23.824	2.02×10^{-13}	***	0.037
TIME	6	92,000	15,333	163.674	$<2 \times 10^{-16}$	***	0.529
BC:FERT	9	602	67	0.714	0.6957	ns	0.000
BC:TIME	18	17,973	999	10.658	$<2 \times 10^{-16}$	***	0.094
FERT:TIME	18	20,224	1124	11.993	$<2 \times 10^{-16}$	***	0.107
BC:FERT:TIME	54	7223	134	1.428	0.0392	*	0.012
Residuals	224	20,985	94				0.182

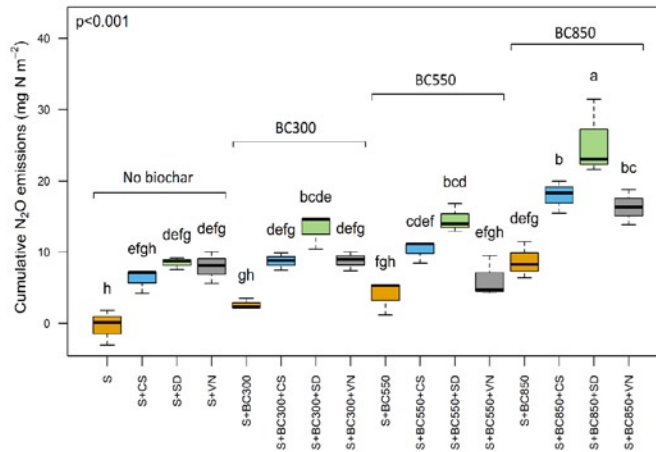


Figure 1. Total cumulative N₂O fluxes (mg N m⁻²) for each treatment (S: Soil; BC300: biochar produced at 300 °C; BC550: biochar produced at 550 °C; BC850: biochar produced at 850 °C; CS: cattle slurry; SD: slurry digestate; VN: vinasse) for the considered period (20 days). Different letters indicate different groups according Tukey’s honest significant difference (HSD) test ($\alpha = 0.05$). p -value for two-way ANOVA for biochar temperature production and fertilizer type. Colors indicate fertilizer treatment (orange: no fertilizer; blue: cattle slurry; green: slurry digestate; and gray: vinasse).

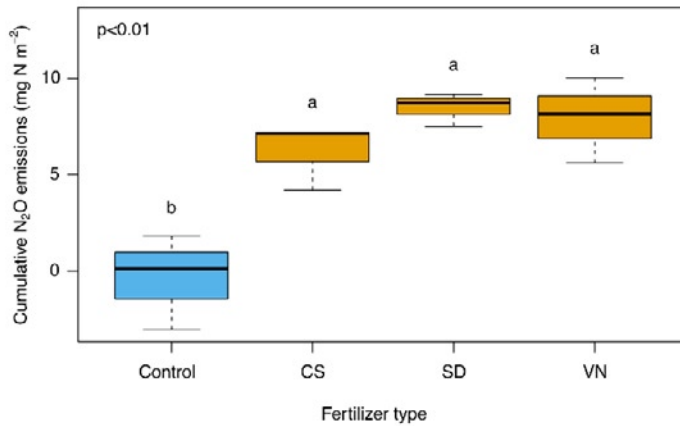


Figure 2. Total cumulative N₂O fluxes (mg N m⁻²) for the different studied fertilizers (Control: soil; CS: cattle slurry; SD: slurry digestate; VN: vinasse) without biochar amendment for the considered period (20 days). *p*-value for one-way ANOVA for fertilizer type.

The effect of biochar on N₂O emissions was influenced by its production temperature and increased with it (Figure 1), but only fluxes from BC850 differed significantly from the control. Emissions from BC850 were also significantly higher than those of BC300 ($p < 0.05$), but not from those of BC550 (Figure 3).

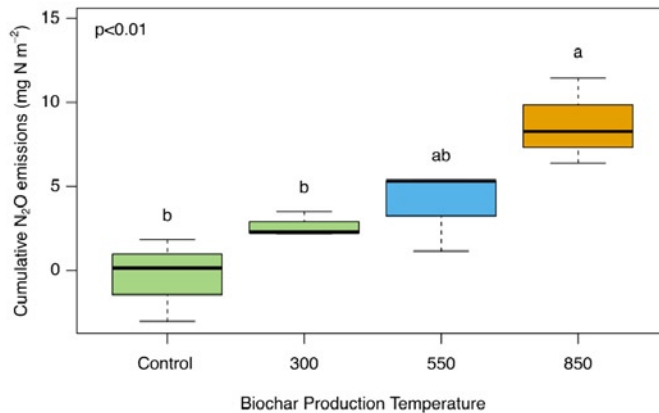


Figure 3. Total cumulative N₂O fluxes (mg N m⁻²) for the different production temperatures of biochar (Control: soil; BC300: biochar produced at 300 °C; BC550: biochar produced at 550 °C; BC850: biochar produced at 850 °C) without fertilizer for the considered period (20 days). *p*-value for one-way ANOVA for biochar production temperature. Different letters and colors indicate different groups according to Tukey's HSD test ($\alpha = 0.05$).

Biochar mixing with organic fertilizer significantly increased N₂O emissions ($p < 0.001$, for non-paired *t*-test) compared to the fertilizer treatment alone (Figure 1). That result is opposite to our hypothesis as we expected that biochar addition to organic fertilizer would reduce N₂O emissions.

N₂O emissions were significantly influenced by the number of days passed after BC and fertilizer incorporation into soil (factor time) (Table 4, Figure 4). The differences between treatments were

statistically significant ($p < 0.05$) only for the first two sampling dates (days 3 and 9 after the application of the organic fertilizers and biochar) of the duration of the experiment (40 days) (Figure 4). After 9 days, N_2O emissions decreased and stabilized in all treatments (including control).

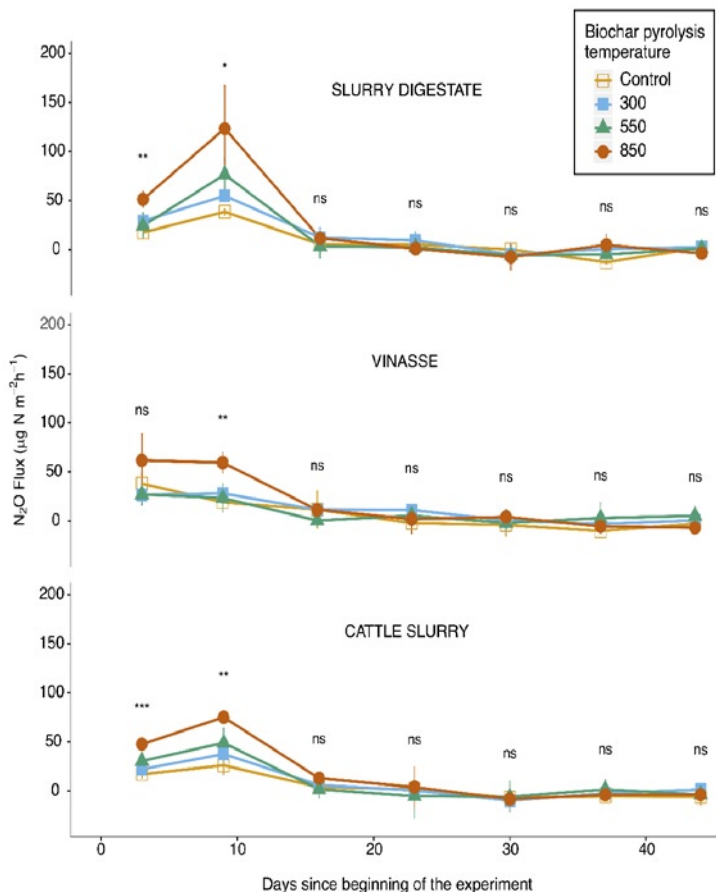


Figure 4. N_2O -N fluxes for each fertilizer and production temperature biochar during the studied period (BC300: Biochar produced at 300 °C; BC550: Biochar produced at 550 °C; BC850: Biochar produced at 850 °C). Stars indicate significant differences according ANOVA (*: $p < 0.05$; **: $p < 0.01$; ***: $p < 0.001$; ns: not significant).

The total cumulative emission for the peak period (20 days) was the greatest from the treatments where organic fertilizers had been mixed with biochar (13.485 mg N/ha), followed by treatments where only organic fertilizer (7.528 mg N/ha) and biochar (5.105 mg N/ha) were applied and the smallest flux was from the control treatment (−0.357 mg N/ha). Among the combination of organic fertilizer and biochar treatments, the greatest total cumulative emission was from treatments where BC850 had been mixed with the fertilizer (19.862 mg N/ha).

Final pH values ranged between 5.08 and 6.09 for all substrate combinations for both treatments (Table 5), while final total carbon content (%) ranged between 1.10 and 1.33 and total nitrogen content (%) between 0.052 and 0.073 among the different treatments (Supplementary Table S1).

Table 5. Final pH_{KCl} for the different treatment level combinations.

		Biochar			
		no-bc	300	550	850
Fertilizer	no-fert	5.15	5.44	5.82	5.77
	CS	5.20	5.67	6.09	6.05
	VN	5.20	5.56	5.91	5.87
	SD	5.08	5.42	5.95	5.88

no-bc: no biochar; BC300: biochar produced at 300 °C; BC550: biochar produced at 550 °C; BC850: biochar produced at 850 °C; no-fert: no fertilizer, CS: cattle slurry; SD: slurry digestate; VN: vinasse.

No significant correlation was found between total emitted N₂O with the properties of the organic fertilizers (pH_{KCl}, NH₄⁺-N, NO₃⁻-N, P, K, Ca, Mg) nor with the properties of biochar (pH, ash content, neutralization ability, surface area, cumulative pore volume) or nutrient content (N_{tot}, C_{tot}, P_{tot}, K_{tot}, Ca_{tot}, Mg_{tot}). N₂O flux in BC treatments was influenced by the release of nutrients from biochar. A linear model was fit between nitrous oxide fluxes and both released C_{tot} and N_{tot} in the studied period (Table 6), showing a significant fit for both C_{tot} ($p < 0.05$, slope = 0.25) and N_{tot} ($p < 0.05$, slope = 7.04) (Figure 5).

Table 6. Initial and final content (%) of N_{tot} and C_{tot}, in biochar at the beginning and at the end of the experiment, and C_{tot} and N_{tot} released by the biochar during the experiment, proportion of total (% w/w).

	Biochar	N _{tot}	C _{tot}
Initial (%)	300	2.82	53.5
	550	2.92	65.9
	850	2.56	68.1
Final (%)	300	1.76	35.9
	550	1.32	33.3
	850	0.79	28.9
Released (difference %, w:w)	300	1.06	17.6
	550	1.60	32.6
	850	1.77	39.2

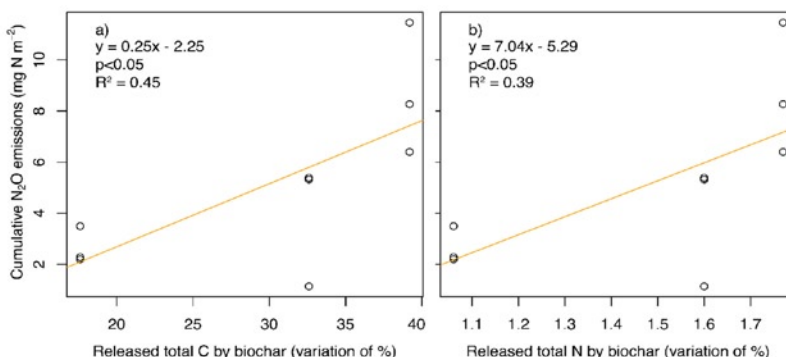


Figure 5. Linear regression for the cumulative N₂O fluxes of the selected period (20 days) with (a) released total C, and (b) released total N.

Nutrient uptake by the plant cover was negligible in the first two weeks of the experiment (when the highest N₂O emissions as well as the biggest differences between treatments were monitored),

as the plants had not emerged yet or were in the sprout or seedlings stages. Total final nitrogen uptake by the plant cover was significantly different ($p < 0.05$) between fertilizers (control, CS, SD, and VN), but no difference ($p > 0.05$) was found in nitrogen uptake between biochars for the different fertilizers (control, CS, SD, and VN) ((Supplementary Table S2). Regarding P_{tot} , K_{tot} , Ca_{tot} , and Mg_{tot} , uptake by the crop cover between biochar treatments for the different fertilizer treatments showed significant differences ($p < 0.05$) only for total phosphorus [53].

The pyrolyzation process resulted in the breaking of the cellulose, hemicellulose, and lignin functional groups (1500–1000 cm^{-1} region), present in BC300 but not in BC850, as shown by FTIR analysis (Supplementary Figure S1) [63–66], with intermediate absorbance peaks for BC550, especially for lignin (1593 and 1032 cm^{-1}). An increase in aromatic groups (region 1000–400 cm^{-1}) was observed with increasing pyrolysis temperature, especially for BC850, with BC550 also showing intermediate peaks. Principal component analysis (PCA) of the FTIR spectra (Supplementary Figures S2 and S3) shows that BC850 is differentiated from BC300 and BC550 on differences of aromatic, aliphatic, and hydroxyl groups (first component, 70.6% of variability explained), while differences in cellulose, hemicellulose, and lignin content differentiate the three different production temperature biochars (first and second principal components).

4. Discussion

Organic fertilization significantly increased N_2O emissions as a consequence of the large amount of $\text{NH}_4^+\text{-N}$ being incorporated into the soil with the addition of fertilizer. Although, according to pH values, conditions were mostly favorable for denitrification in the soil, some nitrification spots would have allowed oxidation of the ammonium from the organic fertilizers into nitrates, especially in the initial period. Emissions were not influenced by the lower pH or the higher content of K, Ca, and Mg in vinasse.

It is well known that biochar can affect the water-holding capacity of the substrates [22], but because of the small relative weight of biochar amendment (0.272% of total soil weight; 0.725% for the 0–10 cm layer), no significant effect on soil moisture compared to control, nor on differences in soil moisture between treatments, is expected. Moisture was also assumed to be not significantly different between treatments, as no significant effect on soil water-holding capacity was expected, watering was the same for all treatments, no leaching or negligible leaching was monitored, uptake by plants was not different [53], and, as the relative amount of amended biochar was small and the biochar pellets were mixed, albedo of the soil should not be affected, therefore not affecting evaporation.

Contrary to our hypothesis, amendment with biochar did not reduce N_2O emissions. Biochar addition into soil resulted in higher emissions of N_2O ($p < 0.05$). Moreover, emissions were higher with higher temperature biochar. The ineffectiveness of the studied biochar in reducing N_2O emissions could be explained by its low C/N values (Table 2), as the C/N values of the studied biochars were much lower compared to those commonly reported in the literature [21], even for biochar produced from herbaceous residues [23]. Previous research has documented that N-rich biochars with low C/N had no mitigation effect on N_2O emissions [21]. A meta-analysis by Cayuela et al. [23] found that biochars with a low C/N ratio (<30) did not reduce N_2O emissions. Spokas and Reicosky [31] found that, from 16 different studied biochars, only biochar with high N content, high labile organic matter, and a low C/N ratio, increased N_2O emissions, with only one of the 16 different biochars, with a C/N ratio of 19.4, resulted in higher N_2O emissions on all soils, while the other biochar generating higher emissions in different soil types presented C/N ratios between 21.85 and 207.5. Clough et al. [46] showed that biochar can increase N_2O emissions, if soil moisture is favorable for denitrification, but also when large amounts of C and N are released from biochar. This is in line with our results, as the biggest losses of C and N were found for BC850, from which the highest emissions were also measured. Although BC850 presented the lowest initial N content (Table 2), and extractable carbon and nitrogen were higher for lower production temperature biochar (Supplementary Table S1), the higher release of nutrients measured with higher temperature biochar could be a consequence of the pH of

the soil–biochar interface being closer to the optimal for ammonification, increasing the mineralization rate of biochar. The idea that BC's enhancing effect on N_2O emissions comes from C and N release is supported by the positive significant relation found from the linear fit between N_2O flux and the released C and N amount. Released carbon becoming available would promote denitrifiers' growth, and reduce O_2 availability in the substrates, indirectly promoting denitrification too [14]. Available C is a key factor controlling denitrification [67–69], which was the predominant process involved in N_2O production in the substrates, as a consequence of soil pH during the experiment and soil moisture, as the measurements were carried out the day after watering. The pH values at the end of the experiment for the substrate mixes were in the range between 5.08 and 6.09 (Table 5), which are below the optimum for nitrification (7.8–8.9) [70]. Denitrification is less sensitive to pH than nitrification, and, at lower values of pH, the ratio $N_2O:N_2$ increases [71], supporting that denitrification was the predominant process involved in the N_2O emissions. Moreover, Hütsch et al. [72] reported the biggest losses due to denitrification, mainly N_2O , for pH values of 5.2 and 5.9 for sandy and loamy soils respectively, which are almost coincident with the final pH values of the substrates tested in this experiment. It has also been reported that fast increases in soil pH can cause a sharp increase in denitrification potential, due to the solubilization of organic matter [73]. It has been documented that denitrifying bacteria recover faster when soils are rewetted after dry periods [74], and that rewetting after dry periods increases the concentration of dissolved organic carbon (DOC) [75] and C availability [76,77]. This would explain why the emissions peaked after the initial watering of the dry soil, and why the biggest differences among treatments were measured during the first two weeks. Firestone and Davidson [6] established that large increases in N_2O emissions, like those observed after rewetting, are more typical for denitrification than for nitrification, which supports our assumption that conditions in the substrates were more favorable for denitrification, and that denitrification was the main reason for the observed emissions. According to Petersen [78], denitrification in manure slurries is promoted by the readily assimilable carbon. This would explain why biochar amendment does not reduce emissions with organic fertilization. In fact, organic carbon input can promote anaerobic conditions, even at low water-filled pore space (WFPS) values, increasing denitrification potential and N_2O emissions [79]. Higher losses of C with the highest production temperature biochar would explain why this biochar presented the highest emissions.

The higher pH from higher pyrolysis temperature biochars could have also contributed to the differences in N_2O fluxes, for higher rates of denitrification are expected under slightly alkaline than under acid conditions [80]. Finally, higher phosphorus content in higher production temperature biochar could have also promoted higher N_2O emissions, as P content promotes N_2O emissions from both nitrification and denitrification processes [81].

An alternative mechanism for explaining the differences in emissions after application of the different biochars could be a combination of biochar-mediated soil organic matter mineralization enhancement, in parallel with NH_4^+ sorption by the biochar which, in turn, reduces the nitrification potential. Although biochar has been reported to have opposed effects on mineralization [46], meta-analyses show a general increase in mineralization activity in biochar-amended soils [22,23], an increase that is usually attributed to the priming effect of biochar, by stimulating microorganisms to mineralize recalcitrant soil organic matter in response to the C input [21,41,46]. This would lead to an increase of nitrification activity [21], due to the NH_4^+ becoming available as a result of the ammonification process. Ammonification is not so sensitive to low pH as nitrification [82,83]. In parallel, NH_4^+ sorption by biochar would decrease nitrification activity, explaining the differences in the final N_2O emissions from different treatments. As sorption takes place in the surface of biochar, it will be conditioned mostly by the biochar pH and not by the pH of the substrates. The different pH and, consequently, NH_4^+ sorption capacity of the different biochars would result in different NH_4^+ availability and, therefore, nitrification activity. Higher temperature biochar presents lower NH_4^+ sorption potential [84,85], leading to more available NH_4^+ in soil for nitrification. Although ammonium sorption capacity increases with increasing pH [84,85], higher pH values will cause a shift in the

ammonium-ammonia equilibrium towards ammonia [86]. Wang et al. [86,87] observed that adjusting the pH of the solution to 7 resulted in increased NH_4^+ sorption. Assuming that the three biochars enhanced mineralization, then BC300, with its pH close to 7 and higher content of negatively charged functional groups present in cellulose, hemicellulose, and lignin with lower temperatures, as shown in the FTIR analysis (Supplementary Figure S1), would have been the one with the highest NH_4^+ sorption capacity, followed by BC550. However, the low levels of organic N and P in the soil would limit ammonification, and the low pH of the substrates would limit nitrification, therefore seeming unlikely that the combination of ammonification and NH_4^+ sorption could cause the measured differences in the N_2O fluxes. Even for biochar and fertilizer combined amendment, where N was not limiting due to the addition of NH_4^+-N , as the interaction between biochar and fertilizer was not significant, this mechanism of combined ammonification and nitrification did not play a significant role, with the low pH for nitrification being the most likely limiting factor.

5. Conclusions

Organic fertilizers increased N_2O emissions in comparison to the control as expected, but the increase was not different among fertilizers. Biochar amendment did not mitigate the increase in N_2O emissions that resulted from organic fertilization, as biochar itself produced higher emissions. No significant interaction between biochar and fertilizer treatments was found. Biochar addition also increased emissions, with this difference being significant only for higher temperature production biochar. Our findings support the idea that biochar cannot be considered as a universal tool for the reduction of GHG emissions, and that each biochar, depending on its physical and chemical properties, can have a different effect. A low C/N ratio and a high N content in biochar can lead to higher emissions in biochar-amended soils. This study highlights the need for more research, focusing on different feedstocks and production methods of biochar, to provide a better understanding and allow future modeling of the mechanisms relating biochar properties and N_2O emissions. This is particularly important for biochars produced from non-woody source materials, and especially with low C/N ratios, more likely to have an unexpected and undesired effect on GHG emissions.

Supplementary Materials: The following are available online at <http://www.mdpi.com/2073-4395/10/1/109/s1>, Figure S1: Fourier-transform infrared spectroscopy (FTIR) spectrum of the studied biochars (300°, 550°, and 850°) with identified functional groups. Figure S2: Biplot of the first two components of the principal component analysis (PCA) of the Fourier-transform infrared spectroscopy (FTIR) spectrum values for the three production temperature biochars (300°, 550°, and 850°). Figure S3: Scatterplot of wavenumber values and eigenvalues for the first two principal components of the principal component analysis (PCA) of the Fourier-transform infrared spectroscopy (FTIR) spectrum data. Table S1: Extractable Nitrogen and Carbon of the different production temperature biochar after 120 h. Table S2: Final pH_{KCl} , C_{tot} and N_{tot} values for the different treatment level combinations.

Author Contributions: Conceptualization, H.R. and A.A.; methodology, A.A., K.S. and M.S.; validation, H.R. and M.S.; formal analysis, J.E.-G.; investigation, J.E.-G., H.R. and M.S.; resources, H.R., A.A., M.S. and K.S.; data curation, J.E.-G., H.R. and A.A.; writing—original draft preparation, J.E.-G.; writing—review and editing, H.R., A.A., K.S. and M.S.; visualization, J.E.-G.; supervision, H.R., A.A., M.S. and K.S.; project administration, H.R.; funding acquisition, H.R. and A.A. All authors have read and agreed to the published version of the manuscript.

Funding: The research was funded by the Estonian Agricultural Registers and Information Board (ARIB) program “Support for development of new products, practices, processes, and technologies” (RT I, 31.07.2015, 6).

Acknowledgments: We would like to thank the research contractor Taivo Roomann from Leedi farm in Raplamaa and the “Biosyngas production from torrefied hay” project coordinator Tommy Biene.

Conflicts of Interest: The authors declare no conflict of interest.

References

1. UNFCCC. Adoption of the Paris Agreement. FCCC/CP/2015/L.9/Rev.1. In Proceedings of the United Nations Framework Convention on Climate Change: 21st Conference of the Parties, Paris, France, 30 November–11 December 2015.
2. IPCC. *Climate Change 2014: Synthesis Report. Contribution of Working Groups I, II and III to the Fifth Assessment Report of the Intergovernmental Panel on Climate Change*; Meyer, L.A., Pachauri, R.K., Eds.; Core Writing Team: Geneva, Switzerland, 2014; p. 151.
3. Ravishankara, A.R.; Daniel, J.S.; Portmann, R.W. Nitrous oxide (N₂O): The dominant ozone-depleting substance emitted in the 21st century. *Science* **2009**, *326*, 123–125. [[CrossRef](#)] [[PubMed](#)]
4. Ussiri, D.; Lal, R. *Soil Emission of Nitrous Oxide and Its Mitigation*; Springer: Dordrecht, The Netherlands, 2013; Volume XVIII, p. 378.
5. Park, S.; Croteau, P.; Boering, K.A.; Etheridge, D.M.; Ferretti, D.; Fraser, P.J.; Kim, K.R.; Krummel, P.B.; Langenfelds, R.L.; van Ommen, T.D.; et al. Trends and seasonal cycles in the isotopic composition of nitrous oxide since 1940. *Nat. Geosci.* **2012**, *5*, 261–265. [[CrossRef](#)]
6. Firestone, M.K.; Davidson, E.A. Microbiological Basis of NO and N₂O Production and Consumption in Soils. In *Exchange of Trace Gases between Terrestrial Ecosystems and the Atmosphere*; Andreae, M.O., Schimel, D.S., Eds.; John Wiley and Sons: New York, NY, USA, 1989; pp. 7–21.
7. Braker, G.; Conrad, R. Diversity, Structure, and Size of N₂O-Producing Microbial Communities in Soils—What Matters for Their Functioning? In *Advances in Applied Microbiology*; Academic Press: Cambridge, MA, USA, 2011; Volume 75, pp. 33–70.
8. Shen, J.; Treu, R.; Wang, J.; Nicholson, F.; Bhogal, A.; Thorman, R. Modeling nitrous oxide emissions from digestate and slurry applied to three agricultural soils in the United Kingdom: Fluxes and emission factors. *Environ. Pollut.* **2018**, *243*, 1952–1965. [[CrossRef](#)] [[PubMed](#)]
9. Jones, S.K.; Rees, R.M.; Skiba, U.M.; Ball, B.C. Influence of organic and mineral N fertiliser on N₂O fluxes from a temperate grassland. *Agric. Ecosyst. Environ.* **2007**, *121*, 74–83. [[CrossRef](#)]
10. van Groenigen, J.W.; Kasper, G.J.; Velthof, G.L.; van den Pol-van Dasselaar, A.; Kuikman, P.J. Nitrous oxide emissions from silage maize fields under different mineral nitrogen fertilizer and slurry applications. *Plant Soil* **2004**, *263*, 101–111. [[CrossRef](#)]
11. Marchaim, U. *Biogas Processes for Sustainable Development*; FAO: Rome, Italy, 1992.
12. Ciborowski, P. *Anaerobic Digestion of Livestock Manure for Pollution Control and Energy Production: A Feasibility Assessment*; Minnesota Pollution Control Agency: St. Paul, MN, USA, 2001; p. 233.
13. Petersen, S.O. Greenhouse gas emissions from liquid dairy manure: Prediction and mitigation. *J. Dairy Sci.* **2018**, *101*, 6642–6654. [[CrossRef](#)]
14. Holly, M.A.; Larson, R.A.; Powell, J.M.; Ruark, M.D.; Aguirre-Villegas, H. Greenhouse gas and ammonia emissions from digested and separated dairy manure during storage and after land application. *Agric. Ecosyst. Environ.* **2017**, *239*, 410–419. [[CrossRef](#)]
15. Lourenco, K.S.; Rossetto, R.; Vitti, A.C.; Montezano, Z.F.; Soares, J.R.; Sousa, R.M.; do Carmo, J.B.; Kuramae, E.E.; Cantarella, H. Strategies to mitigate the nitrous oxide emissions from nitrogen fertilizer applied with organic fertilizers in sugarcane. *Sci. Total Environ.* **2019**, *650*, 1476–1486. [[CrossRef](#)]
16. Carmo, J.B.D.; Filoso, S.; Zotelli, L.C.; de Sousa Neto, E.R.; Pitombo, L.M.; Duarte-Neto, P.J.; Vargas, V.P.; Andrade, C.A.; Gava, G.J.C.; Rossetto, R.; et al. Infield greenhouse gas emissions from sugarcane soils in Brazil: Effects from synthetic and organic fertilizer application and crop trash accumulation. *GCB Bioenergy* **2013**, *5*, 267–280. [[CrossRef](#)]
17. Lehmann, J.; Joseph, S. *Biochar for Environmental Management: Science and Technology*; Earthscan: London, UK, 2009.
18. Sohi, S.P. Carbon storage with benefits. *Science* **2012**, *338*, 1034–1035. [[CrossRef](#)]
19. Crane-Droesch, A.; Abiven, S.; Jeffery, S.; Torn, M.S. Heterogeneous global crop yield response to biochar: A meta-regression analysis. *Environ. Res. Lett.* **2013**, *8*. [[CrossRef](#)]
20. Jeffery, S.; Abalos, D.; Prodana, M.; Bastos, A.C.; van Groenigen, J.W.; Hungate, B.A.; Verheijen, F. Biochar boosts tropical but not temperate crop yields. *Environ. Res. Lett.* **2017**, *12*. [[CrossRef](#)]

21. Borchard, N.; Schirrmann, M.; Cayuela, M.L.; Kammann, C.; Wrage-Monnig, N.; Estavillo, J.M.; Fuertes-Mendizabal, T.; Sigua, G.; Spokas, K.; Ippolito, J.A.; et al. Biochar, soil and land-use interactions that reduce nitrate leaching and N₂O emissions: A meta-analysis. *Sci. Total Environ.* **2019**, *651*, 2354–2364. [[CrossRef](#)] [[PubMed](#)]
22. Liu, Q.; Zhang, Y.; Liu, B.; Amonette, J.E.; Lin, Z.; Liu, G.; Ambus, P.; Xie, Z. How does biochar influence soil N cycle? A meta-analysis. *Plant Soil* **2018**, *426*, 211–225. [[CrossRef](#)]
23. Cayuela, M.L.; van Zwieten, L.; Singh, B.P.; Jeffery, S.; Roig, A.; Sánchez-Monedero, M.A. Biochar's role in mitigating soil nitrous oxide emissions: A review and meta-analysis. *Agric. Ecosyst. Environ.* **2014**, *191*, 5–16. [[CrossRef](#)]
24. Scheer, C.; Grace, P.R.; Rowlings, D.W.; Kimber, S.; Van Zwieten, L. Effect of biochar amendment on the soil-atmosphere exchange of greenhouse gases from an intensive subtropical pasture in northern New South Wales, Australia. *Plant Soil* **2011**, *345*, 47–58. [[CrossRef](#)]
25. Suddick, E.C.; Six, J. An estimation of annual nitrous oxide emissions and soil quality following the amendment of high temperature walnut shell biochar and compost to a small scale vegetable crop rotation. *Sci. Total Environ.* **2013**, *465*, 298–307. [[CrossRef](#)]
26. Rittl, T.F.; Butterbach-Bahl, K.; Basile, C.M.; Pereira, L.A.; Alms, V.; Dannenmann, M.; Couto, E.G.; Cerri, C.E.P. Greenhouse gas emissions from soil amended with agricultural residue biochars: Effects of feedstock type, production temperature and soil moisture. *Biomass Bioenergy* **2018**, *117*, 1–9. [[CrossRef](#)]
27. Buchkina, N.P.; Hüppi, R.; Leifeld, J. Biochar and short-term N₂O and CO₂ emission from plant residue-amended soil with different fertilisation history. *Zemdirb. Agric.* **2019**, *106*, 99–106. [[CrossRef](#)]
28. Van Zwieten, L.; Singh, B.; Joseph, S.; Kimber, S.; Cowie, A.; Chan, K.Y. Biochar and Emissions of Non-CO₂ Greenhouse Gases from Soil. In *Biochar for Environmental Management: Science and Technology*; Lehmann, J., Joseph, S., Eds.; Routledge: London, UK, 2009. [[CrossRef](#)]
29. Clough, T.J.; Bertram, J.E.; Ray, J.L.; Condron, L.M.; O'Callaghan, M.; Sherlock, R.R.; Wells, N.S. Unweathered Wood Biochar Impact on Nitrous Oxide Emissions from a Bovine-Urine-Amended Pasture Soil. *Soil Sci. Soc. Am. J.* **2010**, *74*, 852–860. [[CrossRef](#)]
30. Verhoeven, E.; Six, J. Biochar does not mitigate field-scale N₂O emissions in a Northern California vineyard: An assessment across two years. *Agric. Ecosyst. Environ.* **2014**, *191*, 27–38. [[CrossRef](#)]
31. Spokas, K.A.; Reicosky, D.C. Impacts of Sixteen Different Biochars on Soil Greenhouse Gas Production. *Ann. Environ. Sci.* **2009**, *3*, 179–193.
32. Malghani, S.; Gleixner, G.; Trumbore, S.E. Chars produced by slow pyrolysis and hydrothermal carbonization vary in carbon sequestration potential and greenhouse gases emissions. *Soil Biol. Biochem.* **2013**, *62*, 137–146. [[CrossRef](#)]
33. Sánchez-García, M.; Roig, A.; Sánchez-Monedero, M.A.; Cayuela, M.L. Biochar increases soil N₂O emissions produced by nitrification-mediated pathways. *Front. Environ. Sci.* **2014**, *2*, 25. [[CrossRef](#)]
34. Christel, W.; Zhu, K.; Hofer, C.; Kreuzeder, A.; Santner, J.; Bruun, S.; Magid, J.; Jensen, L.S. Spatiotemporal dynamics of phosphorus release, oxygen consumption and greenhouse gas emissions after localised soil amendment with organic fertilisers. *Sci. Total Environ.* **2016**, *554–555*, 119–129. [[CrossRef](#)] [[PubMed](#)]
35. Wang, C.; Lu, H.; Dong, D.; Deng, H.; Strong, P.J.; Wang, H.; Wu, W. Insight into the effects of biochar on manure composting: Evidence supporting the relationship between N₂O emission and denitrifying community. *Environ. Sci. Technol.* **2013**, *47*, 7341–7349. [[CrossRef](#)] [[PubMed](#)]
36. Harter, J.; Krause, H.M.; Schuettler, S.; Ruser, R.; Fromme, M.; Scholten, T.; Kappler, A.; Behrens, S. Linking N₂O emissions from biochar-amended soil to the structure and function of the N-cycling microbial community. *ISME J.* **2014**, *8*, 660–674. [[CrossRef](#)] [[PubMed](#)]
37. Hüppi, R.; Felber, R.; Neftel, A.; Six, J.; Leifeld, J. Effect of biochar and liming on soil nitrous oxide emissions from a temperate maize cropping system. *Soil* **2015**, *1*, 707–717. [[CrossRef](#)]
38. Obia, A.; Cornelissen, G.; Mulder, J.; Dorsch, P. Effect of Soil pH Increase by Biochar on NO, N₂O and N₂ Production during Denitrification in Acid Soils. *PLoS ONE* **2015**, *10*, e0138781. [[CrossRef](#)]
39. Bird, M.I.; Wynn, J.G.; Saiz, G.; Wurster, C.M.; McBeath, A. The Pyrogenic Carbon Cycle. *Annu. Rev. Earth Planet. Sci.* **2015**, *43*, 273–298. [[CrossRef](#)]
40. Santin, C.; Doerr, S.H.; Merino, A.; Bucheli, T.D.; Bryant, R.; Ascough, P.; Gao, X.; Masiello, C.A. Carbon sequestration potential and physicochemical properties differ between wildfire charcoals and slow-pyrolysis biochars. *Sci. Rep.* **2017**, *7*, 11233. [[CrossRef](#)] [[PubMed](#)]

41. Nelissen, V.; Rütting, T.; Huygens, D.; Staelens, J.; Ruyschaert, G.; Boeckx, P. Maize biochars accelerate short-term soil nitrogen dynamics in a loamy sand soil. *Soil Biol. Biochem.* **2012**, *55*, 20–27. [[CrossRef](#)]
42. Joseph, S.D.; Camps-Arbestain, M.; Lin, Y.; Munroe, P.; Chia, C.H.; Hook, J.; van Zwieten, L.; Kimber, S.; Cowie, A.; Singh, B.P.; et al. An investigation into the reactions of biochar in soil. *Soil Res.* **2010**, *48*, 501–515. [[CrossRef](#)]
43. Enders, A.; Hanley, K.; Whitman, T.; Joseph, S.; Lehmann, J. Characterization of biochars to evaluate recalcitrance and agronomic performance. *Bioresour. Technol.* **2012**, *114*, 644–653. [[CrossRef](#)]
44. Ahmad, M.; Lee, S.S.; Dou, X.; Mohan, D.; Sung, J.K.; Yang, J.E.; Ok, Y.S. Effects of pyrolysis temperature on soybean stover- and peanut shell-derived biochar properties and TCE adsorption in water. *Bioresour. Technol.* **2012**, *118*, 536–544. [[CrossRef](#)]
45. Ippolito, J.A.; Novak, J.M.; Busscher, W.J.; Ahmedna, M.; Rehrh, D.; Watts, D.W. Switchgrass biochar affects two aridisols. *J. Environ. Qual.* **2012**, *41*, 1123–1130. [[CrossRef](#)]
46. Clough, T.; Condron, L.; Kammann, C.; Müller, C. A Review of Biochar and Soil Nitrogen Dynamics. *Agronomy* **2013**, *3*, 275–293. [[CrossRef](#)]
47. Biederman, L.A.; Harpole, W.S. Biochar and its effects on plant productivity and nutrient cycling: A meta-analysis. *GCB Bioenergy* **2013**, *5*, 202–214. [[CrossRef](#)]
48. Feng, Z.; Zhu, L. Impact of biochar on soil N₂O emissions under different biochar-carbon/fertilizer-nitrogen ratios at a constant moisture condition on a silt loam soil. *Sci. Total Environ.* **2017**, *584–585*, 776–782. [[CrossRef](#)]
49. Tybirk, K.; Luostarinen, S.; Hamelin, L.; Rodhe, L.; Haneklaus, S.; Poulsen, H.D.; Jensen, A.L.S. *Sustainable Manure Management in the Baltic Sea Region*; Jokioinen, Finland, 2013. Available online: http://eu.baltic.net/Project_Database.5308.html?contentid=58&contentaction=single (accessed on 1 October 2019)
50. Jeffery, S.; Verheijen, F.G.A.; van der Velde, M.; Bastos, A.C. A quantitative review of the effects of biochar application to soils on crop productivity using meta-analysis. *Agric. Ecosyst. Environ.* **2011**, *144*, 175–187. [[CrossRef](#)]
51. Bates, R.B.; Ghoniem, A.F. Biomass torrefaction: Modeling of volatile and solid product evolution kinetics. *Bioresour. Technol.* **2012**, *124*, 460–469. [[CrossRef](#)] [[PubMed](#)]
52. Hagemann, N.; Spokas, K.; Schmidt, H.-P.; Kägi, R.; Böhler, M.; Bucheli, T. Activated Carbon, Biochar and Charcoal: Linkages and Synergies across Pyrogenic Carbon's ABCs. *Water* **2018**, *10*, 182. [[CrossRef](#)]
53. Raave, H.; Escuer-Gatius, J.; Kauer, K.; Shanskiy, M.; Tönutare, T.; Astover, A. Pyrolysis temperature influence on nutrient release from hay biochar and on the biochar impact on perennial ryegrass nutrient uptake and yield. Manuscript submitted for publication.
54. Hutchinson, G.L.; Livingston, G.P. Use of chamber systems to measure trace gas fluxes. In *Agricultural Ecosystem Effects on Trace Gases and Global Climate Change*; Harper, L.A., Mosier, A.R., Duxbury, J.M., Rolston, D.E., Eds.; American Society of Agronomy: Madison, WI, USA, 1993; pp. 63–78. [[CrossRef](#)]
55. Järveoja, J.; Peichl, M.; Maddison, M.; Soosaar, K.; Vellak, K.; Karofeld, E.; Teemusk, A.; Mander, Ü. Impact of water table level on annual carbon and greenhouse gas balances of a restored peat extraction area. *Biogeosciences* **2016**, *13*, 2637–2651. [[CrossRef](#)]
56. Lofffield, N.; Flessa, H.; Augustin, J.; Beese, F. Automated Gas Chromatographic System for Rapid Analysis of the Atmospheric Trace Gases Methane, Carbon Dioxide, and Nitrous Oxide. *J. Environ. Qual.* **1997**, *26*, 560–564. [[CrossRef](#)]
57. Livingston, G.P.; Hutchinson, G.L. Enclosure-based measurement of trace gas exchange: Applications and sources of error. In *Biogenic Trace Gases: Measuring Emissions from Soil and Water*; Matson, P.A., Harriss, R.C., Eds.; Blackwell Publishing: Oxford, UK, 1995; pp. 14–51.
58. Parkin, T.B.; Venterea, R.T.; Follett, R.F. Chapter 3. *Chamber-Based Trace Gas Flux Measurements*; USDA-ARS: Beltsville, MD, USA, 2010.
59. Vinzent, B.; Fuß, R.; Maidl, F.-X.; Hülsbergen, K.-J. N₂O emissions and nitrogen dynamics of winter rapeseed fertilized with different N forms and a nitrification inhibitor. *Agric. Ecosyst. Environ.* **2018**, *259*, 86–97. [[CrossRef](#)]
60. R Development Core Team. *R: A Language and Environment for Statistical Computing*; R Foundation for Statistical Computing: Vienna, Austria, 2016.
61. Mendiburu, F.D. *Agricolae: Statistical Procedures for Agricultural Research*; R Package Version 1.2-3; The Comprehensive R Archive Network: Vienna, Austria, 2015.

62. Tukey, J.W. *Exploratory Data Analysis*; Addison-Wesley Publishing Company: Reading, MA, USA, 1977.
63. Yang, H.; Yan, R.; Chen, H.; Lee, D.H.; Zheng, C. Characteristics of hemicellulose, cellulose and lignin pyrolysis. *Fuel* **2007**, *86*, 1781–1788. [[CrossRef](#)]
64. Keiluweit, M.; Nico, P.S.; Johnson, M.G.; Kleber, M. Dynamic molecular structure of plant biomass-derived black carbon (biochar). *Environ. Sci. Technol.* **2010**, *44*, 1247–1253. [[CrossRef](#)]
65. Song, K.; Zhang, H.; Wu, Q.; Zhang, Z.; Zhou, C.; Zhang, Q.; Lei, T. Structure and thermal properties of tar from gasification of agricultural crop residue. *J. Therm. Anal. Calorim.* **2014**, *119*, 27–35. [[CrossRef](#)]
66. Horikawa, Y.; Hirano, S.; Mihashi, A.; Kobayashi, Y.; Zhai, S.; Sugiyama, J. Prediction of Lignin Contents from Infrared Spectroscopy: Chemical Digestion and Lignin/Biomass Ratios of *Cryptomeria japonica*. *Appl. Biochem. Biotechnol.* **2019**, *188*, 1066–1076. [[CrossRef](#)]
67. Firestone, M.K.; Tiedje, J.M. Temporal change in nitrous oxide and dinitrogen from denitrification following onset of anaerobiosis. *Appl. Environ. Microbiol.* **1979**, *38*, 673–679. [[CrossRef](#)]
68. Clemens, J.; Huschka, A. The effect of biological oxygen demand of cattle slurry and soil moisture on nitrous oxide emissions. *Nutr. Cycl. Agroecosystems* **2001**, *59*, 193–198. [[CrossRef](#)]
69. Butterbach-Bahl, K.; Baggs, E.M.; Dannenmann, M.; Kiese, R.; Zechmeister-Boltenstern, S. Nitrous oxide emissions from soils: How well do we understand the processes and their controls? *Philos. Trans. R. Soc. Lond. B Biol. Sci.* **2013**, *368*, 20130122. [[CrossRef](#)] [[PubMed](#)]
70. Halling-Sørensen, B.; Jørgensen, S.E. Process Chemistry and Biochemistry of Nitrification. In *Studies in Environmental Science*; Halling-Sørensen, B., Jørgensen, S.E., Eds.; Elsevier Science: Amsterdam, The Netherlands, 1993; Volume 54, pp. 55–118.
71. Simek, M.; Cooper, J.E. The influence of soil pH on denitrification: Progress towards the understanding of this interaction over the last 50 years. *Eur. J. Soil Sci.* **2002**, *53*, 345–354. [[CrossRef](#)]
72. Hütsch, B.W.; Zhang, S.; Feng, K.; Yan, F.; Schubert, S. Effect of pH on denitrification losses from different arable soils. *Plant Nutr.* **2001**, 962–963. [[CrossRef](#)]
73. Anderson, C.R.; Peterson, M.E.; Frampton, R.A.; Bulman, S.R.; Keenan, S.; Curtin, D. Rapid increases in soil pH solubilise organic matter, dramatically increase denitrification potential and strongly stimulate microorganisms from the Firmicutes phylum. *PeerJ* **2018**, *6*, e6090. [[CrossRef](#)] [[PubMed](#)]
74. Smith, M.S.; Parsons, L.L. Persistence of Denitrifying Enzyme Activity in Dried Soils. *Appl. Environ. Microbiol.* **1985**, *49*, 316–320. [[CrossRef](#)] [[PubMed](#)]
75. Kalbitz, K.; Solinger, S.; Park, J.H.; Michalzik, B.; Matzner, E. Controls on the Dynamics of Dissolved Organic Matter in Soils: A Review. *Soil Sci.* **2000**, *165*, 277–304. [[CrossRef](#)]
76. Lundquist, E.J.; Jackson, L.E.; Scow, K.M.; Hsu, C. Changes in microbial biomass and community composition, and soil carbon and nitrogen pools after incorporation of rye into three California agricultural soils. *Soil Biol. Biochem.* **1999**, *31*, 221–236. [[CrossRef](#)]
77. Ruser, R.; Flessa, H.; Russow, R.; Schmidt, G.; Buegger, F.; Munch, J.C. Emission of N₂O, N₂ and CO₂ from soil fertilized with nitrate: Effect of compaction, soil moisture and rewetting. *Soil Biol. Biochem.* **2006**, *38*, 263–274. [[CrossRef](#)]
78. Petersen, S.O. Nitrous Oxide Emissions from Manure and Inorganic Fertilizers Applied to Spring Barley. *J. Environ. Qual.* **1999**, *28*, 1610–1618. [[CrossRef](#)]
79. Chen, Z.; Ding, W.; Luo, Y.; Yu, H.; Xu, Y.; Müller, C.; Xu, X.; Zhu, T. Nitrous oxide emissions from cultivated black soil: A case study in Northeast China and global estimates using empirical model. *Glob. Biogeochem. Cycles* **2014**, *28*, 1311–1326. [[CrossRef](#)]
80. Yamulki, S.; Harrison, R.M.; Goulding, K.W.T.; Webster, C.P. N₂O, NO and NO₂ fluxes from a grassland: Effect of soil pH. *Soil Biol. Biochem.* **1997**, *29*, 1199–1208. [[CrossRef](#)]
81. Mori, T.; Ohta, S.; Ishizuka, S.; Konda, R.; Wicaksono, A.; Heriyanto, J.; Hardjono, A. Effects of phosphorus addition on N₂O and NO emissions from soils of an *Acacia mangium* plantation. *Soil Sci. Plant Nutr.* **2010**, *56*, 782–788. [[CrossRef](#)]
82. Dancer, W.S.; Peterson, L.A.; Chesters, G. Ammonification and Nitrification of N as Influenced by Soil pH and Previous N Treatments¹. *Soil Sci. Soc. Am. J.* **1973**, *37*, 67–69. [[CrossRef](#)]
83. Haynes, R.J.; Swift, R.S. Effect of rewetting air-dried soils on pH and accumulation of mineral nitrogen. *J. Soil Sci.* **1989**, *40*, 341–347. [[CrossRef](#)]

84. Yang, H.I.; Lou, K.; Rajapaksha, A.U.; Ok, Y.S.; Anyia, A.O.; Chang, S.X. Adsorption of ammonium in aqueous solutions by pine sawdust and wheat straw biochars. *Environ. Sci. Pollut. Res. Int.* **2018**, *25*, 25638–25647. [[CrossRef](#)] [[PubMed](#)]
85. Fidel, R.B.; Laird, D.A.; Spokas, K.A. Sorption of ammonium and nitrate to biochars is electrostatic and pH-dependent. *Sci. Rep.* **2018**, *8*, 17627. [[CrossRef](#)] [[PubMed](#)]
86. Wang, B.; Lehmann, J.; Hanley, K.; Hestrin, R.; Enders, A. Adsorption and desorption of ammonium by maple wood biochar as a function of oxidation and pH. *Chemosphere* **2015**, *138*, 120–126. [[CrossRef](#)]
87. Wang, B.; Lehmann, J.; Hanley, K.; Hestrin, R.; Enders, A. Ammonium retention by oxidized biochars produced at different pyrolysis temperatures and residence times. *RSC Adv.* **2016**, *6*, 41907–41913. [[CrossRef](#)]





© 2020 by the authors. Licensee MDPI, Basel, Switzerland. This article is an open access article distributed under the terms and conditions of the Creative Commons Attribution (CC BY) license (<http://creativecommons.org/licenses/by/4.0/>).

- II** Stegarescu, G., **Escuer-Gatius, J.**, Soosaar, K., Kauer, K., Tõnutare, T., Astover, A., Reintam, E. 2020. Effect of Crop Residue Decomposition on Soil Aggregate Stability. *Agriculture* 10(11), 527.

Article

Effect of Crop Residue Decomposition on Soil Aggregate Stability

Gheorghe Stegarescu ^{1,*}, Jordi Escuer-Gatius ¹, Kaido Soosaar ² , Karin Kauer ¹,
Tõnu Tõnutare ¹, Alar Astover ¹  and Endla Reintam ¹

¹ Institute of Agricultural and Environmental Sciences, Estonian University of Life Sciences, 51006 Tartu, Estonia; jordi.escuer@gmail.com (J.E.-G.); Karin.Kauer@emu.ee (K.K.); tonu.tonutare@emu.ee (T.T.); alar.astover@emu.ee (A.A.); endla.reintam@emu.ee (E.R.)

² Department of Geography, Institute of Ecology and Earth Sciences, University of Tartu, 50090 Tartu, Estonia; kaido.soosaar@ut.ee

* Correspondence: gheorghe.stegarescu@emu.ee

Received: 13 October 2020; Accepted: 3 November 2020; Published: 5 November 2020



Abstract: The decomposition of fresh crop residues added to soil for agricultural purposes is complex. This is due to different factors that influence the decomposition process. In field conditions, the incorporation of crop residues into soil does not always have a positive effect on aggregate stability. The aim of this study was to investigate the decomposition effects of residues from two different cover crops (*Brassica napus* var. *oleifera* and *Secale cereale*) and one main crop (wheat straw) on soil aggregate stability. A 105-day incubation experiment was conducted in which crop residues were mixed with sandy loam soil at a rate of 6 g C kg⁻¹ of soil. During the incubation, there were five water additions. The decomposition effects of organic matter on soil conditions during incubation were evaluated by determining the soil functional groups; carbon dioxide (CO₂), nitrous oxide (N₂O), and methane (CH₄) emissions; soil microbial biomass carbon (MBC); and water-stable aggregates (WSA). The functional groups of the plant residues and the soil were analyzed using Fourier transform infrared spectroscopy (FTIR) and a double exponential model was used to estimate the decomposition rates. The results show that the decomposition rate of fresh organic materials was correlated with the soil functional groups and the C/N ratio. Oilseed rape and rye, with lower C/N ratios than wheat straw residues, had faster decomposition rates and higher CO₂ and N₂O emissions than wheat straw. The CO₂ and N₂O flush at the start of the experiment corresponded to a decrease of soil aggregate stability (from Day 3 to Day 10 for CO₂ and from Day 19 to Day 28 for N₂O emissions), which was linked to higher decomposition rates of the labile fraction. The lower decomposition rates contributed to higher remaining C (carbon) and higher soil aggregate stability. The results also show that changes in the soil functional groups due to crop residue incorporation did not significantly influence aggregate stability. Soil moisture (SM) negatively influenced the aggregate stability and greenhouse gas emissions (GHG) in all treatments (oilseed rape, rye, wheat straw, and control). Irrespective of the water addition procedure, rye and wheat straw residues had a positive effect on water-stable aggregates more frequently than oilseed rape during the incubation period. The results presented here may contribute to a better understanding of decomposition processes after the incorporation of fresh crop residues from cover crops. A future field study investigating the influence of incorporation rates of different crop residues on soil aggregate stability would be of great interest.

Keywords: aggregate stability; cover crops; decomposition rates; greenhouse gas emissions; microbial biomass

1. Introduction

Crop residue incorporation in the soil such as cover crops and cash crops can improve soil quality in organic farming and conservation agriculture. A previous study observed that freshly added organic matter (crop residues) has a temporary effect on soil aggregate stability [1]. Abiven et al. [2] found that the efficiency of crop residue applications on soil aggregate stability depended on their initial chemical (carbon to nitrogen ratio (C/N)) and biochemical composition. Liu et al. [3] also showed that the effectiveness of the crop residues on soil aggregate stability depended on the addition rates, composition, and decomposability. In terms of the biochemical composition of crop residues, Angst et al. [4] observed that crop residues with a higher concentration of recalcitrant (lignin, lipids, cellulose, etc.) material had lower decomposition rates and longer-term effects on the aggregate stability. Apart from these examples, Abiven et al. [5] noted that few studies have linked soil aggregate stability with the biochemical composition of crop residues. A recent study showed that with the incorporation of fresh crop residues in the soil, the microorganisms concentrate their energy on the decomposition of easily decomposable compounds (sugars, proteins, etc.) [6]. In exchange, soil aggregate-binding agents are liberated from microorganisms (fungal hyphae and polysaccharides). Thus, crop residues improve the soil aggregate stability during their decomposition by soil bacteria and fungi. However, the more advanced the decomposition stage, the lower the microbial activity and aggregate stability [7]. The decomposition study of Mizuta et al. [8] showed that decomposition rates of pure compounds such as starch and cellulose influence aggregate formation but not soil aggregate stability.

The decomposition rates of the crop residues are influenced by the type of incorporated crop residues, soil water content, aeration regime and plant water content [9,10]. The results of Cosentino et al. [11] showed that crop residues could increase the microbial biomass and soil aggregate stability, but these effects were diminished by frequent soil drying and wetting cycles. Additionally, another past study observed that not all crop residues incorporated in the soil increased the soil aggregate stability [12] and that the effect of crop residues on soil aggregate stability is influenced by the soil type, climate zone, and agricultural management. A meta-analysis by Blanco-Canqui et al. [13] also found that not all studies that involved cover crops as crop residues affect the soil aggregate stability. Previous and recent studies have found that the location of crop residues (crop residues left on the surface or incorporated into the soil) can influence decomposition rates as well as soil biological properties and soil aggregate stability [14–16]. Thus, the crop residues left on the surface will decompose much more slowly than incorporated crop residues. Another study based on two years of data from a humid temperate zone showed a decrease in soil aggregate stability after crop residue incorporation by tillage [17]. Balesdent et al. [18] reported that in conventional tillage, the amount of decomposed fresh organic matter was much higher than in a no-till system. The incorporation of crop residues by tillage increases the access of microorganisms to fresh organic materials, leading to fast decomposition and creating a transient effect on soil aggregate stability.

At present, the literature still does not fully cover the extent of the beneficial effects of the decomposition rate of incorporated crop residues on soil aggregate stability since many interfering factors can influence crop residue decomposition. Additionally, in most previous studies of aggregate stability, the experiments conducted in a laboratory studied the effects using only oven-dried material from crop residues or post-harvest crop residues with a high content of dry matter [2,7,19]. The focus of our paper was to study the effect of the decomposition rate on soil aggregate stability when incorporating fresh crop residues from two cover crops widely used in Nordic climate conditions and wheat straw. We suppose that by incorporating cover crop residues into the soil, the destabilizing effect on soil structural stability is related to unstable and rapid decomposition rates associated with 'young' organic matter. In this case, the 'young' organic matter refers to freshly incorporated crop residues.

2. Materials and Methods

2.1. Soil and Crop Residue Preparation

The incubation experiment comprised four treatments, each containing four replications. Three of the treatments consisted of soil mixed with either fresh green crop residues of oilseed rape (OR), fresh green residues of rye (Rye), or dry wheat straw (WS). Pots filled with soil without any added organic matter comprised a control treatment (Control). The field soil used for the pot experiment was sampled from the top 0–20 cm layer, dried at room temperature, and sieved through a 10 mm sieve. The soil had a sandy loam texture with the following characteristics: 57.4% sand, 32.3% silt, and 10.3% clay. According to the World Reference Base for Soil Resources (IUSS Working Group WRB 2006), the soil can be described as an Albic Stagnic Luvisol. The dry soil was placed in 4000 mL pots ($\varnothing = 21$ cm, $h = 19.3$ cm) at a rate of 3000 g per pot. The chemical characteristics of the soil are shown in Table 1.

Table 1. Initial physicochemical properties of the soil used in the incubation experiment.

pH _{KCl}	TC	TN	P	K	Mg	Ca	CEC	Particles Content, %		
								>0.063	<0.002	0.002–0.063
			g kg ⁻¹			meq 100 g ⁻¹				
5.7	14.8	1.2	30.1	27.6	43.1	191.3	9.5	57.4	10.3	32.3

Two of the most common cover crop residues in the Nordic region were selected, oilseed rape (*Brassica napus* var. *oleifera*) and cereal rye (*Secale cereale*) as well as wheat straw residue. The shoots and leaves of oilseed rape and rye were collected from the field at the tillering stage. From the collected plant material, a subsample was used to determine the initial total carbon (TC) and total nitrogen (TN) (Table 2). The TC and TN were determined in a total elemental analyzer (VarioMAX CNS, elemental Analysensysteme GmbH, Langenselbold, Germany). Plant functional groups were analyzed using FTIR according to the procedure described below (Section 2.3.4).

Table 2. Initial chemical properties of plant residues.

Crop Residues	Total C, g C kg ⁻¹	Total N, g N kg ⁻¹	C/N	Dry Matter, g kg ⁻¹
Oilseed rape	424	41	10	153
Wheat straw	451	5	98	796
Rye	429	36	12	194

2.2. Experiment Design

Fresh crop residues were chopped into small pieces (about 4 cm long) and evenly incorporated into the dry soil in the pots at a rate of 6 g C kg⁻¹ of soil before water addition (considered as Day 0). This quantity is equivalent to 22.5 Mg C ha⁻¹ in field conditions, given a 25 cm soil depth and a bulk density of 1500 kg m⁻³. All four treatments were brought up to the field capacity for water (24% gravimetric) by adding distilled water 24 h after mixing dry soil with crop residues; in total, five wetting procedures were applied at 1, 11, 26, 46, and 75 days. The treatments were incubated for 105 days at a room temperature of 23 °C (± 0.8) and covered with a dark plastic film to allow some gas exchange. The experiment was conducted in two phases: the oilseed rape, wheat straw, and control treatments first, followed by rye.

2.3. Sampling and Analysis

2.3.1. Water-Stable Aggregates

The sampling for water-stable aggregates, FTIR analyses, and soil total carbon and nitrogen was done at Day 0 before residue addition, then again at 3, 10, 13, 19, 25, 28, 45, 48, 74, 77, and 105 days.

The soil was sampled from every pot at a 0–5 cm depth. The sampled soil was dried at room temperature and sieved through a 2 mm sieve. The aggregate stability was determined based on the method of Kemper and Rosenau [20]. Firstly, 4 g of dry soil from each sample (aggregates ≤ 2 mm) were placed in a set of sieves with 0.25 mm openings and shaken in cans with 100 mL of distilled water for 3 min on the wet sieving apparatus (Eijkelkamp, Giesbeek, The Netherlands). The distilled water cans were replaced by cans with a 0.4% NaOH solution and then shaken in continuous mode until all aggregates were dissolved. Finally, both types of cans were dried in a water bath at 95 °C for 12 h and then in a drying oven at 105 °C for 1 h. The percentage of stable aggregates was obtained by dividing the weight of soil remaining in the NaOH solution cans by the sum of the soil weight from the distilled water can and the weight of the soil from the NaOH solution can. Each sample from every single pot was measured with four repetitions ($n = 16$).

2.3.2. Gas Emissions Analysis

Gas emissions were measured using the closed chamber method [21]. Gas samples from each treatment were taken at Day 0, on the first day after residue incorporation, and then at Days 3, 5, 10, 13, 19, 25, 28, 45, 48, 74, 77, and 105. Three-liter pots were used as chambers, each with a diameter of 17 cm and height of 15.6 cm. The pots were inserted upside down into the soil pots to a depth of approximately 1 cm, achieving hermetic closing of the neck. Two holes were made in each chamber, one for a gas collection pipe and the other for a temperature sensor. Gas samples were taken over a one-hour period, at regular intervals of 20 min (i.e., at 0, 20, 40, and 60 min), using 12 mL pre-evacuated (0.3 mbar) bottles [22]. The CO₂, N₂O, and CH₄ concentrations of samples were determined using a GC-2014 gas chromatography system (Shimadzu Corporation, Kyoto, Japan equipped with ECD, TCD, and FID sensors as described by Lofffield et al. [23]. Soil conditions, such as soil temperature, electrical conductivity (EC), and soil moisture (SM), were simultaneously measured using an electronic tensiometer sensor (Procheck GS3, Decagon Devices, MeterGroup, Pullman, WA, USA).

2.3.3. Microbial Biomass Carbon

Sampling for microbial biomass was performed separately at Days 3, 10, 13, 19, 25, 28, 45, 48, 74, 77, and 105. Samples were taken from every pot, and analyses immediately performed once for each sample. Microbial biomass carbon was determined according to the modified method of Fließbach and Mäder [24]. Each analysis was performed with a 20 g chloroform-fumigated and unfumigated fresh soil sample over 24 h. Extraction was performed using 80 mL of a 0.01 M CaCl₂ solution. To determine C in the fumigated and non-fumigated samples, a total elemental analyzer was used (VarioMAX CNS, Elementar Analysensysteme GmbH, Langenselbold, Germany). The concentration was displayed as mg C kg⁻¹ of dry soil.

2.3.4. Fourier Transform Infrared Spectroscopy (FTIR) Analysis

After drying, the soil samples were crushed by hand between 1 and 5 min in an agate mortar. The soil functional groups were determined by Thermo-Nicolet iS10 Fourier Transform Infrared Spectrophotometer (FTIR, Thermo Fisher Scientific, Waltham, MA, USA). The data was collected at a 4 cm⁻¹ resolution over a range of 4000 to 400 cm⁻¹. For each sample, 32 scans were performed in three repetitions. Spectra replicates were corrected against the spectrum for ambient air as background, and the automatic baseline correction was applied. Peak heights were obtained using OMNIC software (Nicolet Instruments Corp., Madison, WI, USA). Relative absorbance was measured following the procedure described in Gerzabek et al. [25]. The parameters (base1/peak/base2) chosen for each peak were as follows: 3000/2920/2800, 1740/1630/1495, 1495/1410/1320, and 1320/1005/825. The relative absorbance was calculated by dividing the height of a distinct peak by the total sum of all peak heights. The soil spectra from the FTIR analyses are represented in Figure 1. The results show two peaks, at 3694 and 3617 cm⁻¹, which are associated with O–H stretching in kaolinite [26]. The same O–H bond specific for carboxyl and hydroxyl groups was also found in this region, at 3400 cm⁻¹ [27].

The peak at 2920 cm⁻¹ is due to the asymmetric C–H vibration of aliphatic compounds, also known as the hydrophobic component [28]. Further along the soil spectra, the hydrophilic component at 1630 cm⁻¹ can be seen, which represents the aromatic C = C and C = O vibrations of amide I groups [29]. The next band, at 1410 cm⁻¹, is characteristic of C–O bond vibrations as well as vibrations in C–N (amide III) [30,31]. The sharp peak at 1005 cm⁻¹ corresponds to the Si–O–Si stretching of silicates and clay minerals as well as the C–O–C stretching of polysaccharides [32]. Three other peaks in the soil samples were found at 795, 775, and 695 cm⁻¹, which are due to Si–O bonds in quartz material [26].

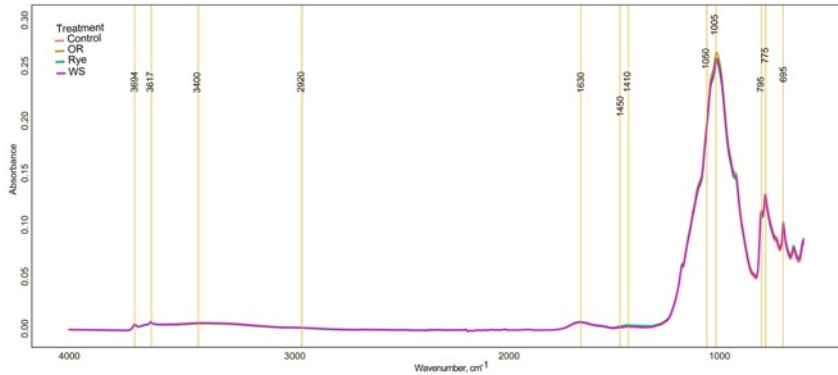


Figure 1. Average FTIR spectra obtained from analyses of the soil in each of four treatment conditions over a 105-day incubation period: soil only (Control), soil mixed with oilseed rape residues (OR), soil mixed with rye residues (Rye), and soil mixed with wheat straw (WS).

2.4. Decomposition Rates

The C decomposition of crop residues was estimated based on the initial input of carbon into the soil [33] and expressed as:

$$netC_{evolved} = C_{amended} - C_{control} \tag{1}$$

In Equation (1), $netC_{evolved}$ is the difference between amended carbon ($C_{amended}$) as plant residues and carbon flushed from the control treatment ($C_{control}$). The percentage of remaining C ($\%C_{remaining}$) was estimated as a function of:

$$\%C_{remaining} = ((C_{initial} - C_{evolved}) / C_{initial}) \times 100 \tag{2}$$

$C_{initial}$ is the C concentration of the added residue, and $C_{evolved}$ is the C emitted as CO₂ during incubation. A double exponential model was used to calculate the decomposition rate:

$$C_t = C_a(e^{-k_a t}) + C_p(e^{-k_p t}). \tag{3}$$

The model divides the incorporated fresh organic matter from oilseed rape, wheat straw, and rye treatments into two pools of rapidly decomposing C_a and slow decomposing C_p . In the model, C_t is the percentage of remaining C from the residue at time t , k_a is the decomposition rate of the rapidly decomposing pool, and k_p is the decomposition rate of the stable fraction C_p . The percentage of remaining C should be between 0 and 100. The model does not consider the transformation of labile material into more recalcitrant material, which can occur during microbial activity.

2.5. Statistical Analysis

Two-way ANOVA was used to estimate the variation across all parameters using time and treatment factors as well as their interaction. One-way ANOVA was applied to determine the treatment

effect for each parameter on a specific day. One-way ANOVA followed by post hoc Tukey's HSD was used to study the differences between treatments for the final cumulative gas fluxes. The daily gas emissions between measurement points were estimated by linear interpolation [34]. The interpolation was performed to obtain a more realistic value of the percentage of remaining C in the soil, which was calculated from the cumulative CO₂. Pearson correlation and stepwise regression analysis was performed for all data to identify the relationships between parameters. R programming language (R core team, Vienna, Austria, 2019) was used for all statistical analyses. To fit the double exponential model, the 'nlxb' function from the 'nlslr' package was used.

3. Results

3.1. Soil Aggregate Stability

Dry soil at Day 0, before crop residue addition and wetting, had high aggregate stability across all treatments: there were no significant differences between them (Figure 2). However, after water addition on Day 3, the stability decreased significantly with reductions of 25% in the control and rye treatments, 19% in the oilseed rape treatment, and 29% in the wheat straw treatment. Until Day 19, aggregate stability only significantly increased within wheat straw and rye treatments compared to Day 3, reaching a value of 39.36% (± 1.35) and 32.26% (± 0.72) stable aggregates, respectively. Nevertheless, this growth was 10% and 15% lower in wheat straw and rye, respectively, compared to Day 0. In both treatments, aggregate stability further decreased between Days 19 and 28. Afterwards, aggregate stability did not change significantly in wheat straw treatment. In the rye treatment, stability increased continuously between Days 28 and 77. In the oilseed rape treatment, aggregate stability decreased progressively until Day 28. Oilseed rape treatment resulted in a significant increase in aggregate stability at Day 45, and at the end of incubation at Day 105. In the control treatment, a significant decrease also happened on Day 74, followed by an increase at Day 105.

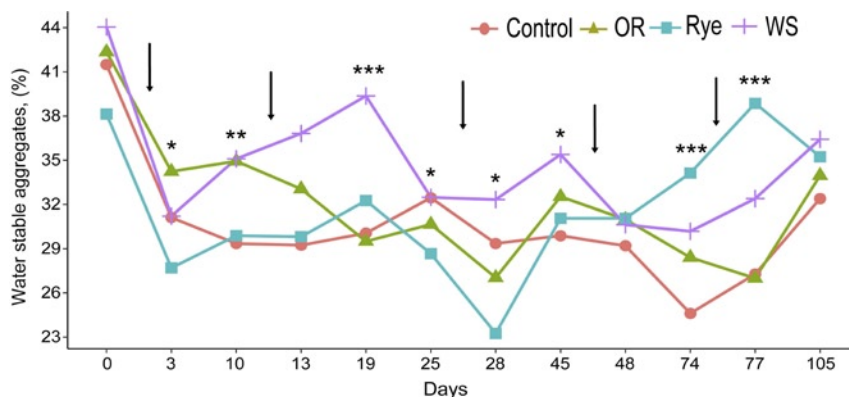


Figure 2. The evolution of water-stable aggregates in each of four treatment conditions over a 105-day incubation period: soil only (Control), soil mixed with oilseed rape residues (OR), soil mixed with rye residues (Rye), and soil mixed with wheat straw (WS). Arrows indicate the water addition events. Stars indicate significant differences between treatments within the same day according to one-way ANOVA (* $p < 0.05$, ** $p < 0.01$, and *** $p < 0.001$).

Comparing the percentage of water-stable aggregates (WSA) on Day 3 of the experiment and after Day 105, there was a higher overall rate of stable aggregates in the rye (>21%) and wheat straw (>14%) treatments. The WSA showed significant variability between and within the treatments during the incubation period (Table 3).

Table 3. Results of two-way ANOVA for the effect of treatment, days, and the interaction of treatment by days for each parameter: soil moisture (SM), soil temperature (Temp.), electrical conductivity (EC), water-stable aggregates (WSA), microbial biomass carbon (MBC), total nitrogen (TN), and total carbon (TC); P1005: relative absorbance of the FTIR peak for silicates and clay minerals as well as C–O–C stretching in polysaccharides; P1410: relative absorbance of the FTIR peak for C–O bond vibrations and also the vibrations in C–N (amide III); P1630: relative absorbance of the FTIR peak for the aromatic C = C and C = O vibrations of amide I groups; P2920: relative absorbance of the FTIR peak for asymmetric C–H vibration of aliphatic compounds.

Parameters	Treatment		Days		Treatment × Days	
	F Value	P	F Value	P	F Value	P
N ₂ O (μg m ⁻² h ⁻¹)	264.239	0.000 ***	76.997	0.000 ***	33.715	0.000 ***
CO ₂ (mg m ⁻² h ⁻¹)	660.949	0.000 ***	237.662	0.000 ***	89.538	0.000 ***
CH ₄ (μg m ⁻² h ⁻¹)	3.936	0.005 **	3.172	0.000 ***	0.873	0.708
SM (m ⁻³ m ⁻³)	442.689	0.000 ***	103.543	0.000 ***	6.866	0.000 ***
Temp. (°C)	149.701	0.000 ***	1859.010	0.000 ***	78.681	0.000 ***
EC (mS cm ⁻¹)	918.884	0.000 ***	98.949	0.000 ***	30.498	0.000 ***
WSA (%)	13.325	0.000 ***	10.291	0.000 ***	3.555	0.000 ***
MBC (mg C kg ⁻¹)	99.688	0.000 ***	12.786	0.000 ***	4.564	0.000 ***
TN (%)	1547.048	0.000 ***	2.832	0.000 ***	1.414	0.036 *
TC (%)	2158.979	0.000 ***	0.725	0.758	1.003	0.477
P2920 (%)	2.151	0.095	2.657	0.104	0.598	0.617
P1630 (%)	3.549	0.015 *	20.296	0.000 ***	5.640	0.001 **
P1410 (%)	55.169	0.000 ***	4.534	0.034 *	3.163	0.025 *
P1005 (%)	14.694	0.000 ***	8.601	0.003 **	2.614	0.052

* $p < 0.05$, ** $p < 0.01$, and *** $p < 0.001$.

There were significant differences between the control and other treatments on Day 10 of the incubation (Figure 2). On Days 10 and 19, a significant increase occurred in wheat straw as compared to other treatments. A significant growth of aggregate stability with respect to other treatments was found in the rye and wheat straw treatments on Days 74 and 77.

3.2. Gas Emissions

The treatments had a significant effect on the evolution of greenhouse gases (Table 3). Oilseed rape and rye treatments had significantly higher CO₂ emissions than other treatments ($p < 0.05$). In both cases, the emissions were highest in the first 25 days of the incubation, after which the emissions stabilized (Figure 3A). The highest peak of emissions in oilseed rape treatment was observed immediately after the addition of the residue, at Day 0, until Day 3, in which there was a decrease from 827.2 (±30.27) mg to 795.08 (±59.98) mg C m⁻² h⁻¹, respectively. For the rye treatment, the maximum CO₂ emissions value was reached on the third day, at 927.06 (±35.41) mg C m⁻² h⁻¹. Wheat straw-treated soil yielded lower emissions than soil with fresh residues, but significantly higher emissions than those of the control treatment. In the oilseed rape and rye treatments, the CO₂ fluxes stabilized after Day 45, whereas in the wheat straw treatment, CO₂ emissions were significantly higher in the last 60 days of the experiment. The cumulative CO₂ emissions in the oilseed rape treatment were 8% higher than in the rye treatment (Figure 3D), 76% higher than in the wheat straw treatment, and 95% higher than in the control treatment.

During the incubation, oilseed rape and rye treatments showed significantly higher N₂O emissions (Figure 3B) than the other treatments. The emissions in oilseed rape and rye began to increase three days after the addition of water, reaching 1.65 (±0.22) mg N m⁻² h⁻¹ in the rye treatment and 0.41 (±0.05) mg N m⁻² h⁻¹ in the oilseed rape treatment. Whilst the N₂O emissions continued to rise in the oilseed rape treatment, for rye treatment, the emissions decreased on Days 5 and 10. After the second water addition, the emissions in both rye and oilseed rape treatments increased

and only stabilized after Day 74. Rye emissions peaked between Days 25 and 28 at a maximum of $5.15 (\pm 0.42) \text{ mg N m}^{-2} \text{ h}^{-1}$.

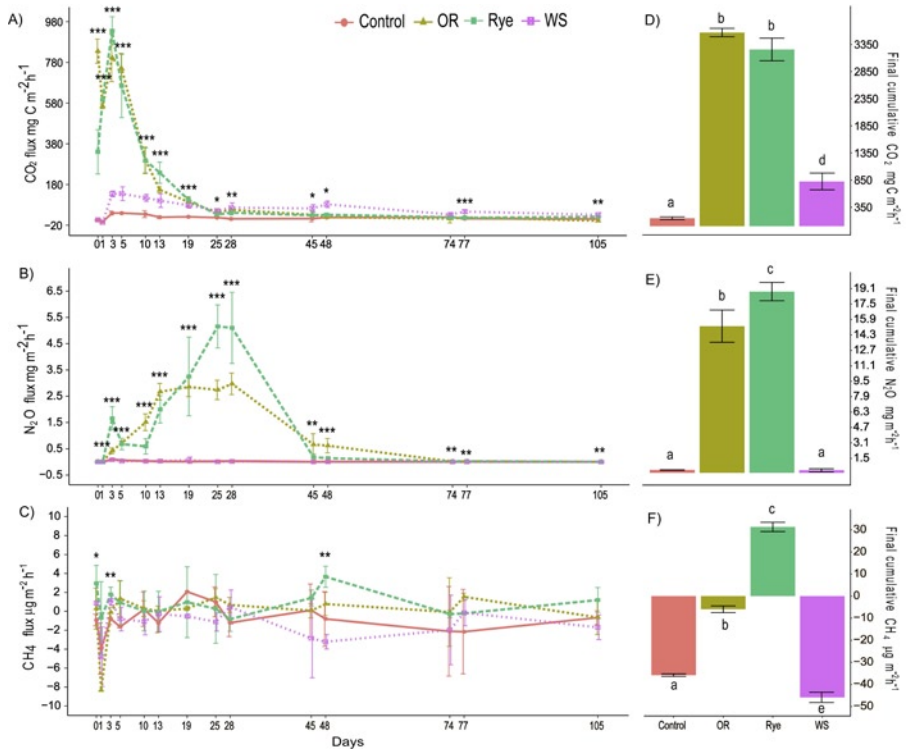


Figure 3. Evolution of CO₂ (A), N₂O (B), and CH₄ (C) flux (mean ± standard error) and average final cumulative flux in each of four treatment conditions over a 105-day incubation period (D), (E), (F): soil only (Control), soil mixed with oilseed rape residues (OR), soil mixed with rye residues (Rye), and soil mixed with wheat straw (WS). Stars indicate significant differences between treatments within the same day according to one-way ANOVA (* $p < 0.05$, ** $p < 0.01$, and *** $p < 0.001$). The different letters represent significant differences between treatments according to Tukey’s HSD test.

By contrast, oilseed rape peak N₂O emissions values were maintained for a more extended period, although the maximum value was significantly lower than for the rye treatment at $2.97 (\pm 0.2) \text{ mg N m}^{-2} \text{ h}^{-1}$. The highest cumulative N₂O emissions were registered in the rye treatment, at $18.79 (\pm 0.48) \text{ mg N m}^{-2} \text{ h}^{-1}$ (Figure 3E). The oilseed rape treatment showed 19% lower cumulative emissions as compared with rye treatment, and 98% higher as compared with control and wheat straw treatments. In both control and wheat straw treatments, the N₂O emissions were not significantly different from each other after 105 days of incubation.

Methane (CH₄) fluxes varied significantly throughout the incubation experiment across all treatments (Figure 3C). Negative CH₄ fluxes were detected in all treatments at specific sampling dates during the experiment. Notably, in the control treatment, negative emissions were registered on 71% of the measured days, and on 80%, 28%, and 35% of the measured days in the wheat straw, oil rapeseed, and rye treatments, respectively. Positive cumulative fluxes were only observed in the rye treatment ($11.04 \text{ μg C m}^{-2} \text{ h}^{-1}$, ± 4.38) (Figure 3F). In all other treatments, cumulative fluxes were negative.

3.3. Microbial Biomass Carbon

The plant residues incorporated into the soil influenced the microbial biomass carbon (MBC) in different ways (Figure 4). The concentration of MBC varied significantly for time (days) and treatment (Table 3), although higher variability was noted between the treatments. In the rye and oilseed rape treatments, MBC was significantly increased on the third day after the first water addition, at $982.7 (\pm 49.73)$ and $415.98 (\pm 84.16)$ mg C kg⁻¹ of dry soil, respectively (Figure 4). In both treatments with fresh residues, MBC dropped significantly on Day 10. After that, it remained relatively stable until Day 25. Between Days 28 and 48, the MBC decreased substantially in the oilseed rape treatment. By contrast, the rye treatment recorded a gradual increase in MBC, starting after 48 days and continuing until the end of the experiment. The wheat straw soil treatment reached its peak more gradually, and only after Day 25. With every water addition, the MBC in the wheat straw decreased until Day 77, which was followed by an increase.

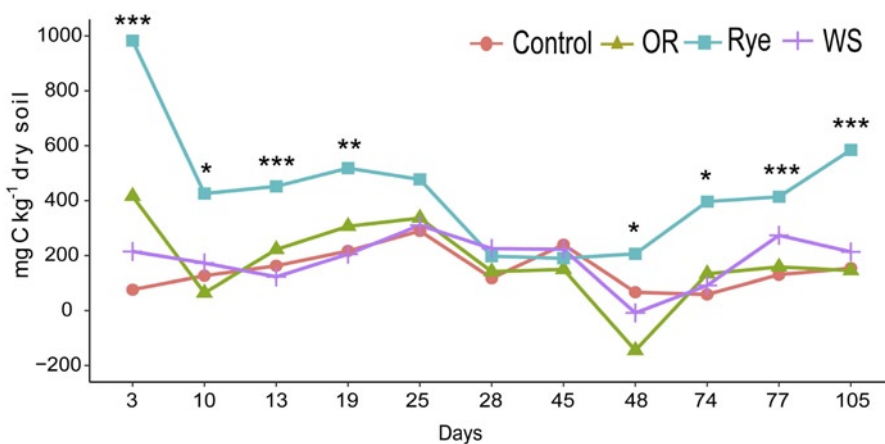


Figure 4. The microbial biomass carbon (MBC) evolution in each of four treatment conditions over a 105-day incubation period: soil only (Control), soil mixed with oilseed rape residues (OR), soil mixed with rye residues (Rye), and soil mixed with wheat straw (WS). Stars indicate significant differences between treatments within the same day according to one-way ANOVA (* $p < 0.05$, ** $p < 0.01$, and *** $p < 0.001$).

3.4. Soil Functional Groups

The treatment and incubation period did not have a significant effect on all identified peaks from the FTIR spectra (Table 3). Overall, the addition of rye plant residues had the greatest effect on the relative absorbance of the aromatic (1630 cm^{-1}) and C–O compounds (1410 cm^{-1}) (Table 4). At Day 105, the rye treatment showed a 25% and a 63% increase in relative absorbance at the peaks of 1630 cm^{-1} and 1410 cm^{-1} , respectively. The mineral compound at the 1005 cm^{-1} peak decreased by 2% in relative absorbance at Day 105 compared to Day 0. The initial biochemical state of the wheat straw treatment did not change significantly after 105 days of incubation, nor were significant changes recorded in the control treatment after Day 105. In the oilseed rape treatment, a 44% increase in relative absorbance was observed at the 1410 cm^{-1} peak (corresponding to C–O and amide (III) compounds). None of the aliphatic compounds in any of the treatments underwent significant changes as reflected in their peak at 2920 cm^{-1} (Table 4).

Table 4. Differences in relative absorbance (%) from the FTIR spectra (mean \pm standard error) in different treatment conditions: Control, OR (soil mixed with oilseed rape residues), Rye (soil mixed with rye residues), and WS (soil mixed with wheat straw residues), at Day 0 (before residue incorporation) and at Day 105.

Treatment	2920	1630	1410	1005
Day 0				
Control	0.00 (± 0.00) a *	2.55 (± 0.08) a	0.55 (± 0.04) a	96.91 (± 0.10) a
Rye	0.00 (± 0.00) a	2.68 (± 0.07) a	0.27 (± 0.07) c	97.06 (± 0.12) a
WS	0.16 (± 0.07) a	2.61 (± 0.10) a	0.43 (± 0.04) ac	96.80 (± 0.17) a
OR	0.16 (± 0.09) a	2.78 (± 0.08) a	0.45 (± 0.01) a	96.61 (± 0.11) a
105 days				
Control	0.20 (± 0.06) a	2.78 (± 0.05) a	0.51 (± 0.05) a	96.52 (± 0.11) a
Rye	0.20 (± 0.06) a	3.59 (± 0.08) b ** \uparrow	0.74 (± 0.06) c \uparrow	95.47 (± 0.15) c \downarrow
WS	0.14 (± 0.06) a	2.77 (± 0.05) a	0.42 (± 0.01) a	96.67 (± 0.06) a
OR	0.14 (± 0.06) a	2.63 (± 0.05) a	0.80 (± 0.03) c \uparrow	96.43 (± 0.08) a

* The different letters indicate the significant difference between the treatments on specific days, according to Tukey's comparison test. ** Arrows indicate a significant decrease or increase in relative absorbance within each treatment as compared to the initial values at Day 0 according to Tukey's comparison test.

4. Discussion

After 105 days of incubation, there was a total of 58.04% and 60.77% remaining C in the oilseed rape and rye treatments, respectively, and 71.19% in the wheat straw treatment (Table 5). Based on the percentage of remaining C, the double exponential model was applied, which divides the incorporated organic material into labile and stable fractions. C_a , which is initial labile C content in the crop residues, was between 38% and 40% in the rye and oilseed rape treatments, respectively.

Table 5. Observed remaining carbon (C) in soil with added crop residues after 105 days of incubation, and kinetic coefficients calculated from the double exponential model (Equation (3)). Values in the brackets are standard errors of the mean ($n = 3$). Soil mixed with wheat straw (WS), soil mixed with fresh green oilseed rape residues (OR), and soil mixed with fresh green rye residues (Rye).

Treatment	Observed Remaining C %	C_a * %	C_p * %	k_a * %C d $^{-1} \times 10^2$	k_p * %C d $^{-1} \times 10^4$
WS	71.19 (± 4.73)	27.03 (± 6.67)	72.97 (± 6.67)	0.7 (± 0.00)	-32.9 (± 0.00)
OR	58.04 (± 0.95)	38.38 (± 0.26)	61.62 (± 0.26)	13.2 (± 0.00)	5.7 (± 0.00)
Rye	60.77 (± 2.18)	39.23 (± 2.39)	60.77 (± 2.39)	12.7 (± 0.00)	4.3 (± 0.00)

* C_a : initial %C in the rapidly decomposing organic material; C_p : initial %C in the slow decomposing organic material; k_a : decomposition rate of C_a ; k_p : decomposition rate of C_p .

The decomposition rates for the labile fraction k_a in the rye and oilseed rape treatments were 12.7×10^2 and 13.7×10^2 %C d $^{-1}$, respectively. The stable fraction k_p registered a slower decomposition rate in rye residues, of 4.3×10^4 %C d $^{-1}$, compared to oilseed rape, at 5.7×10^4 %C d $^{-1}$. In case of wheat straw, a negative result was observed for the decomposition rate of stable fraction k_p (-32.9×10^4 , %C d $^{-1}$). The negative decomposition rate is the result of compounds in the labile fraction that are less readily decomposed, taking a longer time to decompose and delaying the start of the decomposition of the stable fraction. Furthermore, in terms of the labile fraction, wheat straw had a much lower positive decomposition rate of the labile fraction k_a compared to other residues (0.7×10^2 , %C d $^{-1}$). Generally, these findings are consistent with the findings of Johnson et al. [33] and Barel et al. [35], who found that crop residues with lower C/N have higher decomposition rates. Jama and Nair [36] also found, in a decomposition study, that the decomposition speed of the labile fraction is more strongly correlated to the C/N ratio than that of the stable fraction. Additionally, Ajwa and Tabatai [37] noticed that decomposition rates increase with the higher total N of crop residues. It is worth noting

that the dry matter in crop residues decreases in the following order: wheat straw > rye > oilseed rape. Consequently, the decomposition rates were inversely proportional to the dry matter content in the crop residues. This means that at lower dry matter content, the decomposition rates are higher (oilseed rape < rye < wheat straw).

In this study, it was hypothesized that low aggregate stability is related to the high decomposition rates of 'young' organic matter. Both rye and oilseed rape had high decomposition rates at the beginning of incubation, which resulted in a flush of CO₂ and N₂O emission, even before water addition (on the first day) (Figure 3A,B). The high CO₂ emissions and decomposition rates in rye and oilseed rape treatments are in agreement with Ghimire et al. [38], who showed that crop residues with a higher labile fraction generate a higher CO₂ efflux. The period of the highest CO₂ emissions rate occurred during the first 10 days of incubation (Figure 3A). After Day 10, the CO₂ emissions started to slow down in all the treatments with crop residues. Thus, starting from Day 10, the aggregate stability in the rye and wheat straw treatments increased for a short period. In the oilseed rape treatment, the aggregate stability declined after 10 days. Furthermore, wheat straw with a lower decomposition rate and CO₂ emissions had higher aggregate stability from Day 10 to 19 compared with rye and oilseed rape treatments. In this study, no significant correlation between the soil aggregate stability and CO₂ emissions was found. However, other studies suggest that the higher the aggregate stability is, the higher the CO₂ emissions might be [39,40]. That can happen due to higher C concentrations inside the stable aggregates. The increase in N₂O emissions was significantly influenced by the decrease in aggregate stability (Table 6). The result is in line with previous literature [41] showing that aggregates disruption can serve as spots of N₂O emissions. In the rye treatment, the highest N₂O fluxes were observed from Day 19 to Day 28 of the incubation period (Figure 3B).

Meanwhile, the aggregate stability in this treatment decreased starting from Day 25 (Figure 2). In the oilseed rape treatment, the highest N₂O emissions correspond to the period between Days 13 and 28 (Figure 3B). By contrast, aggregate stability for this period, compared with Day 10, decreased to even lower values (Figure 2). The more advanced the decomposition stage, the more organic matter is decomposed, which makes the organic matter become more porous and retain more water [42]. During the 28 days of incubation, three water additions were made according to the gravimetric field capacity of the soil and the weight of the pots after the first water addition. The decomposed organic matter increased the retention capacity of the soil mass. Additionally, this influenced the high amount of N₂O emissions because conditions favorable for the denitrification process were created by increasing the water content. Kravchenko et al. [43] confirmed that crop residues tend to increase water content by absorbing water from the soil and increasing N₂O emissions.

Overall, the observed remaining C in the soil proved to have a significant positive influence on soil aggregate stability (Table 6). After 28 days of incubation, the decomposition rates slowed down; consequently, less carbon was flushed from the soil leaving, in turn, a more stable fraction in the soil, which resulted in an increase in aggregate stability after 28 days of incubation for the rye and wheat straw treatments.

Slower decomposition rates generate slower microbial activity which, in the long term, stabilizes the soil organic matter inside the aggregates [44]. At the same time, a slower decomposition rate occurs with less decomposable compounds (cellulose, lignin, lipids, etc.). This could explain the increase in MBC (Figure 4) and aggregate stability (Figure 2) after 48 days of rye and wheat straw treatment. Besides the chemical composition of crop residues, which influences the decomposition rates, the soil moisture and temperature are two important factors that can speed up decomposition [45]. Soil moisture positively influenced the N₂O emissions and CH₄. The present finding also supports Schaufler et al. [46], who concluded that soil moisture positively influences nitrous oxide and methane emissions. In our research, the link between soil moisture and CO₂ emissions was negative.

Table 6. Correlation matrix between different parameters for all data (CO₂: carbon dioxide emissions; N₂O: nitrous oxide emissions; CH₄: methane emissions; SM: soil moisture; Temp.: soil temperature; EC: electrical conductivity; WSA: water-stable aggregates; MBC: microbial biomass carbon; TN: total nitrogen; TC: total carbon; P1005: relative absorbance of the FTIR peak for silicates and clay minerals as well as C–O–C stretching in polysaccharides; P1410: relative absorbance of the FTIR peak for C–O bond vibrations and also the vibrations in C–N (amide III); P1630: relative absorbance of the FTIR peak for the aromatic C=C and C=O vibrations of amide I groups; P2920: relative absorbance of the FTIR peak for asymmetric C–H vibration of aliphatic compounds; C_{remain}: observed remaining carbon from crop residues in the soil after 105 days).

	N ₂ O	CO ₂	CH ₄	SM	Temp	EC	MBC	WSA	TN	TC	P1005	P1410	P1630
CO ₂	NS												
CH ₄	NS	NS											
SM	0.3 ***	-0.2 *	0.2 *										
Temp	NS	0.2 *	NS	-0.6 ***									
EC	0.7 ***	NS	0.3 ***	0.2 **	-0.2 ***								
MBC	0.3 ***	0.5 ***	0.2 **	NS	-0.2 *	NS							
WSA	-0.3 **	NS	-0.2 **	-0.5 ***	0.2 ***	-0.3 ***	NS						
TN	0.4 ***	NS	0.2 *	NS	NS	0.7 ***	0.2 **	NS					
TC	0.4 ***	0.2 *	0.2 **	NS	NS	0.4 ***	0.4 ***	NS	0.7 ***				
P1005	-0.3 **	NS	NS	-0.2 **	0.4 **	-0.3 ***	-0.3 ***	NS	-0.4 ***	-0.4 ***			
P1410	0.4 **	NS	NS	NS	NS	0.6 ***	0.3 ***	NS	0.6 ***	0.4 ***	-0.7 ***		
P1630	NS	NS	NS	0.2 **	NS	-0.2 **	NS	NS	0.2 *	0.2 ***	-0.8 ***	0.2 ***	
P2920	0.3 *	NS	NS	0.2 *	-0.3 *	0.3 **	0.3 ***	NS	NS	0.2 *	-0.6 ***	0.3 ***	NS
C _{remain}	-0.5 ***	NS	-0.3 ***	-0.3 **	NS	-0.8 ***	NS	0.4 ***	-0.8 ***	-0.5 ***	0.5 ***	-0.8 ***	NS

NS: not significant, * $p < 0.05$, ** $p < 0.01$, and *** $p < 0.001$.

Schaufler et al. found that CO₂ emissions are higher at an intermediate soil moisture content, which is in agreement with our findings showing that CO₂ emissions are lower at higher moisture contents and lower temperatures. Regarding methane emissions, only the rye treatment had positive cumulative emissions, which could be explained by the creation of anaerobic hotspots by microorganisms that consume oxygen during intense activity.

In this study, soil moisture served as a trigger for the decrease in soil aggregate stability (Table 6). The disruption of aggregates occurs as a result of the water addition procedure. The results from stepwise regression analysis show that soil moisture or soil electric conductivity can serve as significant predictor variables for soil aggregate stability in all treatments. Both rye and oilseed rape treatments had higher soil electric conductivity (see Figure S1) and higher crop residue TN (Table 2). Soil electric conductivity was also positively correlated with N₂O emissions and soil moisture (Table 6). Thus, it can be concluded that a higher soil moisture content increases the soil electrical conductivity and N₂O emissions, and indirectly influences soil aggregate stability. The negative correlation between aggregate stability and soil moisture was previously confirmed by Perfect et al. [47]. The decrease of aggregate stability after wetting may be related to the presence of entrapped air inside the aggregates, which triggers aggregate slaking [48].

The incorporation of crop residues had a significant effect on the soil functional groups (Table 3). This is the result of differences in the functional groups of crop residues analyzed by FTIR (see Figure S2). Thus, the incorporation of crop residues in soil increased the levels of amide I group or protein compounds (1630 cm⁻¹) in the soil mixed with rye residues (Table 4). The peak responsible for carbohydrates and the amide III group at 1410 cm⁻¹ also showed an increase due to the incorporation of rye and oilseed rape residues. Only wheat straw treatment did not have a significant effect on soil functional groups. This was probably due to the duration of the experiment, since the biochemical compounds in the wheat require a longer time to decompose.

The small changes in the relative absorbance of peaks at 1630 and 1410 cm⁻¹ in the rye and oilseed rape treatments did not appear to have any effect on aggregate stability as no significant correlation was found (Table 6). Stepwise regression analysis identified two treatments (rye and wheat straw) in which soil functional group changes influenced aggregate stability (Table 7). In the wheat straw treatment, the aliphatic group (2920 cm⁻¹) had a positive influence on the soil aggregate stability. This can be directly correlated with the decomposition of the labile fraction from wheat straw at the beginning of the experiment and the high total carbon content of the crop residue. Demyan et al. [27] specified that the aliphatic group could result from the increase in labile organic matter.

Table 7. Results of stepwise multiple regression analysis showing the influence of different factors (N₂O: nitrous oxide emissions; SM: soil moisture; Temp.: soil temperature; EC: electrical conductivity; MBC: microbial biomass carbon; TN: total nitrogen; TC: total carbon; P1005: relative absorbance of the FTIR peak for silicates and clay minerals as well as C–O–C stretching in polysaccharides; P1410: relative absorbance of the FTIR peak for C–O bond vibrations and also the vibrations in C–N (amide III); P2920: relative absorbance of the FTIR peak for asymmetric C–H vibration of aliphatic compounds) on water-stable aggregates within different treatments after 105 days.

	Partial R2	Model R2	F-Value	P > F
Control				
SM	0.069	0.062	10.202	0.057
EC	0.112	0.099	8.616	0.0091 **
TC	0.229	0.212	13.441	0.000 ***
N ₂ O	0.246	0.222	10.362	0.0832
Rye				
SM	0.268	0.245	11.371	0.0048 **
TN	0.390	0.349	9.584	0.0002 ***
Temp	0.525	0.476	10.701	0.2437
P1410	0.584	0.525	9.835	0.0101 *
P1005	0.631	0.563	9.249	0.0739

Table 7. Cont.

	Partial R2	Model R2	F-Value	P > F
WS				
P2920	0.209	0.183	8.182	0.0009 ***
MBC	0.313	0.268	6.845	0.0201 *
EC	0.408	0.347	6.668	0.0395 *
OR				
EC	0.274	0.250	11.674	0.0006 ***
TC	0.509	0.476	15.563	0.0002 ***

* $p < 0.05$, ** $p < 0.01$, and *** $p < 0.001$.

Meanwhile, in the rye treatment, the aggregate stability was significantly influenced by the carbohydrates/amide III group represented by the 1410 cm^{-1} peak (Table 7). This is based on the significantly higher relative absorbance of this peak (Table 4) in the rye treatment. However, this compound is also influenced considerably by the TN and TC content in soil (Table 6), which proved to be significantly higher in the rye treatment compared to other treatments.

5. Conclusions

This study examined the short-term effects of cover crop residue addition on water-stable aggregates in soil. The chemical composition of organic matter was demonstrated to play an essential role in increasing the levels of water-stable aggregates. The decomposition rates of different types of organic matter were highly dependent on their C/N ratio. The lower C/N ratio in rye and oilseed rape residues resulted in higher decomposition rates. Residues with a low C/N ratio were associated with higher CO_2 and N_2O emissions. The high decomposition rates of crop residues and water addition in the early stages of incubation each led to a significant decrease in aggregate stability. The addition of the crop residues had a short transient effect on the soil aggregate stability. The degree of soil moisture negatively affected aggregate stability in untreated field soil as well as in soil with added rye, oilseed rape, or wheat straw. The results also show that a higher amount of remaining C in the soil can positively influence soil aggregate stability. General correlation analysis between soil biochemical compounds and soil aggregate stability did not show any significant relationships, although stepwise regression analysis showed that aliphatic compounds (2920 cm^{-1}) and the carbohydrates/amide III group (1410 cm^{-1}) from the wheat straw and rye treatments, respectively, can significantly influence the aggregate stability.

Further study is needed to fully understand the relationship between soil moisture and the water retention capacity of crop residues and influence on aggregate stability. However, it is also essential that future studies characterize the addition rates of crop residue that can improve aggregate stability, irrespective of soil moisture content and decomposition rates.

Supplementary Materials: The following are available online at <http://www.mdpi.com/2077-0472/10/11/527/s1>, Figure S1: The evolution of soil moisture (a), electrical conductivity (b) and soil temperature (c) (mean and \pm standard error) in each of four treatment conditions: soil only (Control), soil mixed with oilseed rape residues (OR), soil mixed with rye residues (Rye), soil mixed with wheat straw (WS), over a 105-day incubation period. Stars indicate significant differences between treatments within the same day according to one-way ANOVA (* $p < 0.05$, ** $p < 0.01$, and *** $p < 0.001$), Figure S2: FT-IR spectra of the crop residues incorporated in the soil.

Author Contributions: Conceptualization, E.R. and T.T.; methodology, E.R., G.S., J.E.-G. and T.T.; validation, E.R.; formal analysis, G.S., K.K. and K.S.; resources, E.R. and A.A.; data curation, J.E.-G. and G.S.; writing—original draft, G.S.; writing—review and editing, J.E.-G., K.S., K.K., E.R. and A.A.; visualization, G.S.; supervision, E.R. and T.T.; project administration, E.R.; funding acquisition, E.R. and A.A. All authors have read and agreed to the published version of the manuscript.

Funding: The research was funded by the European Union's European Regional Development Fund (Estonian University of Life Sciences ASTRA project [2014-2020.4.01.16-0036] "Value-chain based bio-economy") and the Horizon 2020 project iSQAPER [project number 635750].

Acknowledgments: We would like to thank our colleagues Imbi Albre and Raja Kährik for analyzing the initial soil chemical properties.

Conflicts of Interest: The authors declare no conflict of interest.

References

1. Tisdall, J.M.; Oades, J.M. Organic matter and water-stable aggregates in soils. *J. Soil Sci.* **1982**, *33*, 141–163. [[CrossRef](#)]
2. Abiven, S.; Menasseri, S.; Angers, D.A.; Leterme, P. Dynamics of aggregate stability and biological binding agents during decomposition of organic materials. *Eur. J. Soil Sci.* **2007**, *58*, 239–247. [[CrossRef](#)]
3. Liu, A.; Ma, B.L.; Bomke, A.A. Effects of Cover Crops on Soil Aggregate Stability, Total Organic Carbon, and Polysaccharides. *Soil Sci. Soc. Am. J.* **2005**, *69*, 2041–2048. [[CrossRef](#)]
4. Angst, G.; Mueller, K.E.; Kögel-Knabner, I.; Freeman, K.H.; Mueller, C.W. Aggregation controls the stability of lignin and lipids in clay-sized particulate and mineral associated organic matter. *Biogeochemistry* **2017**, *132*, 307–324. [[CrossRef](#)]
5. Abiven, S.; Menasseri, S.; Chenu, C. The effects of organic inputs over time on soil aggregate stability—A literature analysis. *Soil Biol. Biochem.* **2009**, *41*, 1–12. [[CrossRef](#)]
6. Shahbaz, M.; Kuzyakov, Y.; Sanaullah, M.; Heitkamp, F.; Zelenev, V.; Kumar, A.; Blagodatskaya, E. Microbial decomposition of soil organic matter is mediated by quality and quantity of crop residues: Mechanisms and thresholds. *Biol. Fertil. Soils* **2017**, *53*, 287–301. [[CrossRef](#)]
7. Sarker, T.C.; Incerti, G.; Spaccini, R.; Piccolo, A.; Mazzoleni, S.; Bonanomi, G. Linking organic matter chemistry with soil aggregate stability: Insight from ¹³C NMR spectroscopy. *Soil Biol. Biochem.* **2018**, *117*, 175–184. [[CrossRef](#)]
8. Mizuta, K.; Taguchi, S.; Sato, S. Soil aggregate formation and stability induced by starch and cellulose. *Soil Biol. Biochem.* **2015**, *87*, 90–96. [[CrossRef](#)]
9. Dungait, J.A.J.; Hopkins, D.W.; Gregory, A.S.; Whitmore, A.P. Soil organic matter turnover is governed by accessibility not recalcitrance. *Glob. Chang. Biol.* **2012**, *18*, 1781–1796. [[CrossRef](#)]
10. Parr, J.F.; Papendick, R.I. Factors Affecting the Decomposition of Crop Residues by Microorganisms. *Crop Residue Manag. Syst.* **2015**, *31*, 101–129.
11. Cosentino, D.; Chenu, C.; Le Bissonnais, Y. Aggregate stability and microbial community dynamics under drying-wetting cycles in a silt loam soil. *Soil Biol. Biochem.* **2006**, *38*, 2053–2062. [[CrossRef](#)]
12. Macrae, R.J.; Mehuys, G.R. The effect of green manuring on the physical properties of temperate-area soils. *Adv. Soil Sci.* **1985**, *3*, 71–94. [[CrossRef](#)]
13. Blanco-Canqui, H.; Shaver, T.M.; Lindquist, J.L.; Shapiro, C.A.; Elmore, R.W.; Francis, C.A.; Hergert, G.W. Cover Crops and Ecosystem Services: Insights from Studies in Temperate Soils. *Agron. J.* **2015**, *107*, 2449. [[CrossRef](#)]
14. Coppens, F.; Garnier, P.; De Gryze, S.; Merckx, R.; Recous, S. Soil moisture, carbon and nitrogen dynamics following incorporation and surface application of labelled crop residues in soil columns. *Eur. J. Soil Sci.* **2006**, *57*, 894–905. [[CrossRef](#)]
15. Chahal, I.; Van Eerd, L.L. Cover crop and crop residue removal effects on temporal dynamics of soil carbon and nitrogen in a temperate, humid climate. *PLoS ONE* **2020**, *15*, e0235665. [[CrossRef](#)]
16. Muhammad, I.; Wang, J.; Sainju, U.M.; Zhang, S.; Zhao, F.; Khan, A. Cover cropping enhances soil microbial biomass and affects microbial community structure: A meta-analysis. *Geoderma* **2021**, *381*, 114696. [[CrossRef](#)]
17. Sánchez de Cima, D.; Tein, B.; Eremeev, V.; Luik, A.; Kauer, K.; Reintam, E.; Kahu, G. Winter cover crop effects on soil structural stability and microbiological activity in organic farming. *Biol. Agric. Hortic.* **2015**, *8765*, 1–12. [[CrossRef](#)]
18. Balesdent, J.; Chenu, C.; Balabane, M. Relationship of soil organic matter dynamics to physical protection and tillage. *Soil Tillage Res.* **2000**, *53*, 215–230. [[CrossRef](#)]
19. Deneff, K.; Six, J.; Bossuyt, H.; Frey, S.D.; Elliott, E.T.; Merckx, R.; Paustian, K. In fluence of dry-wet cycles on the interrelationship between aggregate, particulate organic matter, and microbial community dynamics. *Soil Tillage Res.* **2001**, *33*, 1599–1611. [[CrossRef](#)]
20. Kemper, W.D.; Rosenau, R.C. Aggregate Stability and Size Distribution. In *Methods of Soil Analysis, Part 1—Physical and Mineralogical Methods*; Wiley Online Library: Hoboken, NJ, USA, 1986; Volume 9, pp. 425–442, ISBN 978-0891188414.
21. Hutchinson, G.L.; Livingston, G.P. Use of chamber systems to measure trace gas fluxes. *Agric. Ecosyst. Eff. Trace Gases Glob. Clim. Chang.* **1993**, *55*, 63–78.

22. Escuer-Gatius, J.; Shanskiy, M.; Soosaar, K.; Astover, A.; Raave, H. High-temperature hay biochar application into soil increases N₂O fluxes. *Agronomy* **2020**, *10*, 109. [[CrossRef](#)]
23. Lofffield, N.; Flessa, H.; Augustin, J.; Beese, F. Automated Gas Chromatographic System for Rapid Analysis of the Atmospheric Trace Gases Methane, Carbon Dioxide, and Nitrous Oxide. *J. Environ. Qual.* **1997**, *26*, 560–564. [[CrossRef](#)]
24. Fließbach, A.; Mäder, P. Microbial biomass and size-density fractions differ between soils of organic and conventional agricultural systems. *Soil Biol. Biochem.* **2000**, *32*, 757–768. [[CrossRef](#)]
25. Gerzabek, M.H.; Antil, R.S.; Kögel-Knabner, I.; Knicker, H.; Kirchmann, H.; Haberhauer, G. How are soil use and management reflected by soil organic matter characteristics: A spectroscopic approach. *Eur. J. Soil Sci.* **2006**, *57*, 485–494. [[CrossRef](#)]
26. Bernier, M.H.; Levy, G.J.; Fine, P.; Borisover, M. Organic matter composition in soils irrigated with treated wastewater: FT-IR spectroscopic analysis of bulk soil samples. *Geoderma* **2013**, *209*, 233–240. [[CrossRef](#)]
27. Demyan, M.S.; Rasche, F.; Schulz, E.; Breulmann, M.; Müller, T.; Cadisch, G. Use of specific peaks obtained by diffuse reflectance Fourier transform mid-infrared spectroscopy to study the composition of organic matter in a Haplic Chernozem. *Eur. J. Soil Sci.* **2012**, *63*, 189–199. [[CrossRef](#)]
28. Parolo, M.E.; Savini, M.C.; Loewy, R.M. Characterization of soil organic matter by FT-IR spectroscopy and its relationship with chlorpyrifos sorption. *J. Environ. Manag.* **2017**, *196*, 316–322. [[CrossRef](#)]
29. Toosi, E.R.; Kravchenko, A.N.; Mao, J.; Quigley, M.Y.; Rivers, M.L. Effects of management and pore characteristics on organic matter composition of macroaggregates: Evidence from characterization of organic matter and imaging. *Eur. J. Soil Sci.* **2017**, *68*, 200–211. [[CrossRef](#)]
30. Baumann, K.; Schöning, I.; Schrupf, M.; Ellerbrock, R.H.; Leinweber, P. Rapid assessment of soil organic matter: Soil color analysis and Fourier transform infrared spectroscopy. *Geoderma* **2016**, *278*, 49–57. [[CrossRef](#)]
31. Tatzber, M.; Mutsch, F.; Mentler, A.; Leitgeb, E.; Englisch, M.; Zehetner, F.; Djukic, I.; Gerzabek, M.H. Mid-infrared spectroscopy for topsoil layer identification according to litter type and decomposition stage demonstrated on a large sample set of Austrian forest soils. *Geoderma* **2011**, *166*, 162–170. [[CrossRef](#)]
32. Poirier, N.; Sohi, S.P.; Gaunt, J.L.; Mahieu, N.; Randall, E.W.; Powlson, D.S.; Evershed, R.P. The chemical composition of measurable soil organic matter pools. *Org. Geochem.* **2005**, *36*, 1174–1189. [[CrossRef](#)]
33. Johnson, J.M.F.; Barbour, N.W.; Weyers, S.L. Chemical composition of crop biomass impacts its decomposition. *Soil Sci. Soc. Am. J.* **2007**, *71*, 155–162. [[CrossRef](#)]
34. Vinzent, B.; Fuß, R.; Maidl, F.X.; Hülsbergen, K.J. N₂O emissions and nitrogen dynamics of winter rapeseed fertilized with different N forms and a nitrification inhibitor. *Agric. Ecosyst. Environ.* **2018**, *259*, 86–97. [[CrossRef](#)]
35. Barel, J.M.; Kuyper, T.W.; Paul, J.; de Boer, W.; Cornelissen, J.H.C.; De Deyn, G.B. Winter cover crop legacy effects on litter decomposition act through litter quality and microbial community changes. *J. Appl. Ecol.* **2019**, *56*, 132–143. [[CrossRef](#)]
36. Jama, B.A.; Nair, P.K.R. Decomposition- and nitrogen-mineralization patterns of *Leucaena leucocephala* and *Cassia siamea* mulch under tropical semiarid conditions in Kenya. *Plant Soil* **1996**, *179*, 275–285. [[CrossRef](#)]
37. Ajwa, H.A.; Tabatabai, M.A. Decomposition of different organic materials in soils. *Biol. Fertil. Soils* **1994**, *18*, 175–182. [[CrossRef](#)]
38. Ghimire, B.; Ghimire, R.; VanLeeuwen, D.; Mesbah, A. Cover Crop Residue Amount and Quality Effects on Soil Organic Carbon Mineralization. *Sustainability* **2017**, *9*, 2316. [[CrossRef](#)]
39. Chaplot, V.; Cooper, M. Soil aggregate stability to predict organic carbon outputs from soils. *Geoderma* **2015**, *243*, 205–213. [[CrossRef](#)]
40. Gispert, M.; Emran, M.; Pardini, G.; Doni, S.; Ceccanti, B. The impact of land management and abandonment on soil enzymatic activity, glomalin content and aggregate stability. *Geoderma* **2013**, *202*, 51–61. [[CrossRef](#)]
41. Ball, B.C. Soil structure and greenhouse gas emissions: A synthesis of 20 years of experimentation. *Eur. J. Soil Sci.* **2013**, *64*, 357–373. [[CrossRef](#)]
42. Iqbal, A.; Beaugrand, J.; Garnier, P.; Recous, S. Tissue density determines the water storage characteristics of crop residues. *Plant Soil* **2013**, *367*, 285–299. [[CrossRef](#)]
43. Kravchenko, A.N.; Toosi, E.R.; Guber, A.K.; Ostrom, N.E.; Yu, J.; Azeem, K.; Rivers, M.L.; Robertson, G.P. Hotspots of soil N₂O emission enhanced through water absorption by plant residue. *Nat. Geosci.* **2017**, *10*, 496–500. [[CrossRef](#)]

44. Golchin, A.; Oades, J.M.; Skjemstad, J.O.; Clarke, P. Soil structure and carbon cycling. *Soil Res.* **1994**, *32*, 1043–1068. [[CrossRef](#)]
45. Kauer, K.; Raave, H.; Köster, T.; Viiralt, R.; Noormets, M.; Keres, I.; Laidna, T.; Parol, A.; Selge, A. The decomposition of turfgrass clippings is fast at high air humidity and moderate temperature. *Acta Agric. Scand. Sect. B Soil Plant Sci.* **2012**, *62*, 224–234. [[CrossRef](#)]
46. Schaufler, G.; Schindlbacher, A.; Skiba, U.; Kitzler, B.; Zechmeister-Boltenstern, S.; Sutton, M.A. Greenhouse gas emissions from European soils under different land use: Effects of soil moisture and temperature. *Eur. J. Soil Sci.* **2010**, *61*, 683–696. [[CrossRef](#)]
47. Perfect, E.; Kay, B.D.; Van Loon, W.K.P.; Sheard, R.W.; Pojasok, T. Factors influencing soil structural stability within a growing season. *Soil Sci. Soc. Am. J.* **1990**, *54*, 173–179. [[CrossRef](#)]
48. Hillel, D. Soil Physical Attributes. *Soil Environ.* **2008**, 55–77. [[CrossRef](#)]

Publisher’s Note: MDPI stays neutral with regard to jurisdictional claims in published maps and institutional affiliations.



© 2020 by the authors. Licensee MDPI, Basel, Switzerland. This article is an open access article distributed under the terms and conditions of the Creative Commons Attribution (CC BY) license (<http://creativecommons.org/licenses/by/4.0/>).

III

III Escuer-Gatius, J., Shanskiy, M., Mander, Ü., Kauer, K., Astover, A., Vahter, H., Soosaar, K. 2020. Intensive rain hampers the effectiveness of nitrification inhibition in controlling N₂O emissions from dairy slurry fertilised soils. *Agriculture* 10(11), 497.

Article

Intensive Rain Hampers the Effectiveness of Nitrification Inhibition in Controlling N₂O Emissions from Dairy Slurry-Fertilized Soils

Jordi Escuer-Gatius ¹, Merrit Shanskiy ¹, Ülo Mander ², Karin Kauer ¹, Alar Astover ¹, Hanna Vahter ² and Kaido Soosaar ^{2,*}

¹ Institute of Agricultural and Environmental Sciences, Estonian University of Life Sciences, 51006 Tartu, Estonia; jordi.escuer@emu.ee (J.E.-G.); merrit.shanskiy@emu.ee (M.S.); karin.kauer@emu.ee (K.K.); alar.astover@emu.ee (A.A.)

² Institute of Ecology and Earth Sciences, University of Tartu, 51014 Tartu, Estonia; ulo.mander@ut.ee (Ü.M.); hanna.vahter@ut.ee (H.V.)

* Correspondence: kaido.soosaar@ut.ee

Received: 3 September 2020; Accepted: 21 October 2020; Published: 24 October 2020



Abstract: Nitrification inhibitors have been proposed as a tool to mitigate nitrous oxide (N₂O) emissions from agriculture, which are caused mainly by fertilization. The nitrification inhibitor 3,4-Dimethylpyrazole phosphate (DMPP) was tested in a winter rapeseed field after dairy slurry application in Central Estonia. N₂O emissions were monitored using the closed chamber method. Soil and leachate chemical parameters were also analyzed. N₂O emissions increased from pre-slurry application values of 316 and 264 µg m⁻² h⁻¹ for the control and treatment plot, respectively, to maximum values of 3130.71 and 4834 µg m⁻² h⁻¹, with cumulative emissions during the study period of 12.30 kg ha⁻¹ for the control plot and 17.70 kg ha⁻¹ for the treatment plot. The intense precipitation period that began with the application of the slurry resulted in changes in soil moisture and water-filled pore space (WFPS), modifying the nitrification/denitrification balance. Positive significant correlations ($p = 0.016$ and $p = 0.037$, for the control and treatment plot, respectively) were found between N₂O fluxes and WFPS. Future studies should consider the role of nitrifier and denitrifier communities in order to better assess in-field nitrification inhibitor effectiveness.

Keywords: denitrification; DMPP; nitrous oxide; water-filled pore space

1. Introduction

Climate change is one of the most pressing environmental issues of our time. The urge to reduce emissions of greenhouse gasses (GHG) such as nitrous oxide (N₂O) is generally acknowledged [1]. Although N₂O only accounts for approximately 6% of total annual anthropogenic GHG emissions, while carbon dioxide (CO₂) represents 76%, N₂O has a global warming potential 265 times (over 100 year period) that of CO₂ [2]. Moreover, it currently constitutes the most important ozone-depleting substance [3].

Anthropogenic sources represent almost 40% of global N₂O emissions, of which agriculture accounts for 67–80% of emissions [4]. The main reason that explains the contribution of agriculture to N₂O emissions is fertilization, both organic and inorganic, as well as N-fixing crops [4,5]. N₂O emissions from the soil are the product of three main processes: nitrification, denitrification, and nitrifier denitrification [6–11]. Nitrification is the aerobic oxidation of ammonia or ammonium into nitrates, and it is divided into two steps: the first is the oxidation of ammonium to nitrites, and the second is the oxidation of nitrites to nitrates. Nitrification is carried out by ammonia-oxidizing bacteria (AOB) and ammonia-oxidizing archaea (AOA) [12]. Although recent studies have suggested that AOA

populations are more significant than those of AOB [13,14], AOB still remain accepted as the main cause of nitrification [12,15–19], especially in N-rich soils [20], and specifically after ammonia application [17]. The main bacterial genera responsible for each step of nitrification in agricultural soils are *Nitrosomonas*, especially in N-amended soils [8,21,22], and *Nitrobacter* [23,24], respectively. Denitrification is the anaerobic reduction of nitrates to dinitrogen, with nitrites, nitric oxide, and nitrous oxide as intermediate products [25]. The main key factors regulating nitrification and denitrification in soils are soil water content, temperature, pH, soil ammonium and nitrate content, and carbon (C) availability [26,27]. Low pH limits both nitrification and denitrification, although nitrification is more sensitive to soil acidity, and will be limited by values below 4.5, while denitrification can still take place at values as low as 3.5 [28–31]. Ammonium (NH_4^+) and nitrates (NO_3^-) are the source of nutrients for nitrification and denitrification, respectively [32]. NH_4^+ availability is the most important factor conditioning autotrophic nitrification [6], while NO_3^- and C, which are the energy source for denitrifier organisms, are essential for denitrification [30,33]. The water-filled pore space (WFPS) is used as a measure of soil moisture that considers not only soil water content but also soil porosity [10]. As nitrification is an aerobic process and denitrification is anaerobic, their prevalence is directly controlled by oxygen availability in the soil; thus, WFPS is commonly used to estimate the prevalence of each of these processes [34–37], as well as their importance.

Nitrogen is an essential element for plants, as it is a part of the plant proteins, DNA, and chlorophyll, constituting the most determinant mineral element of crop yield obtained from the soil by plants [38]. Plants are able to use N in the form of NO_3^- and NH_4^+ , but NO_3^- is characterized by a low soil retention [39], increasing the chances of losses through leaching. Reducing the production of NO_3^- will reduce nitrogen losses beyond the root's reach due to leaching [40]. Reducing the oxidation of NH_4^+ to NO_3^- will also indirectly reduce denitrification, as there will be no additional source of NO_3^- for denitrification, and therefore, losses through N_2O and N_2 from denitrification will be also reduced. Nitrification inhibitors (NIs) have been proposed as a tool to reduce nitrogen losses from different ecosystems by inhibiting the nitrification process [41]. By slowing down nitrification, NIs stabilize nitrogen in the soil in the form of NH_4^+ , which can be then gradually absorbed by plants [42]. Different chemical compounds are commercially distributed as nitrification inhibitors, although the most commonly used and studied in the last years are dicyandiamide (DCD) and 3,4-dimethylpyrazole phosphate (DMPP). Their effectiveness has been assessed profusely; however, DCD has attracted the most attention (Table S1, [43–45]), with the studies dedicated to DMPP being more scarce when considering only croplands. Nevertheless, in recent years, increasing attention has been focused on DMPP due to it not showing effects on non-target soil microorganisms. It has also been reported to be very effective for inhibiting the activity of ammonia-oxidizing bacteria (AOB) and increasing nitrogen use efficiency (NUE) and crop yield [46]. A meta-analysis by Yang et al. [45] established an average reduction of N_2O emissions of 47.6% for DMPP, compared to 44.7% for DCD. The effect of the nitrification inhibitor DMPP is based on the delay of the oxidation of ammonium to nitrite (and subsequently to nitrate), by slowing down the activity of the chemoautotrophic bacteria of the genus *Nitrosomonas* spp. [47–49]. Both DMPP and DCD, as well as other NIs including Nitrapyrin and 3,4-dimethylpyrazole succinic (DMPSA), slow down the oxidation of NH_4^+ to NO_2^- by inhibiting the activity of the enzyme ammonia monooxygenase (AMO) [41,50]. Although the specific mechanism by which DMPP inhibits the activity is not clear, Ruser and Schulz [41] suggested that the inhibition of nitrification occurs via Cu chelation, reducing the availability of Cu, which is a requirement of ammonia monooxygenase [51,52].

The duration of the effect of manure application on N_2O emissions depends on several factors, but it is mainly controlled by precipitation and temperature [53,54]. Increases in N_2O emissions after nitrogen (N) application can last for about 6 weeks [55], with 77% of N_2O emissions taking place in the first 4 weeks after N fertilization in grasslands [26] and 67% of the total N_2O emissions taking place in the 7 weeks after slurry application [56]. On the other hand, the expected effect of DMPP on *Nitrosomonas* lasts between 6–8 weeks depending mainly on soil temperature and moisture [22].

Rapeseed (*Brassica napus* L.) is a key crop because it is cultivated for seed oil for human consumption, with animal feed as a byproduct, but also as an energy crop. It is currently the primary raw material for biodiesel production in the EU, accounting for 45% of the total production in 2017 [57]. While rapeseed has been extensively grown for biodiesel production, uncertainties exist regarding the real impact of rapeseed cultivation on climate warming [58]. Astover et al. [59] estimated, based on the 'BioGrace greenhouse gas calculation tool version 4d' [60], that rapeseed cultivation had the highest potential emissions per yield, both for global GHG and specifically for N₂O emissions, for Estonia. In other studies, significant N₂O emissions from rapeseed fields have also been measured [27,61]. Also, in order to fulfill the reduction requirements of the European Green Deal, establishing no net emissions of greenhouse gases by 2050 [62], it is essential to minimize emissions from the production of materials used as biodiesel. For instance, the Revised Renewable Energy Directive (2018/2001/EU) [63] on the promotion of the use of energy from renewable sources requires a reduction of GHG emissions from the use of rapeseed biodiesel of at least 52%. However, Pehnelt and Vietze [58] estimated reductions of GHG emissions for different scenarios smaller than 35% with the use of rapeseed biofuels, highlighting the need to reduce emissions from rapeseed production.

This experiment aimed to assess the effectiveness of the nitrification inhibitor DMPP on reducing N₂O fluxes in acid soils in a winter rapeseed field in Central Estonia. The hypothesis was that the application of DMPP would reduce N₂O emissions, slowing down the oxidation of NH₄⁺ into NO₃⁻ thus increasing the availability of NH₄⁺ in soil for plants.

2. Materials and Methods

2.1. Study Site and Experiment Set-Up

The experimental site is located in the central part of Estonia (Kehtna parish, Rapla county; 58°55'22" N 24°50'52" E; Figure 1). The field has a total size of 18.13 ha and the type of soil is sandy-loam Gleysol (FAO, 2014) (Republic of Estonia Land Board's Geoportal, <https://xgis.maaamet.ee/maps/XGis>). The field had been sown the previous year with a grassland mix with a 20% of N-fixing species (Tetraploid *Trifolium pratense*, 10%; Diploid *Trifolium pratense*, 5%; *Trifolium repens*, 5%; *Lolium perenne*, 35%; *Dactylis glomerata*, 10%; *Festulolium*, 20%; *Festuca pratensis*, 15%; Older Seeds OÜ, Saku, Estonia). In 1964, a drainage system was installed in the field. The drainage system (Figure 1) can be divided according to the direction of the flow: the western section of the field pours into the ditch bordering the west side of the field, while the central and north sections pour to the Kuusiku river in the north. In our study, the field was divided into two different plots: a control, and a treatment plot, with five replications (chambers) each. Soil chemical parameters for both plots are shown in Table 1. The division was based on the direction of the water leaching, allowing us to collect leaching samples from both plots separately. Winter rapeseed (*Brassica napus* 'DK Sequoia') was sown in both plots on the 10th of August of 2016 and harvested on the 26th of August 2017. On the 6th of August of 2016, a dairy slurry with a pH of 8.02 and a content of NH₄⁺ of 6132 mg kg⁻¹ (Table 2) was applied to the field at a rate of 30 t ha⁻¹. The slurry application was done via injection followed by the use of a rotary harrow. On the control plot, the slurry was applied alone; on the treatment plot, the slurry was mixed with the nitrification inhibitor DMPP (BASE, Ludwigshafen, Germany), at a rate of 3 L ha⁻¹. The duration of the study was 50 days, a period covering both the period of increased N₂O emissions after slurry application and of the expected action of DMPP.



Figure 1. The location of the experimental trial at Kehtna parish (Rapla county, 58°55′22″ N 24°50′52″ E) in Central Estonia. The white lines represent the main drainage system collectors. The red circles indicate the ends of drainage pipes where the leachate collection was carried out. The orange line indicates the in-field separation between the control and treatment plot.

Table 1. The initial (pre-slurry application) main soil chemical parameters for the control and the treatment plot.

Parameter	Control Plot	Treatment Plot
BD (g cm ⁻³)	1.107	1.124
pH _{KCl}	4.75	4.76
DM (%)	68.36	69.04
NO ₃ ⁻ -N (mg kg ⁻¹)	51.11	50.99
NH ₄ ⁺ -N (mg kg ⁻¹)	3.08	4.35
P (mg kg ⁻¹)	40.09	61.52
K (mg kg ⁻¹)	105	147
OM (mg kg ⁻¹)	12.04	10.91
N (%)	0.66	0.60
C (%)	6.82	6.09
S (%)	0.11	0.08
DN (mg kg ⁻¹)	110	120
DOC (mg kg ⁻¹)	370	387

BD: bulk density; DM: dry matter; OM: organic matter, DN: dissolved nitrogen; DOC: dissolved organic carbon. Italic characters indicate a significant difference ($p < 0.05$) according to the Wilcoxon signed-rank test.

Table 2. Chemical parameters of the applied slurry (nutrient content values refer to DM part).

DM (%)	pH _{KCl}	NH ₄ -N (mg kg ⁻¹)	NO ₃ -N (mg kg ⁻¹)	P (%)	K (%)	Mg (%)	Ca (%)
7.88	8.02	6132	0.00	0.96	2.37	0.59	1.42
OM (%)	C (%)	N (%)	S (%)	DN (%)	DIC (%)	DC (%)	DOC (%)
70.97	42.02	2.65	0.75	1.67	1.30	4.70	3.40

DM: dry matter; OM: organic matter; DN: dissolved nitrogen; DIC: dissolved inorganic carbon; DC: dissolved carbon; DOC: dissolved organic carbon.

2.2. Environmental Parameters

At both study plots, the soil temperature was measured at four depths 5, 10, 20, and 30 cm with a four-channel PT1000 temperature sensors (COMET SYSTEM, s.r.o, Rožnov pod Radhoštěm, Czech Republic). Soil moisture and electrical conductivity were measured with a GS3 sensor connected to a ProCheck handheld reader (Decagon Devices, Pullman, WA, USA). Field soil parameters were measured for each plot on all GHG sampling dates.

Water-filled pore space (WFPS) was calculated using the equation [64]:

$$WFPS (\%) = 100 \cdot \frac{VWC}{TP} \quad (1)$$

where VWC is volumetric soil moisture content (m³ m⁻³), and TP is total porosity (%) calculated as [65]:

$$TP = 1 - \frac{BD}{D_p} \quad (2)$$

where BD is bulk density, and D_p particle density (both in g cm⁻³).

Climatological data (atmospheric pressure, precipitation, humidity, sunshine, air temperature, air temperature at 2 cm of height, soil temperature, minimum soil temperature, maximum soil temperature, visibility and wind direction) were obtained from the Kuusiku weather station (WMO code 26134, 58°58'23.3" N 24°44'02.4" E, Estonian Weather Service, <https://www.ilmateenistus.ee/ilmateenistus/vaatlusvork/kuusiku-meteoroloogijaajaam/>), which is located approximately eleven kilometers from the experiment location.

2.3. Soil and Leachate Sampling and Analysis

Soil and leachate samples were collected during the study period. Soil samples from a depth of 0–20 cm were taken in three replications, each one a mix of 10 different randomly collected samples with the aid of a soil probe, from each plot in a 2-m radius around the chambers. Leaching water was collected from the end of the drainage pipes (Figure 1). Soil and leaching water samples were taken initially in a 2-day interval after the application of the slurry, and with smaller frequency afterward. Sampling of leaching water was limited by the water level rising higher than the drainage pipes ends, although it was possible to collect 8 days samples during the first 10 days.

Soil dry matter (DM) was measured by drying soil samples at 105 °C for 16 h. Soil organic matter (OM) was determined by loss-upon-ignition following heating at 500 °C for four hours. Soil pH was determined in a 2.5:1 KCl soil (*v:w*) suspension. Soil NO₃⁻-N and NH₄⁺-N were determined in 2M KCl extract of soil by a flow injection analyzer FIAStar 5000 (Foss Tecator AB, Höganäs, Sweden). Soil available P and K were extracted with ammonium lactate (0.1 M NH₄CH₂CH(OH)COO⁻ + 0.4 M CH₃COOH, pH 3.75) [66]. Available P in the extraction solution was determined by flow injection analysis by Tecator ASTN 9/84. Available K was determined from the same solution by the flame photometric method. Total carbon (C), nitrogen (N), and sulphur (S) were determined using a vario MAX CNS Element Analyzer (Elementar Analysensysteme GmbH, Langenselbold, Germany). Leaching water NO₃⁻-N and NH₄⁺-N were measured via a flow injection analyzer FIAStar 5000 (Foss Tecator AB, Höganäs, Sweden). Dissolved organic carbon (DOC) concentration was determined according to the EVS-EN 1484

standard with a VARIO TOC analyzer (Elementar Analysensysteme GmbH, Langenselbold, Germany) and dissolved nitrogen (DN) concentration according to the EVS-EN 12260 standard. Leaching soil water DOC and DN concentrations were measured according to the same standards after extraction with H₂O.

Slurry DM was determined by oven drying for 2 h at 135 °C [67] and organic matter by loss on ignition [68]. Phosphorus was determined by Stannous Chloride and Ca by the o-Cresolphthalein Complexone method, in Kjeldahl Digest by Fiastar 5000; K by the Flame Photometric method; Mg by Titan Yellow method by Fiastar 5000 ASTN 90/92 and NH₄-N using flow injection analyses by Tecator ASN 65-32/84 [69]. Total C, N, and S were determined using a vario MAX CNS Element Analyzer (Elementar Analysensysteme GmbH, Langenselbold, Germany). For the determination of total soluble nitrogen (DN), total soluble carbon (DC), total soluble organic carbon (TOC), and total soluble inorganic carbon (DIC) content in the slurry, H₂O was used as extractant with solution in a 1:10 ratio (*m/v*), extracted for 2 h, and then filtered through a 0.45 µm filter. TOC was determined according to the standard EN 1484:1997, with the instrument VARIO TOC (Elementar Analysensysteme GmbH, Langenselbold, Germany, temperature 850 °C). DN was determined according to the standard EN 12260. Oxidation of the sample containing nitrogen via catalytic combustion occurred in an oxygen atmosphere at >700 °C with nitrogen oxides. The quantification of the nitrogen concentration was carried out by chemiluminescence detection, using VARIO TOC with HORIBA APNA-370 chemiluminescence detector. Dissolved organic, inorganic, total carbon content, and dissolved nitrogen content were expressed on the basis of oven-dried soil. The limit of quantitation for DC, TOC, and DIC was 20 mg kg⁻¹ and for DN 5 mg kg⁻¹.

2.4. Flux Measurements

Nitrous oxide flux measurements were carried out with the closed chamber method [70,71], using white opaque PVC chambers, with a height of 40 cm, a diameter of the collar of 50 cm, and a total headspace volume of 65.5 L. Five chambers were used in each of the plots. Collars were installed on-site 24 h before the first measurement to allow system stabilization. The N₂O flux was measured on 17 occasions from the 5th of August until the 22nd of September of 2016. The N₂O flux measurements were carried out in a higher frequency during the first two weeks after the application of the slurry, and then with decreasing frequency, becoming weekly for the rest of the period. This was done to capture the expected higher flux variability after the slurry application. Gas samples for N₂O measurement were collected over an hour in 20 min intervals (0, 20, 40, 60 min) into 20-mL pre-evacuated (0.04 mbar) bottles.

The nitrous oxide concentration in the collected air samples was determined using the Shimadzu GC-2014 gas chromatography system equipped with ECD, TCD, and FID sensors. The system is based on the automated gas chromatographic system described by Lofffield et al. [72] and located in the lab of the Department of Geography of the Institute of Ecology and Earth Sciences at the University of Tartu in Estonia.

The N₂O flux was calculated from the slope of the least-squares linear regression of the N₂O concentrations versus time (*dC/dt*), using the equation [73]:

$$f = \frac{dC}{dt} \cdot \frac{V}{A} \quad (3)$$

where *f* is the gas flux of N₂O (µg m⁻² h⁻¹); *C* is the N₂O concentration in the chamber air (µg m⁻³); *t* is time (h); *V* is the volume (m³); and *A* is the surface area (m²) entailed by the chamber.

The adjusted *R*² value of the linear regression was used to filter the data, discarding one of the observations if necessary, using the remaining three [73] for flux calculation. Minimum *R*² values of 0.90 and 0.99 were used to check the linearity of the measurements for four (*n* = 4) and three (*n* = 3) measurement points, respectively. A chamber session was discarded when the *R*² value did not meet the criteria, but always leaving a minimum of three chamber measurements.

Cumulative emissions were estimated by the time-integration of daily fluxes after gap-filling by linear interpolation between sampling points [74].

2.5. Statistical Analysis

All statistical analyses were carried out using the R programming language [75]. No additional package was required for the statistical analysis. Unless stated otherwise, the Wilcoxon signed-rank test was used to compare treatments, and the Spearman's rank correlation to analyze correlations between N_2O flux and soil and leachate chemical parameters and environmental data. Box-and-whisker plots are presented following the conventions described by Tukey [76].

3. Results

3.1. Nitrous Oxide Flux

Nitrous oxide fluxes raised from the initial non-significantly different values of 316 and $265 \mu\text{g m}^{-2} \text{h}^{-1}$ for the control and the treatment plot, respectively, to $4834 \pm 733.20 \mu\text{g m}^{-2} \text{h}^{-1}$ in the treatment plot and $1843 \pm 554.53 \mu\text{g m}^{-2} \text{h}^{-1}$ in the control plot, one day after the slurry application (Figure 2). Fluxes from the treatment plot were significantly higher on two of the four-day periods following the application of the slurry. Fluxes were higher in the control plot between the 10th and the 14th day, and after that were again higher in the treatment plot, but differences were not significant. The maximum flux, $3130.71 \pm 725.74 \mu\text{g m}^{-2} \text{h}^{-1}$, was reached in the control plot on the 13th day. At the end of the studied period, fluxes had stabilized around similar values (43 and $50 \mu\text{g m}^{-2} \text{h}^{-1}$ for control and treatment, respectively), and no significant differences between the plots. The total cumulative emissions during the study period were $12.30 \pm 1.81 \text{ kg ha}^{-1}$ for the control plot and $17.70 \pm 1.54 \text{ kg ha}^{-1}$ for the treatment plot. The final cumulative emissions were not significantly different ($p > 0.05$).

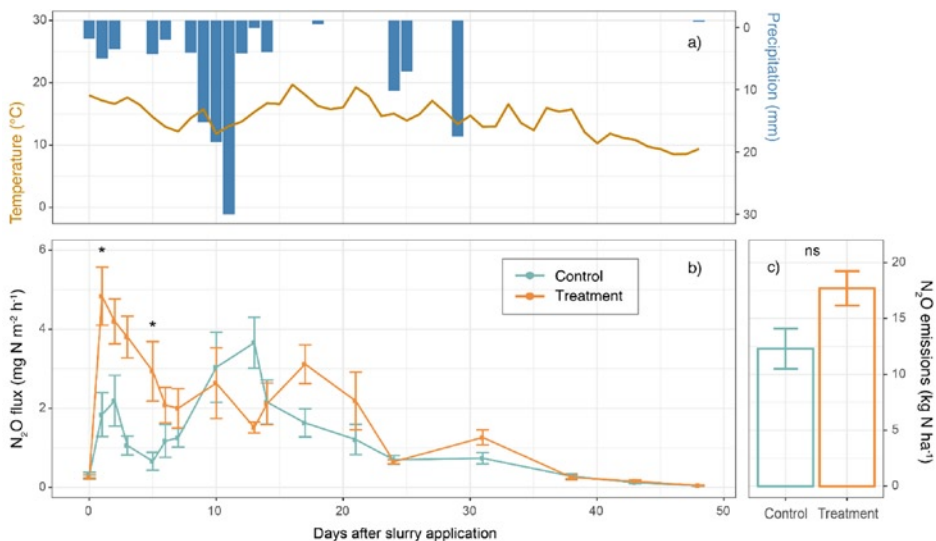


Figure 2. Measured (a) daily average soil temperature ($^{\circ}\text{C}$) and daily total precipitation (mm) in the Kuusiku weather station; (b) daily N_2O fluxes ($\text{mg N m}^{-2} \text{h}^{-1}$); and (c) total emissions (kg N ha^{-1}) for the full study period (mean and standard error). Stars indicate significant differences for the daily flux between the control and treatment plot for a non-paired Wilcoxon-test (ns: non-significant; *: $p < 0.05$).

3.2. Environmental Data

A strong precipitation event was monitored beginning on the same day of the application of slurry and lasting for approximately two weeks, having the biggest intensity on the second week (Figure 2). A total of 105.8 mm of precipitation was recorded during the first two weeks after the slurry application, while only 28.7 mm was recorded during the two weeks prior to the application. Moreover, July was a slightly drier month than the average (75 versus 87 mm for the 1961–1990 period) (Estonian Weather Service, <https://www.ilmateenistus.ee/ilmateenistus/vaatlusvork/kuusiku-meteoroloogijaam/>).

Correlation analysis between N_2O fluxes and environmental parameters (Table S2) shows that N_2O flux was correlated with both air and soil temperature, but this correlation was stronger in the treatment plot ($\rho = 0.439$ with $p = 0.000$ for treatment; and $\rho = 0.256$ with $p = 0.021$ for control plot; for the average 24-h temperature). A significant correlation between the N_2O flux and precipitation recorded at the Kuusiku Weather Station at the moment of the measurement was found only for the treatment plot; however, the correlation was significant ($p < 0.01$) for both plots for the accumulated precipitation for the 2-h, 24-h, and 72-h periods prior to the moment of measurement. The highest correlation between the N_2O flux and precipitation was found for the three-day cumulative precipitation, being stronger in the control than in the treatment plot ($\rho = 0.674$ for control and $\rho = 0.448$ for treatment plot, $p < 0.001$). A strong correlation was found between the average ground temperature for a 24 and 72-h period prior to the measurement for the treatment plot ($\rho = 0.439$ and $\rho = 0.509$, $p < 0.001$). This correlation was much weaker for the control plot ($\rho = 0.256$, $p = 0.021$; $\rho = 0.235$, $p = 0.035$).

3.3. Soil Parameters

The control and the treatment plots showed different WFPS ($p = 0.021$) (Figure 3) for the studied period. A correlation analysis between WFPS and N_2O flux was tested for the day-of-experiment WFPS, three-day, five-day, and seven-day averaged WFPS prior to the experiment, after linear interpolation of the missing values (Table S2). The correlation between the N_2O flux and WFPS was only significant for the control plot for the 3-day averaged measured WFPS (WFPS3d), while it was significant for all considered WFPS periods for the treatment plot. The Spearman's rank correlation coefficient between N_2O flux and WFPS3d was $\rho = 0.267$ ($p = 0.016$) and $\rho = 0.248$ ($p = 0.037$) for the control and treatment plot, respectively.

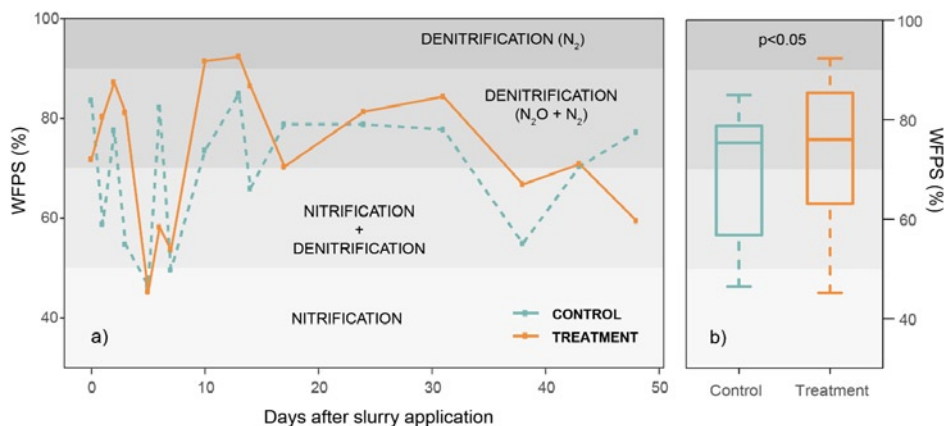


Figure 3. The water-filled pore space (WFPS) evolution (a) and distribution of values (b) for the studied period for treatment (orange) and control (blue) plots. Nitrification and denitrification optimal WFPS limits are from Focht [34], Davidson [35], Bouwman [36], Ruser et al. [37], Hansen et al. [29] and Ussiri and Lal [4].

The correlation analysis between N_2O fluxes and the environmental parameters (Table S2) showed that N_2O flux was strongly correlated with temperature for the treatment plot ($p = 0.005$ for 5 cm depth, and $p < 0.001$ for depths 10, 20, and 30 cm), but this correlation was not significant for the control plot.

3.4. Soil Chemical Properties

From all analyzed soil parameters (Table 1), only dissolved nitrogen (DN) was statistically different ($p = 0.047$) between the control and the treatment plot prior to the beginning of the experiment. Initial pH had almost the same value on both plots (4.76 and 4.75) and was not significantly different. After the slurry application, pH increased, but this increase was stronger in the treatment plot, where it remained higher for almost all the studied period, although the difference between the treatment and the control soil pH was not significant.

Nitrate content and ammonium were not significantly different between the plots prior to the slurry application (Table 1), although ammonium content was higher in the treatment plot. No significant differences were found in NO_3^- -N nor NH_4^+ -N content between control and treatment plots during the period (Figure 4). No statistically significant correlation for N_2O flux with soil nitrates was found for either plot. The correlation with soil ammonium was only statistically significant for the control plot ($\rho = 0.464$, $p = 0.004$).

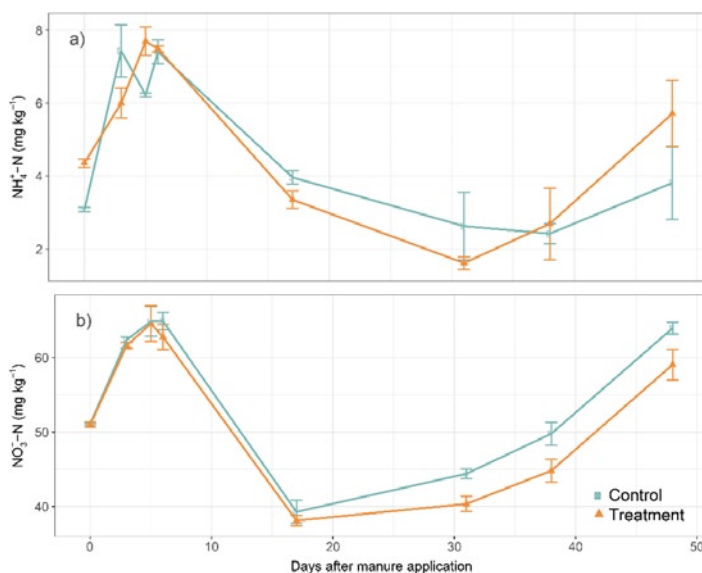


Figure 4. Measured soil NO_3^- -N (a) and NH_4^+ -N (b) mean concentration for the treatment and control plots. Error bars represent the standard error.

Soil total carbon was highly correlated with N_2O ($\rho = 0.546$, $p < 0.001$) for the treatment plot, while such correlation was not significant for the control plot. Negative significant correlation existed with DOC ($\rho = -0.397$, $p = 0.015$) for the control plot.

3.5. Leaching

The intense precipitation caused the leachate collection points at both the control and treatment plots to be overflowed by the ditch and the river, respectively, during part of the experiment, limiting the leachate sampling (Figures S1 and S2). Although it was possible to measure the first and last 10 days of the period, no sound conclusions can be drawn about the total losses of nitrogen through

leachate for the whole period. Nevertheless, no significant differences were found for NH_4^+ or NO_3^- leaching between plots for the dates when data was available (Figures S3 and S4). The correlation analysis (Table S2) between N_2O fluxes and leachate properties showed a significant negative correlation in the control plot with the NO_3^- concentration ($\rho = -0.394$; $p = 0.004$) but a positive correlation with NH_4^+ ($\rho = 0.388$; $p = 0.005$), while for the treatment plot a negative correlation was found with NH_4^+ ($\rho = -0.586$; $p = 0.022$) and a positive one with the NO_3^- concentration ($\rho = 0.832$; $p < 0.001$).

4. Discussion

Contrary to the experiment hypothesis, N_2O emissions were higher in the plot where the nitrification inhibitor was applied, with significant differences during the initial period. This poses two questions: why the application of the nitrification inhibitor did not reduce N_2O fluxes; and why the emissions were higher in the plot where the nitrification inhibitor had been applied. These two questions can be answered according to the information provided by field and climatic data. The most determining factor was the high precipitation event that started on the same day as the slurry and DMPP application, resulting in changes in soil moisture. The effectiveness of NIs in reducing N_2O emissions is known to be conditioned by soil moisture and rainfall, soil pH, and temperature [20,51]. Soil moisture, which is directly dependent on precipitation, controls the availability of oxygen, which is one of the key factors regulating denitrification [6]. Higher soil moisture promotes anaerobic conditions in soil and, therefore, a more important role of denitrification, which is not affected by the inhibitory effect of DMPP [12,77]. Nitrification and denitrification, and subsequently N_2O production, are controlled by several factors, particularly soil moisture, affected by rainfall and drainage among other aspects. The importance of rainfall and soil water content in N_2O emissions has been noted extensively in the literature [78–82], and specifically for denitrification [83–85]. A positive relationship between increasing soil water content and increasing N_2O emission from both lab and field studies has been explained by an increase in the denitrification activity [37]. Stevens and Luahglin [86] and Lohila et al. [33] established that the restricted availability of oxygen, as well as the presence of NO_3^- and the availability of labile carbon, are the most important prerequisites for denitrification. Moreover, Loro et al. [87] found that both denitrification activity and N_2O emissions from denitrification were correlated with soil water content, but not with NO_3^- content, when the latter is not limiting. This is in accordance with the findings of Dobbie and Smith [26] that water-filled pore space (WFPS) is the main factor conditioning N_2O emissions when soil NO_3^- concentration and temperature are not limiting. In fact, Dobbie et al. [79] found that the biggest N_2O fluxes appeared at WFPS between 70–90%, and Ruser et al. [37] reported a strong increase in N_2O emissions for WFPS above 60–70%, suggesting that it was denitrification and not nitrification that was the main process involved in the emissions. At higher values of WFPS, above 90%, the process may switch from the production of N_2O to N_2 [34,35], but, at lower values of pH like those of the study field soil, the ratio $\text{N}_2:\text{N}_2\text{O}$ decreases [88,89] due to the sensitivity of nitrous oxide reductase to the pH [90]. According to the WFPS values (Figure 3), both plots were predominantly under denitrification conditions. The significant positive correlation between N_2O fluxes and WFPS values found for both plots confirms that the higher fluxes were related to denitrification in both cases. With denitrification being the main source of emissions, the inhibition of nitrification was not effective in reducing N_2O emissions. Dobbie et al. [79] also reported a strong positive correlation between the cumulative N_2O emissions and the rainfall during the 4-week period beginning one week before the N application. Several studies have reported that rainfall events usually produce immediate peaks in N_2O emissions [26,78,91], and that denitrification is the main process responsible for N_2O emissions following rainfall events [92,93]. Correlation between N_2O emissions and denitrification activity has been found in manured soils [94], and Clemens & Huschka [95] found that denitrification dominates N_2O emissions processes after slurry application and suggested that the NO_3^- present in the soil can be used to oxidize the organic substances present in the slurry. The readily available C in slurries and manures is used for denitrifiers in anaerobic conditions as an energy source [30].

N₂O emissions from denitrification could also have been enhanced by the drier soil conditions prior to the moment of the slurry application; total precipitation two weeks before application of the slurry and two weeks after was 28.7 and 105.8 mm, respectively. Rewetting after drought has been observed to boost mineralization and denitrification [96]. It has been documented that denitrifying bacteria recover faster when soils are rewetted after dry periods [97]. Smith et al. [98] found an increase in N₂O emissions and denitrification rate after the apparition of anaerobic conditions. Firestone and Davidson [6] established that bold increases in N₂O emissions, like those observed after rewetting, are more typical for denitrification than for nitrification, which suggests that denitrification was the main thing responsible for the observed emissions. It has been suggested that rewetting after dry periods increases the concentration of DOC [37]. As the importance of carbon in denitrification has been well established in the literature [95,99–101], denitrification in manure slurries is promoted by the readily assimilable C [102]. Moreover, carbon availability can promote anaerobic conditions, even at low WFPS, increasing denitrification potential and N₂O emissions and explaining higher emissions found in organic fertilization than in inorganic fertilization [91]. Crop residues present in the field after harvesting the grassland cover (*Lolium perenne*, *Festulolium*, *Trifolium pratense*, *Festuca pratensis*) from the previous season would have increased C availability and denitrification rates once they were mixed with the soil at the moment of the slurry application; high denitrification rates have been found after plant damage or cutting, and this has been attributed to the increase in C availability in the soil from the decomposition of roots [30,103], which would also be enhanced by the increase in soil moisture due to precipitation. Once it has been established that denitrification was the source of the emission peaks during the studied period, the question of why emissions were higher from the treatment plot than from the control plot during the initial period still needs to be answered. This can be explained by a higher WFPS in the treatment plot for most of the period and therefore higher denitrification rate (Figure 3), resulting in higher N₂O emissions, as the activity of N₂O reductase should have been inhibited by the low soil pH. The different evolution of WFPS in the treatment plot was a consequence of differences in soil moisture as soil porosity was similar in both plots. Although the plots were established according to the similar soil properties and micro-topographical characteristics, moisture evolution was slightly different in both plots after the intense precipitation. Although the correlation between N₂O and precipitation was stronger in the control plot than in the treatment plot for cumulative precipitation (2-h, 1-day, 3-day), this correlation was not significant for precipitation at the moment of the measurement, while it was significant for the treatment plot. Possible explanations could be the distance from the weather station (approximately 11 km), or that the 2-h cumulative precipitation before measurement is a better predictor of soil conditions than a single, momentary precipitation measurement. However, we hypothesize that the correlation between N₂O flux and precipitation at the moment of measurement was not significant for the control plot because the influence of precipitation on the N₂O flux in the control plot could be delayed in comparison to the treatment plot, which would explain why the peak of N₂O emissions for the control plot took place on the 13th day of measurements. The WFPS, initially lower for the treatment plot, became higher in treatment on the first day of measurement, but it was higher again for the control plot on the 6th day (Figure 3), showing that the effect of precipitation was more rapid in the treatment plot, and the correlation between N₂O flux and WFPS was significant for the control plot only for 3-day averaged values (WFPS3d), while it was significant in all cases for the treatment plot. Important in-field spatial variability is known to exist both for soil water content and N₂O fluxes [7,33], and it is one of the main causes of uncertainty in N₂O measurements from agro-ecosystems [32]. Factors such as soil NO₃⁻ and NH₄⁺ concentration, labile C content, as well as bulk density, can show a variable spatial distribution, resulting in the spatial variability of nitrification and denitrification rates [104]. Cowan et al. [32] reported differences in N₂O flux of 2 orders of magnitude in distances smaller than 10 m in a grassland, and that only 1.1% of the area of the field contributed to over 55% of the total N₂O flux, highlighting the importance of hotspots in N₂O fluxes. In our study, initial NO₃⁻, NH₄⁺, C content, and bulk density

were not significantly different between both plots, but differences in soil moisture evolution could explain the difference in temporal behavior regarding N_2O fluxes.

The application of slurries results in pronounced increases of NH_4^+ content in the soil. Afterward, the NH_4^+ concentration is expected to decrease and NO_3^- to increase, as NH_4^+ is oxidized into NO_3^- . The rate at which NH_4^+ is oxidized into NO_3^- is an indicator of nitrification activity. The application of a nitrification inhibitor should slow down this process in the treatment plot, retaining N in the form of NH_4^+ for a longer period than in the control plot. However, soil analyses during the experiment show, after the expected initial increase in NH_4^+ concentration, that both plots behaved identically regarding the oxidation of NH_4^+ into NO_3^- (Figure 4). This means that nitrification was taking place in both plots. This can be attributed to a lack of effectiveness of DMPP in the first days after application. Results from Kong et al. [46] show a time lag in the effect of DMPP on N_2O emissions, as well as NH_4^+ and NO_3^- evolution in the soil; in a field experiment (cultivation after spraying the plant cover with DMPP) the effect appeared only approximately two weeks after it was applied. This is observed for the N_2O emissions, but also for NH_4^+ and NO_3^- , which show a similar evolution for the first two weeks with and without DMPP. Although a delay in the effectiveness of DMPP is not universal, it could be sometimes masked by an insufficient sampling frequency during the first days after application. Nevertheless, a several days delay in the effect of DMPP can also be observed in the results from Beltran-Rendon et al. [105], De Antoni Migliorati et al. [106] and Kou et al. [107] under a range of different conditions. The slightly higher initial content of NH_4^+ in the treatment plot may have also contributed to a higher initial nitrification activity in our experiment.

The significant correlation (Table S2) between N_2O flux and soil NH_4^+ content only for the control plot but not for the treatment plot suggests that nitrification was a significant N_2O source during the full duration of the experiment in control, but not in the treatment plot. This correlation is also significant for leachate from the control plot, where higher N_2O fluxes are correlated with a higher concentration of NH_4^+ , and with a lower concentration of NO_3^- , suggesting a predominance of nitrification, while the opposite trend is observed in the treatment plot (a higher concentration of NO_3^- and a lower of NH_4^+ resulted in higher N_2O fluxes), suggesting again the predominance of denitrification.

The low pH of the soils, combined with low oxygen availability and high availability of NH_4^+ after the slurry application, could indicate that nitrifier denitrification was partially responsible for the high N_2O emissions, as it has been proposed to be a major pathway for N_2O emissions when there is high availability of NH_4^+ and low oxygen [9,108]. However, the increase of NO_3^- content in the soils (Figure 4), from the oxidation of the NH_4^+ incorporated with the slurry, show that nitrifier-denitrification was not the main source of the measured high fluxes.

5. Conclusions

This study showed that the use of nitrification inhibitors does not result necessarily in a reduction in N_2O emissions as environmental factors can conceal its effectiveness. High N_2O emissions were measured in both the control and treatment plot after slurry application, with high spatial variability inside the plots. An intense precipitation event, beginning the same day of the application of the manure, resulted in an increase of soil moisture and changes in WFPS values. The high WFPS values in combination with the significant correlation between N_2O flux and WFPS indicate that the peaks of emissions were the product of denitrification, explaining the absence of a nitrification inhibition effect in the treatment plot. This highlights the importance of climatic factors, and especially precipitation, in the performance of nitrification inhibitors. The relationship between precipitation, soil moisture, and subsequently, nitrification/denitrification activity is well-known, but how this can affect the inhibitory effect is sometimes neglected, as it is in-field spatial variability. Our results emphasize the necessity for further studies of the factors conditioning the action of nitrification inhibitors, with a special focus on in-field application, to achieve maximum effectiveness. Also, microbiological analyses of the populations of nitrifiers and denitrifiers should help to assess the role of each community regarding the effectiveness of nitrification inhibitors. Finally, long-term studies with a repeated

application of DMPP should allow us to detect long-term changes in microbial populations and the effect on N₂O emissions.

Supplementary Materials: The following are available online at <http://www.mdpi.com/2077-0472/10/11/497/s1>, Figure S1: Evolution of ammonium (NH₄⁺-N) concentration in leachate (mg L⁻¹), Figure S2: Evolution of nitrate (NO₃⁻-N) concentration in leachate (mg L⁻¹), Figure S3: Ammonium (NH₄⁺-N) concentrations in leachate (mg L⁻¹), Figure S4: Nitrate (NO₃⁻-N) concentrations in leachate (mg L⁻¹), Table S1: Number of studies on DCD and DMPP included in Akiyama et al. (2009), Abalos et al. (2014), Gilsanz et al. (2016) and Quan et al. (2017), Table S2: Correlations between N₂O flux and (a) climatic parameters, (b) soil analysis, (c) field data and (d) leachate analysis.

Author Contributions: Conceptualization, K.S.; methodology, K.S. and K.K.; validation, J.E.-G. and K.S.; formal analysis, J.E.-G. and H.V.; investigation, J.E.-G. and H.V.; resources, K.S., A.A., Ü.M. and K.K.; data curation, J.E.-G.; writing—original draft preparation, J.E.-G. and K.S.; writing—review and editing, J.E.-G., K.S., M.S., Ü.M., K.K., H.V. and A.A.; visualization, J.E.-G.; supervision, K.S., M.S., A.A. and Ü.M.; project administration, K.S.; funding acquisition, K.S., A.A. and Ü.M. All authors have read and agreed to the published version of the manuscript.

Funding: This research was funded by the Estonian Research Council (the IUT2-16 and PRG352 grants) and the EU through the European Regional Development Fund (Centre of Excellence EcolChange, Estonia; and Estonian University of Life Sciences ASTRA project ‘Value-chain based bio-economy’).

Acknowledgments: The authors would like to thank Marko Satsi from Kehtna Mõisa OÜ and BASF SE for their support.

Conflicts of Interest: The authors declare no conflict of interest.

References

1. IPCC. *Global Warming of 1.5 °C. An IPCC Special Report on the Impacts of Global Warming of 1.5 °C above Pre-Industrial Levels and Related Global Greenhouse Gas EMISSION pathways, in the Context of Strengthening the Global Response to the Threat of Climate Change, Sustainable Development, and Efforts to Eradicate Poverty*; Intergovernmental Panel on Climate Change: Geneva, Switzerland, 2018; p. 630.
2. IPCC. *Climate Change 2014: Synthesis Report. Contribution of Working Groups I, II and III to the Fifth Assessment Report of the Intergovernmental Panel on Climate Change*; Core Writing Team: Geneva, Switzerland, 2014; p. 151. ISBN 978-92-9169-143-2.
3. Ravishankara, A.R.; Daniel, J.S.; Portmann, R.W. Nitrous oxide (N₂O): The dominant ozone-depleting substance emitted in the 21st century. *Science* **2009**, *326*, 123–125. [[CrossRef](#)] [[PubMed](#)]
4. Ussiri, D.; Lal, R. *Soil Emission of Nitrous Oxide and Its Mitigation*; Springer Netherlands: Dordrecht, The Netherlands, 2013; Volume XVIII, p. 378.
5. Park, S.; Croteau, P.; Boering, K.A.; Etheridge, D.M.; Ferretti, D.; Fraser, P.J.; Kim, K.R.; Krummel, P.B.; Langenfelds, R.L.; van Ommen, T.D.; et al. Trends and seasonal cycles in the isotopic composition of nitrous oxide since 1940. *Nat. Geosci.* **2012**, *5*, 261–265. [[CrossRef](#)]
6. Firestone, M.K.; Davidson, E.A. Microbiological Basis of NO and N₂O Production and Consumption in Soils. In *Exchange of Trace Gases between Terrestrial Ecosystems and the Atmosphere*; Andreae, M.O., Schimel, D.S., Eds.; John Wiley and Sons: New York, NY, USA, 1989; pp. 7–21.
7. Parton, W.J.; Mosier, A.R.; Ojima, D.S.; Valentine, D.W.; Schimel, D.S.; Weier, K.; Kulmala, A.E. Generalized model for N₂ and N₂O production from nitrification and denitrification. *Glob. Biogeochem. Cycles* **1996**, *10*, 401–412. [[CrossRef](#)]
8. Bremner, J.M. Sources of nitrous oxide in soils. *Nutr. Cycl. Agroecosyst.* **1997**, *49*, 7–16. [[CrossRef](#)]
9. Wrage, N.; van Groenigen, J.W.; Oenema, O.; Baggs, E.M. A novel dual-isotope labelling method for distinguishing between soil sources of N₂O. *Rapid Commun. Mass Spectrom.* **2005**, *19*, 3298–3306. [[CrossRef](#)]
10. Smith, K.A.; Thomson, P.E.; Clayton, H.; McTaggart, I.P.; Conen, F. Effects of temperature, water content and nitrogen fertilisation on emissions of nitrous oxide by soils. *Atmos. Environ.* **1998**, *32*, 3301–3309. [[CrossRef](#)]
11. Braker, G.; Ralf, C. Diversity, Structure, and Size of N₂O-Producing Microbial Communities in Soils—What Matters for Their Functioning? In *Advances in Applied Microbiology*; Academic Press: Cambridge, MA, USA, 2011; Volume 75, pp. 33–70.

12. Duan, Y.F.; Kong, X.W.; Schramm, A.; Labouriau, R.; Eriksen, J.; Petersen, S.O. Microbial N Transformations and N₂O Emission after Simulated Grassland Cultivation: Effects of the Nitrification Inhibitor 3,4-Dimethylpyrazole Phosphate (DMPP). *Appl. Environ. Microbiol.* **2017**, *83*. [[CrossRef](#)]
13. Leininger, S.; Urich, T.; Schloter, M.; Schwark, L.; Qi, J.; Nicol, G.W.; Prosser, J.I.; Schuster, S.C.; Schleper, C. Archaea predominate among ammonia-oxidizing prokaryotes in soils. *Nature* **2006**, *442*, 806–809. [[CrossRef](#)]
14. Taylor, A.E.; Zeglin, L.H.; Wanzek, T.A.; Myrold, D.D.; Bottomley, P.J. Dynamics of ammonia-oxidizing archaea and bacteria populations and contributions to soil nitrification potentials. *ISME J.* **2012**, *6*, 2024–2032. [[CrossRef](#)]
15. Jia, Z.; Conrad, R. Bacteria rather than Archaea dominate microbial ammonia oxidation in an agricultural soil. *Environ. Microbiol.* **2009**, *11*, 1658–1671. [[CrossRef](#)]
16. Morimoto, S.; Hayatsu, M.; Takada Hoshino, Y.; Nagaoka, K.; Yamazaki, M.; Karasawa, T.; Takenaka, M.; Akiyama, H. Quantitative Analyses of Ammonia-oxidizing Archaea (AOA) and Ammonia-oxidizing Bacteria (AOB) in Fields with Different Soil Types. *Microbes Environ.* **2011**, *26*, 248–253. [[CrossRef](#)] [[PubMed](#)]
17. Di, H.J.; Cameron, K.C.; Shen, J.P.; Winefield, C.S.; O’Callaghan, M.; Bowatte, S.; He, J.Z. Nitrification driven by bacteria and not archaea in nitrogen-rich grassland soils. *Nat. Geosci.* **2009**, *2*, 621–624. [[CrossRef](#)]
18. Di, H.J.; Cameron, K.C.; Shen, J.P.; Winefield, C.S.; O’Callaghan, M.; Bowatte, S.; He, J.Z. Ammonia-oxidizing bacteria and archaea grow under contrasting soil nitrogen conditions. *FEMS Microbiol. Ecol.* **2010**, *72*, 386–394. [[CrossRef](#)] [[PubMed](#)]
19. Di, H.J.; Cameron, K.C.; Sherlock, R.R.; Shen, J.-P.; He, J.-Z.; Winefield, C.S. Nitrous oxide emissions from grazed grassland as affected by a nitrification inhibitor, dicyandiamide, and relationships with ammonia-oxidizing bacteria and archaea. *J. Soils Sediments* **2010**, *10*, 943–954. [[CrossRef](#)]
20. Di, H.J.; Cameron, K.C.; Podolyan, A.; Robinson, A. Effect of soil moisture status and a nitrification inhibitor, dicyandiamide, on ammonia oxidizer and denitrifier growth and nitrous oxide emissions in a grassland soil. *Soil Biol. Biochem.* **2014**, *73*, 59–68. [[CrossRef](#)]
21. Briones, A.M.; Okabe, S.; Umemiya, Y.; Ramsing, N.B.; Reichardt, W.; Okuyama, H. Influence of different cultivars on populations of ammonia-oxidizing bacteria in the root environment of rice. *Appl. Environ. Microbiol.* **2002**, *68*, 3067–3075. [[CrossRef](#)]
22. Villar, J.M.; Guillaumes, E. Use of nitrification inhibitor DMPP to improve nitrogen recovery in irrigated wheat on a calcareous soil. *Span. J. Agric. Res.* **2010**, *8*. [[CrossRef](#)]
23. Gerardi, M.H. Nitrifying Bacteria. In *Nitrification and Denitrification in the Activated Sludge Process*; John Wiley & Sons, Inc.: New York, NY, USA, 2002; pp. 43–54. [[CrossRef](#)]
24. Cabello, P.; Roldán, M.D.; Castillo, F.; Moreno-Vivián, C. Nitrogen Cycle. In *Encyclopedia of Microbiology*; Academic Press: Cambridge, MA, USA, 2009; pp. 299–321. [[CrossRef](#)]
25. Wrage, N.; Velthof, G.L.; van Beusichem, M.L.; Oenema, O. Role of nitrifier denitrification in the production of nitrous oxide. *Soil Biol. Biochem.* **2001**, *33*, 1723–1732. [[CrossRef](#)]
26. Dobbie, K.E.; Smith, K.A. Nitrous oxide emission factors for agricultural soils in Great Britain: The impact of soil water-filled pore space and other controlling variables. *Glob. Chang. Biol.* **2003**, *9*, 204–218. [[CrossRef](#)]
27. Vinzent, B.; Fuß, R.; Maidl, F.-X.; Hülsbergen, K.-J. N₂O emissions and nitrogen dynamics of winter rapeseed fertilized with different N forms and a nitrification inhibitor. *Agric. Ecosyst. Environ.* **2018**, *259*, 86–97. [[CrossRef](#)]
28. Halling-Sørensen, B. Process Chemistry and Biochemistry of Nitrification. In *Studies in Environmental Science*; Halling-Sørensen, B., Jørgensen, S.E., Eds.; Elsevier Science: Amsterdam, The Netherlands, 1993; Volume 54, pp. 55–118.
29. Hansen, R.; Mander, Ü.; Soosaar, K.; Maddison, M.; Löhmus, K.; Kupper, P.; Kanal, A.; Söber, J. Greenhouse gas fluxes in an open air humidity manipulation experiment. *Landsc. Ecol.* **2012**, *28*, 637–649. [[CrossRef](#)]
30. Saggar, S.; Jha, N.; Deslippe, J.; Bolan, N.S.; Luo, J.; Giltrap, D.L.; Kim, D.G.; Zaman, M.; Tillman, R.W. Denitrification and N₂O:N₂ production in temperate grasslands: Processes, measurements, modelling and mitigating negative impacts. *Sci. Total Environ.* **2013**, *465*, 173–195. [[CrossRef](#)]
31. Borchard, N.; Schirrmann, M.; Cayuela, M.L.; Kammann, C.; Wrage, M.N.; Estavillo, J.M.; Fuertes, M.T.; Sigua, G.; Spokas, K.; Ippolito, J.A.; et al. Biochar, soil and land-use interactions that reduce nitrate leaching and N₂O emissions: A meta-analysis. *Sci. Total Environ.* **2019**, *651*, 2354–2364. [[CrossRef](#)] [[PubMed](#)]
32. Cowan, N.J.; Norman, P.; Famulari, D.; Levy, P.E.; Reay, D.S.; Skiba, U.M. Spatial variability and hotspots of soil N₂O fluxes from intensively grazed grassland. *Biogeosciences* **2015**, *12*, 1585–1596. [[CrossRef](#)]

33. Lohila, A.; Aurela, M.; Hatakka, J.; Pihlatie, M.; Minkkinen, K.; Penttilä, T.; Laurila, T. Responses of N₂O fluxes to temperature, water table and N deposition in a northern boreal fen. *Eur. J. Soil Sci.* **2010**, *61*, 651–661. [[CrossRef](#)]
34. Focht, D.D. Methods for Analysis of Denitrification in Soils. In *Soil–Plant–Nitrogen Relationships*; Nielsen, D.R., MacDonald, J.G., Eds.; Academic Press: Cambridge, MA, USA, 1978; pp. 433–490. [[CrossRef](#)]
35. Davidson, E.A. Fluxes of nitrous oxide and nitric oxide from terrestrial ecosystems. In *Microbial Production and Consumption of Greenhouse Gases: Methane, Nitrogen Oxides, and Halomethanes*; Rogers, J.E., Whitman, W.B., Eds.; American Society for Microbiology: Washington, DC, USA, 1991; pp. 219–235.
36. Bouwman, A.F. Direct emission of nitrous oxide from agricultural soils. *Nutr. Cycl. Agroecosyst.* **1996**, *46*, 53–70. [[CrossRef](#)]
37. Ruser, R.; Flessa, H.; Russow, R.; Schmidt, G.; Buegger, F.; Munch, J.C. Emission of N₂O, N₂ and CO₂ from soil fertilized with nitrate: Effect of compaction, soil moisture and rewetting. *Soil Biol. Biochem.* **2006**, *38*, 263–274. [[CrossRef](#)]
38. Allison, F.E. Nitrogen and Soil Fertility. In *Yearbook of Agriculture 1957*; United States Department of Agriculture: Washington, WA, USA, 1957; p. 784.
39. Bouchet, A.-S.; Laperche, A.; Bissuel-Belaygue, C.; Snowdon, R.; Nesi, N.; Stahl, A. Nitrogen use efficiency in rapeseed. A review. *Agron. Sustain. Dev.* **2016**, *36*. [[CrossRef](#)]
40. Yu, L.; Kang, R.; Mulder, J.; Zhu, J.; Dörsch, P. Distinct fates of atmospheric NH₄⁺ and NO₃[−] in subtropical, N-saturated forest soils. *Biogeochemistry* **2017**, *133*, 279–294. [[CrossRef](#)]
41. Ruser, R.; Schulz, R. The effect of nitrification inhibitors on the nitrous oxide (N₂O) release from agricultural soils—a review. *J. Plant Nutr. Soil Sci.* **2015**, *178*, 171–188. [[CrossRef](#)]
42. Di, H.J.; Cameron, K.C. Inhibition of nitrification to mitigate nitrate leaching and nitrous oxide emissions in grazed grassland: A review. *J. Soils Sediments* **2016**, *16*, 1401–1420. [[CrossRef](#)]
43. Akiyama, H.; Yan, X.; Yagi, K. Evaluation of effectiveness of enhanced-efficiency fertilizers as mitigation options for N₂O and NO emissions from agricultural soils: Meta-analysis. *Glob. Chang. Biol.* **2009**, *16*, 1837–1846. [[CrossRef](#)]
44. Gilsanz, C.; Báez, D.; Misselbrook, T.H.; Dhanoa, M.S.; Cárdenas, L.M. Development of emission factors and efficiency of two nitrification inhibitors, DCD and DMPP. *Agric. Ecosyst. Environ.* **2016**, *216*, 1–8. [[CrossRef](#)]
45. Yang, M.; Fang, Y.; Sun, D.; Shi, Y. Efficiency of two nitrification inhibitors (dicyandiamide and 3, 4-dimethylpyrazole phosphate) on soil nitrogen transformations and plant productivity: A meta-analysis. *Sci. Rep.* **2016**, *6*, 22075. [[CrossRef](#)]
46. Kong, X.; Eriksen, J.; Petersen, S.O. Evaluation of the nitrification inhibitor 3,4-dimethylpyrazole phosphate (DMPP) for mitigating soil N₂O emissions after grassland cultivation. *Agric. Ecosyst. Environ.* **2018**, *259*, 174–183. [[CrossRef](#)]
47. Zerulla, W.; Barth, T.; Dressel, J.; Erhardt, K.; Horchler von Locquenghien, K.; Pasda, G.; Rädle, M.; Wissemeyer, A. 3,4-Dimethylpyrazole phosphate (DMPP)—A new nitrification inhibitor for agriculture and horticulture. *Biol. Fertil. Soils* **2001**, *34*, 79–84. [[CrossRef](#)]
48. Guillaumes, E.; Villar, J.M. Effects of DMPP [3,4-dimethylpyrazole phosphate] on the growth and chemical composition of ryegrass (*Lolium perenne* L.) raised on calcareous soil. *Span. J. Agric. Res.* **2004**, *2*. [[CrossRef](#)]
49. Trenkel, M.E. *Slow-and Controlled-Release and Stabilized Fertilizers: An Option for Enhancing Nutrient Use Efficiency in Agriculture*; International Fertilizer Industry Association (IFA): Paris, France, 2010.
50. Byrne, M.P.; Tobin, J.T.; Forrestal, P.J.; Danaher, M.; Nkwonta, C.G.; Richards, K.; Cummins, E.; Hogan, S.A.; O’Callaghan, T.F. Urease and Nitrification Inhibitors—As Mitigation Tools for Greenhouse Gas Emissions in Sustainable Dairy Systems: A Review. *Sustainability* **2020**, *12*, 6018. [[CrossRef](#)]
51. Barrena, I.; Menéndez, S.; Correa-Galeote, D.; Vega-Mas, I.; Bedmar, E.J.; González-Murua, C.; Estavillo, J.M. Soil water content modulates the effect of the nitrification inhibitor 3,4-dimethylpyrazole phosphate (DMPP) on nitrifying and denitrifying bacteria. *Geoderma* **2017**, *303*, 1–8. [[CrossRef](#)]
52. Godfrey, L.V.; Glass, J.B. The geochemical record of the ancient nitrogen cycle, nitrogen isotopes, and metal cofactors. *Methods Enzym.* **2011**, *486*, 483–506. [[CrossRef](#)]
53. Velthof, G.L.; Mosquera, J.; Mosquera, J.; Veld, J.W.H.H.i.t.; Hummelink, E.W.J. *Effect of Manure Application Technique on Nitrous Oxide Emission from Agricultural Soils*; Alterra Wageningen UR: Wageningen, The Netherlands, 2010; p. 74.

54. Zhu, Y.; Merbold, L.; Leitner, S.; Pelster, D.E.; Okoma, S.A.; Ngetich, F.; Onyango, A.A.; Pellikka, P.; Butterbach-Bahl, K. The effects of climate on decomposition of cattle, sheep and goat manure in Kenyan tropical pastures. *Plant Soil* **2020**, *451*, 325–343. [CrossRef]
55. Mosier, A.R. Soil processes and global change. *Biol. Fertil. Soils* **1998**, *27*, 221–229. [CrossRef]
56. Lessard, R.; Rochette, P.; Gregorich, E.G.; Pattey, E.; Desjardins, R.L. Nitrous Oxide Fluxes from Manure-Amended Soil under Maize. *J. Environ. Qual.* **1996**, *25*. [CrossRef]
57. Flach, B.; Lieberz, S.; Lappin, J.; Bolla, S. *EU Biofuels Annual 2018*; USDA Foreign Agricultural Service: Washington, DC, USA, 2018.
58. Pehnelt, G.; Vietze, C. *Uncertainties about the GHG Emissions Saving of Rapeseed Biodiesel*; Friedrich-Schiller University of Jena: Jena, Germany, 2012.
59. Astover, A.; Shanskiy, M.; Lauringson, E. *Development and Application of the Methodology for the Calculation of Average Greenhouse Gas Emissions from the Cultivation of Rapeseed, Wheat, Rye, Barley and Triticale in Estonia*; Ministry of the Environment of the Republic of Estonia: Tartu, Estonia, 2015.
60. BioGrace. BioGrace Greenhouse Gas Calculation Tool Version 4d. Available online: <http://www.biograce.net/> (accessed on 26 February 2020).
61. Vinzent, B.; Fuß, R.; Maidl, F.-X.; Hülsbergen, K.-J. Efficacy of agronomic strategies for mitigation of after-harvest N₂O emissions of winter oilseed rape. *Eur. J. Agron.* **2017**, *89*, 88–96. [CrossRef]
62. European Commission. *Communication from the Commission: The European Green Deal*; European Commission: Brussels, Belgium, 2019.
63. *The European Parliament and of the Council of the European Union. Directive (EU) 2018/2001 of the European Parliament and of the Council of 11 December 2018 on the Promotion of the Use of Energy from Renewable Sources*; Council of the European Union: Strasbourg, France, 2018.
64. Oo, A.Z.; Gonai, T.; Sudo, S.; Thuzar Win, K.; Shibata, A. Surface application of fertilizers and residue biochar on N₂O emission from Japanese pear orchard soil. *Plantsoil Environ.* **2018**, *64*, 597–604. [CrossRef]
65. Carter, M.R.; Gregorich, E.G. *Soil Sampling and Methods of Analysis*; CRC Press: Boca Raton, FL, USA, 2007. [CrossRef]
66. Egnér, H.; Riehm, H.; Domingo, W.R. Untersuchungen über die chemische Bodenanalyse als Grundlage für die Beurteilung des Nährstoffzustandes der Böden. II. Chemische Extraktionsmethoden zur Phosphor- und Kaliumbestimmung. *K. Lantbr. Ann.* **1960**, *26*, 199–215.
67. Association of official analytical chemists (AOAC). *Official Methods of Analysis*, 15th ed.; Association of Official Analytical Chemists: Washington, DC, USA, 1990.
68. Schulte, E.E.; Hopkins, B.G. Estimation of Soil Organic Matter by Weight Loss-On-Ignition. In *Soil Organic Matter: Analysis and Interpretation*; Magdoff, F.R., Tabatabai, M.A., Jr., Edward, A.H., Eds.; Soil Science Society of America, Inc.: Madison, WI, USA, 1996; Volume 46. [CrossRef]
69. Ruzicka, J.; Hansen, E.H. *Flow Injection Analysis*, 2nd ed.; Wiley: New York, NY, USA, 1988.
70. Hutchinson, G.L.; Livingston, G.P. Use of chamber systems to measure trace gas fluxes. In *Agricultural Ecosystem Effects on Trace Gases and Global Climate Change*; Harper, L.A., Mosier, A.R., Duxbury, J.M., Rolston, D.E., Eds.; American Society of Agronomy: Madison, WI, USA, 1993; pp. 63–78. [CrossRef]
71. Mander, U.; Maddison, M.; Soosaar, K.; Teemusk, A.; Kanal, A.; Uri, V.; Truu, J. The impact of a pulsing groundwater table on greenhouse gas emissions in riparian grey alder stands. *Environ. Sci. Pollut. Res. Int.* **2015**, *22*, 2360–2371. [CrossRef]
72. Lofthfield, N.; Flessa, H.; Augustin, J.; Beese, F. Automated Gas Chromatographic System for Rapid Analysis of the Atmospheric Trace Gases Methane, Carbon Dioxide, and Nitrous Oxide. *J. Environ. Qual.* **1997**, *26*. [CrossRef]
73. Livingston, G.P.; Hutchinson, G.L. Enclosure-based measurement of trace gas exchange: Applications and sources of error. In *Biogenic Trace Gases: Measuring Emissions from Soil and Water*; Matson, P.A., Harriss, R.C., Eds.; Blackwell Publishing: Oxford, UK, 1995; pp. 14–51.
74. Volpi, I.; Ragagnini, G.; Nasso, N.; Bonari, E.; Bosco, S. Soil N₂O emissions in Mediterranean arable crops as affected by reduced tillage and N rate. *Nutr. Cycl. Agroecosyst.* **2019**, *116*, 117–133. [CrossRef]
75. R Core Team. *R: A Language and Environment for Statistical Computing*; R Foundation for Statistical Computing: Vienna, Austria, 2016.
76. Tukey, J.W. *Exploratory Data Analysis*; Addison-Wesley Publishing Company: Reading, MA, USA, 1977.

77. Müller, C.; Stevens, R.J.; Laughlin, R.J.; Azam, F.; Ottow, J.C.G. The nitrification inhibitor DMPP had no effect on denitrifying enzyme activity. *Soil Biol. Biochem.* **2002**, *34*, 1825–1827. [[CrossRef](#)]
78. Flessa, H.; Dörsch, P.; Beese, F. Seasonal variation of N₂O and CH₄ fluxes in differently managed arable soils in southern Germany. *J. Geophys. Res.* **1995**, *100*. [[CrossRef](#)]
79. Dobbie, K.E.; McTaggart, I.P.; Smith, K.A. Nitrous oxide emissions from intensive agricultural systems: Variations between crops and seasons, key driving variables, and mean emission factors. *J. Geophys. Res. Atmos.* **1999**, *104*, 26891–26899. [[CrossRef](#)]
80. Schaufler, G.; Kitzler, B.; Schindlbacher, A.; Skiba, U.; Sutton, M.A.; Zechmeister-Boltenstern, S. Greenhouse gas emissions from European soils under different land use: Effects of soil moisture and temperature. *Eur. J. Soil Sci.* **2010**, *61*, 683–696. [[CrossRef](#)]
81. Wang, F.; Li, J.; Wang, X.; Zhang, W.; Zou, B.; Neher, D.A.; Li, Z. Nitrogen and phosphorus addition impact soil N₂O emission in a secondary tropical forest of South China. *Sci. Rep.* **2014**, *4*, 5615. [[CrossRef](#)]
82. Dhadli, H.S.; Brar, B.S.; Kingra, P.K. Temporal Variations in N₂O Emissions in Maize and Wheat Crop Seasons: Impact of N-Fertilization, Crop Growth, and Weather Variables. *J. Crop Improv.* **2016**, *30*, 17–31. [[CrossRef](#)]
83. Ryden, J.C. Denitrification loss from a grassland soil in the field receiving different rates of nitrogen as ammonium nitrate. *J. Soil Sci.* **1983**, *34*, 355–365. [[CrossRef](#)]
84. Mori, T.; Ohta, S.; Ishizuka, S.; Konda, R.; Wicaksono, A.; Heriyanto, J.; Hardjono, A. Effects of phosphorus addition on N₂O and NO emissions from soils of anAcacia mangiumplantation. *Soil Sci. Plant Nutr.* **2010**, *56*, 782–788. [[CrossRef](#)]
85. Keil, D.; Niklaus, P.A.; von Riedmatten, L.R.; Boeddinghaus, R.S.; Dormann, C.F.; Scherer-Lorenzen, M.; Kandeler, E.; Marhan, S. Effects of warming and drought on potential N₂O emissions and denitrifying bacteria abundance in grasslands with different land-use. *FEMS Microbiol. Ecol.* **2015**, *91*. [[CrossRef](#)]
86. Stevens, R.J.; Laughlin, R.J. Cattle Slurry Applied Before Fertilizer Nitrate Lowers Nitrous Oxide and Dinitrogen Emissions. *Soil Sci. Soc. Am. J.* **2002**, *66*, 647–652. [[CrossRef](#)]
87. Loro, P.J.; Bergstrom, D.W.; Beauchamp, E.G. Intensity and Duration of Denitrification following Application of Manure and Fertilizer to Soil. *J. Environ. Qual.* **1997**, *26*, 706–713. [[CrossRef](#)]
88. Simek, M.; Cooper, J.E. The influence of soil pH on denitrification: Progress towards the understanding of this interaction over the last 50 years. *Eur. J. Soil Sci.* **2002**, *53*, 345–354. [[CrossRef](#)]
89. Hénault, C.; Bourennane, H.; Ayzac, A.; Ratié, C.; Saby, N.P.A.; Cohan, J.P.; Eglin, T.; Gall, C.L. Management of soil pH promotes nitrous oxide reduction and thus mitigates soil emissions of this greenhouse gas. *Sci. Rep.* **2019**, *9*, 20182. [[CrossRef](#)] [[PubMed](#)]
90. McMillan, A.M.S.; Pal, P.; Phillips, R.L.; Palmada, T.; Berben, P.H.; Jha, N.; Saggari, S.; Luo, J. Can pH amendments in grazed pastures help reduce N₂O emissions from denitrification?—The effects of liming and urine addition on the completion of denitrification in fluvial and volcanic soils. *Soil Biol. Biochem.* **2016**, *93*, 90–104. [[CrossRef](#)]
91. Chen, Z.; Ding, W.; Luo, Y.; Yu, H.; Xu, Y.; Müller, C.; Xu, X.; Zhu, T. Nitrous oxide emissions from cultivated black soil: A case study in Northeast China and global estimates using empirical model. *Glob. Biogeochem. Cycles* **2014**, *28*, 1311–1326. [[CrossRef](#)]
92. Thornton, F.C.; Shurpali, N.J.; Bock, B.R.; Reddy, K.C. N₂O and no emissions from poultry litter and urea applications to Bermuda grass. *Atmos. Environ.* **1998**, *32*, 1623–1630. [[CrossRef](#)]
93. Cantarel, A.A.M.; Bloor, J.M.G.; Deltroy, N.; Soussana, J.-F. Effects of Climate Change Drivers on Nitrous Oxide Fluxes in an Upland Temperate Grassland. *Ecosystems* **2010**, *14*, 223–233. [[CrossRef](#)]
94. Calderón, F.J.; McCarty, G.W.; Reeves, J.B. Analysis of manure and soil nitrogen mineralization during incubation. *Biol. Fertil. Soils* **2005**, *41*, 328–336. [[CrossRef](#)]
95. Clemens, J.; Huschka, A. The effect of biological oxygen demand of cattle slurry and soil moisture on nitrous oxide emissions. *Nutr. Cycl. Agroecosyst.* **2001**, *59*, 193–198. [[CrossRef](#)]
96. Guo, X.; Drury, C.F.; Yang, X.; Daniel Reynolds, W.; Fan, R. The Extent of Soil Drying and Rewetting Affects Nitrous Oxide Emissions, Denitrification, and Nitrogen Mineralization. *Soil Sci. Soc. Am. J.* **2014**, *78*, 194–204. [[CrossRef](#)]
97. Smith, M.S.; Parsons, L.L. Persistence of Denitrifying Enzyme Activity in Dried Soils. *Appl. Environ. Microbiol.* **1985**, *49*, 316–320. [[CrossRef](#)]
98. Smith, M.S.; Firestone, M.K.; Tiedje, J.M. The Acetylene Inhibition Method for Short-term Measurement of Soil Denitrification and its Evaluation Using Nitrogen-131. *Soil Sci. Soc. Am. J.* **1978**, *42*. [[CrossRef](#)]

99. Firestone, M.K.; Tiedje, J.M. Temporal change in nitrous oxide and dinitrogen from denitrification following onset of anaerobiosis. *Appl. Environ. Microbiol.* **1979**, *38*, 673–679. [[CrossRef](#)] [[PubMed](#)]
100. Paul, J.W.; Beauchamp, E.G. Denitrification and fermentation in plant-residue-amended soil. *Biol. Fertil. Soils* **1989**, *7*. [[CrossRef](#)]
101. Tenuta, M.; Bergstrom, D.W.; Beauchamp, E.G. Denitrifying enzyme activity and carbon availability for denitrification following manure application. *Commun. Soil Sci. Plant Anal.* **2008**, *31*, 861–876. [[CrossRef](#)]
102. Petersen, S.O. Nitrous Oxide Emissions from Manure and Inorganic Fertilizers Applied to Spring Barley. *J. Environ. Qual.* **1999**, *28*. [[CrossRef](#)]
103. Beck, H.; Christensen, S. The effect of grass maturing and root decay on N₂O production in soil. *Plant Soil* **1987**, *103*, 269–273. [[CrossRef](#)]
104. Oenema, O.; Velthof, G.L.; Yamulki, S.; Jarvis, S.C. Nitrous oxide emissions from grazed grassland. *Soil Use Manag.* **1997**, *13*, 288–295. [[CrossRef](#)]
105. Beltran-Rendon, D.; Rico-Fragozo, K.; Farfan-Caceres, L.; Restrepo-Diaz, H.; Hoyos-Carvajal, L. The effect of nitrification inhibitor 3,4-dimethylpyrazole phosphate (DMPP) on nitrifying organism populations under in vitro conditions. *Agric. Sci.* **2011**, *2*, 198–200. [[CrossRef](#)]
106. De Antoni, M.M.; Scheer, C.; Grace, P.R.; Rowlings, D.W.; Bell, M.; McGree, J. Influence of different nitrogen rates and DMPP nitrification inhibitor on annual N₂O emissions from a subtropical wheat–maize cropping system. *Agric. Ecosyst. Environ.* **2014**, *186*, 33–43. [[CrossRef](#)]
107. Kou, Y.P.; Wei, K.; Chen, G.X.; Wang, Z.Y.; Xu, H. Effects of 3,4-dimethylpyrazole phosphate and dicyandiamide on nitrous oxide emission in a greenhouse vegetable soil. *Plant Soil Environ.* **2016**, *61*, 29–35. [[CrossRef](#)]
108. Wrage-Mönnig, N.; Horn, M.A.; Well, R.; Müller, C.; Velthof, G.; Oenema, O. The role of nitrifier denitrification in the production of nitrous oxide revisited. *Soil Biol. Biochem.* **2018**, *123*, A3–A16. [[CrossRef](#)]

Publisher’s Note: MDPI stays neutral with regard to jurisdictional claims in published maps and institutional affiliations.



© 2020 by the authors. Licensee MDPI, Basel, Switzerland. This article is an open access article distributed under the terms and conditions of the Creative Commons Attribution (CC BY) license (<http://creativecommons.org/licenses/by/4.0/>).

IV Escuer-Gatius, J., Lõhmus, K., Shanskiy, M., Kauer, K., Vahter, H., Mander, Ü., Astover, A., Soosaar, K. 2022. Critical points for closing the carbon and nitrogen budgets in a winter rapeseed field. Nutrient Cycling in Agroecosystems.



Critical points for closing the carbon and nitrogen budgets in a winter rapeseed field

Jordi Escuer-Gatius · Krista Lõhmus ·
Merrit Shanskiy · Karin Kauer · Hanna Vahter ·
Ülo Mander · Alar Astover · Kaido Soosaar

Received: 23 August 2021 / Accepted: 24 March 2022
© The Author(s), under exclusive licence to Springer Nature B.V. 2022

Abstract The main C and N fluxes of a winter rapeseed field in Central Estonia were quantified for one year to identify the highest fluxes and major sources of uncertainty. Greenhouse gas emissions were measured with the closed chamber method, leaching losses were estimated by combining the soil water balance and leachate analyses, and soil C and N changes were also monitored. Gross primary production (GPP) and di-nitrogen (N_2) fluxes were estimated from the C and N mass balance, respectively. The field was a net C sink ($3366 \text{ kg C ha}^{-1} \text{ yr}^{-1}$) because of the high C absorption rate through GPP ($17,215 \text{ kg C ha}^{-1} \text{ yr}^{-1}$). The N outputs markedly exceeded the inputs, which translated into soil N losses. The highest measured N fluxes were those

of N leaching ($44 \text{ kg N ha}^{-1} \text{ yr}^{-1}$) and nitrous oxide (N_2O) emissions ($26 \text{ kg N ha}^{-1} \text{ yr}^{-1}$). Approximately 60% of the total N_2O emissions occurred during the first 50 days after slurry application, promoted by field and weather conditions. The unaccounted soil N loss was attributed to N_2 emissions (estimated at $668 \text{ kg N ha}^{-1} \text{ yr}^{-1}$). After conversion to CO_2 -eq, the positive balance of carbon dioxide (CO_2) emissions remained the dominant flux ($34,571 \text{ kg CO}_2\text{-eq ha}^{-1} \text{ yr}^{-1}$), but N_2O emissions were also notable ($11,218 \text{ kg CO}_2\text{-eq ha}^{-1} \text{ yr}^{-1}$). The methodology used in this study provided estimates for the main fluxes in the C and N cycles, but also allowed the identification of methodological limitations and challenges.

Supplementary Information The online version contains supplementary material available at <https://doi.org/10.1007/s10705-022-10202-8>.

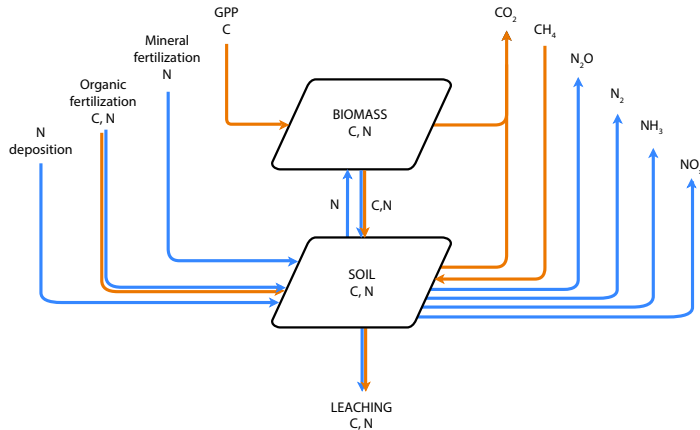
J. Escuer-Gatius (✉) · M. Shanskiy · K. Kauer ·
A. Astover
Institute of Agricultural and Environmental Sciences,
Estonian University of Life Sciences, Tartu, Estonia
e-mail: Jordi.EscuerGatius@emu.ee

K. Lõhmus · H. Vahter · Ü. Mander · K. Soosaar
Institute of Ecology and Earth Sciences, University
of Tartu, Tartu, Estonia

Published online: 15 April 2022

Springer

Graphical abstract Main components of the C (orange) and N (blue) budget considered in the study.



Keywords Carbon dioxide · Carbon sequestration · DMPP · Nitrous oxide · N_2 emissions · N leaching

Introduction

The increasing human population worldwide, which is expected to reach 10 billion by 2050, has created a growing need for food and is anticipated to increase agricultural demand by around 50% in 2050 compared with 2013 levels (FAO 2017). The intensification of production may result in higher greenhouse gas (GHG) emissions from production inputs such as fertilizers. Agricultural intensification can also result in soil degradation, again enhancing GHG emissions (EEA 2000), as well as eutrophication, ozone formation, and soil acidification (Ammann et al. 2009). Adverse impacts such as GHG emissions and soil degradation need to be minimized to mitigate the effect of agriculture on the environment. However, efficient and sustainable agricultural practices can only be achieved with a comprehensive understanding of the mechanistic processes giving rise to these negative impacts. Full carbon (C) and nitrogen (N) budget quantifications, considering all inputs and outputs, are essential to understand these processes, as C and N cycling is a major control on emissions of carbon dioxide (CO_2), nitrous oxide (N_2O), and methane (CH_4).

Atmospheric concentrations of GHGs continue to increase (NOAA 2020). Agriculture is responsible for approximately 11% of total GHG emissions in the EU member states (EEA 2016) and 10% in the US (EPA 2020). Nitrous oxide is an especially relevant GHG as it has a global warming potential 273 times that of CO_2 (IPCC 2021) and is recognized as the main ozone-depleting substance (Ravishankara et al. 2009). Anthropogenic emissions represent approximately 50% of total N_2O emissions (Ciais et al. 2013), around two thirds of which can be attributed to agriculture (Davidson and Kanter 2014). In contrast, croplands can act as sinks or sources of CO_2 depending on the crop and the applied agro-technology (Lal 2001).

Nutrient losses also have an important economic detrimental effect on agriculture, as they increase the necessity of inputs, which can eventually make agriculture economically unsustainable (Oenema and Velthof 2002). Losses of N from croplands can be as high as 37% in maize, 46% in wheat, and 56% in rice (Prasad and Hobbs 2018). In Europe, N recovery (the amount of N recovered in the crop per amount of N applied with fertilization) is around 30–60% for cereals, which means that between 40 and 70% of the N applied with fertilization is lost (Sutton et al. 2011). Globally, only 47% of the reactive N added to croplands through fertilization is converted into harvest (Lassaletta et al. 2014).

Emission reduction goals established in the Kyoto Protocol (UNFCCC 1997), the Paris Agreement (UNFCCC 2015), and the “Global Warming of 1.5 °C” report (IPCC 2018) stress the need for precise accounting of emissions, at both field and global scales, because effective policies cannot be implemented without accurate source identification (Davidson and Kanter 2014). Field nutrient budgets are also necessary for large-scale model development and validation, given the existing uncertainties of these models (Bouwman et al. 1995; Philibert et al. 2012). Moreover, although a large amount of literature is available regarding cropland emissions, in many cases there are no accompanying data on the size of other relevant C and N fluxes and pools, or other essential ancillary data may be missing (Burke et al. 2002; Eagle et al. 2017; Ladha et al. 2016; Leip et al. 2007; Öborn et al. 2003; Oenema et al. 2003; Rosenstock et al. 2013). As a result, a complete picture of the processes by which these elements are added and lost at field level is not available.

Rapeseed (*Brassica napus* L.) is the main crop in the EU for the production of biofuels (USDA Foreign Agricultural Service 2018), and the third most important crop for oil production worldwide (Bouchet et al. 2016). The consequences of biofuel production in future emissions remain unclear, but biofuel production and use could become the most important source of GHG emissions in the future (Davidson and Kanter 2014). Furthermore, concerns have been raised regarding the quantification of emissions from the use of rapeseed-derived biofuels (Pehnelt and Vietze 2012). Rapeseed is also cultivated for oil consumption by humans because of its high protein content and because it also generates an animal feed byproduct. Unfortunately, rapeseed has one of the highest N-application rates of all crops (Jensen et al. 2011) and has a low N-use efficiency (Malagoli et al. 2005), which results in negative environmental and economic impacts. Increased understanding of the C and N fluxes in rapeseed cultivation are needed to allow accurate evaluation of the environmental impact of this crop.

The aim of this study was to assemble a set of methodologies for the estimation of the C and N budgets at the field scale under winter rapeseed production, and identify methodological challenges and limitations, as well as to propose methodological improvements.

Material and methods

Experimental set-up

The study field is located in central Estonia (58° 55′ 21″ N, 24° 50′ 52″ E; Kehtna parish, Rapla county; Fig. S1). The field has a total surface of 18.13 ha, and the dominant soil type is Gleysol with a loam texture (FAO 2015). The mean values for the soil properties were as follows (mean ± standard error): bulk density (g cm^{-3}), 1.11 ± 0.21 ; pH_{KCl} , 4.75 ± 0.01 ; organic matter (OM, %), 11.45 ± 0.09 ; $\text{NH}_4^+\text{-N}$ (mg kg^{-1}), 3.715 ± 0.085 ; $\text{NO}_3^-\text{-N}$ (mg kg^{-1}), 51.05 ± 0.24 ; C (%), 6.45 ± 0.09 ; N (%), 0.63 ± 0.005 ; Ca (mg kg^{-1}), 2326 ± 74 ; K (mg kg^{-1}), 126 ± 6.29 ; Mg (mg kg^{-1}), 333 ± 6 ; P (mg kg^{-1}), 50.80 ± 1.14 ; S (%), 0.095 ± 0.005 ; and dissolved organic carbon (DOC, mg kg^{-1}), 378.5 ± 4.6 . A tile drainage system was installed in the field in 1964 (Republic of Estonia Land Board’s Geoportaal, <https://xgis.maaamet.ee/maps/XGis>) and it is still present and in working condition. The drainage system can be divided according to the discharge point (Fig. S1): in the western part of the field, the drainage system discharges into a ditch. In the central and eastern parts, the drainage system discharges into the Rõue River (also known as Kuusiku River) to the north. In the previous year to the studied period, the field had been sown with a grassland mix (*Lolium perenne*, 35%; *Festulolium*, 20%; *Festuca pratensis*, 15%; *Dactylis glomerata*, 10%; *Trifolium pratense*, 15%; and *Trifolium repens*, 5%).

Measurements of GHG and soil and leachate analyses were taken for a period of one year (August 5, 2016–August 17, 2017) to cover the full growing season of the winter rapeseed. As a part of a study of the effect of 3,4-Dimethylpyrazole phosphate (DMPP; BASF, Ludwigshafen, Germany) application on N_2O emissions and NO_3^- leaching, the study field was divided into two different plots with similar soil properties. A more detailed description of the experiment, focusing on the losses during the first 50 days after the application of the slurry, to test the effectiveness of the nitrification inhibitor DMPP in reducing N_2O emissions and NO_3^- leaching after dairy slurry application can be found in Escuer-Gatius et al. (2020). The same division was also used for the estimation of the C and N budgets. The division was based on the direction of the water drainage system, allowing

the collection of leachate samples for each of the two plots separately (Fig. S1). Slurry was applied to the field on August 6, 2016. In the control plot, cattle slurry was mixed with the upper layer of the soil at a rate of 30 t ha⁻¹ (equivalent to 1019 kg C ha⁻¹ and 64 kg N ha⁻¹) using the injection technique followed by tillage with a rotary harrow. In the treatment plot, the slurry was mixed with the nitrification inhibitor DMPP, before being applied with the same technique and at the same rate. The DMPP application rate was 3 L ha⁻¹. Winter rapeseed (*B. napus* 'DK Sequoia') was sown on August 10, 2016 and harvested on August 26, 2017. Mineral fertilization was applied as calcium ammonium nitrate (CAN) and ammonium sulphate nitrate (ASN) on three occasions in 2017: April 4, 250 kg ha⁻¹ of CAN 27; May 1, 160 kg ha⁻¹ of ASN 26 N+13S; and May 8, 160 kg ha⁻¹ of ASN 26 N+13S.

Climatic data (pressure, precipitation, humidity, sunshine, air temperature, air temperature at 20 mm above the ground, ground temperature, visibility, wind direction, wind speed, and maximum wind speed) were obtained from the Kuusiku weather station (Estonian Weather Service, WMO code 26,134; 58° 58' 23" N, 24° 44' 02" E), located approximately 11 km from the experimental field. The total precipitation during the duration of the experiment was 646 mm, the mean air temperature 5.9 °C, with a minimum temperature of -21 °C and a maximum temperature of 28.1 °C (Fig. S2).

Methods

Nutrient balance

The equation for the calculation of the C mass balance was derived from Soussana et al. (2010) as:

$$\Delta C_{\text{soil}} = F_{\text{slurry}} + F_{\text{min.fertilizer}} + F_{\text{gas.fluxes}} - F_{\text{seeds}} - F_{\text{cropresidues+weeds}} - F_{\text{leaching}} \quad (1)$$

where ΔC_{soil} is the change in total C content in soil; $F_{\text{gas.fluxes}}$ comprises the main gaseous interchange between soil and the atmosphere, including CO₂, CH₄, volatile organic compounds (VOC), and fluxes caused by fire ($F_{\text{CO}_2} - F_{\text{CH}_4} - F_{\text{VOC}} - F_{\text{fire}}$), with F_{CO_2} including gross primary productivity (GPP) and ecosystem respiration (soil respiration and above-ground plant respiration); fertilization is divided into

slurry application (F_{slurry}) and mineral fertilization ($F_{\text{min.fertilizer}}$); F_{seeds} is the C in the harvested seeds; $F_{\text{cropresidues+weeds}}$ is the C in crop residues and weeds; and F_{leaching} represents the losses through leaching. Since no losses by fire took place in the field in the studied period and we assume that VOC emissions are negligible (Hutchings and Webb, 2019; Wohlfahrt et al., 2012), these factors were omitted. No erosion was observed in the field. All fluxes are expressed as kg C ha⁻¹ yr⁻¹.

Similarly, an equation to estimate the change of N content in the soil was derived following Sainju (2017) and Cameron et al. (2013) (Eq. 2). It was assumed that the N input by biological fixation during the rapeseed growing season was negligible, as there were no N-fixing species.

$$\Delta N_{\text{soil}} = F_{\text{slurry}} + F_{\text{min.fertilizer}} - F_{\text{gas.fluxes}} + N_{\text{deposition}} - F_{\text{seeds}} - F_{\text{cropresidues+weeds}} - F_{\text{leaching}} \quad (2)$$

where ΔN_{soil} is the change of N content in soil during the study period, F_{slurry} considers the addition of N through manure application, $F_{\text{min.fertilizer}}$ represents the addition of N as mineral fertilizer, $N_{\text{deposition}}$ is the input of reactive nitrogen from the atmosphere; F_{seeds} is the N removed with harvested seeds, $F_{\text{cropresidues+weeds}}$ represents the crop residues and weed biomass not extracted with the harvest; and F_{leaching} is the N loss through leaching. $F_{\text{gas.fluxes}}$ comprises the main gaseous interchange between soil and the atmosphere, and can be decomposed as follows:

$$F_{\text{gas.fluxes}} = F_{\text{N}_2\text{O}} + F_{\text{N}_2} + F_{\text{NH}_3} + F_{\text{NO}_x} \quad (3)$$

where $F_{\text{N}_2\text{O}}$, F_{N_2} , F_{NH_3} , and F_{NO_x} are the fluxes of N₂O, dinitrogen (N₂), ammonia (NH₃), and nitrogen oxides (NO_x), respectively. All fluxes are expressed as kg N ha⁻¹ yr⁻¹.

For the budget calculation, input fluxes at soil or field-scale have a positive sign, whereas output fluxes have a negative sign.

GHG flux measurements

The CO₂, N₂O, and CH₄ measurements were carried out using the closed chamber method (Hutchinson and Livingston 1993). Five white opaque PVC chambers (0.40 m height, 0.50 m base diameter, and 65.5 L headspace volume) were used in each of the plots (10

chambers in total). The collars were installed on site 24 h before the beginning of the measurements. Trace gas fluxes were measured from August 5, 2016 until August 14, 2017, at 2–3 day intervals during the first week after the application of the slurry, with a total of 13 measurements in the first 30 days, and a regular weekly frequency after that. Gas samples for trace gas measurement were collected at 0, 20, 40, and 60 min after chamber closure into 12 ml pre-evacuated (0.04 mbar) bottles, using a gas-tight syringe to remove the air in the system before sampling. The CO₂ fluxes measured with the opaque chambers represent ecosystem respiration (R_{ECO}) (Poyda et al. 2017). From June 2, 2017, extensions made from the same material as the chambers and with the same diameter as the chambers at the base and 1 m height were added to the chambers, to expand the height and volume (making a total height of 1.4 m) to accommodate the rapeseed plants.

The gas concentration in the air samples collected in the field was determined in the lab with a Shimadzu GC-2014 gas chromatograph (Shimadzu Corporation, Kyoto, Japan) integrated into an automated gas chromatographic system as described by Loftfield et al. (1997). Gas fluxes were estimated from the slope of the least-squares linear regression of the gas concentrations in the samples over time (Livingston and Hutchinson 1995; Soosaar et al. 2011) as follows:

$$f = \frac{dC}{dt} \cdot \frac{V}{A} \quad (4)$$

where f is the flux of the studied gas ($\mu\text{g m}^{-2} \text{h}^{-1}$), dC/dt is the rate of change in concentration with time ($\mu\text{g m}^{-3} \text{h}^{-1}$), C is the trace gas concentration at a certain moment t ($\mu\text{g m}^{-3}$), t is time (h), and V and A are the chamber headspace (m^3) and the area of the surface covered by the chamber (m^2).

The adjusted R^2 value of the linear fit was used to determine the goodness-of-fit of each chamber session, validating conditions of chamber stability and flux linearity (Livingston and Hutchinson 1995). One of the four observations was discarded as an outlier if necessary and the remaining three were used for flux calculation. The minimum R^2 values of 0.90 and 0.99 were used to check the linearity of the measurements for four ($n=4$) and three ($n=3$) measurement points, respectively. A chamber session was discarded when the R^2 value did not meet the criteria, but a minimum

of three chamber measurements for each plot were retained.

Cumulative fluxes were calculated by integration of total daily fluxes (time integration) over the whole period (Vinzent et al. 2018), after gap-filling by linear interpolation between sampling points. Linear interpolation was used also for gap filling of missing flux values (Vinzent et al. 2018).

The N₂O and CH₄ emissions were converted into CO₂-eq ha⁻¹ considering a global warming potential (GWP) over a 100-year period of 273 for N₂O and 28 for CH₄ (IPCC, 2021).

Soil C and N change

Three representative soil samples of the first 0.20 m of soil, resulting from the mix of ten subsamples each, were collected from each plot in the area adjacent to the chambers, with the aid of a soil sampler probe, at the beginning and end of the study period. The change in soil C and N was estimated based on the difference between the initial and final contents (Sainju 2017).

The conversion between laboratory analysis data (mg kg^{-1}) to field data was performed assuming an active soil depth of 0.20 m, where most soil C and N is found (Allison 1973; Del Grosso et al. 2000). The bulk density was determined at the beginning of the experiment at different soil depths with 50 mm increments for the topsoil using steel cylinders. Soil dry matter (DM) was measured by drying soil samples at 105 °C for 16 h. Soil organic matter (OM) was determined by loss-upon-ignition following heating at 500 °C for 4 h. Soil pH was determined in a 2.5:1 KCl soil (v:w) suspension. Soil NO₃⁻-N and NH₄⁺-N were determined in 2 M KCl extract of soil by a flow injection analyzer FIAStar 5000 (Foss Tecator AB, Höganäs, Sweden). Total C and N were determined using a VarioMAX CNS Element Analyzer (Elementar Analysensysteme GmbH, Langenselbold, Germany). Linear interpolation was used to estimate missing data for field, soil, and leachate parameters (Kersebaum et al. 2004; Øygarden and Botterweg 1998).

Leachate analysis and leachate losses

Leachate samples were collected during the study period. Leaching water was collected separately for

the two study plots from the ends of the drainage pipes (Fig. S1). Samples were initially collected at a daily frequency during the first week after the application of the slurry, followed by a lower frequency afterwards, giving 11 measurements in the first 50 days of the experiment and a total of 27 measurements (days) during the whole study period. Of these, 6 were discarded because either the ditch or the river was flooded above the drainage pipe end level. Collection of leaching water samples was limited temporarily by flooding of the drainage pipes, and also by freezing and drought.

Daily C and N losses due to leaching were calculated from the daily C and N concentrations in leachate, after linear interpolation between measurements, applied to the total amount of estimated daily percolation. Total C and N losses were then estimated from the temporal integration of daily values for the whole period.

Total daily percolation (PC) was estimated using the soil water balance (Goyal 2014):

$$P + I = ET_c + R + PC + \Delta S \quad (5)$$

where P is precipitation, I is water supplied by irrigation, ET_c is evapotranspiration, R is superficial runoff, and ΔS is the net change in water storage (all in $L \text{ d}^{-1}$). The soil water balance was considered to 0.3 m soil depth, the depth of the relatively homogeneous topsoil horizon, which includes all roots, and is delimited below by a poorly permeable clay layer. Because there was no irrigation, $I=0$, and assuming no runoff due to the flat topography of the field and no visible runoff, $R=0$, thus PC was calculated as follows (Arregui and Quemada 2006):

$$PC = P - ET_c - \Delta S \quad (6)$$

Precipitation (P) was obtained from the Kuusiku meteorological station. The change in soil moisture (ΔS) was estimated from daily changes in measured soil moisture in the field, after linear interpolation between measurement days. Crop evapotranspiration (ET_c) was calculated with the FAO-56 methodology as described in Allen et al. (1998) (Supplementary Methodology S1).

Leaching water NO_3^- -N and NH_4^+ -N concentrations were measured via a flow injection analyzer FIAStar 5000 (Foss Tecator AB, Höganäs, Sweden). The DOC concentration was determined according

to the EVS-EN 1484 standard with a Vario TOC analyzer (Elementar Analysensysteme GmbH, Langensfeld, Germany) and the dissolved nitrogen (DN) concentration was determined according to the EVS-EN 12,260 standard. Leaching soil water DOC and DN concentrations were measured according to the same standards after extraction with H_2O .

Slurry analyses

Slurry DM was determined by oven drying for 2 h at 135 °C (AOAC 1990) and the organic matter content was determined by loss on ignition (Schulte and Hopkins 1996). The NH_4^+ -N content was determined using flow injection analyses by Tecator ASN 65-32/84 (Ruzicka and Hansen 1988). Total C and N were determined using a Vario MAX CNS Element Analyzer (Elementar Analysensysteme GmbH, Langensfeld, Germany). For the determination of total soluble nitrogen (DN), total soluble carbon (DC), total soluble organic carbon (TOC), and total soluble inorganic carbon (DIC) content in the slurry, H_2O was used as extractant with solution in a 1:10 ratio (m/v), extracted for 2 h, and then filtered through a 0.45- μm filter. TOC was determined according to the standard EN 1484:1997, with a Vario TOC analyzer (Elementar Analysensysteme GmbH, Langensfeld, Germany, temperature 850 °C). The DN content was determined according to the standard EN 12,260. The quantification of the DN concentration was carried out by chemiluminescence detection, using a Vario TOC analyzer (Elementar Analysensysteme GmbH, Langensfeld, Germany) with a HORIBA APNA-370 (HORIBA, Ltd., Kyoto, Japan) chemiluminescence detector. The DOC, DIC, DC, and DN contents were expressed on the basis of oven-dried soil. The limit of quantitation for DC, DOC, and DIC was 20 mg kg^{-1} and 5 mg kg^{-1} for DN.

Field soil parameters

Soil temperature, moisture, and electrical conductivity were measured on each GHG flux sampling day. Soil temperature was measured for each plot at four different depths (0.05, 0.10, 0.20, and 0.30 m) with a four-channel temperature datalogger S0141 (COMET SYSTEM, Rožnov pod Radhoštěm, Czech Republic) with four PT1000 sensors. Soil moisture and electrical conductivity were measured at 0.05 m depth with

a GS3 sensor connected to a ProCheck handheld reader (Decagon Devices, Pullman, WA, USA).

Biomass production

Plant samples were collected from the field before harvest at the end of the season separately for both plots. Ten 1 m² quadrats were sampled for each plot, positioned next to each GHG chamber ring. The first quadrat was located at a distance of 1 m from each GHG sampling collar, and the second was positioned 1 m from the first quadrat. All aboveground plant biomass collected from each quadrat was weighed. Winter rapeseed and weeds were weighed separately.

One representative model plant was collected randomly from each quadrat, giving a total of ten model plants per plot. For each model plant, a soil monolith was removed around the plant to 0.30 m depth, including the full root system of the winter rapeseed but also weed roots. The winter rapeseed plant root system and the bigger weed roots were separated and washed free from soil. The remaining soil with small weed roots was weighed, a 200 cm³ subsample taken and weighed, and another subsample was taken to estimate the dry matter content. Weed roots were washed out using a 0.5 mm sieve and sorted from the soil debris under the microscope. The DM of small weed roots per unit dry matter of a 200 cm³ subsample was included for biomass calculation after extrapolation. The winter rapeseed plant samples were processed and divided into three aboveground compartments (stems and branches, seedpods, and seeds) and three belowground compartments (tap or main root, coarse roots with ≥ 2 mm diameter, and fine roots with < 2 mm diameter). No undecomposed winter rapeseed leaves or flowers were identified, as leaf senescence had taken place long before seed maturity. For weeds, the above- and belowground parts were considered together.

All parts of the plants were dried at 70 °C until constant weight was achieved. The C and N contents were determined for each plant compartment. The C and N uptake per plant was calculated by multiplying the aboveground DM content per plant and compartment of the plant by the aboveground biomass C and N concentration of each plant and compartment (Aosaar et al. 2016). The total biomass C and N content was then extrapolated to the field scale.

Other gaseous N fluxes

The di-nitrogen (N₂) fluxes were estimated using the mass balance approach (Ammann et al. 2009) as the difference between all the measured or estimated N inputs (N input with mineral fertilizer, N input with slurry, and N deposition) and outputs (N₂O emissions, leaching N losses, NO_x and NH₃ emissions, and plant biomass N content) considering soil N change, as described in Eq. (2).

The NH₃ volatilization was estimated with the equations described in Sommer and Olesen (1991) and Sommer et al. (1991) (Supplementary Methodology S2). The obtained reference value of emissions was corrected to take into account the application procedure of the slurry in the soil (injection followed by rotary harrow) with a factor derived from Sommer and Hutchings (2001).

The NO_x emissions and N deposition for the period were obtained from regional budgets. Measurements from the three closest NitroEurope network stations to the experimental site (Lahemaa, Estonia; Vilsandi, Estonia; and Zosēni, Latvia) from Vet et al. (2014) were interpolated to obtain estimates of N deposition and NO_x emissions. The estimated values of N deposition were in agreement with the average of the sum of oxidized and reduced N for Estonia from Klein et al. (2016).

GPP

The GPP, defined as the total amount of C captured through photosynthesis in a given period, was calculated from the mass balance, as the difference between all C inputs (manure, CH₄ oxidation) and outputs (soil and plant respiration, leaching, and C in plant biomass) (Smith et al. 2020; Soussana et al. 2010).

Nitrogen-use efficiency (NUE)

Two different approaches were used for NUE calculation. We defined NUE_{crop} as the N content in seed yield per unit of N fertilizer input (Congreves et al. 2021; Oenema et al. 2015). We calculated NUE_{soil} according to Moll et al. (1982), as the production yield (seeds) per unit of available N in the soil. The DN value was used for the estimation of indigenous available N in the soil. This soil-based approach to

NUE calculation was chosen as it considers background (indigenous) soil N content (Congreves et al. 2021). The NUE_{soil} calculation can be divided into two different components: N uptake efficiency (NU_{pE}), which considers the amount of N available in the soil that is taken up by plants; and the N utilization efficiency (NU_{tE}), which is the amount of plant N that is used for seed production.

Statistical analysis

All statistical analysis was carried out in the R programming language (R Core Team 2016). Unless stated otherwise, the Mann–Whitney U test was used to compare treatments, and the correlation analysis values refer to the Spearman's rank correlation coefficient (ρ). Analysis of variance (ANOVA) followed by a post-hoc Tukey's HSD (honest significant difference) analysis was applied to find differences between monthly flux values. Statistical differences were considered significant at a level of $p < 0.05$. The Tukey's HSD test was performed with the package 'agricolae' in R (Mendiburu 2015). Results of the correlation analysis are included in the Supplementary Materials (Tables S1, S2, S3, and S4).

Results

GHG fluxes

The CO_2 flux showed an initial increase following the slurry incorporation (Fig. 1) and soil mixing, which enhanced the mineralization of the residues of the previous crop. In the final period (starting on May 2017), CO_2 emissions increased with higher temperatures and rapeseed plant growth. The N_2O emissions remained relatively stable except for the period following slurry application (0–40 days) and peaks in autumn (December 2016) and spring (second half of March 2017), caused by the freeze–thaw process. The CH_4 fluxes remained negative throughout almost the whole period, with a slightly higher soil CH_4 -C oxidation in the control plot. There were no significant differences in cumulative emissions during the full study period between plots for any of the measured GHG fluxes (Fig. 1).

Excluding the fluxes measured during the first 40 days of the experiment (which include the expected effect of the manure application), higher N_2O fluxes were only measured at soil temperatures between 0 and 2 °C, independently of the WFPS (Fig. 2).

When all fluxes were converted to CO_2 -eq ha^{-1} and the C input with GPP was considered, the field was found to be a net C sink, with an average balance for both plots of 34,571 kg CO_2 -eq ha^{-1} (Table 1). However, N_2O emissions counteracted almost a third of the global warming mitigation of the CO_2 balance and CH_4 oxidation by soils, with an average N_2O emission of 11,218 CO_2 -eq ha^{-1} .

Leaching

The total amount of leachate was 605 and 597 $\text{L m}^{-2} \text{yr}^{-1}$ for the control and treatment plots, respectively, and was mainly driven by precipitation and the evapotranspiration of the growing rapeseed plants and weeds. Cumulative losses through leaching were similar between the plots for total C, but differed for total N (Fig. 3. Daily (left) and cumulative (right) C and N losses through leaching (kg ha^{-1}). Error bars represent standard error), with higher losses observed in the control plot. The total amount of N loss through leaching was significantly higher ($p < 0.001$) in the control plot than in the treatment plot, with values of 54.3 ± 7.03 and 34.5 ± 3.70 kg ha^{-1} , respectively. The total amount of leachate was similar for both plots, but the total N content in leachate was 16.3% higher in the control plot. Although the NH_4^+ -N content in the leachate was not significantly different through the year between plots, the leachate NO_3^- -N content in the treatment plot was 15.6% lower than that in the control plot ($p = 0.023$).

Biomass production

Total rapeseed dry biomass was 13,202 and 14,070 kg ha^{-1} for the treatment and control plots, respectively, with 48.32% and 1.98% of C and N for the control plot, respectively, and 49.11% and 2.19% for the treatment plot. The plant density was 6.90 and 10.56 plants m^{-2} for the control and treatment plots, respectively. No significant differences were found in the distribution of total biomass, C or N content between the two plots within each plant part.

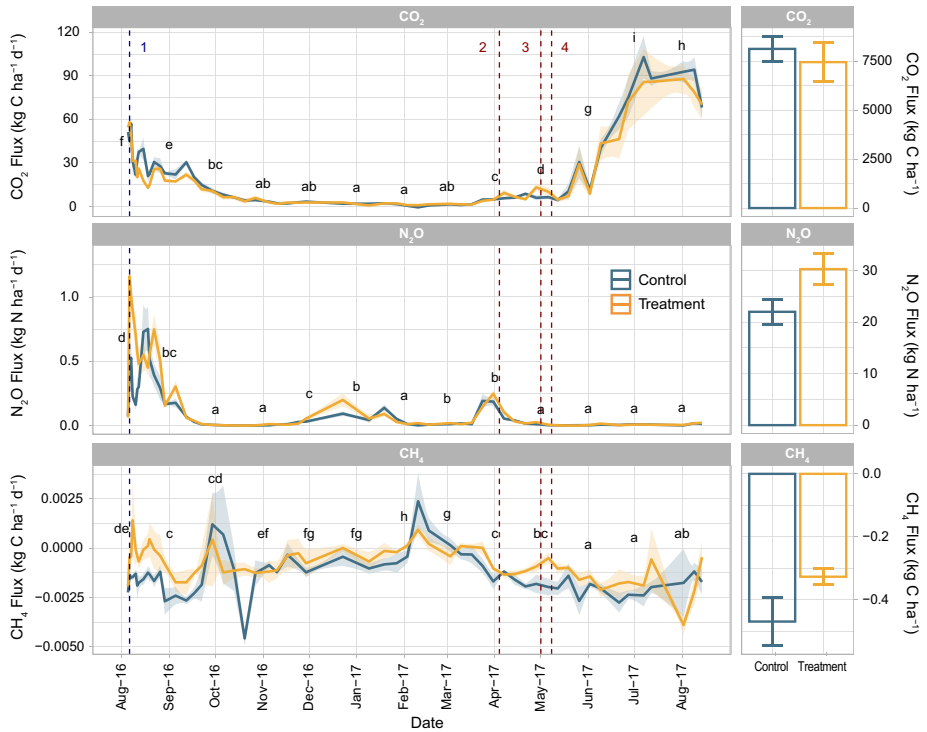


Fig. 1 Daily (left) and cumulative (right) fluxes of CO₂-C, N₂O-N, and CH₄-C (kg ha⁻¹) from control and treatment plots during the experimental period. Shaded areas and error bars represent standard error. 1: slurry application; 2: calcium

ammonium nitrate (CAN) application; 3 and 4: ammonium sulphate nitrate (ASN) application. Different letters indicate significant differences in flux values between different months according to a post-hoc Tukey HSD test ($\alpha=0.05$)

The C was similarly distributed among the different plant parts, whereas N was predominantly found in the seeds (Fig. 4. Total plant dry biomass and total C (Ctot) and N (Ntot) in the different rapeseed plant pools (kg ha⁻¹); Table S5). Final seedpod and seed weight represented 64% and 55% of the total plant weight, for the treatment and control plot, respectively. Seed yield was 5365 and 4959 t ha⁻¹ for treatment and control plot, respectively. Seeds represented 41% and 35% of the total weight of the plant for the control and treatment plot, respectively, while the N content in seeds was 71% and 70% of the total plant N content, respectively. No leaves were collected from the rapeseed plants. In addition, the undecomposed

litter content in the soil was negligible. No significant differences were found in the weight or the C and N contents for any of the plant compartments between the control and treatment plots.

The total weight of weed biomass was approximately 20 and 40 times smaller than the weight of rapeseed plant biomass for the treatment plot (657 kg ha⁻¹) and control plot (368 kg ha⁻¹), respectively, but the proportions of total C (268 and 151 kg C ha⁻¹, respectively) and total N (16.2 and 8.1 kg N ha⁻¹, respectively) were similar to those from rapeseed plants.

Fig. 2 N₂O-N flux (daily value per plot) depending on soil temperature (at a 0.05 m depth) for three water-filled pore space (WFPS) intervals (25–50%, 50–75%, and 75–100%). Error bars represent standard error values. Black color indicates fluxes measured during the first 40 days of the experiment (expected effect of slurry application)

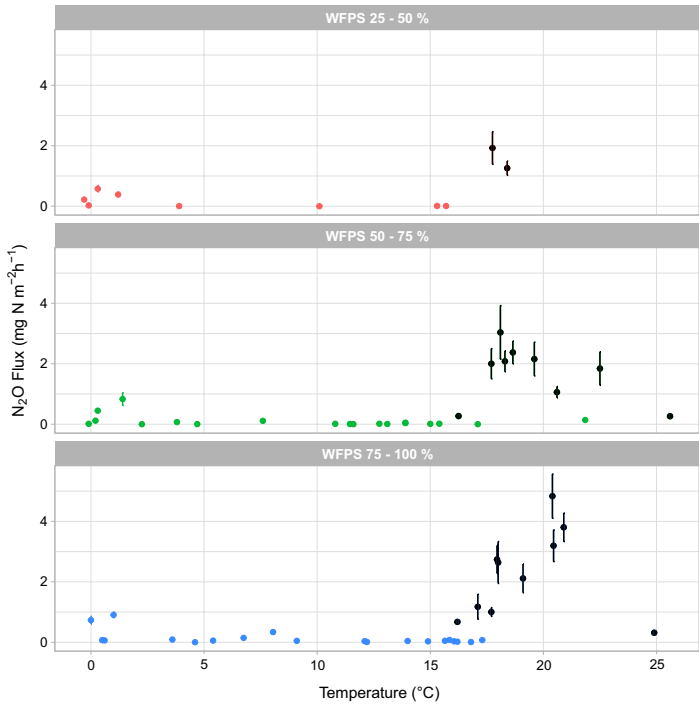


Table 1 Cumulative CO₂, N₂O, and CH₄ emissions for the studied period

GPP gross primary production; R_{ECCO} ecosystem respiration; GWP over a 100-year period: [†]273, [‡]27.9 (IPCC 2021)

	Cumulative emissions (kg ha ⁻¹)				Cumulative emissions (kg CO ₂ -eq ha ⁻¹)			
	CO ₂ -C	N ₂ O-N	CH ₄ -C	GPP	R _{ECCO}	R _{ECCO} -GPP	N ₂ O [†]	CH ₄ [‡]
Control	8124.12	22.00	-0.47	17,185	29,788	-33,223	9440	-17.48
Treatment	7448.18	30.29	-0.33	17,244	27,310	-35,918	12,996	-12.17
Average for both plots	7786.15	26.15	-0.40	17,215	28,549	-34,571	11,218	-14.83

Seed NUE and field N balance

The values of NUE_{crop} were very similar for both plots and were both above 1 (1.30 and 1.34 for control and treatment, respectively) when considering the entire harvest (seeds and harvested crop residues). NUE_{soil} was higher for the control than for the treatment plot (45 and 40%), with a higher NUpE by plants (63% and 57%, for the control and treatment

plots, respectively) and a slightly lower NUtE in the treatment plot (72% and 70%).

The total N input with fertilization to the field was 215.0 kg N ha⁻¹ (64.3 kg N ha⁻¹ as manure and 150.7 kg N ha⁻¹ as fertilization), while average N output with harvested rapeseed seeds was 202 kg N ha⁻¹, with a final field N balance between input with fertilization and output with harvest of 13.0 kg ha⁻¹. The N recovery was 0.94 kg N in crop harvest (seeds) per

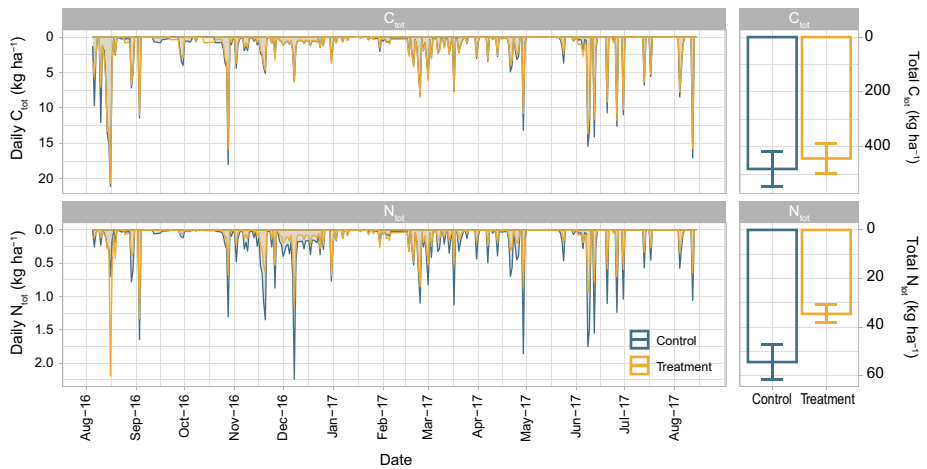


Fig. 3 Daily (left) and cumulative (right) C and N losses through leaching (kg ha^{-1}). Error bars represent standard error values

kg of applied N with fertilization, (0.91 and 0.97 for control and treatment plots, respectively).

Ecosystem C and N balance

The estimated mean soil C pool change during the considered period, as the difference between the initial and the final situation, was $3135 \text{ kg C ha}^{-1}$, representing an increase of 2.2% of the initial value, whereas the mean soil N pool decreased by 819 kg N ha^{-1} , a loss of 5.8% of the initial soil N content (Table S6).

Photosynthetically captured $\text{CO}_2\text{-C}$ by the rape-seed plants ($17,185$ and $17,244 \text{ kg C ha}^{-1} \text{ yr}^{-1}$ for the control and treatment plots, respectively) and weeds surpassed the C captured through NPP (6949 and $6752 \text{ kg C ha}^{-1} \text{ yr}^{-1}$ for the control and treatment plots, respectively) (Table 2). At the field scale, considering the change in soil C content and the incorporation of plant residues (roots) after harvest, the C balance was positive, resulting in an input for the control and treatment plot of 2872 and $3860 \text{ kg ha}^{-1} \text{ yr}^{-1}$. If the entirety of the crop residues had been incorporated into the soil, the C balance would have been

6766 and $7292 \text{ kg ha}^{-1} \text{ yr}^{-1}$ for the control and treatment plot, respectively.

The N inputs were limited to N application with the organic and synthetic fertilizer, and N deposition. The highest measured fluxes were the N in plants (287 and $305 \text{ kg ha}^{-1} \text{ yr}^{-1}$ for control and treatment plots, respectively), whereas the remaining fluxes, including N_2O emissions, were considerably smaller (Table 2). The difference in the N mass balance (661 and $676 \text{ kg N ha}^{-1} \text{ yr}^{-1}$, for control and treatment plots, respectively) was attributed to N_2 emissions. At the field scale, considering the incorporation of plant residues and the change in soil N content, the N balance remained negative, and the total soil N losses for the control and treatment plots were 804 and $825 \text{ kg N ha}^{-1} \text{ yr}^{-1}$, respectively.

Discussion

Evolution of the GHG fluxes during the measurement period

The CO_2 fluxes behaved as expected and were mainly controlled by soil respiration and plant growth. As expected, CO_2 emissions were strongly correlated with soil temperature for both plots ($\rho=0.818$,

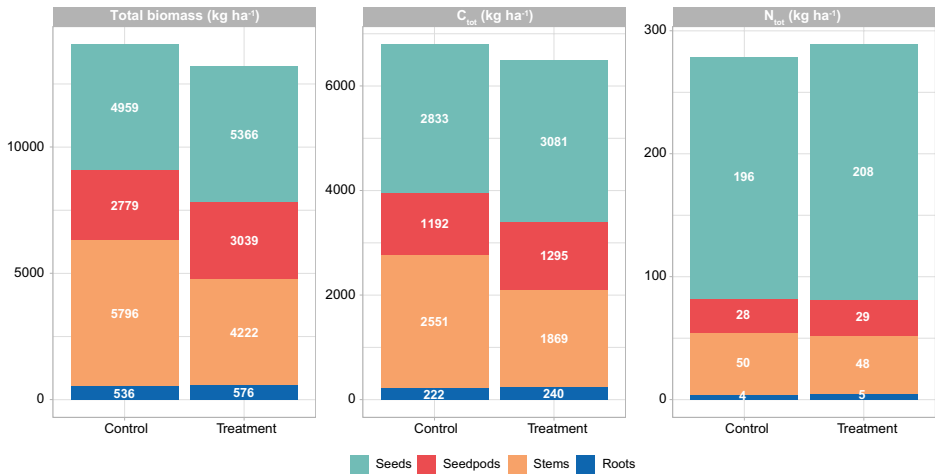


Fig. 4 Total plant dry biomass and total C (C_{tot}) and N (N_{tot}) in the different rapeseed plant pools (kg ha⁻¹)

$p < 0.001$ and $\rho = 0.883$, $p < 0.001$ for the control and treatment plots, respectively; Table S1). The increase in CO_2 emissions with temperature was related to enhanced soil respiration (Lloyd and Taylor 1994) and, most importantly, to rapeseed plant growth, which peaked in summer with maximum plant development and decreased as plants started to dry before harvest (Béziat et al. 2009). Atmospheric carbon sequestration by CH_4 oxidation in soils was slightly higher during warmer periods, but the overall CH_4 -C sequestration was low compared with the soil and plant respiration, which is common for agricultural soils (Smith and Conen 2004).

Significant emissions of N_2O were only measured after the application of the slurry and during two periods with temperatures between 0 and 2 °C (Figs. 1, 2), indicating that the N_2O was likely produced and/or released during freeze-thaw cycles. The maximum values of soil N_2O fluxes measured after slurry application ($\sim 6 \text{ mg m}^{-2} \text{ h}^{-1}$ for the treatment plot) are very similar to those reported by Herr et al. (2020) in the first year of an experiment with slurry applied by injection. The huge N_2O emissions after slurry application were attributed to a peak in denitrifying activity caused by a combination of intense precipitation after a relatively dry period resulting in soil rewetting, enhanced C availability from slurry

and crop residue mineralization, and NH_4^+ addition with slurry (Escuer-Gatius et al. 2020). The N_2O emissions from the first 50 days represented 57.94% and 62.68% of the total emissions for the control and treatment plot, respectively. No significant differences were detected in N_2O flux during the initial period after mixing of the slurry with or without nitrification inhibitor (Escuer-Gatius et al. 2020).

Especially interesting are the N_2O fluxes measured in December of 2016 and on the second half of March and April of 2017 (Fig. 1), which occurred during a period of low but positive soil temperatures (0–2 °C) that followed a period dominated by negative temperatures (Figure S2). These fluxes, reaching values of approximately $1 \text{ mg m}^{-2} \text{ h}^{-1}$, are most likely the result of freeze-thaw processes. Freeze-thaw is known to have a significant effect on N_2O emissions from croplands (Saggar et al. 2013; Wagner-Riddle et al. 2017), with notable emissions even at temperatures close to zero (Flessa et al. 1995; Pärn et al. 2018). Two main hypotheses have been given to explain freeze-thaw fluxes: release of physically trapped N_2O under and/or within frozen surface layers, and emission of newly produced N_2O at the onset of thaw (Ejack and Whalen 2021; Risk et al. 2013). Newly produced N_2O is usually attributed to denitrification triggered by the changes in physical and chemical soil

Table 2 Annual ecosystem carbon and nitrogen balance (kg ha⁻¹ yr⁻¹)

Flux	C			N		
	(kg C ha ⁻¹ yr ⁻¹)			(kg N ha ⁻¹ yr ⁻¹)		
	Control	Treatment	Average	Control	Treatment	Average
CH ₄ oxidation	0.47 ± 0.07	0.33 ± 0.02	0.40 ± 0.045			
Ecosystem respiration (R _{ECO} : CO ₂ emissions)	-8124 ± 650	-7448 ± 1010	-7786 ± 830			
N ₂ O emissions				-22.0 ± 2.44	-30.3 ± 2.98	-26.15 ± 2.71
Leaching	-481 ± 64	-443 ± 54	-462 ± 59	-54.3 ± 7.03	-34.5 ± 3.70	-44.4 ± 5.37
Slurry	1019	1019	1019	64.32	64.32	64.32
Mineral fertilizer				150.7	150.7	150.7
Plant sequestration	-6949 ± 1121	-6752 ± 903	-6851 ± 1012			
<i>Seeds</i>	<i>-2833 ± 498</i>	<i>-3081 ± 403</i>	<i>-2957 ± 313</i>			
<i>Crop residues and weeds</i>	<i>-4116 ± 636</i>	<i>-3671 ± 500</i>	<i>-3894 ± 568</i>			
N in plant biomass				-287 ± 49	-305 ± 51	-296 ± 50
<i>Seeds</i>				<i>-196 ± 33</i>	<i>-208 ± 27</i>	<i>-202 ± 21</i>
<i>Crop residues and weeds</i>				<i>-91 ± 16</i>	<i>-97 ± 23</i>	<i>-94 ± 15</i>
N ₂ emissions				-661	-676	-668
N depositions				5.5	5.5	5.5
NH ₃ -N emissions				-1.7	-1.7	-1.7
NO _x -N emissions				-3	-3	-3
GPP	17,185	17,244	17,214			
Soil change	2650	3620	3135	-809	-830	-819.5
Ecosystem/Field change	3860	2872	3366	-804	-825	-815

An additional breakdown 'Seeds' and 'Crop residues and weeds' is provided (in italics) but note that these data are already included in 'Plant sequestration' and 'N in plant biomass'

conditions produced by thaw onset and the sudden increase in biological activity (Flessa et al. 1995; Risk et al. 2013). A notable proportion of the N₂ emissions estimated from the mass balance method could have in fact originated during these freeze-thaw events and not only from the period following organic fertilization (Wu et al. 2020).

No noticeable peaks were detected after mineral fertilization. The higher fluxes measured at the end of March and beginning of April can be attributed to freeze-thaw and not to mineral fertilization, as the highest peak of emissions for this period was measured on March 31, several days before the first mineral fertilization took place (April 4). However, mineral fertilization could have partially contributed to prolonging the emissions from the freeze-thaw event, and may be partly responsible for the emissions measured during April 4–28. The combination of several mechanisms could explain the absence of emission

peaks caused by mineral fertilization as opposed to those observed with organic fertilization: (i) the lack of soil disturbance; (ii) the absence of changes in soil moisture or increases in soil labile C upon addition of mineral fertilizer; (iii) no re-wetting effect from precipitation in the moment of mineral fertilization; and (iv) uptake from the small plants present at the times of synthetic fertilization application, which were not present when organic fertilizer was applied.

The annual N₂O fluxes presented here are much higher than those estimated for Estonia or the Baltic countries for rapeseed crops (Astover et al. 2015; Fridrihsone et al. 2018; Fridrihsone et al. 2020). They are also 2–3 times higher than those measured for winter rapeseed in several different sites across Germany (Ruser et al. 2017), and 3–4 times higher than those estimated for different sites across Europe (Walter et al. 2014) and Finland (Regina et al. 2013). The main factor differentiating our study is most

likely the high soil N content of the field. However, it is known that soil N surplus is common in the European Union (Huygens et al. 2020; van Grinsven et al. 2012), and that over-fertilization and a low efficiency in the use of manure are frequent in the Baltic Sea region (McCrackin et al. 2018). This suggests that the situation presented here is not uncommon. Therefore, a special focus should be put on reducing N use in such agro-ecosystems, especially in the form of manure. The weather conditions at key moments (such as at the time of slurry application) could also partly explain the high N₂O fluxes.

Considering the entire balance, the field was a net C sink, mainly resulting from the R_{ECCO}-GPP balance, with negligible CH₄ flux. Accumulation of C from CO₂ capture in photosynthesis by crops is common, although the positive effect of CO₂ sequestration is reduced by harvest removal (Maas et al. 2013). Winter rapeseed acting as a net C sink was also reported by Béziat et al. (2009). However, almost a third of this global warming mitigation benefit was counteracted by N₂O emissions when all GHG fluxes were converted to CO₂-eq by adjustment with GWP (Table 1). On average, 57% of N₂O emissions were measured in the 40 days after slurry application. This highlights the role of organic fertilization in the total GHG emissions from croplands, and the potential to tackle emissions through appropriate changes to fertilizer management. Lessard et al. (1996) found that during a 270 day growing season, 67% of N₂O was emitted in the first 7 weeks after manure application. Moreover, Li et al. (2012) reported that 60% of the total N₂O emissions during a year were emitted during the first 3–5 days after fertilizer application. These high emissions are aggravated by the lack of synchrony between slurry application and crop demand, resulting in the majority of the N being lost before plants can make use of it (Gomes et al. 2009; Hansen et al. 2019); however, plant uptake was insufficient to mitigate the gaseous losses due to the soil high N content (Giweta et al. 2017). This puts into question fertilization management practices in winter crops, when crops are too small to make much use of the nutrients incorporated into the soil (Crews and Peoples 2005).

Correlation analyses of fluxes and leachate chemical parameters suggest different patterns for the control and treatment plots, to which the nitrification inhibitor had been applied. The N₂O correlated positively with NO₃⁻-N content in leachate ($\rho=0.954$,

$p<0.001$) for the treatment plot; however, there was no significant correlation with NH₄⁺ content (Table S4). In contrast, for the control plot, there was a positive correlation with NH₄⁺ content and a significant negative correlation with NO₃⁻ content in leachate ($\rho=0.266$, $p<0.05$; $\rho=-0.544$, $p<0.001$). A significant negative correlation was also found for N₂O flux and NO₃⁻ content in soil in the control plot ($\rho=-0.429$, $p<0.01$; Table S3). This may indicate that the fluxes in the treatment plot were predominantly determined by denitrification, whereas they were mostly driven by nitrification in the control plot. This is consistent with the conclusions of Escuer-Gatius et al. (2020) regarding the different levels of importance of nitrification and denitrification in the control and treatment plots.

Leaching losses during the growing season

The total amount of N loss through leaching (54.3 ± 7.03 and 34.5 ± 3.70 kg ha⁻¹ yr⁻¹ for the control and treatment plots, respectively) was in the range of commonly reported values (12–75 kg N ha⁻¹; Sainju 2017). The values of N leaching were significantly different between plots ($p<0.001$); however, there was no difference in the total amount of leachate, indicating that the difference was a consequence of different N contents in the leachate. Although the leachate NH₄⁺-N content was not significantly different between plots, the NO₃⁻-N content was significantly higher in the control plot than in the treatment plot ($p=0.023$). This represents a reduction in total N loss through leaching of 36%, and could be related to the nitrification inhibition activity of DMPP and resulting in the 16% lower average leachate NO₃⁻ content in the treatment plot. This is in accordance with the results of Quemada et al. (2013), who reported an average reduction of 17% of the nitrate leaching after NI application, but much smaller than the 57% reduction reported by Yang et al. (2016) for DMPP. Although no differences were found in the period immediately after the application of the slurry nor in the cumulative N₂O emissions for the whole growing season, the DMPP application can explain the lower leachate NO₃⁻ concentration and thus the final smaller N losses through leaching in the treatment plot. DMPP may have reduced nitrification but this did not affect denitrification, which is assumed to be the source of most of the measured N₂O emissions,

if NO_3^- availability is not limiting. Nair et al. (2020) reported the opposite results: a reduction of N_2O emission with no reduction of NO_3^- leaching. Thers et al. (2019) reported an increase of soil NH_4^+ content with the application of DMPP but no significant difference in N_2O emissions, although the increase of NH_4^+ did not translate into a decrease of NO_3^- . The lack of similar results could be due to the limited number of long-term studies with DMPP considering both N_2O emissions and NO_3^- leaching, especially in a N-rich agro-ecosystem like the one studied here.

Leaching losses may have been underestimated as we could not take leachate samples when the ends of the drainage pipes were covered by water during the intense precipitation event that followed the slurry application (leaching samples were collected during the first 10 days immediately after slurry application, but sampling was then not possible for approximately two weeks after that), when important nutrient losses through leaching are likely to have occurred.

Biomass production

Rapeseed seed yield (5162 kg ha^{-1}) was more than double the average production for Estonia (2356 kg ha^{-1} for the period 2014–2018; Statistics Estonia, 2019), but within the range observed in previous research (Assefa et al. 2018; Begna et al. 2017; O'Neill et al. 2021; Ratajczak et al. 2017). Although the density (6.90 and $10.56 \text{ plants m}^{-2}$ for the control and treatment plot, respectively) was much lower than considered optimal ($60\text{--}80 \text{ plants m}^{-2}$), much lower densities are required by hybrids (Rathke et al., 2006), such as DK Sequoia (Carruthers et al. 2017). However, a lower plant density can be compensated by a larger leaf area and a higher number of pods per plant, leading to similar seed yields (Mendham et al. 1981). This explains the similar biomass in both plots (Fig. 4) despite the differences in plant density. Final seedpod and seed weight represented 63.6% and 55.0% of the total plant weight for the treatment and control plot, respectively, which is in accordance with previous studies (Malagoli et al. 2005). This was partly due to the transfer of N to the pods from other plant parts, especially from leaves. No leaves were collected at the end of the season, as a consequence of leaf senescence, which usually begins with flowering. During leaf senescence, nutrients are reallocated to stems and afterwards to pods and seeds,

with photosynthesis still taking place in stems and pods (Béziat et al. 2009; Bouchet et al. 2016). Early leaf senescence results in leaf litter being completely decomposed by harvesting time.

The small size of roots was most likely a consequence of the high nutrient availability in the soil, especially the high N content, requiring a smaller soil volume exploration by roots (Bouchet et al. 2016). It may also relate to special characteristics of the cultivar (Bouchet et al. 2016). The high nutrient availability can also explain the high seed yield of the field.

There were no significant differences in plant production between the control and treatment plots. This was probably because soil N was not a limiting factor for plant growth and crop yield (Herr et al. 2020; McCormick et al. 1984).

High carbon sequestration by the rapeseed crop

The field was a net sink of C, even after removal of the seeds with the harvest. This was a consequence of the high GPP of the rapeseed plants that surpassed CO_2 emissions and C losses through leaching. However, this positive balance could be partly counteracted by the enhanced CO_2 emissions from mineralization of crop residues left in the field after harvesting (Lee et al. 2007), which can lead to high emissions from rapeseed crop residues (Stegarescu et al. 2020). Stegarescu et al. (2020) estimated in a pot experiment that more than 40% of the carbon incorporated into the soil with rapeseed crop residues was lost in a 105 day period. This means that more than 90 kg C ha^{-1} on average could be lost as CO_2 emissions during the first few months after harvest. Likewise, the presence of non-mineralized C in the crop residues from the previous season in the soil at the beginning of the study could have also resulted in an overestimation of GPP as a result of the use of the mass balance approach.

High N losses from gaseous emissions

The contents of the soil N pool (initial and final N content of 14,135 and $13,317 \text{ kg N ha}^{-1}$, respectively; Table S6) were above the typical range ($2000\text{--}12,000 \text{ kg N ha}^{-1}$) (Cameron et al. 2013). This could be the result of the repeated slurry application over the years (Webb et al. 2013), but also because the sowing of grassland mix in the previous year

contained N-fixing species (15% *T. pratense* and 5% *T. repens*).

The highest flux in the N balance were N_2 emissions estimated with the mass balance approach, although this value has to be taken carefully as the mass balance calculation may be biased by the estimation of the initial and final soil N contents. However, this is in accordance with the conclusions of Velthof et al. (2007), stating that N_2 emissions from denitrification are the largest N source from agroecosystems in Europe. The high measured N_2O and estimated N_2 emissions are likely to have been related to both field and meteorological conditions (high WFPS, available C from slurry and NO_3^- in soil from nitrification of the slurry NH_4^+) during and immediately after slurry application, resulting in high denitrification levels (Escuer-Gatius et al. 2020). The crop residues present in the soil at the beginning of the experiment were probably mineralized relatively rapidly after slurry application as a result of ploughing and the associated increase of soil moisture. The slurry application promoted mineralization (Maidl and Fischbeck 1989) during periods without vegetation cover. This contributed to the high losses through gaseous N emissions and leaching. The high precipitation, combined with the slurry application and mineralization of the crop residues, explains the high initial N emissions, both as N_2 and N_2O (Chen et al. 2014; Dobbie and Smith 2003; Saggar et al. 2013; Smith et al. 1999).

Overall, the N applied with slurry was not available to plants due to the asynchrony of N organic fertilization and plant uptake, combined with large and rapid losses from gaseous emissions and leaching (Table 2). Gaseous losses were especially intense following slurry application when the plants had yet not germinated (germination started on August 22, 2016) or their root system was very small, limiting plant uptake. Shifting to a spring rapeseed cultivar would avoid the losses in the fall period (AEAT 1998), reducing emissions per hectare (Fridrihsone et al. 2018), although it could increase emissions per tonne of harvest (Fridrihsone et al. 2020). In contrast, plants could benefit from mineral fertilizer application in May in three different applications in smaller amounts and at short intervals. The rest of the annual requirement by plants was covered by net N mineralization. With the high initial soil N pool, the applied fertilization may have been excessive; however,

NUE_{soil} values may indicate reasonable N management because of the high N losses after slurry application, whereas other parameters indicate quite the opposite. However, this approach does not consider N mineralization occurring in the soil during the season. Conversely, NUE_{crop} indicates a net removal of N, with a value > 1 (Congreves et al. 2021), which may be interpreted as relating to insufficient N fertilization. Therefore, these approaches for NUE calculation are probably not a valid measure of fertilization effectiveness in this scenario of high soil N initial content, and other approaches to calculate NUE could be more suitable in these conditions (Congreves et al. 2021).

Harvest, considering only seeds, represented 19% of total N input (including soil N change). When harvest also included the harvested aboveground plant biomass, this percentage increased to 28%, which is still a low N recovery rate (Galloway and Cowling 2002; Lal and Stewart 2018; Liu et al. 2016; Prasad and Hobbs 2018). It has already been proposed that plants do not directly benefit from N application with slurry, but this management mainly leads to refilling of soil N stocks (Schlingmann et al. 2020). However, this potential refilling is limited by high N losses after slurry application, and may be insufficient to maintain soil N stocks (Schlingmann et al. 2020), explaining the negative soil N balance in our study and confirming the abovementioned inefficacies of the current slurry management.

The average emission factor (EF) for both plots was 0.12 kg N_2O-N kg N applied⁻¹ (0.10 and 0.14 kg N_2O-N kg N applied⁻¹ for the control and treatment plot, respectively). This estimated EF is more than 10 times the Tier 1 value from IPCC (2019) (0.01), and almost 20 times the average value proposed by Mathivanan et al. (2021) (0.0066). These high emissions took place mostly in the first weeks after the slurry application and are attributable to high denitrification rates resulting from the combination of high initial soil N content, the slurry application, rewetting of the soil due to intensive rain, mineralization of crop residues, and soil mixing in the moment of slurry application (Escuer-Gatius et al. 2020).

The ratio between the calculated N_2 losses from the mass balance and the measured N_2O emissions is 30 and 22 for control and treatment plot, respectively. Weier et al. (1993) reported $N_2:N_2O$ ratios between 0 and 549 for soils with pH between 6.5 and 7.4, whereas Dannenmann et al. (2008) reported values

of $N_2:N_2O$ ratio between 21 and 220 for pH ranging between 6.3 and 7.3. Considering the acidity of the studied soil (pH 4.75–4.76), we expect the $N_2:N_2O$ ratio for the field to be in the lower part of the range because of the sensitivity of N_2O -reductase to low pH (Baggs et al. 2010). Simek and Cooper (2002) stated that the lower $N_2:N_2O$ ratio attributed to soils with low pH could be caused by lower organic C and mineral N availability for the denitrifying organisms under acid conditions rather than a direct effect on denitrification enzymes at low pH. If this were true, a lower $N_2:N_2O$ ratio would not be expected for the study field.

The estimated NH_3 volatilization was 1.7 kg N ha^{-1} , which represents 2.69% of the N applied with slurry. This value is at the lower end of the expected range of 2–35% (Sainju 2017). The low estimation is also the result of applying a correction factor considering the application method (injection followed by rotary harrow). The application method is a key factor determining NH_3 emissions after slurry application (Herr et al. 2020; Sommer and Hutchings 2001; Webb et al. 2010). Moreover, Thompson and Meisinger (2002) reported reductions in NH_3 emissions of 85% and 96% in two studies following the immediate incorporation by harrowing. This low estimation is also reasonable considering the environmental conditions at the moment of application, as rain increases infiltration into the soil and limits volatilization (Sommer et al. 2003).

Although NO emissions can be relevant at lower soil WFPS, reaching the same magnitude or even bigger than that of N_2O emissions, given the high WFPS in our study in the weeks after slurry application (Fig. S3), NO emissions should not have been especially high (Meixner and Yang 2006; Oswald et al. 2013). Nitrogen is mostly emitted as NO at $WFPS < 30\%$ –60% while N_2O and N_2 are the main N-related emissions at $WFPS > 60\%$ –65% (Medinets et al. 2015). Moreover, the WFPS during these weeks suggests that nitrous acid (HONO) emissions would have been negligible (Oswald et al. 2013). By applying the EF for organic fertilization and temperate climate from the meta-analysis by Liu et al. (2017), we obtained an estimated NO emission of $0.42 \text{ kg N ha}^{-1}$ (CI: 0.37–1.84) for organic fertilization, and $2.73 \text{ kg N ha}^{-1}$ (CI: 1.10–2.37) for synthetic fertilization, with a total estimated NO emission of 3.15 kg ha^{-1} from fertilization. From average values

of EF suggested by Skiba et al. (2020) for croplands we obtained 0.76 and $2.52 \text{ kg N ha}^{-1}$ for the manure and the synthetic fertilizer application, respectively, and a total of $3.28 \text{ kg N ha}^{-1}$. Both values are only slightly higher than the value estimated from the NitroEurope data (3 kg N ha^{-1}). However, these reference EF values may not be relevant for the studied site because of the unusually high N content.

The underestimation of the NO flux would have resulted in an overestimation of the N_2 flux. Considering similar potential maximum values for NO and N_2O flux (Davidson 1991; Davidson et al. 2000), which was highly unlikely here, the underestimation of the NO flux would have resulted in a maximum overestimation of the N_2 flux by 3.4% and 5.1% for the control and treatment plot, respectively.

Limitations and potential improvements of the proposed methodologies

The use of the mass balance approach for flux estimation, as in the case of N_2 and GPP, is sensitive to the bias in the estimation of the other fluxes involved in the balance, and this is particularly important in the case of the biggest fluxes. Correspondingly, the estimation of the N_2 flux was highly conditioned by the calculation of soil N change, and a bias in the initial or final N soil content analyses would have caused a bias in the N_2 estimation. The choice of soil depth is also crucial, and the common 0.2 m depth may not always be appropriate. The same can be said for the soil depth used for the soil water content change in the soil water balance.

In general, a higher spatial and temporal frequency of measurements of the fluxes and pools would increase the reliability of the output values, but this entails a direct increase of cost, which is frequently the most limiting factor. A bias from the effect of temperature must be considered, as measurements were carried out exclusively during daytime. The effect of temperature should have been especially important for soil respiration (Lloyd and Taylor 1994), but soil respiration was only a small part of the total ecosystem respiration. The use of automated chambers for GHG flux measurement would provide a more complete profile of daily fluxes, capturing day–night variations. In addition, the use of transparent chambers would allow direct GPP measurements.

Leachate sampling from the end of drainage pipes, where a drainage system is located in the field, is a non-expensive option, but the source area of the leachate should always be considered. The distribution and condition of the drainage system, as well as the homogeneity of the field, will be key factors determining the suitability of this approach.

Overall, the combination of methodologies proposed in this study can be adapted to any field study in which GHG fluxes, leachate data, soil analysis, and meteorological data are available, and anthropogenic inputs and outputs are known.

Conclusion

In this study, we assembled a series of different methodologies, which together allowed us to calculate all relevant fluxes and pools in the C and N cycles. Differences in the fluxes obtained in the present study with values from previous studies or statistics (e.g., high yield compared to national average, high N losses from gaseous emissions and leaching, or small root size) can be attributed to field characteristics (e.g., large soil N content) or weather conditions (e.g., rain event in the moment of slurry application).

In the study field, CO₂ emissions were the main source of GHG emissions, but they were surpassed by CO₂ fixed through photosynthesis. Thus the field was a net sink of C because of the high C fixation rate through GPP, although a part of the sequestered C would be lost with the mineralization of the remaining crop residues. Estimated N₂ emissions from the mass balance were the highest N flux, surpassing the N removal through seed harvest. Nitrogen losses caused by N₂ and N₂O emissions and leaching resulted in a decrease in the soil N content. The N₂O emissions were a major source of GHG emissions, especially in the weeks after organic fertilization, partially counteracting field C sequestration, and stressing the need for mitigation of N₂O emissions. When GHG fluxes were converted to CO₂-eq, the positive balance of CO₂ emissions remained the dominant flux, but N₂O emissions were also notable.

Acknowledgements The authors would like to thank the editor and the anonymous reviewers for their valuable suggestions and comments, which helped to significantly improve the manuscript. This research was funded by the Estonian Research Council (the IUT2–16, PRG352, and MOBERC20 Grants) and

the EU through the European Regional Development Fund (Centre of Excellence EcolChange, Estonia).

References

- AEAT (1998) Options to reduce nitrous oxide emissions (Final report). AEAT-4180. directorate-general of the environment, nuclear safety, and protection (European Union), Brussels, Belgium
- Allen RG, Pereira LS, Raes D, Smith M (1998) Crop evapotranspiration - guidelines for computing crop water requirements. FAO, Rome, Italy
- Allison FE (1973) Soil organic matter and its role in crop production. Elsevier, Amsterdam, The Netherlands
- Ammann C, Spirig C, Leifeld J, Nefel A (2009) Assessment of the nitrogen and carbon budget of two managed temperate grassland fields. *Agr Ecosyst Environ* 133:150–162. <https://doi.org/10.1016/j.agee.2009.05.006>
- AOAC (1990) Official Methods of Analysis (15th Edn). Washington, DC, USA: Association of Official Analytical Chemists
- Aosaar J, Mander Ü, Varik M, Becker H, Morozov G, Maddison M et al (2016) Biomass production and nitrogen balance of naturally afforested silver birch (*Betula pendula* Roth.) stand in Estonia. *Silva Fenn.* <https://doi.org/10.14214/sf.1628>
- Arregui LM, Quemada M (2006) Drainage and nitrate leaching in a crop rotation under different N-fertilizer strategies: application of capacitance probes. *Plant Soil* 288:57–69. <https://doi.org/10.1007/s11104-006-9064-9>
- Assefa Y, Prasad PVV, Foster C, Wright Y, Young S, Bradley P et al (2018) Major management factors determining spring and winter canola yield in North America. *Crop Sci* 58:1–16. <https://doi.org/10.2135/cropsci2017.02.0079>
- Astover A, Shanskiy M, Lauringson E (2015) Development and application of the methodology for the calculation of average greenhouse gas emissions from the cultivation of rapeseed, wheat, rye, barley and triticale in Estonia. Ministry of the Environment of the Republic of Estonia, Tartu, Estonia
- Baggs EM, Smales CL, Bateman EJ (2010) Changing pH shifts the microbial source as well as the magnitude of N₂O emission from soil. *Biol Fertil Soils* 46:793–805. <https://doi.org/10.1007/s00374-010-0484-6>
- Begna S, Angadi S, Stamm M, Mesbah A (2017) Winter canola: a potential dual-purpose crop for the United States southern great plains. *Agron J* 109:2508–2520. <https://doi.org/10.2134/agronj2017.02.0093>
- Béziat P, Ceschia E, Dedieu G (2009) Carbon balance of a three crop succession over two cropland sites in South West France. *Agric Meteorol* 149:1628–1645. <https://doi.org/10.1016/j.agrformet.2009.05.004>
- Bouchet A-S, Laperche A, Bissuel-Belaygue C, Snowdon R, Nesi N, Stahl A (2016) Nitrogen use efficiency in rapeseed. A review. *Agron Sustain Dev.* <https://doi.org/10.1007/s13593-016-0371-0>

- Bouwman AF, Van der Hoek KW, Olivier JGJ (1995) Uncertainties in the global source distribution of nitrous oxide. *J Geophys Res.* <https://doi.org/10.1029/94jd02946>
- Burke IC, Lauenroth WK, Confer G, Barrett JE, Mosier A, Lowe P (2002) Nitrogen in the Central Grasslands Region of the United States: current anthropogenic additions of nitrogen to ecosystems of the US central grasslands far outweigh loss of nitrogen through crop removal, resulting in increased nitrogen fluxes with the potential to alter regional-scale biogeochemical cycling. *Bioscience* 52:813–823. [https://doi.org/10.1641/0006-3568\(2002\)052\[0813:nitcgr\]2.0.co;2](https://doi.org/10.1641/0006-3568(2002)052[0813:nitcgr]2.0.co;2)
- Cameron KC, Di HJ, Moir JL (2013) Nitrogen losses from the soil/plant system: a review. *Ann Appl Biol* 162:145–173. <https://doi.org/10.1111/aab.12014>
- Carruthers JM, Cook SM, Wright GA, Osborne JL, Clark SJ, Swain JL et al (2017) Oilseed rape (*Brassica napus*) as a resource for farmland insect pollinators: quantifying floral traits in conventional varieties and breeding systems. *Glob Change Biol Bioenergy* 9:1370–1379. <https://doi.org/10.1111/gcbb.12438>
- Chen Z, Ding W, Luo Y, Yu H, Xu Y, Müller C et al (2014) Nitrous oxide emissions from cultivated black soil: A case study in Northeast China and global estimates using empirical model. *Global Biogeochem Cycles* 28:1311–1326. <https://doi.org/10.1002/2014gb004871>
- Ciais P, Sabine C, Bala G, Bopp L, Brovkin V, Canadell J et al (2013) Carbon and other biogeochemical cycles. In: Stocker TF, Qin D, Plattner G-K, Tignor M, Allen SK, Boschung J et al (eds) *Climate change 2013: the physical science basis. Contribution of working group I to the fifth assessment report of the intergovernmental panel on climate change*. Cambridge University Press, Cambridge, United Kingdom
- Congreves KA, Otchere O, Ferland D, Farzadfar S, Williams S, Arcand MM (2021) Nitrogen use efficiency definitions of today and tomorrow. *Front Plant Sci* 12:637108. <https://doi.org/10.3389/fpls.2021.637108>
- Crews TE, Peoples MB (2005) Can the synchrony of nitrogen supply and crop demand be improved in legume and fertilizer-based agroecosystems? *Rev Nutr Cycl Agroecosyst* 72:101–120. <https://doi.org/10.1007/s10705-004-6480-1>
- Dannenmann M, Butterbach-Bahl K, Gasche R, Willibald G, Papen H (2008) Dinitrogen emissions and the N₂:N₂O emission ratio of a Rendzic Leptosol as influenced by pH and forest thinning. *Soil Biol Biochem* 40:2317–2323. <https://doi.org/10.1016/j.soilbio.2008.05.009>
- Davidson EA (1991) Fluxes of nitrous oxide and nitric oxide from terrestrial ecosystems. In: Rogers JE, Whitman WB (eds) *Microbial production and consumption of greenhouse gases: methane, nitrogen oxides, and halomethanes*. American Society for Microbiology, Washington, WA, United States, pp 219–235
- Davidson EA, Kanter D (2014) Inventories and scenarios of nitrous oxide emissions. *Environ Res Lett.* <https://doi.org/10.1088/1748-9326/9/10/105012>
- Davidson EA, Keller M, Erickson HE, Verchot LV, Veldkamp E (2000) Testing a conceptual model of soil emissions of nitrous and nitric oxides. *Bioscience.* [https://doi.org/10.1641/0006-3568\(2000\)050\[0667:tacmos\]2.0.co;2](https://doi.org/10.1641/0006-3568(2000)050[0667:tacmos]2.0.co;2)
- Del Grosso SJ, Parton WJ, Mosier AR, Ojima DS, Kulmala AE, Phongpan S (2000) General model for N₂O and N₂ gas emissions from soils due to denitrification. *Global Biogeochem Cycles* 14:1045–1060. <https://doi.org/10.1029/1999gb001225>
- Dobbie KE, Smith KA (2003) Nitrous oxide emission factors for agricultural soils in Great Britain: the impact of soil water-filled pore space and other controlling variables. *Glob Change Biol* 9:204–218. <https://doi.org/10.1046/j.1365-2486.2003.00563.x>
- Eagle AJ, Olander LP, Locklier KL, Heffernan JB, Bernhardt ES (2017) Fertilizer management and environmental factors drive N₂O and NO₃ losses in corn: a meta-analysis. *Soil Sci Soc Am J* 81:1191–1202. <https://doi.org/10.2136/sssaj2016.09.0281>
- EEA (2000) *Down to earth: soil degradation and sustainable development in Europe*. European Environment Agency, Copenhagen, Denmark
- EEA (2016) *Sectoral greenhouse gas emissions by IPCC sector* [Online]. EEA. Available: <https://www.eea.europa.eu/data-and-maps/daviz/change-of-co2-emissions-2>. Accessed 6 Apr 2021
- Ejack L, Whalen JK (2021) Freeze-thaw cycles release nitrous oxide produced in frozen agricultural soils. *Biol Fertil Soils* 57:389–398. <https://doi.org/10.1007/s00374-020-01537-x>
- EPA (2020) *Sources of Greenhouse Gas Emissions* [Online]. Congressional Research Service. Available: <https://www.epa.gov/ghgemissions/sources-greenhouse-gas-emissions>. Accessed 6 Apr 2021
- Escuer-Gatius J, Shanskiy M, Mander Ü, Kauer K, Astover A, Vahter H et al (2020) Intensive rain hampers the effectiveness of nitrification inhibition in controlling N₂O emissions from dairy slurry-fertilized soils. *Agriculture.* <https://doi.org/10.3390/agriculture10110497>
- FAO (2015) *World reference base for soilresources 2014. International soil classification system for naming soils and creating legends for soil maps*. Food and Agriculture Organization of the United Nations, Rome, Italy
- FAO (2017) *The future of food and agriculture: trends and challenges*. FAO, Rome, Italy
- Flessa H, Dörsch P, Beese F (1995) Seasonal variation of N₂O and CH₄ fluxes in differently managed arable soils in southern Germany. *J Geophys Res.* <https://doi.org/10.1029/95jd02270>
- Fridrihsone A, Romagnoli F, Cabulis U (2018) Life Cycle Inventory for winter and spring rapeseed production in Northern Europe. *J Clean Prod* 177:79–88. <https://doi.org/10.1016/j.jclepro.2017.12.214>
- Fridrihsone A, Romagnoli F, Cabulis U (2020) Environmental life cycle assessment of rapeseed and rapeseed oil produced in northern Europe: a latvian case study. Sustainability. <https://doi.org/10.3390/su12145699>
- Galloway JN, Cowling EB (2002) Reactive nitrogen and the world: 200 years of change. *Ambio* 31:64–71. <https://doi.org/10.1579/0044-7447-31.2.64>
- Giweta M, Dyck M, Malhi SS (2017) Growing season nitrous oxide emissions from a gray luvisol as a function of long-term fertilization history and crop rotation. *Can J Soil Sci.* <https://doi.org/10.1139/cjss-2016-0106>

- Gomes J, Bayer C, de Souza CF, de Cássia PM, Zanatta JA, Vieira FCB et al (2009) Soil nitrous oxide emissions in long-term cover crops-based rotations under subtropical climate. *Soil Tillage Res* 106:36–44. <https://doi.org/10.1016/j.still.2009.10.001>
- Goyal MR (2014) Management, performance, and applications of micro irrigation systems. Apple Academic Press, New York, United States
- Hansen S, Berland Frøseth R, Stenberg M, Stalenga J, Olesen JE, Krauss M et al (2019) Reviews and syntheses: review of causes and sources of N₂O emissions and NO₃ leaching from organic arable crop rotations. *Biogeosciences* 16:2795–2819. <https://doi.org/10.5194/bg-16-2795-2019>
- Herr C, Mannheim T, Müller T, Ruser R (2020) Effect of nitrification inhibitors on N₂O emissions after cattle slurry application. *Agronomy*. <https://doi.org/10.3390/agronomy10081174>
- Hutchinson GL, Livingston GP (1993) Use of chamber systems to measure trace gas fluxes. In: Harper LA, Mosier AR, Duxbury JM, Rolston DE (eds) *Agricultural ecosystem effects on trace gases and global climate change*. American Society of Agronomy, pp 63–78
- Hutchings N, Webb BA (2019) Crop production and agricultural soils 2019. EMEP/EEA air pollutant emission inventory guidebook 2019. Publications Office of the European Union, Luxembourg
- Huygens D, Orveillon G, Lugato E, Tavazzi S, Comero S, Jones A, et al (2020) Technical proposals for the safe use of processed manure above the threshold established for nitrate vulnerable zones by the nitrates directive (91/676/EEC). Luxembourg
- IPCC (2018) Global warming of 1.5 °C. An IPCC Special Report on the impacts of global warming of 1.5 °C above pre-industrial levels and related global greenhouse gas emission pathways, in the context of strengthening the global response to the threat of climate change, sustainable development, and efforts to eradicate poverty. In: Masson-Delmotte V, Zhai P, Pörtner HO, Roberts D, Skea J, Shukla PR, Pirani A, Moufouma-Okia W, Péan C, Pidcock R, Connors S, Matthews JBR, Chen Y, Zhou X, Gomis MI, Lonnoy E, Maycock T, Tignor M, Waterfield T (eds). Geneva, Switzerland, p 630
- IPCC (2019) Chapter 11: N₂O emissions from managed soils, and CO₂ emissions from lime and urea application. In: Calvo Buendía E, Tanabe K, Kranjc A, Baasansuren J, Fukuda M, Ngarize S et al (eds) 2019 Refinement to the 2006 IPCC guidelines for national greenhouse gas inventories volume 4: agriculture, forestry and other land use. IPCC, Geneva, Switzerland
- Jensen L, Schjoerring J, Van der Hoek K, Poulsen H, Zevenbergen J, Pallière C, et al (2011) Benefits of nitrogen for food, fibre and industrial production. In: Sutton MA, Howard CM, Erisman JW, Billen G, Bleeker A, Grennfelt P, et al (eds) *The European nitrogen assessment: sources, effects and policy perspectives*. pp 32–61
- Kersebaum KC, Hecker J-M, Mirschel W, Wegehenkel M (2004) Modelling water and nutrient dynamics in soil-crop systems. Springer, Münchenberg, Germany, p VIII–272
- Klein H, Gauss M, Nyíri Á, Benedictow A (2016) Transboundary air pollution by main pollutants (S, N, O₃) and PM in 2016. Estonia. MSC-W Data Note The co-operative programme for monitoring and evaluation of the long-range transmission of air pollutants in Europe (EMEP)
- Ladha JK, Tirol-Padre A, Reddy CK, Cassman KG, Verma S, Powlson DS et al (2016) Global nitrogen budgets in cereals: A 50-year assessment for maize, rice, and wheat production systems. *Sci Rep* 6:19355. <https://doi.org/10.1038/srep19355>
- Lal R, Stewart BA (2018) Soil nitrogen uses and environmental impacts
- Lal R (2001) World cropland soils as a source or sink for atmospheric carbon. pp 145–191
- Lassaletta L, Billen G, Grizzetti B, Anglade J, Garnier J (2014) 50 year trends in nitrogen use efficiency of world cropping systems: the relationship between yield and nitrogen input to cropland. *Environ Res Lett*. <https://doi.org/10.1088/1748-9326/9/10/105011>
- Lee DK, Doolittle JJ, Owens VN (2007) Soil carbon dioxide fluxes in established switchgrass land managed for biomass production. *Soil Biol Biochem* 39:178–186. <https://doi.org/10.1016/j.soilbio.2006.07.004>
- Leip A, Dämmgen U, Kuikman P, Van Amstel A (2007) The quality of European (EU-15) greenhouse gas inventories from agriculture. *Environ Sci* 2:177–192. <https://doi.org/10.1080/15693430500393177>
- Lessard R, Rochette P, Gregorich EG, Pattey E, Desjardins RL (1996) Nitrous oxide fluxes from manure-amended soil under maize. *J Environ Qual*. <https://doi.org/10.2134/jeq1996.00472425002500060029x>
- Li H, Qiu J-J, Wang L-G, Xu M-Y, Liu Z-Q, Wang W (2012) Estimates of N₂O emissions and mitigation potential from a spring maize field based on DNDC model. *J Integr Agric* 11:2067–2078. [https://doi.org/10.1016/s2095-3119\(12\)60465-1](https://doi.org/10.1016/s2095-3119(12)60465-1)
- Liu J, Ma K, Ciais P, Polasky S (2016) Reducing human nitrogen use for food production. *Sci Rep* 6:30104. <https://doi.org/10.1038/srep30104>
- Liu S, Lin F, Wu S, Ji C, Sun Y, Jin Y et al (2017) A meta-analysis of fertilizer-induced soil NO and combined NO+N₂O emissions. *Glob Chang Biol* 23:2520–2532. <https://doi.org/10.1111/gcb.13485>
- Livingston GP, Hutchinson GL (1995) Enclosure-based measurement of trace gas exchange: applications and sources of error. In: Matson PA, Harriss RC (eds) *Biogenic trace gases: measuring emissions from soil and water*. Blackwell Publishing, Oxford, United Kingdom, pp 14–51
- Lloyd J, Taylor JA (1994) On the temperature dependence of soil respiration. *Funct Ecol*. <https://doi.org/10.2307/2389824>
- Loftfield N, Flessa H, Augustin J, Beese F (1997) Automated gas chromatographic system for rapid analysis of the atmospheric trace gases methane, carbon dioxide, and nitrous oxide. *J Environ Qual*. <https://doi.org/10.2134/jeq1997.00472425002600020030x>
- Maas SE, Glenn AJ, Tenuta M, Amiro BD (2013) Net CO₂ and N₂O exchange during perennial forage establishment in an annual crop rotation in the Red River Valley. *Manit Can J Soil Sci* 93:639–652. <https://doi.org/10.4141/cjss2013-025>
- Maidl FX, Fischbeck G (1989) Effects of long-term application of slurry on soil nitrogen mineralization. *J Agron Crop*

- Sci 162:310–319. <https://doi.org/10.1111/j.1439-037X.1989.tb00722.x>
- Malagoli P, Laine P, Rossato L, Ourry A (2005) Dynamics of nitrogen uptake and mobilization in field-grown winter oilseed rape (*Brassica napus*) from stem extension to harvest. II. An ¹⁵N-labelling-based simulation model of N partitioning between vegetative and reproductive tissues. *Ann Bot* 95:1187–1198. <https://doi.org/10.1093/aob/mci131>
- Mathivanan GP, Eysholdt M, Zinnbauer M, Rösemann C, Fuß R (2021) New N₂O emission factors for crop residues and fertiliser inputs to agricultural soils in Germany. *Agric Ecosyst Environ*. <https://doi.org/10.1016/j.agee.2021.107640>
- McCormick RA, Nelson DW, Sutton AL, Huber DM (1984) Increased N efficiency from nitrapyrin added to liquid swine manure used as a fertilizer for corn. *Agron J* 76:1010–1014. <https://doi.org/10.2134/agronj1984.00021962007600060034x>
- McCrackin ML, Gustafsson BG, Hong B, Howarth RW, Humborg C, Savchuk OP et al (2018) Opportunities to reduce nutrient inputs to the Baltic Sea by improving manure use efficiency in agriculture. *Reg Environ Change* 18:1843–1854. <https://doi.org/10.1007/s10113-018-1308-8>
- Medinets S, Skiba U, Rennenberg H, Butterbach-Bahl K (2015) A review of soil NO transformation: associated processes and possible physiological significance on organisms. *Soil Biol Biochem* 80:92–117. <https://doi.org/10.1016/j.soilbio.2014.09.025>
- Meixner FX, Yang WX (2006) Biogenic emissions of nitric oxide and nitrous oxide from arid and semi-arid land. *Dryland Ecohydrol* 233–255
- Mendham NJ, Shipway PA, Scott RK (1981) The effects of delayed sowing and weather on growth, development and yield of winter oil-seed rape (*Brassica napus*). *J Agri Sci* 96:389–416. <https://doi.org/10.1017/S002185960006617x>
- Mendiburu FD (2015) *Agricolae: statistical procedures for agricultural research*. R Package Version 1.2–3. The Comprehensive R Archive Network, Vienna, Austria
- Moll RH, Kamprath EJ, Jackson WA (1982) Analysis and Interpretation of factors which contribute to efficiency of nitrogen utilization I. *Agron J* 74:562–564. <https://doi.org/10.2134/agronj1982.00021962007400030037x>
- Nair D, Baral KR, Abalos D, Strobel BW, Petersen SO (2020) Nitrate leaching and nitrous oxide emissions from maize after grass-clover on a coarse sandy soil: mitigation potentials of 3,4-dimethylpyrazole phosphate (DMPP). *J Environ Manag* 260:110165. <https://doi.org/10.1016/j.jenvman.2020.110165>
- NOAA (2020) Rise of carbon dioxide unabated [Online]. Available: <https://research.noaa.gov/article/ArtMID/587/ArticleID/2636/Rise-of-carbon-dioxide-unabated>. Accessed 6 Apr 2021
- O'Neill M, Lanigan GJ, Forristal PD, Osborne BA (2021) Greenhouse gas emissions and crop yields from winter oilseed rape cropping systems are unaffected by management practices. *Front Environ Sci*. <https://doi.org/10.3389/fenvs.2021.716636>
- Öborn I, Edwards AC, Witter E, Oenema O, Ivarsson K, Withers PJA et al (2003) Element balances as a tool for sustainable nutrient management: a critical appraisal of their merits and limitations within an agronomic and environmental context. *Eur J Agron* 20:211–225. [https://doi.org/10.1016/S1161-0301\(03\)00080-7](https://doi.org/10.1016/S1161-0301(03)00080-7)
- Oenema O, Kros H, de Vries W (2003) Approaches and uncertainties in nutrient budgets: implications for nutrient management and environmental policies. *Eur J Agron* 20:3–16. [https://doi.org/10.1016/S1161-0301\(03\)00067-4](https://doi.org/10.1016/S1161-0301(03)00067-4)
- Oenema O, Brentrup F, Lammel J, Bascou P, Billen G, Dobermann A et al (2015) Nitrogen use efficiency (NUE) - an indicator for the utilization of nitrogen in agriculture and food systems. Wageningen, Netherlands
- Oenema O, Velthof GL (2002) Balanced fertilization and regulating nutrient losses from agriculture. In: Steenvorden J, Claessen F, Willems J, Steenvoorden J (eds) *Agricultural effects on ground and surface waters: research at the edge of science and society*, vol 273. IAHS, Wageningen, The Netherlands
- Oswald R, Behrendt T, Ermel M, Wu D, Su H, Cheng Y et al (2013) HONO emissions from soil bacteria as a major source of atmospheric reactive nitrogen. *Science* 341:1233–1235. <https://doi.org/10.1126/science.1242266>
- Øygarden L, Botterweg P (1998) Measuring runoff and nutrient losses from agricultural land in nordic countries: a guideline for good measurement practices. Nordic Council of Ministers, Copenhagen, Denmark
- Pärn J, Verhoeven JTA, Butterbach-Bahl K, Dise NB, Ullah S, Aasa A et al (2018) Nitrogen-rich organic soils under warm well-drained conditions are global nitrous oxide emission hotspots. *Nat Commun* 9:1135. <https://doi.org/10.1038/s41467-018-03540-1>
- Pehnel G, Vietze C (2012) Uncertainties about the GHG emissions saving of rapeseed biodiesel. *Jena economic research papers*. 2012-039. Friedrich-Schiller University of Jena, Jena, Germany
- Philibert A, Loyce C, Makowski D (2012) Quantifying uncertainties in N₂O emission due to N fertilizer application in cultivated areas. *PLoS ONE* 7:e50950. <https://doi.org/10.1371/journal.pone.0050950>
- Poyda A, Reinsch T, Skinner RH, Kluß C, Loges R, Taube F (2017) Comparing chamber and eddy covariance based net ecosystem CO₂ exchange of fen soils. *J Plant Nutr Soil Sci* 180:252–266. <https://doi.org/10.1002/jpln.201600447>
- Prasad R, Hobbs PR (2018) Efficient nitrogen management in the tropics and subtropics. In: Lal R, Stewart BA, (eds) *Soil nitrogen uses and environmental impacts*. New York, NY, p 392
- Quemada M, Baranski M, Nobel-de Lange MNJ, Vallejo A, Cooper JM (2013) Meta-analysis of strategies to control nitrate leaching in irrigated agricultural systems and their effects on crop yield. *Agr Ecosyst Environ* 174:1–10. <https://doi.org/10.1016/j.agee.2013.04.018>
- R Core Team (2016) R: a language and environment for statistical computing. R Foundation for Statistical Computing
- Ratajczak K, Sulewska H, Szymańska G (2017) New winter oilseed rape varieties – seed quality and morphological traits depending on sowing date and rate. *Plant Prod Sci* 20:262–272. <https://doi.org/10.1080/1343943x.2017.1304809>

- Rathke G, Behrens T, Diepenbrock W (2006) Integrated nitrogen management strategies to improve seed yield, oil content and nitrogen efficiency of winter oilseed rape (*Brassica napus* L.): A review. *Agric Ecosyst Environ* 117:80–108. <https://doi.org/10.1016/j.agee.2006.04.006>
- Ravishankara AR, Daniel JS, Portmann RW (2009) Nitrous oxide (N_2O): the dominant ozone-depleting substance emitted in the 21st century. *Science* 326:123–125. <https://doi.org/10.1126/science.1176985>
- Regina K, Kaseva J, Esala M (2013) Emissions of nitrous oxide from boreal agricultural mineral soils—statistical models based on measurements. *Agr Ecosyst Environ* 164:131–136. <https://doi.org/10.1016/j.agee.2012.09.013>
- Risk N, Snider D, Wagner-Riddle C (2013) Mechanisms leading to enhanced soil nitrous oxide fluxes induced by freeze–thaw cycles. *Can J Soil Sci* 93:401–414. <https://doi.org/10.4141/cjss2012-071>
- Rosenstock TS, Rufino MC, Butterbach-Bahl K, Wollenberg E (2013) Toward a protocol for quantifying the greenhouse gas balance and identifying mitigation options in small-holder farming systems. *Environ Res Lett*. <https://doi.org/10.1088/1748-9326/8/2/021003>
- Ruser R, Fuß R, Andres M, Hegewald H, Kesenheimer K, Köbke S et al (2017) Nitrous oxide emissions from winter oilseed rape cultivation. *Agr Ecosyst Environ* 249:57–69. <https://doi.org/10.1016/j.agee.2017.07.039>
- Ruzicka J, Hansen EH (1988) flow injection analysis, 2nd edn. Wiley, New York
- Saggar S, Jha N, Deslippe J, Bolan NS, Luo J, Giltrap DL et al (2013) Denitrification and N_2O/N_2 production in temperate grasslands: processes, measurements, modelling and mitigating negative impacts. *Sci Total Environ* 465:173–195. <https://doi.org/10.1016/j.scitotenv.2012.11.050>
- Sainju UM (2017) Determination of nitrogen balance in agroecosystems. *MethodsX* 4:199–208. <https://doi.org/10.1016/j.mex.2017.06.001>
- Schlingmann M, Tobler U, Berauer B, Garcia-Franco N, Wilfahrt P, Wiesmeier M et al (2020) Intensive slurry management and climate change promote nitrogen mining from organic matter-rich montane grassland soils. *Plant Soil* 456:81–98. <https://doi.org/10.1007/s11104-020-04697-9>
- Schulte EE, Hopkins BG (1996) Estimation of soil organic matter by weight loss-on-ignition. In: Magdoff FR, Tabatabai MA Jr, EAH, (eds) *Soil organic matter: analysis and interpretation*, vol 46. Soil Science Society of America Inc, Madison, Wisconsin
- Simek M, Cooper JE (2002) The influence of soil pH on denitrification: progress towards the understanding of this interaction over the last 50 years. *Eur J Soil Sci* 53:345–354. <https://doi.org/10.1046/j.1365-2389.2002.00461.x>
- Skiba U, Medinets S, Cardenas LM, Carnell EJ, Hutchings N, Amon B (2020) Assessing the contribution of soil NOx emissions to European atmospheric pollution. *Environ Res Lett*. <https://doi.org/10.1088/1748-9326/abd2f2>
- Smith KA, Conen F (2004) Impacts of land management on fluxes of trace greenhouse gases. *Soil Use Manag* 20:255–263. <https://doi.org/10.1079/sum2004238>
- Smith P, Soussana JF, Angers D, Schipper L, Chenu C, Rasse DP et al (2020) How to measure, report and verify soil carbon change to realize the potential of soil carbon sequestration for atmospheric greenhouse gas removal. *Glob Chang Biol* 26:219–241. <https://doi.org/10.1111/gcb.14815>
- Smith K, Bouwman L, Braatz B (1999) N_2O : direct emissions from agricultural soils. In: IPCC (ed) *Background paper to IPCC good practice guidance and uncertainty management in national greenhouse gas inventories*. pp 361–380
- Sommer SG, Hutchings NJ (2001) Ammonia emission from field applied manure and its reduction—invited paper. *Eur J Agron* 15:1–15. [https://doi.org/10.1016/s1161-0301\(01\)00112-5](https://doi.org/10.1016/s1161-0301(01)00112-5)
- Sommer SG, Olesen JE (1991) Effects of dry matter content and temperature on ammonia loss from surface-applied cattle slurry. *J Environ Qual* 20:679–683. <https://doi.org/10.2134/jeq1991.00472425002000030029x>
- Sommer SG, Olesen JE, Christensen BT (1991) Effects of temperature, wind speed and air humidity on ammonia volatilization from surface applied cattle slurry. *J Agric Sci* 117:91–100. <https://doi.org/10.1017/s0021859600079016>
- Sommer SG, Générmont S, Cellier P, Hutchings NJ, Olesen JE, Morvan T (2003) Processes controlling ammonia emission from livestock slurry in the field. *Eur J Agron* 19:465–486. [https://doi.org/10.1016/s1161-0301\(03\)00037-6](https://doi.org/10.1016/s1161-0301(03)00037-6)
- Soosaar K, Mander Ü, Maddison M, Kanal A, Kull A, Lõhmus K et al (2011) Dynamics of gaseous nitrogen and carbon fluxes in riparian alder forests. *Ecol Eng* 37:40–53. <https://doi.org/10.1016/j.ecoleng.2010.07.025>
- Soussana JF, Tallec T, Blanfort V (2010) Mitigating the greenhouse gas balance of ruminant production systems through carbon sequestration in grasslands. *Animal* 4:334–350. <https://doi.org/10.1017/S1751731109990784>
- Stegarescu G, Escuer-Gatius J, Soosaar K, Kauer K, Tõnutare T, Astover A et al (2020) Effect of crop residue decomposition on soil aggregate stability. *Agriculture*. <https://doi.org/10.3390/agriculture10110527>
- Sutton MA, Howard CM, Erisman JW, Billen G, Bleeker A, Grennfelt P et al (2011) *The European nitrogen assessment: sources, effects and policy perspectives*. Cambridge University Press, Cambridge
- Thers H, Petersen SO, Elsgaard L (2019) DMPP reduced nitrification, but not annual N_2O emissions from mineral fertilizer applied to oilseed rape on a sandy loam soil. *GCB Bioenergy* 11:1396–1407. <https://doi.org/10.1111/gcbb.12642>
- Thompson RB, Meisinger JJ (2002) Management factors affecting ammonia volatilization from land-applied cattle slurry in the Mid-Atlantic USA. *J Environ Qual* 31:1329–1338. <https://doi.org/10.2134/jeq2002.1329>
- UNFCCC (1997) Kyoto protocol to the united nations framework convention on climate change. In: (UNFCCC) UNFCCC (ed) *Kyoto, Japan*
- UNFCCC (2015) Adoption of the paris agreement FCCC/CP/2015/L.9/Rev.1 United Nations framework convention on climate change. In: (UNFCCC) UNFCCC (ed) *21st conference of the parties, Paris, France*
- USDA Foreign Agricultural Service (2018) *EU biofuels annual 2018. GAIN report*. USDA Foreign Agricultural Service, The Hague, The Netherlands

- van Grinsven HJM, ten Berge HFM, Dalgaard T, Fraters B, Durand P, Hart A et al (2012) Management, regulation and environmental impacts of nitrogen fertilization in northwestern Europe under the Nitrates Directive; a benchmark study. *Biogeosciences* 9:5143–5160. <https://doi.org/10.5194/bg-9-5143-2012>
- Velthof GL, Oudendag DA, Oenema O (2007) Development and application of the integrated nitrogen model MITERRA-EUROPE. Task 1 service contract integrated measures in agriculture to reduce ammonia emissions. Alterra Rapport. Alterra, Wageningen, The Netherlands
- Vet R, Artz RS, Carou S, Shaw M, Ro C-U, Aas W et al (2014) A global assessment of precipitation chemistry and deposition of sulfur, nitrogen, sea salt, base cations, organic acids, acidity and pH, and phosphorus. *Atmos Environ* 93:3–100. <https://doi.org/10.1016/j.atmosenv.2013.10.060>
- Vinzent B, Fuß R, Maidl F-X, Hülsbergen K-J (2018) N₂O emissions and nitrogen dynamics of winter rapeseed fertilized with different N forms and a nitrification inhibitor. *Agr Ecosyst Environ* 259:86–97. <https://doi.org/10.1016/j.agee.2018.02.028>
- Wagner-Riddle C, Congreves KA, Abalos D, Berg AA, Brown SE, Ambadan JT et al (2017) Globally important nitrous oxide emissions from croplands induced by freeze–thaw cycles. *Nat Geosci* 10:279–283. <https://doi.org/10.1038/ngeo2907>
- Walter K, Don A, Fuß R, Kern J, Drewer J, Flessa H (2014) Direct nitrous oxide emissions from oilseed rape cropping – a meta-analysis. *GCB Bioenergy* 7:1260–1271. <https://doi.org/10.1111/gcbb.12223>
- Webb J, Pain B, Bittman S, Morgan J (2010) The impacts of manure application methods on emissions of ammonia, nitrous oxide and on crop response—a review. *Agric Ecosyst Environ* 137:39–46. <https://doi.org/10.1016/j.agee.2010.01.001>
- Webb J, Sørensen P, Velthof G, Amon B, Pinto M, Rodhe L et al (2013) An assessment of the variation of manure nitrogen efficiency throughout Europe and an appraisal of means to increase manure-n efficiency. In: Sparks DL (ed) *Advances in agronomy*. Academic Press, Cambridge, pp 371–442
- Weier KL, Doran JW, Power JF, Walters DT (1993) Denitrification and the dinitrogen/nitrous oxide ratio as affected by soil water, available carbon, and nitrate. *Soil Sci Soc Am J* 57:66–72. <https://doi.org/10.2136/sssaj1993.03615995005700010013x>
- Wohlfahrt G, Klumpp K, Soussana J-F (2012) Eddy covariance measurements over grasslands. *Eddy Covariance*, pp. 333–344
- Wu X, Chen Z, Kiese R, Fu J, Gschwendter S, Schloter M et al (2020) Dinitrogen (N₂) pulse emissions during freeze-thaw cycles from montane grassland soil. *Biol Fertil Soils* 56:959–972. <https://doi.org/10.1007/s00374-020-01476-7>
- Yang M, Fang Y, Sun D, Shi Y (2016) Efficiency of two nitrification inhibitors (dicyandiamide and 3, 4-dimethylpyrazole phosphate) on soil nitrogen transformations and plant productivity: a meta-analysis. *Sci Rep* 6:22075. <https://doi.org/10.1038/srep22075>

Publisher's Note Springer Nature remains neutral with regard to jurisdictional claims in published maps and institutional affiliations.

CURRICULUM VITAE

First name: Jordi
Last name: Escuer Gatius
Date of birth: March 11th, 1977
E-mail: jordi.escuer@gmail.com

Education

2016–2022 Estonian University of Life Sciences, Institute of Agricultural and Environmental Sciences, PhD studies in Agricultural Sciences
2002–2005 University of Lleida, MSc studies in Agronomy
1995–2001 University of Lleida, BSc studies in Forestry

Employment

2021 – Estonian University of Life Sciences, Institute of Agricultural and Environmental Sciences, Chair of Soil Science, specialist
2016 – 2021 Estonian University of Life Sciences, Institute of Agricultural and Environmental Sciences, Chair of Soil Science, junior researcher
2007 – 2014 LEMA S.C.L., Don Benito, Spain

Professional training

Summer School “Soil & Water”. September 6–16, 2021. Czech Republic and Germany.

Research interests

Greenhouse gas emissions, carbon and nitrogen cycles, nutrient balances, organic fertilisation, greenhouse gas emissions mitigation, nitrification inhibitors, biochar

Dissertations supervised

Hanna Vahter, Master’s Degree, 2019, (sup) Kaido Soosaar, Kuno Kasak, Jordi Escuer Gatius; Nitrifikatsiooni inhibiitori DMPP mõju talirapsi (*Brassica napus* L.) saagikusele ning põllu lämmastikubilansile, University of Tartu.

Funding and projects

V 180265 PKMD (862695) 01.02.2020–31.01.2025

“Towards climate-smart sustainable management of agricultural soils”

Principal Investigator: Alar Astover (Estonian University of Life Sciences, Institute of Agricultural and Environmental Sciences, Chair of Soil Science). Financier: Commission of the European Communities.

PM 180259 PKKH 1.01.2019–31.12.2022

“From bio-waste to high added value products - PKKH. Development of high value-added products from lake sediments”

Principal Investigator: Anu Kisand (Estonian University of Life Sciences, Institute of Agricultural and Environmental Sciences, Chair of Hydrobiology and Fishery). Financier: Estonian University of Life Sciences.

V 190002 PKMD (817819) 1.06.2019–31.05.2024

“Soil biodiversity enhancement in European agroecosystems to promote their stability and resilience by external inputs reduction and crop performance increase”

Principal Investigator: Merrit Shanskiy, Anne Pöder (Estonian University of Life Sciences, Institute of Agricultural and Environmental Sciences, Chair of Soil Science (partner); Estonian University of Life Sciences, Institute of Economy and Social Sciences (partner)); Financier: Commission of the European Communities.

8 P 160194 PKML 4.11.2016–30.06.2017

“Interaction of arbuscular mycorrhiza and biochar on crop P uptake”

Principal Investigator: Alar Astover (Estonian University of Life Sciences, Institute of Agricultural and Environmental Sciences). Financier: Ministry of Education and Research.

T 170144 PKTM (PRIA otsus nr 13-6/315) 1.05.2017–31.03.2021

“Organic fertilizers: decreasing the environmental impact and increasing the efficiency”

Principal Investigator: Henn Raave (Estonian University of Life Sciences, Institute of Agricultural and Environmental Sciences). Financier: NGO Soil Innovation Cluster.

ELULOOKIRJELDUS

Eesnimi: Jordi
Perekonnanimi: Escuer Gatius
Sünniaeg: 11. märts 1977
E-mail: Jordi.EscuerGatius@gmail.com

Haridus:

2016 – 2022 Eesti Maaülikool, Põllumajandus- ja keskkonnainstituut, mullateaduse õppetool, doktoriõpe põllumajanduse erialal
2002 – 2005 Lleida Ülikool, magistriõpe agronoomia erialal
1995 – 2001 Lleida Ülikool, bakalaureuseõpe metsandus erialal

Teenistuskäik:

2021 – Eesti Maaülikool, Põllumajandus- ja keskkonnainstituut, Mullateaduse õppetool, spetsialist
2016 – 2021 Eesti Maaülikool, Põllumajandus- ja keskkonnainstituut, Mullateaduse õppetool, nooremteadur
2007 – 2014 LEMA S.C.L., Badajoz (Hispaania), agronoom.

Enesetäiendus ja koolitused

Suvekool “Soil & Water”. September 6.09-16.09.2021. Tšehhi ja Saksamaa.

Teadustöö põhisuunad

Kasvuhoonegaaside lenduva, süsiniku- ja lämmastikutsüklid, toitainete bilansid, orgaaniline väetamine, kasvuhoonegaaside lenduva vähendamine, nitrifikatsiooni inhibiitorid, biosüsi

Juhendatud väitekirjad

Hanna Vahter, magistrikraad, 2019, (juh) Kaido Soosaar, Kuno Kasak, Jordi Escuer Gatius. Nitrifikatsiooni inhibiitori DMPP mõju talirapsi (*Brassica napus* L.) saagikusele ning põllu lämmastikubilansile. Tartu Ülikool.

Uurimisprojektides osalemine

V 180265 PKMD (862695) 1.02.2020–31.01.2025

“Towards climate-smart sustainable management of agricultural soils”

Vastutav täitja: Alar Astover (Eesti Maaülikool, Põllumajandus- ja keskkonnainstituut, Mullateaduse õppetool). Finantseerija: Euroopa Komisjon.

PM 180259 PKKH 1.01.2019–31.12.2022

“Biojäätmest kõrge lisandväärtusega toodeteni – PKKH. Järvesetest kõrge lisandväärtusega toodete väljatöötamine”

Vastutav täitja: Anu Kisand (Eesti Maaülikool, Põllumajandus- ja keskkonnainstituut, Hüdrobioloogia ja kalanduse õppetool). Finantseerija: Eesti Maaülikool.

V 190002 PKMD (817819) 1.06.2019–31.05.2024

“Soil biodiversity enhancement in European agroecosystems to promote their stability and resilience by external inputs reduction and crop performance increase”

Vastutavad täitjad: Merrit Shanskiy ja Anne Pöder (Eesti Maaülikool, Põllumajandus- ja keskkonnainstituut, Mullateaduse õppetool (partner) ja Eesti Maaülikool, Majandus- ja sotsiaalinstituut (partner)). Finantseerija: Euroopa Komisjon.

8P 160194 PKML 4.11.2016–30.06.2017

“Arbuskulaarse mükoriisa ja biosöe koosmõju põllukultuuride P omastamisele”

Vastutav täitja: Alar Astover (Eesti Maaülikool, Põllumajandus- ja keskkonnainstituut). Finantseerija: Haridus- ja Teadusministeerium.

T 170144 PKTM (PRIA otsus nr 13-6/315) 1.05.2017–31.03.2021

“Orgaaniliste väetiste keskkonnamõju vähendamine ja efektiivsuse suurendamine”

Vastutav täitja: Henn Raave (Eesti Maaülikool, Põllumajandus- ja keskkonnainstituut). Finantseerija: MTÜ Põllukultuuride klaster.

LIST OF PUBLICATIONS

Articles indexed by Thomson Reuters Web of Science or Scopus (1.1)

1. Schindler, T., Mander, Ü., Machacova, K., Espenberg, M., Krasnov, D., **Escuer-Gatius, J.**, Veber, G., Parn, J., Soosaar, K. 2020. Short-term flooding increases CH₄ and N₂O emissions from trees in a riparian forest soil-stem continuum. *Scientific Reports* 10, 3204. doi: 10.1038/s41598-020-60058-7
2. **Escuer-Gatius, J.**, Shanskiy, M., Soosaar, K., Astover, A., Raave, H. 2020. High-Temperature Hay Biochar Application into Soil Increases N₂O Fluxes. *Agronomy* 10(1), 109. doi: 10.3390/agronomy10010109
3. Raave, H., **Escuer-Gatius, J.**, Kauer, K., Shanskiy, M., Tõnutare, T., Astover, A. Permanent grassland hay-derived biochar increases plant N, P and K uptake on an acidic soil. *Zemdirbyste-Agriculture* 107(3):227, 234. doi: 10.13080/z-a.2020.107.029
4. Stegarescu, G., **Escuer-Gatius, J.**, Soosaar, K., Kauer, K., Tõnutare, T., Astover, A., Reintam, E. 2020. Effect of Crop Residue Decomposition on Soil Aggregate Stability. *Agriculture* 10(11), 527. doi: 10.3390/agriculture10110527
5. **Escuer-Gatius, J.**, Shanskiy, M., Mander, Ü., Kauer, K., Astover, A., Vahter, H., Soosaar, K. 2020. Intensive rain hampers the effectiveness of nitrification inhibition in controlling N₂O emissions from dairy slurry-fertilized soils. *Agriculture* 10(11), 497. doi: 10.3390/agriculture10110497
6. Covali, P., Raave, H., **Escuer-Gatius, J.**, Kaasik, A., Tõnutare, T., Astover, A. 2021. The Effect of Untreated and Acidified Biochar on NH₃-N Emissions from Slurry Digestate. *Sustainability* 13(2), 837. doi: 10.3390/su13020837
7. Escuer, O., Karp, K., **Escuer-Gatius, J.**, Raave, H., Teppand, T., Shanskiy, M. 2021. Hardwood biochar as an alternative to reduce peat use for seed germination and growth of *Tagetes patula*. *Acta Agriculturae Scandinavica, Section B – Soil & Plant Science*. doi: 10.1080/09064710.2021.1903986
8. Schindler, T., Machacova, K., Mander, Ü., **Escuer-Gatius, J.**, Soosaar, K. 2021. Diurnal Tree Stem CH₄ and N₂O Flux Dynamics from a Riparian Alder Forest. *Forests*, 12(7):863. doi: 10.3390/f12070863

9. Mander, Ü., Krasnova, A., Schindler, T., Megonigal, J.P., **Escuer-Gatius, J.**, Espenberg, M., Machacova, K., Maddison, M., Pärn, J., Ranniku, R., Pihlatie, M., Kasak, K., Niinemets, Ü., Soosaar, K. Long-term dynamics of soil, tree stem and ecosystem methane fluxes in a riparian forest. *Science of the Total Environment*. 2022 Feb 25; 809:151723. doi: 10.1016/j.scitotenv.2021.151723
10. **Escuer-Gatius, J.**, Lõhmus, K., Shanskiy, M., Kauer, K., Vahter, H., Mander, Ü., Astover, A., Soosaar, K. 2022. Critical points for closing the carbon and nitrogen budgets in a winter rapeseed field. *Nutrient Cycling in Agroecosystems*. doi: 10.1007/s10705-022-10202-8

Articles in proceedings/a chapter in a book or in a collection/specific research publications (3.4)

1. Raave, H., **Escuer-Gatius, J.**, Shanskiy, M. 2018. Lahaheina biomassist toodetud biosöe omadused, mõju mullale ja karjamaa raiheina biomassi saagile. *Agroonoomia* 2018, 171–185. Tartu: Rebellis.

Conference abstracts (5.2)

1. Soosaar, K., Schindler, T., Krasnov, D., Krasnova, A., **Escuer Gatius, J.**, Macháčová, K., Mander, Ü. 2019. The annual budget of CH₄ and N₂O from a riparian forest: balances between the forest floor, tree stems and canopy. *Geophysical Research Abstracts*. EGU2019-13200.
2. Krasnov, D., **Escuer Gatius, J.**, Krasnova, A., Mander, Ü., Noe, S.M., Soosaar, K. 2019. Methods for calculating nitrous oxide and methane from non-steady state automatic chambers. *Geophysical Research Abstracts*. EGU2019-13119.
3. **Escuer Gatius, J.**, Shanskiy, M., Mander, Ü., Kauer, K., Astover, A., Soosaar, K. 2019. Effectiveness of a nitrification inhibitor to reduce N₂O emissions – A case study in Estonia. *Geophysical Research Abstracts*. EGU2019-10613.
4. Stegarescu, G., **Escuer, J.**, Kauer, K., and Reintam, E. 2020. Crop residues amendments quality and effect on greenhouse gas emissions and aggregate stability, EGU General Assembly 2020, Online, 4–8 May 2020. EGU2020-5973. doi: 10.5194/egusphere-egu2020-5973.
5. **Escuer-Gatius, J.**, Lõhmus, K., Shanskiy, M., Kauer, K., Vahter, H., Mander, Ü., Astover, A. and Soosaar, K.. 2021. Carbon and nitrogen budgets of a winter rapeseed field in Estonia: a methodology for the

quantification of all relevant pools and fluxes. EGU General Assembly 2021. EGU21-15668. doi: 10.5194/egusphere-egu21-15668

6. Ranniku, R., Schindler, T., **Escuer-Gatius, J.**, Mander, Ü., Machacova, K., and Soosaar, K. 2022. Greenhouse Gas Dynamics in a Drained Peatland Forest: Annual CH₄ and N₂O Fluxes from Tree Stems and Soil, EGU General Assembly 2022, Vienna, Austria, 23–27 May 2022. EGU22-7493. doi: 10.5194/egusphere-egu22-7493.

VIIS VIIMAST KAITSMIST

KRISTEL PANKSEP

FROM MICROSCOPY TO GENES – UNMASKING TOXIC
CYANOBACTERIA IN A SHALLOW EUTROPHIC LAKE

MIKROSKOOPIAST GEENIDENI, KUIDAS OTSIDA TOKSILISI
SINIVETIKAID MADALAST EUTROOFSEST JÄRVEST

Professor **Veljo Kisand**; teadur **Helen Agasild**; professor **Kaarina Sivonen**
23. mai 2022

REINE KOPPEL

STABILITY OF YIELD AND BAKING QUALITY OF WHEAT
IN BALTIC CONDITIONS

NISU SAAGI JA KÜPSETUSKVALITEEDI STABIILSUS BALTI REGIOONIS

Dotsent **Evelin Loit**, vanemteadur **Mati Koppel**
3. juuni 2022

FARIBA BAHRINI

PATTERN OF URBAN PARK USE, SPATIAL ACCESSIBILITY AND
PREFERANCES OF URBAN PARK USERS IN TEHRAN, IRAN

LINNAPARKIDE KASUTUSMUSTRID, RUUMILINE LIGIPÄÄSETAVUS JA
KASUTAJAEELISTUSED IRAANI PEALINNAS TEHERANIS

Professor **Simon Bell**
10. juuni 2022

ASSAR LUHA

OCCUPATIONAL NOISE EXPOSURE AND HEARING PROBLEMS AMONG
ACTIVE MILITARY SERVICE PERSONNEL IN ESTONIA

MILITAARMÜRA EKSPOSITSIOON JA KUULMISPROBLEEMID
EESTI TEGEVVÄELASTEL

Professor **Eda Merisalu**, kaasprofessor **Hans Orru**
17. juuni 2022

HENRI JÄRV

THE IMPACT OF PROTECTED AREAS GOVERNANCE AND
MANAGEMENT PRACTICES ON HUMAN WELL-BEING AND
LOCAL SOCIOECONOMIC CONDITIONS

KAITSEALADE HALDUSSÜSTEEMI JA KAITSEKORRALDUSLIKE
MEETMETE MÕJU INIMESTE HEAOLULE NING KOHALIKELE
SOTSIAALMAJANDUSLIKELE OLUDELE

Professor **Kalev Sepp**, lektor **Raymond David Ward**
21. juuni 2022

ISSN 2382-7076
ISBN 978-9916-669-53-2 (pdf)